# ARTIFICIAL NEURAL NETWORKS TO PREDICT THE NITRATE DISTRIBUTION IN CIMARRON TERRACE AQUIFER, OKLAHOMA

By

PRATIMA POUDYAL

Bachelor's Degree in Civil Engineering

Tribhuvan University

Institute of Engineering

Pokhara, Nepal

2003

Submitted to the Faculty of the
Graduate College of the
Oklahoma State University
in partial fulfillment of
the requirements for
the Degree of
MASTER OF SCIENCE
December, 2007

ARTIFICIAL NEURAL NETWORKS TO PREDICT THE NITRATE DISTRIBUTION IN CIMARRON TERRACE AQUIFER, OKLAHOMA

Thesis Approved:

Dr. William F. McTernan
Thesis Co-Advisor

Dr. Avdhesh K. Tyagi
Thesis Co-Advisor

Dr. Gregory G. Wilber

Dr. A. Gordon Emslie
Dean of the Graduate College

## ACKNOWLEDGEMENTS

I wish to thank members of my committee for their support and patience, Dr. William F. McTernan, Dr. Avdhesh K. Tyagi, and Dr. Gergroy W. Wilber. Their valuable comments and contributions strengthen this thesis. I would like to take this opportunity to thank Dr. Avdhesh K. Tyagi for providing the financial assistance in the form of research assistantship. The financial support was provided by the city of Enid and the Oklahoma Department of Transportation. I am very grateful and forever indebted to professor Dr. William F. McTernan for his endless support and guidance. Working with him has been a great pleasure for me. I would also like to thank Dr. Gregory G. Wilber for his time, valuable comments and support as a committee member.

I cannot finish without saying how grateful I am with my family. I wish to thank my parents for their love. Most importantly, I would like to thank my brothers Nabin Poudyal and Prabin Poudyal for their love and support in every moment of my life. I would also like to express my warmest thanks to my fiancé Kabindra Joshi for his love and encouragement.

Finally, I would like to thank my invaluable friends Moti K.C. and Roji Manandhar for their help.

## TABLE OF CONTENTS

**Chapter** **Page**

## LIST OF FIGURES

**Figure** **Page**

**Figure** **Page**

**Figure** **Page**



..

## LIST OF TABLES

**Table** **Page**

CHAPTER 1

# INTRODUCTION

## 1.1 Introduction

Groundwater provides approximately 19% of total water consumed in United States (Solley et al., 1998). Generally groundwater is a safe source of drinking water; however, numerous contaminants can render groundwater unsuitable for human consumption. Nitrogen (N), particularly in the form of nitrate ($NO_3$) is the most common groundwater pollutant found in United States (Postma et al., 1991). Several studies showed high association between agriculture and nitrate concentration in groundwater (Mueller et al., 1993; Ryker and Jones, 1995; Ling and El-Kadi, 1998; Shrestha and Ladha, 2002). The Midwestern United States has been identified areas of high nitrate vulnerable areas which also includes north-west Oklahoma (Bukart and Stoner, 2002; Nolan et al., 1999). Highly permeable soils, shallow well depths and intensive fertilizer application are key factors associated with high nitrate levels in this area (Bukart and Stoner, 2002).

Agricultural activities are the main non-point sources of nitrate. When the total nitrogen input exceeds the amount used by plants, nitrate accumulates in the soil and leaches to the underlying aquifer. Nitrate is highly soluble in water and easily moves with water through the soil profile. Landfill leachate, and septic tank effluents are most

frequently reported point sources of nitrate. Private septic system processes serve approximately one quarter of all households in the United States (US Bureau of the Census, 1993). Ammonia is a typical form of nitrogen that is released from septic tanks, but nitrification in the vadose zone can convert ammonia to nitrate, which can leach into groundwater (Makowshi, 2006). Earth's atmosphere consists of 78% nitrogen gas. Naturally occurring nitrate may also cause groundwater nitrate contamination. During lightning storms, atmospheric nitrogen is converted to nitrate and deposited in the soil through precipitation. The infiltrating rainwater can transport the nitrate to the shallow groundwater above the acceptable level for drinking water (Faris et al., 2000).

Nitrate is non-volatile inorganic compound which is highly soluble in water. As nitrate has become one of the common sources of groundwater contamination, its remediation from the drinking water is of key concern. Chlorination, the most common water treatment method, can not remove nitrate from water, however, it may prevent nitrates from being reduced to the toxic nitrite form (Bergsrud et al., 1992). The biological dentrification process is a process which converts nitrate to harmless nitrogen gas (William, 2007). However, biological denitrification process also suffers from several drawbacks including difficulties in maintaining a viable culture of bacteria, high cost of chemicals to maintain the bacterial culture, and unpredictable reaction rates (Murphy, 1997). Reverse osmosis, ion exchange, and electrolysis are several other processes that are currently employed in nitrate removal. However, disposal of the reject water is a major expense and environmental issue related with these processes. Therefore, protection of wells and wellfields from nitrate contamination by the identification and

eventual removal by reduction of potential contaminant sources is more effective action rather than groundwater contaminant remediation.

Identification of unknown contaminant sources, a critical issue in environmental management and regional assessment of ground water quality, is made difficult by the fact that nitrogen sources are spatially distributed (Tesoriero and Voss, 1997). Numerical flow and transport models are extensively used to simulate the fate and transport of nitrogen in soils and groundwater. These models provide valuable information for planning remediation strategies and long term monitoring designs (Li et al., 2006) but there are many fundamental difficulties associated with developing them (Almasri and Kaluarachchi, 2004). The key difficulties are:

- the models are highly data intensive and the data are generally not available and costly to obtain,
- the development of these models require detailed characterization of the study area including the physical, chemical, and biological processes when such processes are not fully known (McGrail, 2001),
- in order to simulate multiple scenarios, these models often require fine spatial and temporal discretization that involves substantial computational resources (Morshed and Kaluarachchi, 1998b and McGrail, 2001), and
- with these forward models it is difficult to identify the source and to solve the problem in inverse direction.

The inverse problem is often ill-posed (Skaggs and Kabala, 1994; Liu and Ball, 1999; Mahinthakumar and Sayeed, 2005) because it is extremely sensitive to errors in the measurement data (Li et al., 2006). To overcome these difficulties in contaminant source

identification, a number of methods have been developed such as geostatistical modeling, nitrogen isotopes tracers (Masoner and Mashburn, 2004), nonlinear optimization modeling (Aral et al., 2001), and dynamic optimization modeling (Liu et al., 2006) among others. Use of artificial neural networks (ANN) is another approach to identify the groundwater contaminant source (McTernan and Bonnet, 2002, Li et al., 2006; Singh et al., 2004).

ANN is a powerful tool which builds a model with a combination of linear and non-linear equations which it formulates as it attempts to link the output data with input data. ANN may be successfully used in a variety of applications because it has ability to "learn" from examples. ANN has found use in successfully determining the spatial distribution of nitrate in an aquifer, and it can also simulate the management alternatives that aim at reducing the groundwater nitrate concentration below maximum contamination level (MCL) by reducing the surface ground nitrogen loading (Almasri and Kaluarachchi, 2005). In addition to that, neural conditional simulations are stochastic tools that define probability of occurrence of output predicted as well as model uncertainties.

## 1.2 Problem statement

Groundwater in the Cimarron River Alluvial Terrace Aquifer is an important economic resource for northwest Oklahoma. Ninety percent of the drinking water requirement for the city of Enid and its surrounding area in Oklahoma is satisfied by Cimarron River Alluvial Terrace Aquifer (KC, 2007). According to the pumpage data provided by the city of Enid, more than 3 billion gallons of groundwater annually are

pumped from the aquifer. In spite of being the main water supply source, previous studies have identified large number of wells and wellfields in this aquifer contaminated with nitrate (Becker, 1994; Maoner and Mashburn, 2004; KC, 2007).

Thirty-one percent of groundwater samples collected from the Cimarron Terrace Aquifer from 1985 to 1993 had nitrate ($NO_3$-N) concentration above the MCL (Becker, 1994). Similarly, a study conducted by USGS and DEQ (2003) showed that 38% of total samples collected in Cimarron Terrace Aquifer had nitrate ($NO_3$-N) concentration in the range of 10.0mg/L to 31.8mg/L (Maoner and Mashburn, 2004). The City of Enid has also performed sampling of four public supply wellfields, Cleo Spring, Ringwood, Ames and Drummond, located at in the central part of the aquifer. A total of 821 samples were collected from 1997 to 2005. Figure 1-1 shows the time series of nitrate ($NO_3$-N) concentration during the sampling period. The average nitrate in the aquifer showed an increasing trend from 1997 to 1999, decreasing trend from 1999 to 2000, again increasing from 2000 to 2002 and fairly constant after 2002 (KC, 2007).

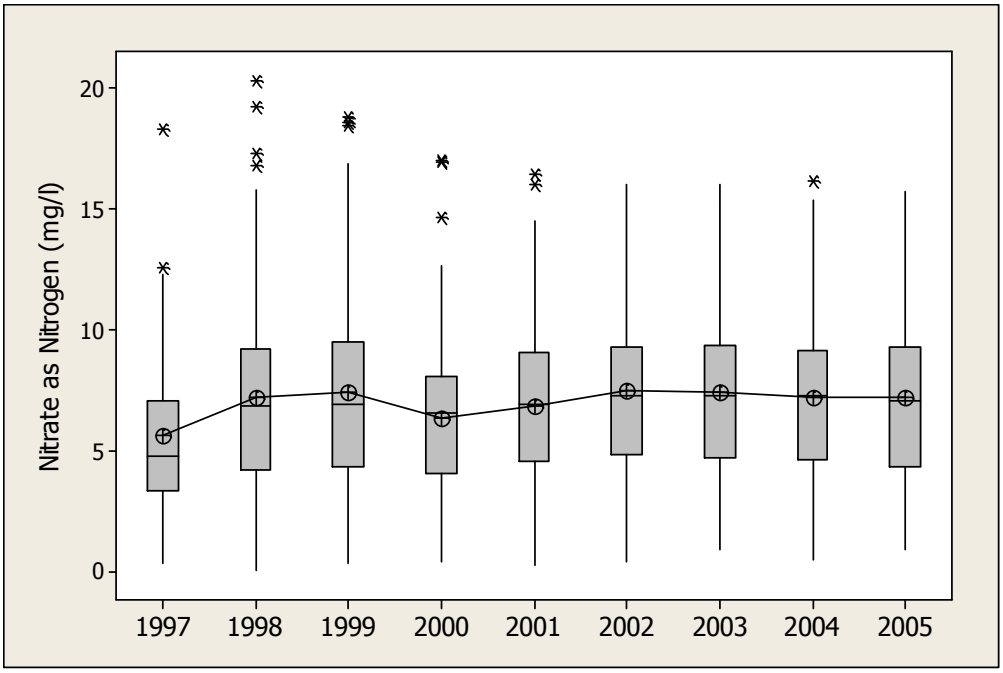


**Figure 1-1. Time series of $NO_3$-N concentration in the Cimarron Terrace Aquifer (KC, 2007)**

The U.S. Environmental Protection Agency (US EPA) has established a Maximum Contaminant Level (MCL) of 10mg/L nitrate-nitrogen ($NO_3$-N) as drinking water criteria (EPA, 1996). Excess levels of nitrate in drinking water are especially problematic in infants because they can cause blue baby syndrome, methemoglobinemia (Weyer, 2001). Methemoglobin is a form of hemoglobin in which the heme iron is reduced to its ferric state ($Fe^{2+}$) and is unable to deliver oxygen (Avery, 1999). Methemoglobinemia results when amounts of methemoglobin in the blood become high, usually 15% of the total circulating hemoglobin (Avery, 1999). Nitrate ingestion is also linked with other health problems such as adult brain and central nervous system tumors, spontaneous abortion, insulin dependent diabetes, and non-Hodgkin lymphoma (Weyer, 2001).

Identification of groundwater nitrate distributions and their probable sources is important for water resources managers and local residents to better protect the water supplies. A primary aim in this study was to extend the closely clustered monitoring data over aquifer space and time. Kriging is a common method of interpolation of concentration point data over space. The semi-variograms of the kriging define the spatial variability of the data. Neural kriging is one of the emerging techniques to extend the monitoring data over space and time (Koike et. al., 2002; Rizzo and Dougherty, 1994; Spichak, 2006). Neural kriging is data-driven and requires no estimation of a covariance function (Rizzo and Dougherty, 1994). The extension of monitoring data in the overall aquifer provides the picture of high nitrate concentration locations and its trend over the study period. Each of the four wellfields in the Cimarron Terrace Aquifer was also modeled separately to determine the pattern of nitrate distribution at those locations.

Another step in this research was to integrate the critical geophysical variables to predict the nitrate concentration in each wellfield. Nitrogen application rates, developed land, percent of clay, and groundwater depth have previously been found to be the four most significant variables that influence nitrate concentration in Cimarron Terrace Aquifer (KC, 2007). Among the most significant variables, surface nitrogen application rate was used as input to predict the nitrate concentrations in the aquifer in this research. A Geographic Information System (GIS) which integrates the National Land Cover Database (NLCD) was used to determine the land use patterns and corresponding nitrogen application rate. A management alternative model was then developed to address options needed to reduce the groundwater nitrate concentration below the MCL. In

addition to this, this research also focused on stochastic (conditional simulation) modeling to define the probability of occurrence of predictions made.

## 1.3 Objectives of study

Groundwater nitrate contamination has become a common problem worldwide. Remediation of contaminated groundwater is always difficult and costly. In order to protect the groundwater, a determination of spatial distribution of contaminant is most important. Following are the specific objectives of this study:

1. Develop a neural kriging model to estimate the spatial nitrate distribution over the entire Cimarron Terrace Aquifer.
2. Develop the neural kriging method to estimate the spatial nitrate distribution in each city of Enid four wellfields.
3. Determine the management alternatives to reduce the groundwater nitrate concentrations below the MCL.
4. Address the probability of occurrence of predicted nitrate concentrations using stochastic conditional simulation.

CHAPTER 2

# STUDY AREA DESCRIPTIONS

## 2.1 Location of study area

The Cimarron Terrace Aquifer is located in northwestern Oklahoma, extending from Freedom to Guthrie as illustrated in Figure 2-1. The aquifer underlies portions of 8 counties of northwest Oklahoma, namely: Woods, Woodward, Alfalfa, Major, Garfield, Blaine, Kingfisher, and Logan. This aquifer consists of 1305 square miles of area underlain by quaternary alluvial, terrace, and dune sand deposits (Adams and Bergman, 1996). The Cimarron Terrace Aquifer lies within the Cimarron River watershed, which has a drainage area of approximately 18,927 square miles (Adams and Bergman, 1996).

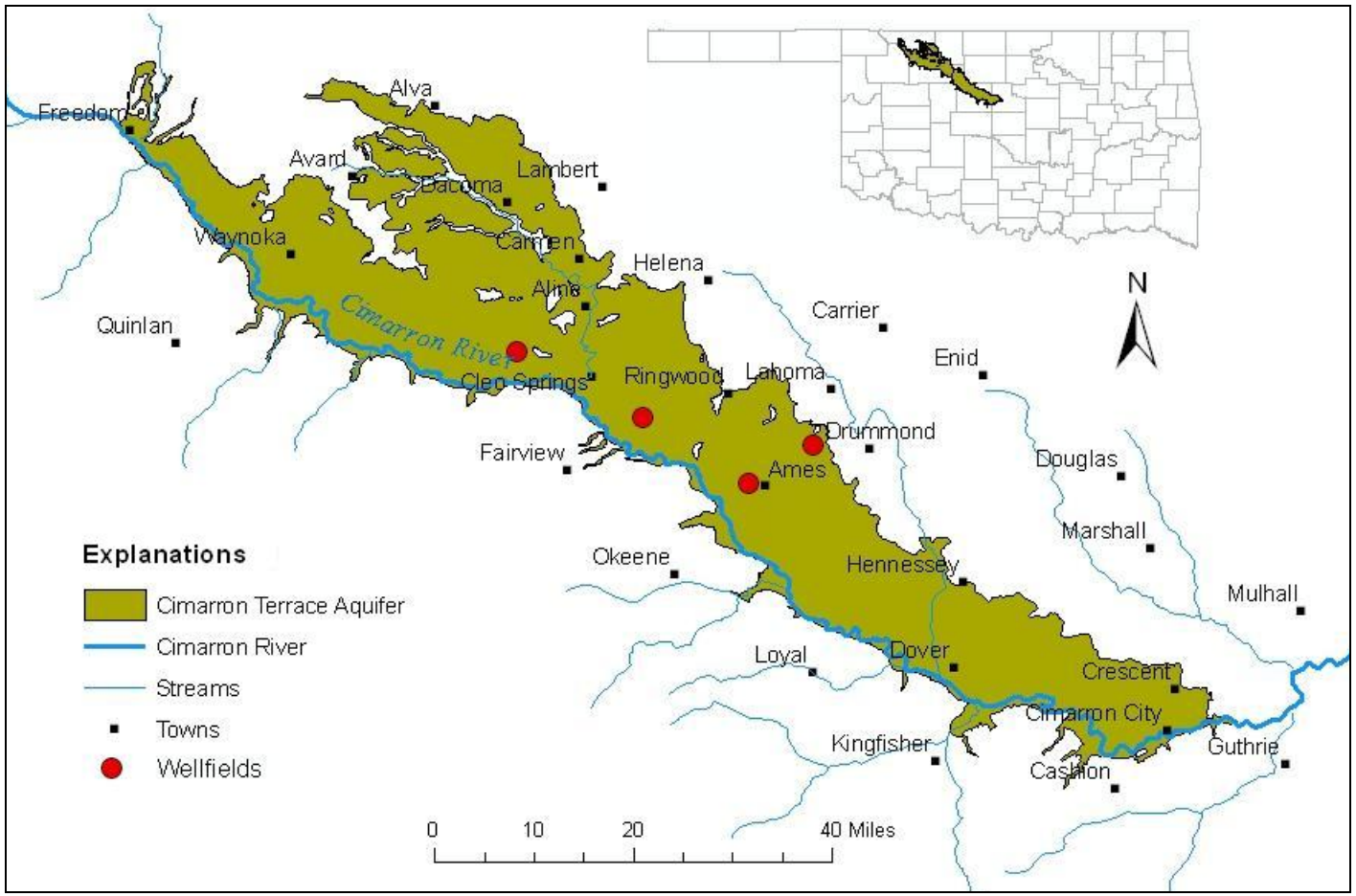


**Figure 2-2. Location map of Cimarron Terrace Aquifer**

## 2.2 Geology

The quaternary alluvial, terrace, and dune sand deposits unconformably overlie the Permian geologic units in Cimarron Terrace Aquifer (Adams and Bergman, 1996). Alluviums in the Cimarron Terrace Aquifer were originally deposited by the southward migration of the ancestral Cimarron River (Adams and Bergman, 1996). The thickness of alluvium deposits ranges from 0 to 50 feet (Adams and Bergman, 1996). The terrace deposits consists of interfingering lenses of clay, sandy clay, and cross-bedded poorly sorted sand and gravel and its thickness varies from 0 to 120 feet (Adams and Bergman, 1996). These terrace sediments have been reworked by water and wind that created sand dunes (Masoner and Mashburn, 2004) up to 70 feet in height. The Permian geologic units, also referred as red bed, in the aquifer are composed of a thick sequence of red shales, fine grained sand-stones, siltstones, dolomite, gypsum, and salt beds (Morton, 1980; Bingham and Bergman, 1980; Bingham and Moore, 1975; and Carr and Bergman, 1976).

## 2.2 Groundwater hydrology

Regional groundwater flow is generally southeast to southwest towards the Cimarron River, except flow direction is influenced by perennial tributaries to the Cimarron River. However, in the northeastern boundary groundwater is flowing away from the Cimarron River and its perennial tributaries to the northeast out of the aquifer (Adams and Bergman, 1996). Regionally, the aquifer is an unconfined aquifer, although it may be confined locally by silt and clay layers (Adams and Bergman, 1996). Over the 1985-1986 period the saturated thickness of the aquifer range from 0 to more than 100

feet, averaging 28 feet (Adams and Bergman, 1996). The regional average groundwater gradient is 0.0035 feet/feet (Reely, 1992). Pump tests on the alluvium and terrace deposits were conducted by Reed et al. (1952) and Engineering Enterprises (1977, 1983) in 23 selected wells. Based on the pumping test results, transmissivity of the aquifer was estimated from 603 $ft^2$/day to 10,184 $ft^2$/day, hydraulic conductivity from 15 feet/day to 542 feet/day, and specific yields from 0.0016 to 0.39 (Adams and Bergman, 1996). Deep percolation of precipitation, irrigation return flow, and subsurface inflow through alluvium are the main sources of recharge to the aquifer (Adams and Bergman, 1996). Seeping water from the aquifer into the Cimarron River and its perennial tributaries is the main discharge from the aquifer (Adams and Bergman, 1996).

## 2.3 Land use

Figure 2-2 shows the National Land Cover Database (NLCD) grid overlying the Cimarron Terrace Aquifer in 2001. Agricultural lands, referring to areas that have been planted or are intensely managed for the production of livestock for food, are the predominant land use in the study area (Masoner and Mashburn, 2004). Among the 46.86 percent of total agricultural land use, 46.54 percent was cultivated crops and 0.32 percent was pasture and hay. Additional land use types in the study area in 2001 were grassland (41.09 percent), developed areas (5.11 percent), shrublands (0.08 percent), and forests (4.25 percent). In comparison with the 1992 NLCD, agricultural land use decreased from 55.21 percent to 46.86 percent in 2001. Due to the development of modern irrigation systems, cultivation of small grains has changed to production of cultivated crops in the 1992 to 2001 interval (KC, 2007). Increased agricultural activity required high nitrogen

application on the agricultural field and consequently produced more threat of increasing nitrate concentration in the underlying aquifer.

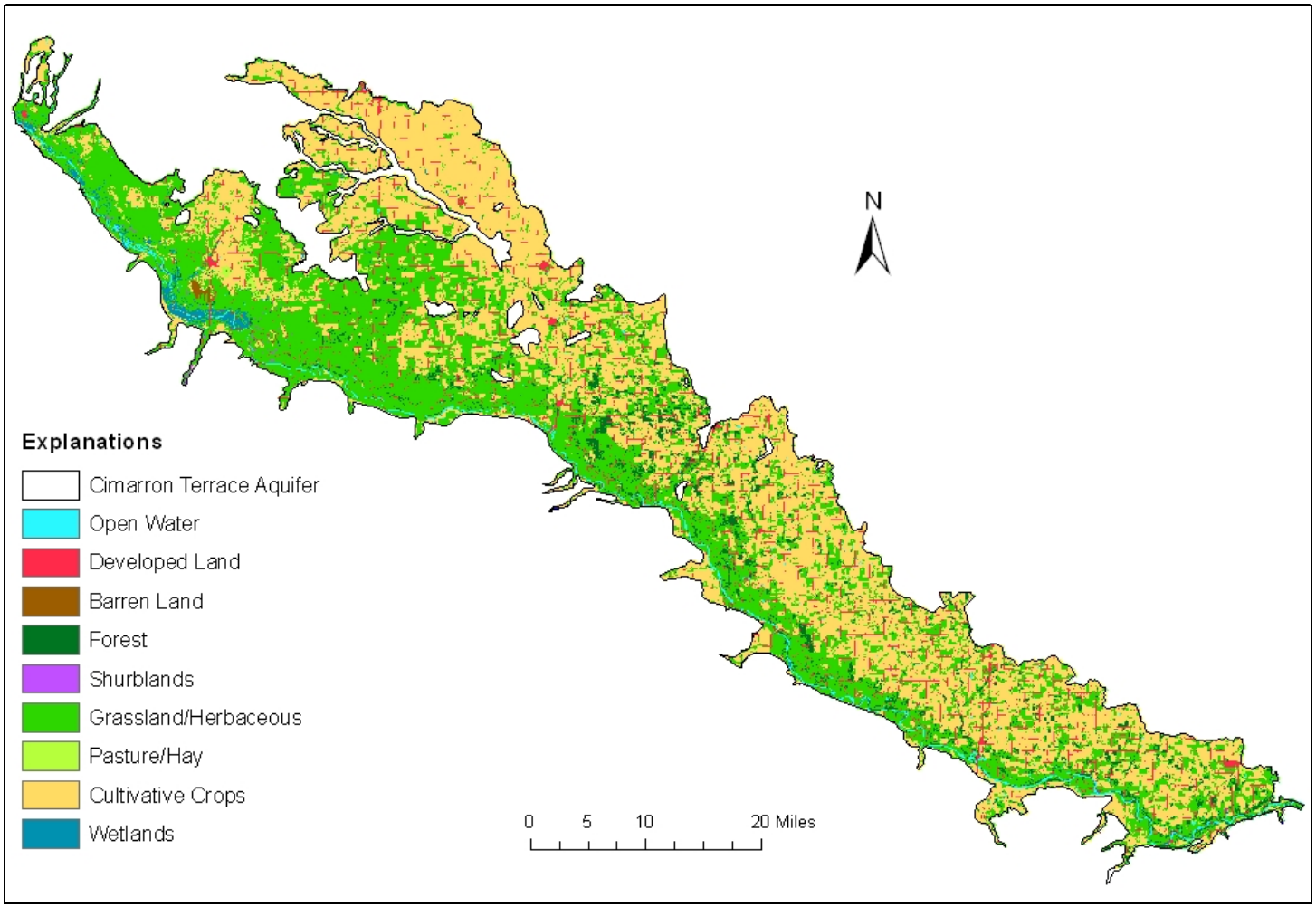


**Figure 2-3. Major land-use determinations from 2001 NLCD**

CHAPTER 3

# NEURAL NETWORKS

## 3.1 Introduction

The human brain is composed of a highly interconnected set of approximately $10^{11}$ neurons (Hagen et al., 1996). Each neuron is composed of three principal components: the dendrites, the cell body (soma and nucleus), and the axon, as shown in Figure 3-1. The dendrites are treelike extensions which are receptors carrying information in the form of electric signals generated by other neurons. The cell body joins the signals from the dendrites and passes on to the axon. The axon (elongated fiber), transmits the neural signal to the cells. The axon transmits the output from each cell to the dendrites of other cells over a bridge called a synaptic junction. The communication over synaptic junction is a complex chemical process and depends on the strength of incoming and outgoing signals (Kumar, 2000). The massive interconnection between neurons and the complex chemical process of communication over synaptic junctions establishes the functioning of biological neural networks (Hagen et al., 1996).

Neural network models are computer architectures based on theories of the human brain. Analogous to the human brain, artificial neural networks work with the interconnected group of artificial neurons. Besides the structure, the similarity between the human brain and neural networks is an ability to “learn” from a phenomenon

and adapt their behavior based on thus learning (Rogers et al., 1995). The neurons in the neural network models are developed by computer algorithms. The iterative computer algorithms are used to develop a combination of linear and non-linear equations for modeling real world complex situations (Kumar, 2000). These computer based models are called artificial neural networks (ANN).

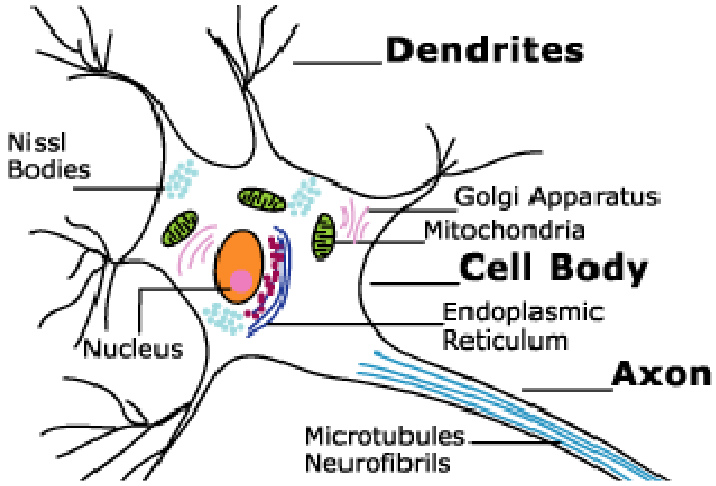


**Figure 3-1. Schematic drawing of biological neuron**
Source: (http://understanding_ocd.tripod.com/ocd_neurons_serotonin.html)

## 3.2 Artificial neural networks

While artificial neural networks are less intricate than the human brain, they exhibit a close correspondence with their biological counterparts because of two key characteristics. Both biological and artificial neural networks use computational devices to process input signals and outputs. The computational devices are highly interconnected and thereby able to model and understand complex situations. Secondly, the behavior of synaptic junctions (interconnection between neurons) in processing the information

determines the functionality of both structures (Hagan et al., 1996). The strength of synaptic junctions are called weights in ANN terminology and "the computational power of the neural network lies the interconnection weights that designate the strength of a node to produce the output at the node to which it is connected (Basheer et al., 1996).

An ANN is a universal approximator and nonlinear in nature (Singh and Datta, 2006). From a mathematical viewpoint it may be helpful to think of artificial neural networks (ANNs) as "nonparametric, nonlinear regression techniques" (Rogers et al., 1995). As opposed to traditional data analysis techniques, where a model is initially selected and then appropriate data are applied, an ANN infer solutions from the data presented to them, often capturing quite subtle relationship (Aggarwal and Song, 1997). This is possible with neural nets because of their ability to "learn" and then apply this learning in a generalized sense to similar situations. In this adaptive learning approach the net undergoes the training process and learns the significance of all data values, which include peaks and plateaus. A neural network not only assigns a significance (or weight) to the magnitude of each relationship among all data points. As more training is executed, a neural network can make better predictions. Consequently the precision with the network can make predictions also increases (Kumar, 2000).

The neural network software "Neuralyst" developed by Cheshire Engineering (1994) was used in this research effort. Neuralyst operates as an Excel add-in and employs the back propagation algorithm. Figure 3-2 illustrates the structure of three layer back propagation algorithm neural model. The input layers describe the problem of concern and the number of input neurons is the number of input variables used to define the problem. The output layer collects the information from the neural processing in the

input and hidden layers and gives a response. As shown in the figure, each layer has all its inputs connected to either a preceding or inputs from the external world, but not with the same layer.

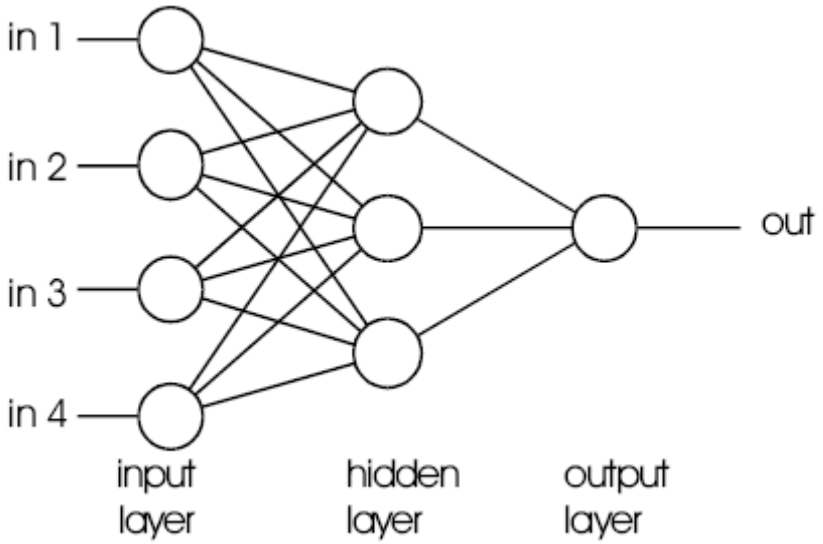


**Figure 3-2. A three layer, four neuron-input layer, three neuron-hidden layer back propagation neural network model**
(Cheshire Engineering, 1994)

Figure 3-3 shows the operation of ANN where the basic processing element of an ANN is the neuron and it performs its work by two basic processes: (i) internal activation; and (ii) activation function. These two processes are described by following equations:

$$Uj = \sum (Xj * wij) \quad \text{.....(1)}$$

$$Yj = Fth(Uj + tj) \quad \text{.....(2)}$$

Every neuron $\boldsymbol{j}$, takes inputs from all the $\boldsymbol{i}$ neurons connected to it. Each input $\boldsymbol{X_i}$, from the input layer is multiplied to a weight, $\boldsymbol{w_{ij}}$. The weights are constantly updated after being randomly assigned initially. Internal activation sums up all weighted inputs

together, resulting the internal value, $U_j$ which is defined as scalar product of the weight and input vector (Zurada, 1997). The internal value, $U_j$, is then biased by a previously established threshold value, $t_j$, and sent through an activation function, $F_{th}$. A typical activation function is sigmoid function. The resulting output, $Y_j$, from the activation function is the neural network response for the given input.

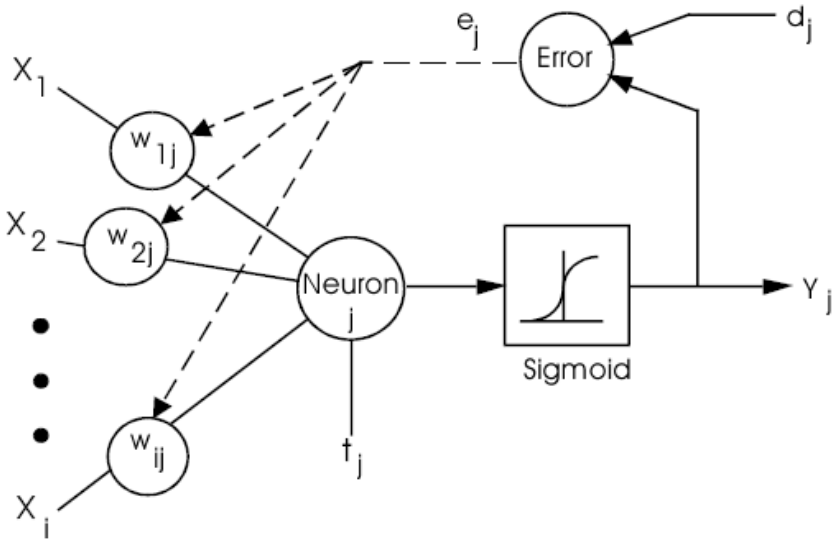


**Figure 3-3. Schematic diagram of neural network operation**
(Cheshire Engineering, 1994)

The process of internal activation and transfer function is repeated several times until the network can produce outputs within a user-specified tolerance. This occurs when the network reaches a plateau in its learning and further runs do not improve its performance (Kumar, 2000). The entire process of repeatedly modifying network weights is called training. Training of an ANN is thus equivalent to performing a minimization procedure of error criterion or calibration in a classic mathematical modeling sense.

The error is called root mean square error (RMS) and it is the sum of the squares of the difference between actual and desired outputs in each of neurons in output layers

and can be expressed as function of the connection weights (McTernan and Bonnett, 2002). A portion of RMS error is passed back through the hidden layers of the network to the input so that the connection weights on all pervious neurons can be altered in such a manner as to minimize the quadratic error between desired and actual outputs (Hagen et al., 1996).

The ANN's ability to learn in the training process defines the accuracy of model predictions. Learning in a multi-layer feed forward network with back propagation training algorithm is achieved in three phases:

- Structure the network, assign the initial random weights, forward feed- input training set, proceed through network from layer to layer applying weights, calculate output.
- Calculate total error as difference between actual output and desired outputs.
- Back propagate the error by passing back through net causing each connection weight to be refined.

In addition to the overall model configuration there are variety of parameters that had significant role in network development in this research. Within each model development, default values were used initially and if the results were not satisfying alternative values were employed over many trials. These tested parameters are listed below with brief description:

*Learning Rate (LR):* Learning rate determines the amount of weight adjustment to be made based on the error passed back. The learning rate did not seem to significantly affect the results therefore the default value of 1.0 was used.

*Momentum:* Momentum allows a change to the weights to persist for a number of adjustment cycles. The default value of 0.9 was used throughout the experiment because changing the momentum was not important to this experiment because we would have liked to have a significant portion of the impact of the old weights affect the newest weight. This minimizes the chance of the network becoming stuck in local minima of the error surface curve (Chim, 1996).

*Training Tolerance:* Training tolerance determines the how much training the neural network undergoes. Once all the training output falls within the target output, plus or minus the training tolerance, the network stops training and scores the output as "Right". Training tolerance does not have effect in learning algorithm. However, the training of network stops when it finds training outputs 100% "Right". The experiments showed that the training tolerance sometimes had to be raised from the default value of 0.1 to 0.27 in order to allow the neural network to finish training.

*Testing Tolerance:* Testing tolerance works in the same way as training tolerance, but for the testing data. It does not have an affect on the neural network results. It is just measure to determine whether or not all of the tested data fall within the specified error.

*Number of layers and number of neurons in hidden layers:* Various studies had recommended that 3 layers neural networks work best (Kumar, 2000; Kumar and DebRoy, 2006; McTernan and Bonnet 2000). Therefore, throughout the experiment 3 layers networks were used. The networks were tested with different number of neurons in the hidden layer in order to achieve best results.

*Initial Weights:* Initial weights are a very important factor in developing neural network models. Different sets of initial weights can significantly affect the results of the model.

In order to achieve more reliable results, tests were repeated for each model with different initial weights. The most frequently occurring results were taken as the final results.

*Activation Function:* Six activation functions: Sigmoid, hyperbolic, linear, Gaussian, augmented ratio, and step are available for the modeling in the neuralyst. The sigmoid function is the default transfer function and all the models in this research effort. Sigmoid function is the most popular function since it is non linear and differentiable (Mendil and Benmahammed, 1999).

# CHAPTER 4

# METHODOLOGY

## 4.1 Background

This chapter explains methods used in this study in order to address problems mentioned in Chapter 1. Artificial neural networks were used in this study effort. A spatial decremental approach was utilized to identify the groundwater nitrate distribution pattern in the overall Cimarron Terrace Aquifer to the individual wellfields in it. The method of determining spatial nitrate distribution using neural network models is called neural kriging (NK) (Rizzo and Dougherty, 1994). Constituent relationship models were developed to predict the nitrate concentration in wells of each wellfield with respect to on ground nitrogen application rate under existing conditions. Management alternatives were simulated with a constituent relationship model in order to predict decreased nitrate concentrations below the MCL. Finally, stochastic modeling was performed using neural conditional simulation to define the probabilities associated with the predicted nitrate concentrations by constituent relationship model for Ames wellfield.

## 4.2 Spatial models

Groundwater nitrate distributions were evaluated in this effort by developing 2D models. The method is known as neural kriging. In this study neural kriging was similar to ordinary kriging but required no estimation of a covariance function.

A neural kringing (NK) network was developed by dividing the entire aquifer into 1000m*1000m grids as shown in Figure 4-1. The grid system was developed in AutoCAD, imported in ArcGIS and projected in NAD_1983_ Albers coordinate system. The origin for NAD (North American Datum) of 1983 is the earth's center of mass. Albers Projection is a conic projection to represent the earth's surface.

A total of 2776 grids were developed and each grid was represented by (X, Y) coordinates. The identification described (coordinates) grid network was implemented in parallelizing algorithm, and applied in GIS to develop maps of discrete spatially distributed groundwater nitrate concentrations. This modeling approach was applied to the entire aquifer, sequentially to the critical central area of the aquifer, and in each of the four wellfields.

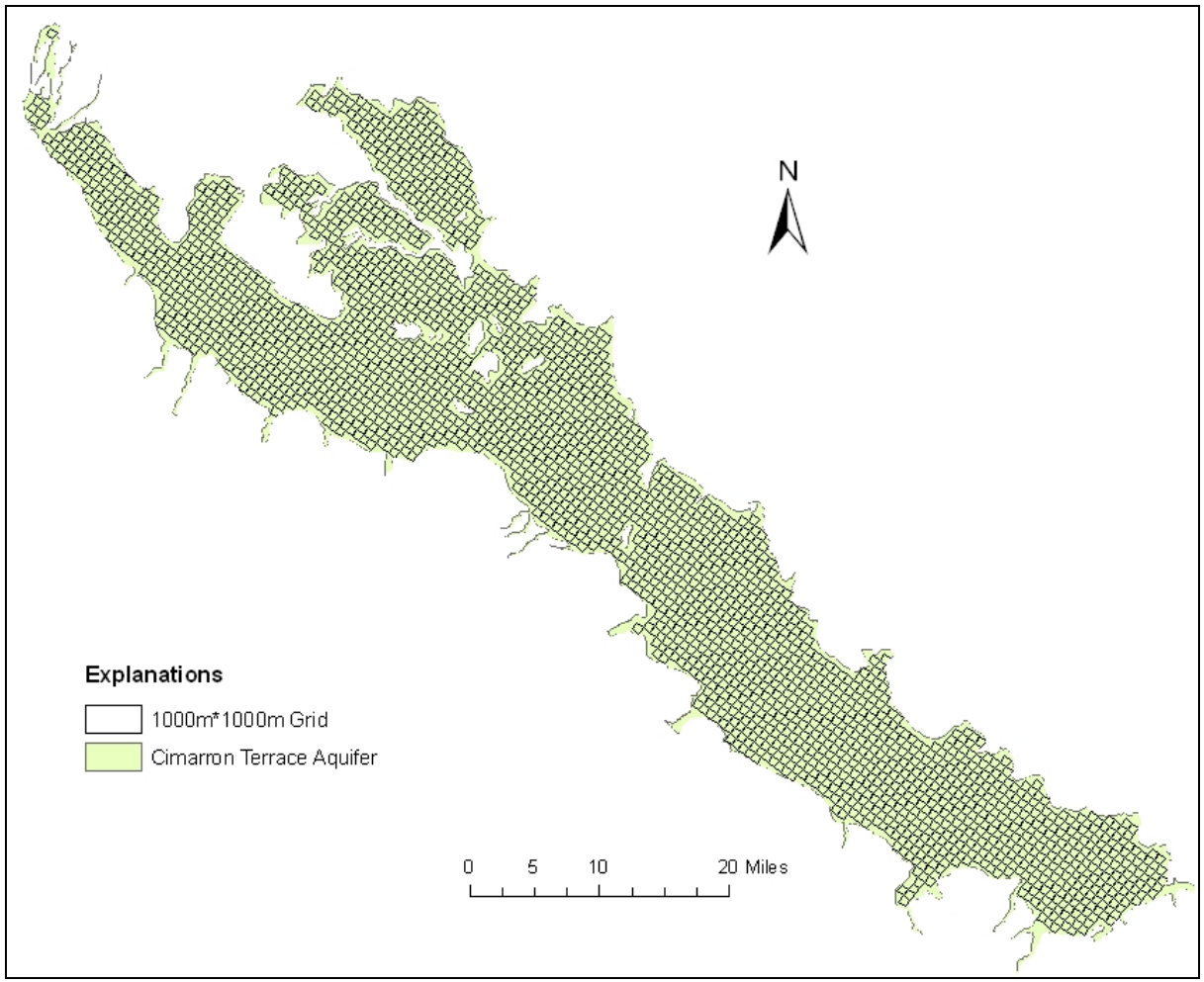


**Figure 4-1. Cimarron Terrace Aquifer with ANN 1000m*1000m grid coordinate system**

### 4.2.1 Overall aquifer model

The city of Enid sampling data were available from 1997 to 2005. The samples were collected from highly clustered wells in four public supply wellfields, located in the central part of the aquifer. Those samples could not represent the nitrate distribution throughout the aquifer. In a study conducted by USGS in cooperation with the DEQ in 2003, an additional 45 private wells were sampled (Maoner and Mashburn, 2004). Figure 4-2 shows the box plot of 2003 nitrate concentrations in the four wellfields and in the USGS study wells. The plot shows that the range of nitrate concentration from USGS study wells was higher then that of from city of Enid wellfields. Nitrate concentration range in USGS study wells was observed from 0.06 mg/L to 31.8 mg/L. However, the plot shows that median nitrate concentration of 9.3 mg/L was observed in Ames wellfield which is the highest value among the city of Enid's four wellfields and the USGS study wells.

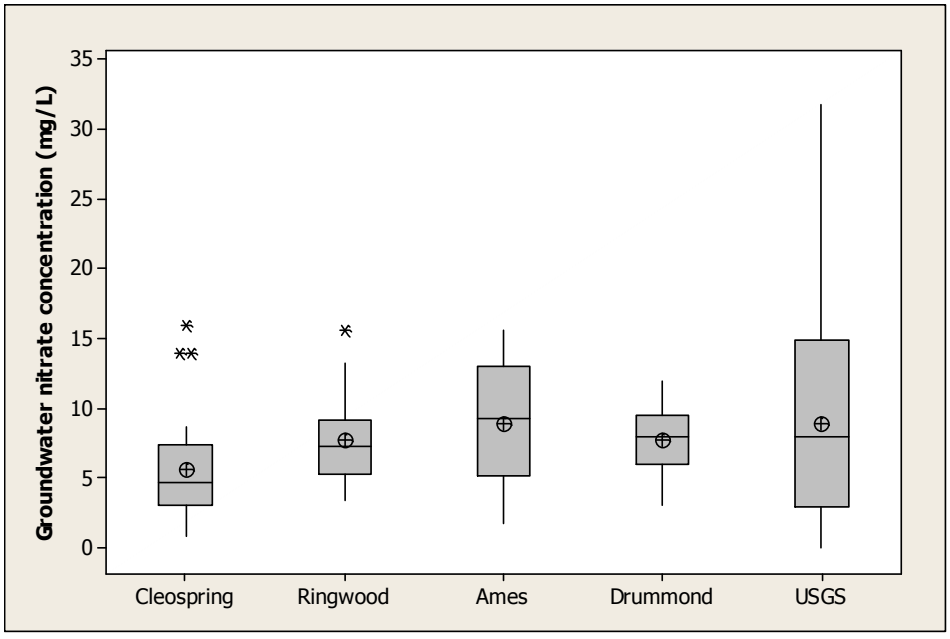


**Figure 4-2. Box plot of nitrate concentrations in city of Enid four wellfiels and in USGS study wells, sampled in 2003**

Figure 4-3 shows that USGS sampling wells were located throughout the aquifer. The first model developed for this effort integrated the 2003 nitrate concentration data from the four wellfields with the USGS data to develop an overall aquifer model of nitrate.

The critical factor in this study was the development of stable and reliable neural network models for making precise predictions. Each well in the study area was represented by the grid (X, Y) coordinates. The nitrate concentration in each well was then represented by the grid having the well in it. The mean value of multiple samples was used to represent the nitrate concentration in those grids which had more then one well. Using the grid coordinates, the entire aquifer was modeled to identify the nitrate distribution pattern. Grid (X, Y) coordinates were used as input. A total 96 nitrate concentration data points were used as the target values. Eighty percent of nitrate concentration data were used for training and 20 percent of randomly selected data were used for testing.

Table 4-1 presents the training and testing data sets for this overall aquifer model. In this table the training data sets are presented first and followed by the testing data sets. The first column in the table shows the identification of wells present in the grid represented by the (X, Y) coordinates presented in second and third column. Origin of the grid coordinates is the bottom left corner of the aquifer. The (X,Y) coordinates are the inputs for this mode. The fourth column presents the observed nitrate concentrations corresponding to the wells in the first column. In the case of multiple wells in a grid, a mean concentration was calculated. The model was trained to predict the nitrate concentrations presented in this column. The fifth column represents the predicted values

of nitrate concentrations after training and testing the data. The blank rows indicate the values before training and testing. The sixth column is known as "mode flag column" which categories the data sets into training and testing as designated in each row of the column.

**Table 4-1. Training and testing data sets for overall aquifer model**

| Well_ID | Input | | Target | Output | MF |
|---|---|---|---|---|---|
| | X-Cord | Y-Cord | $NO_3$_2003 (mg/L) | | |
| W1 | 15 | 9 | 9.37 | | TRAIN |
| W2 | 16 | 22 | 12.30 | | TRAIN |
| W3 | 7 | 36 | 2.19 | | TRAIN |
| W4 | 13 | 32 | 14.80 | | TRAIN |
| W5 | 10 | 43 | 16.80 | | TRAIN |
| W6 | 6 | 50 | 6.14 | | TRAIN |
| W8 | 15 | 48 | 6.93 | | TRAIN |
| W10 | 13 | 54 | 5.83 | | TRAIN |
| W12 | 14 | 61 | 9.01 | | TRAIN |
| W13 | 19 | 61 | 1.11 | | TRAIN |
| A5,W14 | 13 | 72 | 4.71 | | TRAIN |
| A4 | 14 | 72 | 6.80 | | TRAIN |
| A11,W15 | 15 | 71 | 14.50 | | TRAIN |
| A6 | 14 | 73 | 2.47 | | TRAIN |
| A7,A3 | 15 | 72 | 3.70 | | TRAIN |
| A8 | 15 | 73 | 3.60 | | TRAIN |
| A2 | 16 | 72 | 9.30 | | TRAIN |
| A9 | 16 | 73 | 1.80 | | TRAIN |
| D23 | 23 | 65 | 10.73 | | TRAIN |
| A23,A22,A20,W16 | 15 | 75 | 8.14 | | TRAIN |
| A29 | 14 | 77 | 9.40 | | TRAIN |
| A27,A24 | 15 | 76 | 8.20 | | TRAIN |
| A14 | 20 | 70 | 13.00 | | TRAIN |
| A25 | 15 | 77 | 13.40 | | TRAIN |
| A1 | 20 | 71 | 11.73 | | TRAIN |
| D12 | 22 | 69 | 5.43 | | TRAIN |
| D21,D20 | 24 | 67 | 8.07 | | TRAIN |
| D18,D1 | 25 | 66 | 6.27 | | TRAIN |
| A19 | 18 | 75 | 14.00 | | TRAIN |
| D3 | 24 | 69 | 8.50 | | TRAIN |
| D5 | 25 | 68 | 9.80 | | TRAIN |
| D33 | 24 | 70 | 6.00 | | TRAIN |
| D25 | 26 | 69 | 7.68 | | TRAIN |
| D27 | 27 | 70 | 6.90 | | TRAIN |
| D28 | 26 | 71 | 9.60 | | TRAIN |

**Table 4-1. (Continued)**

| Well_ID | Input | | Target | Output | MF |
|---|---|---|---|---|---|
| | X-Cord | Y-Cord | $NO_3$_2003 (mg/L) | | |
| W19 | 23 | 75 | 2.27 | | TRAIN |
| R28,W18 | 15 | 85 | 18.05 | | TRAIN |
| D29 | 26 | 72 | 9.30 | | TRAIN |
| W20 | 20 | 81 | 14.40 | | TRAIN |
| R22 | 14 | 90 | 4.20 | | TRAIN |
| R24,R18 | 15 | 89 | 4.28 | | TRAIN |
| R16,R17,R12,W21 | 15 | 90 | 5.31 | | TRAIN |
| R19,R14,R20 | 16 | 89 | 9.33 | | TRAIN |
| R21 | 17 | 88 | 13.25 | | TRAIN |
| R8,R13 | 16 | 90 | 8.33 | | TRAIN |
| R5 | 15 | 92 | 7.30 | | TRAIN |
| R6,R2,R3,R7 | 16 | 91 | 7.63 | | TRAIN |
| R4 | 17 | 91 | 8.35 | | TRAIN |
| W22 | 18 | 92 | 16.40 | | TRAIN |
| W24 | 17 | 97 | 8.03 | | TRAIN |
| W25 | 22 | 96 | 11.20 | | TRAIN |
| CS29,CS28,CS30,W26 | 16 | 104 | 3.36 | | TRAIN |
| CS10 | 13 | 108 | 8.70 | | TRAIN |
| CS17 | 14 | 107 | 8.40 | | TRAIN |
| CS2 | 11 | 110 | 1.25 | | TRAIN |
| CS25,CS26 | 16 | 105 | 2.33 | | TRAIN |
| CS5,CS3 | 17 | 104 | 5.63 | | TRAIN |
| CS8 | 13 | 109 | 4.60 | | TRAIN |
| CS19 | 15 | 107 | 3.20 | | TRAIN |
| CS22,CS21,CS20 | 16 | 106 | 10.65 | | TRAIN |
| CS4,CS1 | 12 | 111 | 3.83 | | TRAIN |
| CS27 | 17 | 105 | 1.80 | | TRAIN |
| CS12,CS9 | 14 | 109 | 6.10 | | TRAIN |
| CS18 | 16 | 107 | 16.00 | | TRAIN |
| CS23 | 17 | 106 | 3.90 | | TRAIN |
| W27 | 11 | 113 | 8.35 | | TRAIN |
| W29 | 27 | 96 | 0.95 | | TRAIN |
| W28 | 23 | 103 | 2.48 | | TRAIN |
| W30 | 12 | 120 | 14.90 | | TRAIN |
| W33 | 12 | 128 | 3.63 | | TRAIN |
| W35 | 18 | 126 | 1.24 | | TRAIN |
| W37 | 26 | 120 | 3.68 | | TRAIN |
| W36 | 13 | 136 | 0.37 | | TRAIN |
| W39 | 22 | 128 | 2.20 | | TRAIN |
| W39 | 22 | 128 | 2.20 | | TRAIN |
| W40 | 11 | 143 | 8.48 | | TRAIN |
| W45 | 43 | 136 | 17.90 | | TRAIN |
| W11 | 17 | 54 | 15.30 | | TEST |
| A21 | 15 | 74 | 10.70 | | TEST |

**Table 4-1. (Continued)**

| Well_ID | Input | | Target | Output | MF |
|---|---|---|---|---|---|
| | X-Cord | Y-Cord | $NO_3$_2003 (mg/L) | | |
| A18 | 18 | 73 | 14.80 | | TEST |
| A16 | 20 | 72 | 12.40 | | TEST |
| D2 | 23 | 69 | 8.20 | | TEST |
| A17 | 20 | 74 | 15.60 | | TEST |
| D6,D8 | 26 | 68 | 8.6 | | TEST |
| W17 | 22 | 74 | 21.3 | | TEST |
| R25,R27,R26 | 14 | 87 | 7.3 | | TEST |
| R15 | 14 | 91 | 5.3 | | TEST |
| R11,R10 | 15 | 91 | 6.7 | | TEST |
| R9 | 17 | 90 | 9.6 | | TEST |
| R1 | 16 | 92 | 7.4 | | TEST |
| W23 | 23 | 87 | 31.8 | | TEST |
| CS13,CS14 | 14 | 108 | 4.8 | | TEST |
| CS6 | 13 | 110 | 6.8 | | TEST |
| CS11,CS16,CS15 | 15 | 108 | 6.5 | | TEST |
| W31 | 4 | 131 | 0.1 | | TEST |
| W32 | 29 | 102 | 6.0 | | TEST |
| W34 | 23 | 115 | 15.6 | | TEST |

The model set in Table 4-1 was trained to establish the relationship between the grids coordinates and nitrate concentrations. Various networks were evaluated to make the best prediction. Different alternatives were tried by varying the network architecture until some consistency in results in terms of prediction accuracy and numbers of iterations were achieved. Finally, the best model was used to predict the nitrate concentrations at the locations where it was not measured. The best model finalization will be discussed in detail in results chapter.

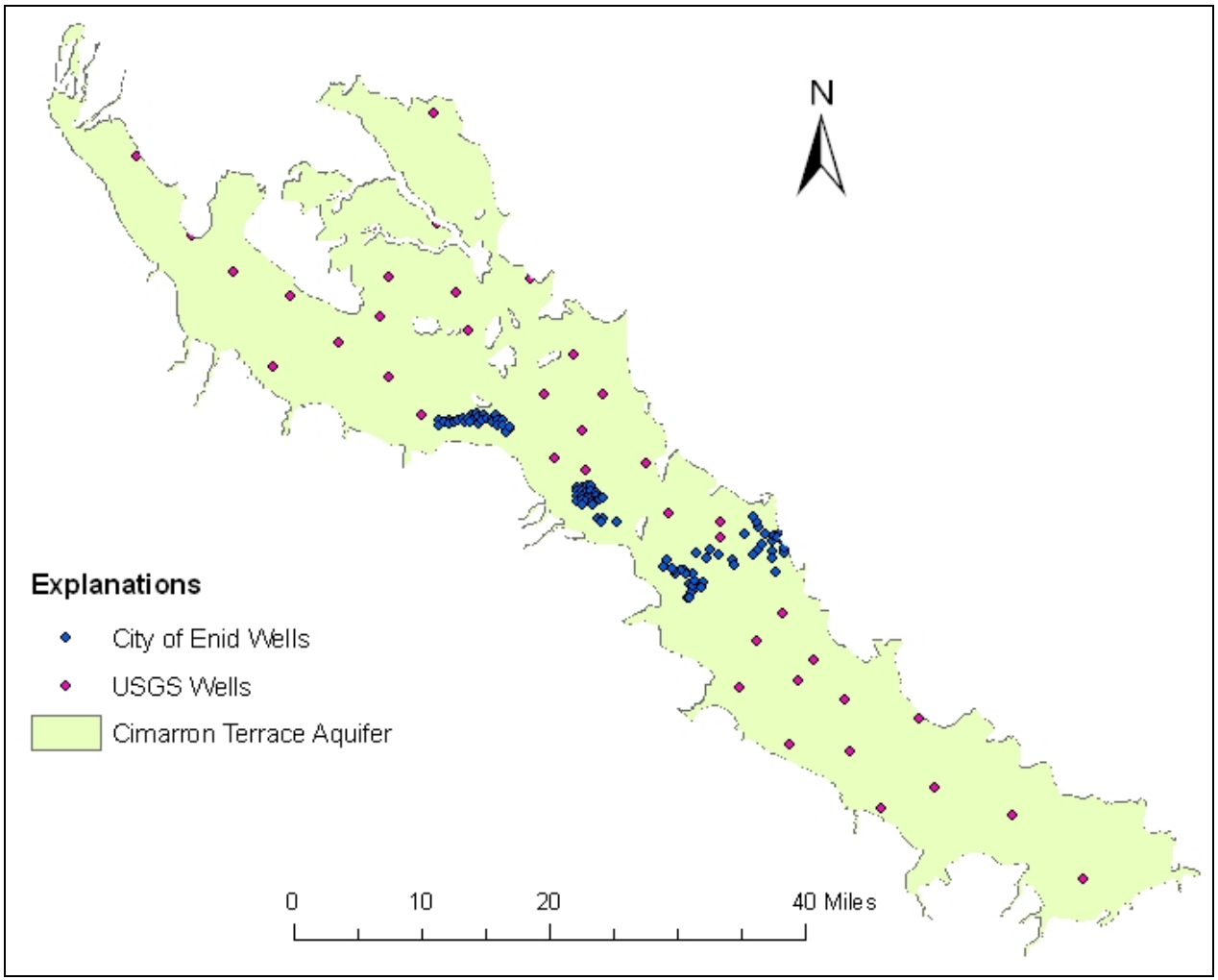


**Figure 4-3. Location of City of Enid sampling wells and USGS sampling wells**

### 4.2.2 Central area model

The modeling approach and grid size of this model was the same as used in the overall aquifer model but in this approach only the central area of the aquifer was addressed. Figure 4-4 shows this central area. The data sets used in this modeling effort were the city of Enid 2003 data set. The USGS data set was not used in this modeling effort to see how well nitrate concentrations can be predicted only with four wellfield data sets since the modeling area is smaller then the overall aquifer model. A total 92 wells were used for this model. Among them 20 percent were randomly selected for testing. Table 4-2 shows the training and testing data sets for the central area model. Data in Table 4-2 are arranged in the same way as in Table 4-1.

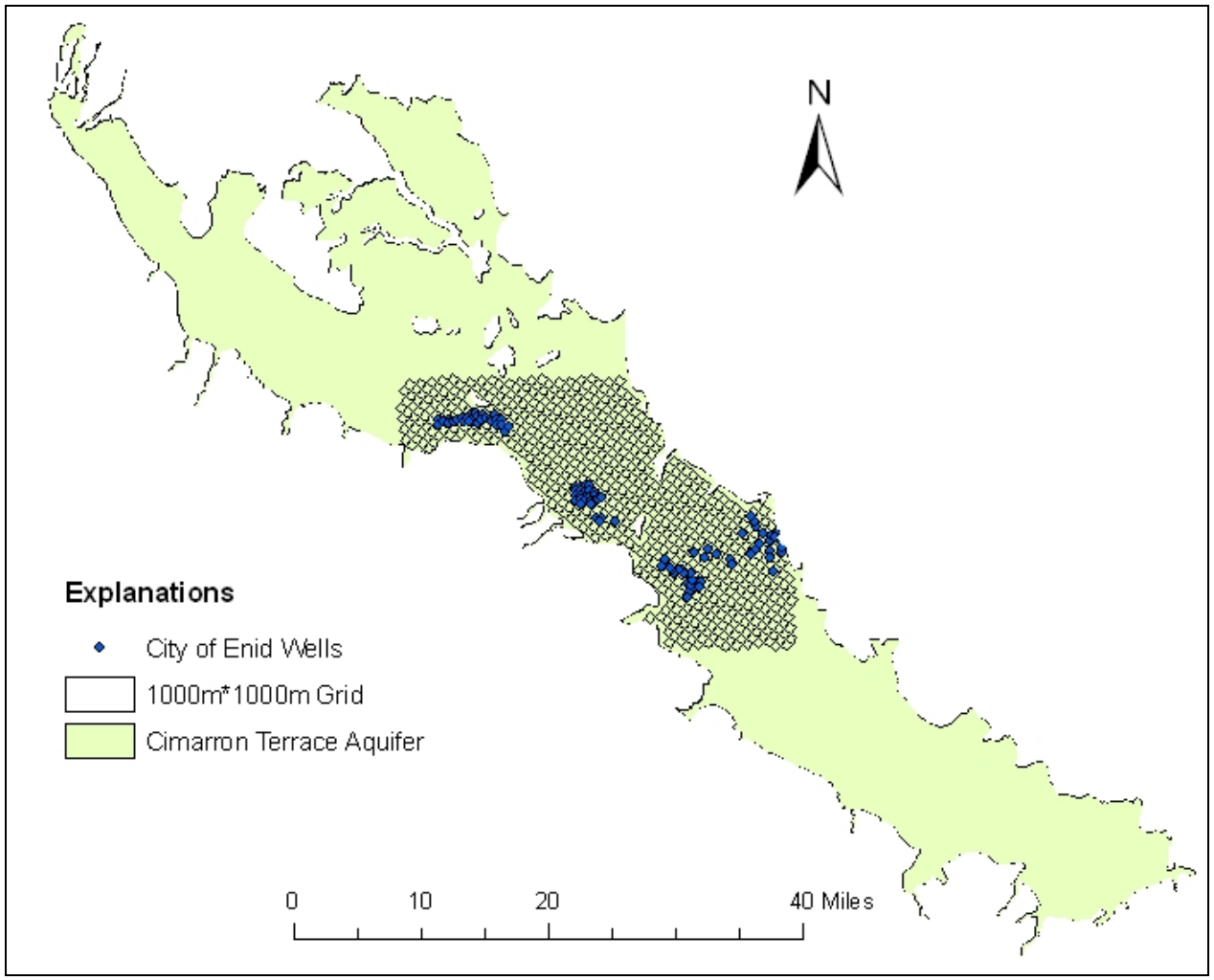


**Figure 4-4. Location of focused area in central area model**

**Table 4-2. Training and testing data sets for central area model**

| Well_ID | Input | | Target | Output | MF |
|---|---|---|---|---|---|
| | X-Cord | Y-Cord | $NO_3$_2003 (mg/L) | | |
| CS29 | 10 | 46 | 0.5 | | TRAIN |
| CS2 | 5 | 54 | 1 | | TEST |
| CS27 | 11 | 48 | 1.5 | | TEST |
| CS25,CS26,CS28 | 10 | 48 | 1.56 | | TRAIN |
| A9 | 10 | 16 | 1.8 | | TRAIN |
| A6 | 8 | 16 | 2.47 | | TEST |
| CS4,CS1 | 6 | 54 | 3.1 | | TRAIN |
| CS19 | 9 | 50 | 3.3 | | TRAIN |
| A8 | 9 | 16 | 3.6 | | TRAIN |
| A3,A7 | 9 | 15 | 3.7 | | TRAIN |
| CS23 | 11 | 49 | 4 | | TEST |
| R22 | 8 | 33 | 4.2 | | TRAIN |
| R24,R18 | 9 | 32 | 4.275 | | TRAIN |
| CS30 | 10 | 47 | 4.4 | | TEST |
| CS13,CS14 | 8 | 51 | 4.5 | | TRAIN |
| A5 | 7 | 15 | 5.2 | | TEST |
| R15 | 8 | 34 | 5.25 | | TRAIN |
| CS8 | 7 | 52 | 5.3 | | TRAIN |
| D12 | 16 | 12 | 5.43 | | TRAIN |
| CS5,CS3 | 6 | 53 | 5.5 | | TEST |
| CS12,CS9 | 8 | 52 | 5.95 | | TRAIN |
| D33 | 18 | 14 | 6 | | TRAIN |
| CS11,CS16,CS15 | 9 | 51 | 6.26 | | TRAIN |
| D18,D1 | 19 | 9 | 6.265 | | TRAIN |
| CS6 | 7 | 53 | 6.4 | | TEST |
| R16,R17,R12 | 9 | 33 | 6.51 | | TRAIN |
| R10,R11 | 9 | 34 | 6.725 | | TRAIN |
| A4 | 8 | 15 | 6.8 | | TRAIN |
| D27 | 20 | 13 | 6.9 | | TRAIN |
| R5 | 9 | 35 | 7.3 | | TRAIN |
| R25,R27,R26 | 8 | 30 | 7.31 | | TRAIN |
| R1 | 10 | 35 | 7.4 | | TEST |
| R6,R2,R3,R7 | 10 | 34 | 7.625 | | TRAIN |
| D25 | 20 | 12 | 7.68 | | TRAIN |
| A23,A22,A20 | 9 | 18 | 7.91 | | TRAIN |
| D21,D20 | 18 | 10 | 8.065 | | TRAIN |
| A27,A24 | 9 | 19 | 8.2 | | TRAIN |
| D2 | 17 | 12 | 8.2 | | TRAIN |
| R13,R8 | 10 | 33 | 8.325 | | TRAIN |
| R4 | 11 | 34 | 8.35 | | TRAIN |
| D6,D8 | 20 | 11 | 8.625 | | TRAIN |
| CS17 | 8 | 50 | 8.7 | | TRAIN |
| D3 | 18 | 12 | 8.85 | | TRAIN |
| CS10 | 7 | 51 | 9.1 | | TRAIN |

**Table 4-2. (Continued)**

| Well_ID | Input | | Target | Output | MF |
|---|---|---|---|---|---|
| | X-Cord | Y-Cord | $NO_3$_2003 (mg/L) | | |
| A2 | 10 | 15 | 9.3 | | TRAIN |
| D29 | 20 | 15 | 9.3 | | TRAIN |
| R19,R14,R20 | 10 | 32 | 9.33 | | TEST |
| A29 | 8 | 20 | 9.4 | | TRAIN |
| R9 | 11 | 33 | 9.6 | | TRAIN |
| D28 | 20 | 14 | 9.6 | | TRAIN |
| CS22,CS21,CS20 | 10 | 49 | 10.4 | | TRAIN |
| A21 | 9 | 17 | 10.7 | | TRAIN |
| A1 | 14 | 14 | 11.73 | | TRAIN |
| A16 | 14 | 15 | 12.4 | | TRAIN |
| A14 | 14 | 13 | 13 | | TRAIN |
| R21 | 11 | 31 | 13.25 | | TRAIN |
| A25 | 9 | 20 | 13.4 | | TRAIN |
| A11 | 9 | 14 | 13.6 | | TRAIN |
| A19 | 12 | 18 | 14 | | TRAIN |
| A18 | 12 | 16 | 14.8 | | TRAIN |
| CS18 | 10 | 50 | 15.4 | | TEST |
| R28 | 9 | 28 | 15.6 | | TRAIN |
| A17 | 14 | 17 | 15.6 | | TRAIN |

In this model, local grid coordinates were assigned for each grid by considering the origin at the bottom left corner of the focused area. Again, grid coordinates were used to predict nitrate concentrations in the central part of the Cimarron Terrace Aquifer. Different alternatives were evaluated by varying the network architecture until some consistency in results in terms of prediction accuracy and numbers of iterations were achieved. Finally, the best model was used to predict the nitrate concentration in each grid of the central area.

### 4.2.3 Individual wellfield spatial models

In order to identify groundwater nitrate distribution within individual wellfields in detail, the grid system was further divided into 200m*200m as shown in Figure 4-5.

Local grid coordinates were assigned and used for each of these models by considering the origin at bottom left of the individual wellfield.

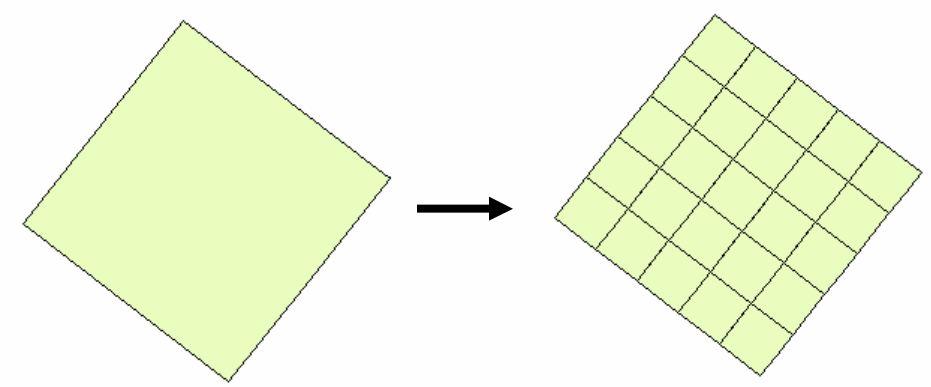

**Figure 4-5. Subdivision of 1000m*1000m grid to 200m*200m grid**

In this modeling effort, the city of Enid database for years 1997-2005 was used. The previously presented Figure 1-1 showed that the nitrate concentration increased from 1995 to 2005 with the exception of 2000. Therefore 2000 data were not included in this study. Among the eight yearly data sets, the 1998 and 2004 data sets were used for testing. Four individual wellfields models were developed in this effort:

- Cleospring wellfield model,
- Ringwood wellfield model,
- Ames wellfield model, and
- Drummond wellfield model.

#### 4.1.3.1 Cleospring wellfield spatial model

The point data of nitrate concentrations at well locations were used to identify the nitrate distribution pattern in the Cleospring wellfield. Figure 4-6 presents the area included in this model. The method employed was the same as was used in the overall aquifer and central area models, but a smaller grid and multiple years' data were used. A

total of 218 nitrate concentration data observed from 1997 to 2005 (except 2000) were used in this modeling. Among them the 1998 and 2004 data were used for testing and the rest for training. Table 4-3 presents the configuration of the Cleospring wellfield model where training datasets are presented first and then the testing data sets. First column of the table shows the year of data observation in wells presented in column two. Column 3 and 4 presents the (X,Y) coordinates of each grid and column 5 presents the nitrate concentration observed in each wells presented in the column 2 in the corresponding year presented in column 1. The results of the model after training and testing will be presented in the output column. The "mode flag" column defines the data points as training and testing.

Networks with varying architectures were executed until model predicted the consistent result in terms of prediction accuracy and time required to train the model. The model architectures and their performances are discussed in detail in results section. Finally, the most consistent model was determined as best model and it was used to predict the nitrate concentrations at the unmeasured locations.

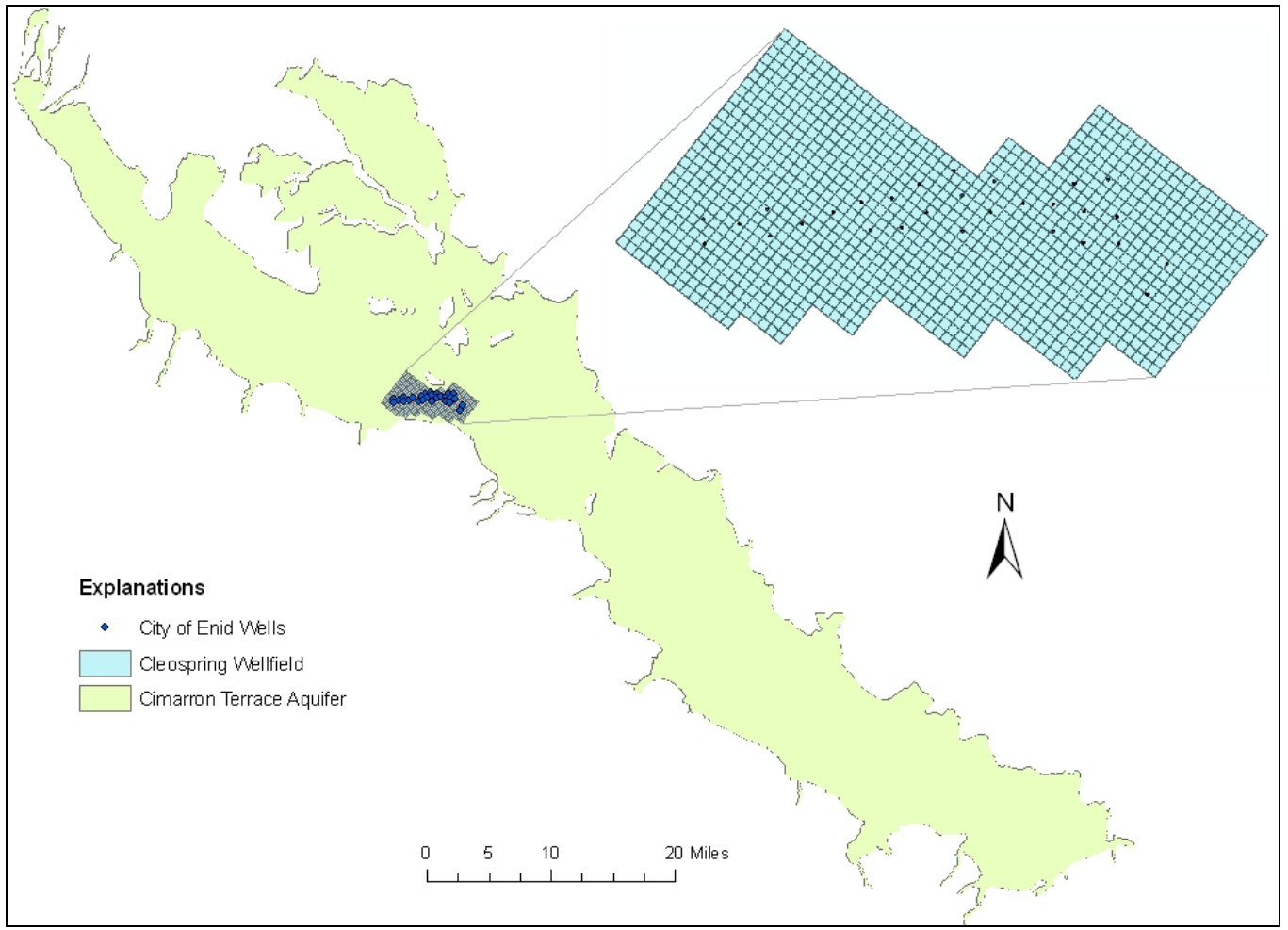


**Figure 4-6. Location of focused area in Cleospring wellfield model**

**Table 4-3. Training and testing data sets for Cleospring wellfield spatial model**

| Year | Well_ID | Input | | Target | Output | MF |
|---|---|---|---|---|---|---|
| | | X-Cord | Y-Cord | $NO_3$ (mg/L) | | |
| 1997 | C1 | 8 | 45 | 4.52 | | TRAIN |
| | C2 | 6 | 44 | 0.90 | | TRAIN |
| | C3 | 12 | 41 | 4.85 | | TRAIN |
| | C4 | 9 | 42 | 3.08 | | TRAIN |
| | C6 | 13 | 37 | 7.70 | | TRAIN |
| | C8 | 16 | 35 | 4.88 | | TRAIN |
| | C10 | 17 | 32 | 6.10 | | TRAIN |
| | C11 | 23 | 31 | 4.06 | | TRAIN |
| | C13 | 22 | 28 | 4.02 | | TRAIN |
| | C14 | 19 | 29 | 3.80 | | TRAIN |
| | C15 | 27 | 29 | 4.78 | | TRAIN |
| | C16 | 25 | 27 | 4.03 | | TRAIN |
| | C17 | 22 | 24 | 4.70 | | TRAIN |
| | C18 | 28 | 25 | 11.26 | | TRAIN |
| | C19 | 26 | 23 | 2.63 | | TRAIN |
| | C20 | 28 | 21 | 11.37 | | TRAIN |
| | C21 | 30 | 19 | 12.20 | | TRAIN |
| | C22 | 28 | 17 | 2.70 | | TRAIN |
| | C23 | 33 | 19 | 2.65 | | TRAIN |
| | C25 | 31 | 16 | 2.24 | | TRAIN |
| | C26 | 29 | 14 | 1.00 | | TRAIN |
| | C27 | 33 | 13 | 1.45 | | TRAIN |
| | C29 | 29 | 6 | 0.38 | | TRAIN |
| | C30 | 32 | 7 | 3.28 | | TRAIN |
| 1998 | C1 | 8 | 45 | 4.47 | | TRAIN |
| | C2 | 6 | 44 | 1.00 | | TRAIN |
| | C3 | 12 | 41 | 6.38 | | TRAIN |
| | C4 | 9 | 42 | 3.63 | | TRAIN |
| | C5 | 10 | 39 | 8.30 | | TRAIN |
| | C6 | 13 | 37 | 9.53 | | TRAIN |
| | C8 | 16 | 35 | 5.27 | | TRAIN |
| | C9 | 18 | 34 | 8.12 | | TRAIN |
| | C10 | 17 | 32 | 8.02 | | TRAIN |
| | C11 | 23 | 31 | 4.82 | | TRAIN |
| | C12 | 21 | 32 | 4.74 | | TRAIN |
| | C13 | 22 | 28 | 4.57 | | TRAIN |
| | C14 | 19 | 29 | 4.47 | | TRAIN |
| | C15 | 27 | 29 | 6.86 | | TRAIN |
| | C16 | 25 | 27 | 5.40 | | TRAIN |
| | C17 | 22 | 24 | 6.80 | | TRAIN |
| | C18 | 28 | 25 | 19.23 | | TRAIN |
| | C19 | 26 | 23 | 2.80 | | TRAIN |
| | C20 | 28 | 21 | 15.63 | | TRAIN |
| | C21 | 30 | 19 | 15.52 | | TRAIN |

**Table 4-3. (Continued)**

| Year | Well_ID | Input | | Target | Output | MF |
|---|---|---|---|---|---|---|
| | | X-Cord | Y-Cord | $NO_3$ (mg/L) | | |
| 1998 | C22 | 28 | 17 | 3.06 | | TRAIN |
| | C23 | 33 | 19 | 3.90 | | TRAIN |
| | C24 | 35 | 16 | 2.70 | | TRAIN |
| | C25 | 31 | 16 | 3.42 | | TRAIN |
| | C26 | 29 | 14 | 0.65 | | TRAIN |
| | C27 | 33 | 13 | 1.38 | | TRAIN |
| | C28 | 31 | 11 | 0.07 | | TRAIN |
| | C29 | 29 | 6 | 0.12 | | TRAIN |
| | C30 | 32 | 7 | 3.60 | | TRAIN |
| 2001 | C1 | 8 | 45 | 3.92 | | TRAIN |
| | C2 | 6 | 44 | 1.36 | | TRAIN |
| | C3 | 12 | 41 | 5.24 | | TRAIN |
| | C4 | 9 | 42 | 5.40 | | TRAIN |
| | C5 | 10 | 39 | 7.90 | | TRAIN |
| | C6 | 13 | 37 | 7.88 | | TRAIN |
| | C8 | 16 | 35 | 4.76 | | TRAIN |
| | C9 | 18 | 34 | 7.30 | | TRAIN |
| | C10 | 17 | 32 | 7.72 | | TRAIN |
| | C11 | 23 | 31 | 4.68 | | TRAIN |
| | C12 | 21 | 32 | 4.56 | | TRAIN |
| | C13 | 22 | 28 | 4.68 | | TRAIN |
| | C14 | 19 | 29 | 4.88 | | TRAIN |
| | C15 | 27 | 29 | 7.86 | | TRAIN |
| | C16 | 25 | 27 | 5.70 | | TRAIN |
| | C17 | 22 | 24 | 6.84 | | TRAIN |
| | C18 | 28 | 25 | 16.44 | | TRAIN |
| | C19 | 26 | 23 | 3.00 | | TRAIN |
| | C20 | 28 | 21 | 13.50 | | TRAIN |
| | C21 | 30 | 19 | 14.36 | | TRAIN |
| | C22 | 28 | 17 | 3.27 | | TRAIN |
| | C23 | 33 | 19 | 3.10 | | TRAIN |
| | C24 | 35 | 16 | 0.88 | | TRAIN |
| | C25 | 31 | 16 | 3.04 | | TRAIN |
| | C26 | 29 | 14 | 0.70 | | TRAIN |
| | C27 | 33 | 13 | 1.52 | | TRAIN |
| | C28 | 31 | 11 | 0.40 | | TRAIN |
| | C29 | 29 | 6 | 0.30 | | TRAIN |
| | C30 | 32 | 7 | 4.24 | | TRAIN |
| 2002 | C1 | 8 | 45 | 3.24 | | TRAIN |
| | C2 | 6 | 44 | 1.40 | | TRAIN |
| | C3 | 12 | 41 | 4.40 | | TRAIN |
| | C4 | 9 | 42 | 4.64 | | TRAIN |
| | C5 | 10 | 39 | 7.90 | | TRAIN |
| | C6 | 13 | 37 | 7.65 | | TRAIN |

**Table 4-3. (Continued)**

| Year | Well_ID | Input | | Target | Output | MF |
|---|---|---|---|---|---|---|
| | | X-Cord | Y-Cord | $NO_3$ (mg/L) | | |
| 2002 | C8 | 16 | 35 | 4.80 | | TRAIN |
| | C9 | 18 | 34 | 7.68 | | TRAIN |
| | C10 | 17 | 32 | 8.08 | | TRAIN |
| | C11 | 23 | 31 | 4.92 | | TRAIN |
| | C12 | 21 | 32 | 4.88 | | TRAIN |
| | C13 | 22 | 28 | 4.68 | | TRAIN |
| | C14 | 19 | 29 | 5.00 | | TRAIN |
| | C15 | 27 | 29 | 7.88 | | TRAIN |
| | C16 | 25 | 27 | 5.75 | | TRAIN |
| | C17 | 22 | 24 | 6.64 | | TRAIN |
| | C18 | 28 | 25 | 15.96 | | TRAIN |
| | C19 | 26 | 23 | 3.36 | | TRAIN |
| | C20 | 28 | 21 | 14.48 | | TRAIN |
| | C21 | 30 | 19 | 14.20 | | TRAIN |
| | C22 | 28 | 17 | 4.05 | | TRAIN |
| | C23 | 33 | 19 | 3.70 | | TRAIN |
| | C24 | 35 | 16 | 0.40 | | TRAIN |
| | C25 | 31 | 16 | 2.55 | | TRAIN |
| | C26 | 29 | 14 | 1.80 | | TRAIN |
| | C27 | 33 | 13 | 1.96 | | TRAIN |
| | C29 | 29 | 6 | 0.80 | | TRAIN |
| | C30 | 32 | 7 | 4.76 | | TRAIN |
| 2003 | C1 | 8 | 45 | 2.95 | | TRAIN |
| | C2 | 6 | 44 | 1.25 | | TRAIN |
| | C3 | 12 | 41 | 3.90 | | TRAIN |
| | C4 | 9 | 42 | 4.70 | | TRAIN |
| | C5 | 10 | 39 | 7.35 | | TRAIN |
| | C6 | 13 | 37 | 6.75 | | TRAIN |
| | C8 | 16 | 35 | 4.60 | | TRAIN |
| | C9 | 18 | 34 | 7.45 | | TRAIN |
| | C10 | 17 | 32 | 8.70 | | TRAIN |
| | C11 | 23 | 31 | 5.00 | | TRAIN |
| | C12 | 21 | 32 | 4.75 | | TRAIN |
| | C13 | 22 | 28 | 4.70 | | TRAIN |
| | C14 | 19 | 29 | 4.80 | | TRAIN |
| | C15 | 27 | 29 | 8.35 | | TRAIN |
| | C16 | 25 | 27 | 6.05 | | TRAIN |
| | C17 | 22 | 24 | 8.40 | | TRAIN |
| | C18 | 28 | 25 | 16.00 | | TRAIN |
| | C19 | 26 | 23 | 3.20 | | TRAIN |
| | C20 | 28 | 21 | 13.95 | | TRAIN |
| | C21 | 30 | 19 | 13.95 | | TRAIN |
| | C22 | 28 | 17 | 4.05 | | TRAIN |

**Table 4-3. (Continued)**

| Year | Well_ID | Input | | Target | Output | MF |
|---|---|---|---|---|---|---|
| | | X-Cord | Y-Cord | $NO_3$ (mg/L) | | |
| 2003 | C23 | 33 | 19 | 3.90 | | TRAIN |
| | C25 | 31 | 16 | 3.00 | | TRAIN |
| | C26 | 29 | 14 | 1.65 | | TRAIN |
| | C27 | 33 | 13 | 1.80 | | TRAIN |
| | C28 | 31 | 11 | 1.00 | | TRAIN |
| | C29 | 29 | 6 | 0.90 | | TRAIN |
| | C30 | 32 | 7 | 5.10 | | TRAIN |
| 2005 | C1 | 8 | 45 | 1.80 | | TRAIN |
| | C2 | 6 | 44 | 1.10 | | TRAIN |
| | C3 | 12 | 41 | 4.08 | | TRAIN |
| | C4 | 9 | 42 | 3.56 | | TRAIN |
| | C5 | 10 | 39 | 6.92 | | TRAIN |
| | C6 | 13 | 37 | 6.00 | | TRAIN |
| | C8 | 16 | 35 | 4.36 | | TRAIN |
| | C10 | 17 | 32 | 9.80 | | TRAIN |
| | C11 | 23 | 31 | 4.80 | | TRAIN |
| | C12 | 21 | 32 | 4.36 | | TRAIN |
| | C13 | 22 | 28 | 4.32 | | TRAIN |
| | C14 | 19 | 29 | 4.76 | | TRAIN |
| | C15 | 27 | 29 | 7.32 | | TRAIN |
| | C16 | 25 | 27 | 5.28 | | TRAIN |
| | C17 | 22 | 24 | 9.56 | | TRAIN |
| | C18 | 28 | 25 | 14.88 | | TRAIN |
| | C19 | 26 | 23 | 3.40 | | TRAIN |
| | C20 | 28 | 21 | 13.04 | | TRAIN |
| | C21 | 30 | 19 | 12.88 | | TRAIN |
| | C22 | 28 | 17 | 3.96 | | TRAIN |
| | C23 | 33 | 19 | 3.40 | | TRAIN |
| | C24 | 35 | 16 | 4.00 | | TRAIN |
| | C25 | 31 | 16 | 2.55 | | TRAIN |
| | C26 | 29 | 14 | 1.10 | | TRAIN |
| | C27 | 33 | 13 | 1.45 | | TRAIN |
| | C29 | 29 | 6 | 0.93 | | TRAIN |
| | C30 | 32 | 7 | 4.30 | | TRAIN |
| 1999 | C1 | 8 | 45 | 3.80 | | TEST |
| | C3 | 12 | 41 | 4.30 | | TEST |
| | C4 | 9 | 42 | 4.40 | | TEST |
| | C6 | 13 | 37 | 8.12 | | TEST |
| | C8 | 16 | 35 | 4.90 | | TEST |
| | C9 | 18 | 34 | 8.60 | | TEST |
| | C10 | 17 | 32 | 8.40 | | TEST |
| | C11 | 23 | 31 | 4.45 | | TEST |
| | C12 | 21 | 32 | 5.60 | | TEST |
| | C13 | 22 | 28 | 4.64 | | TEST |

**Table 4-3. (Continued)**

| Year | Well_ID | Input | | Target | Output | MF |
|---|---|---|---|---|---|---|
| | | X-Cord | Y-Cord | $NO_3$ (mg/L) | | |
| 1999 | C14 | 19 | 29 | 4.83 | | TEST |
| | C15 | 27 | 29 | 7.42 | | TEST |
| | C16 | 25 | 27 | 5.90 | | TEST |
| | C17 | 22 | 24 | 6.20 | | TEST |
| | C18 | 28 | 25 | 18.50 | | TEST |
| | C19 | 26 | 23 | 3.20 | | TEST |
| | C20 | 28 | 21 | 16.90 | | TEST |
| | C21 | 30 | 19 | 15.03 | | TEST |
| | C22 | 28 | 17 | 3.02 | | TEST |
| | C23 | 33 | 19 | 3.66 | | TEST |
| | C25 | 31 | 16 | 3.08 | | TEST |
| | C27 | 33 | 13 | 1.42 | | TEST |
| | C28 | 31 | 11 | 0.37 | | TEST |
| | C29 | 29 | 6 | 0.34 | | TEST |
| | C30 | 32 | 7 | 4.08 | | TEST |
| 2004 | C1 | 8 | 45 | 2.00 | | TEST |
| | C2 | 6 | 44 | 1.00 | | TEST |
| | C3 | 12 | 41 | 3.92 | | TEST |
| | C4 | 9 | 42 | 4.23 | | TEST |
| | C5 | 10 | 39 | 7.07 | | TEST |
| | C6 | 13 | 37 | 6.43 | | TEST |
| | C8 | 16 | 35 | 5.28 | | TEST |
| | C9 | 18 | 34 | 7.40 | | TEST |
| | C10 | 17 | 32 | 9.13 | | TEST |
| | C11 | 23 | 31 | 4.93 | | TEST |
| | C12 | 21 | 32 | 4.53 | | TEST |
| | C13 | 22 | 28 | 4.30 | | TEST |
| | C14 | 19 | 29 | 4.73 | | TEST |
| | C15 | 27 | 29 | 8.33 | | TEST |
| | C16 | 25 | 27 | 5.57 | | TEST |
| | C17 | 22 | 24 | 8.73 | | TEST |
| | C18 | 28 | 25 | 15.37 | | TEST |
| | C19 | 26 | 23 | 3.27 | | TEST |
| | C20 | 28 | 21 | 13.40 | | TEST |
| | C21 | 30 | 19 | 13.67 | | TEST |
| | C22 | 28 | 17 | 4.07 | | TEST |
| | C23 | 33 | 19 | 4.00 | | TEST |
| | C25 | 31 | 16 | 2.60 | | TEST |
| | C26 | 29 | 14 | 1.37 | | TEST |
| | C27 | 33 | 13 | 1.47 | | TEST |
| | C28 | 31 | 11 | 0.70 | | TEST |
| | C29 | 29 | 6 | 0.47 | | TEST |
| | C30 | 32 | 7 | 4.37 | | TEST |

#### 4.1.3.2 Ringwood wellfield spatial model

Groundwater nitrate distribution in Ringwood wellfield area was studied in this effort. Figure 4-7 shows the area included in this model. The method was same as the previously presented Cleospring wellfield model where grid coordinates (X,Y) were used as input to predict the nitrate concentration in the corresponding grid. A total of 205 nitrate concentration data points from 1997 to 2005 (excluding 2000) were used in this model for training and testing. Table 4-4 presents the training and testing data sets used in this model. The values presented in this table are arranged in the same way as in previously explained Table 4-3.

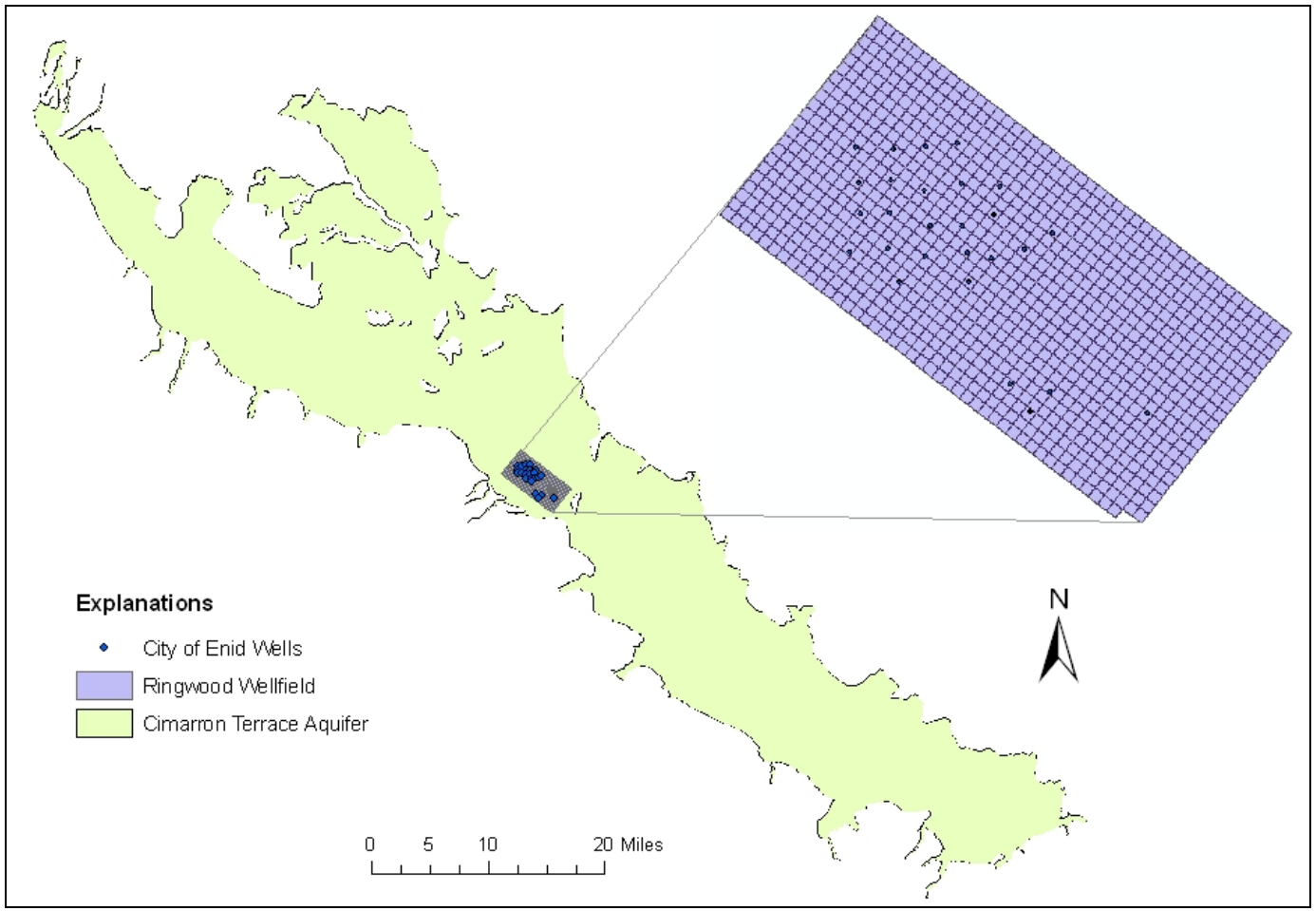


**Figure 4-7. Location of focused area in Ringwood wellfield model**

**Table 4-4. Training and testing data sets for Ringwood wellfield spatial model**

| Year | Well_ID | Input | | Target | Output | MF |
|---|---|---|---|---|---|---|
| | | X-Cord | Y-Cord | $NO_3$ (mg/L) | | |
| 1997 | R1 | 12 | 40 | 5.64 | | TRAIN |
| | R2 | 14 | 37 | 4.28 | | TRAIN |
| | R4 | 18 | 33 | 4.52 | | TRAIN |
| | R5 | 10 | 38 | 5.70 | | TRAIN |
| | R6 | 12 | 36 | 4.46 | | TRAIN |
| | R8 | 15 | 31 | 5.56 | | TRAIN |
| | R9 | 17 | 28 | 5.22 | | TRAIN |
| | R10 | 8 | 36 | 3.38 | | TRAIN |
| | R11 | 10 | 34 | 3.70 | | TRAIN |
| | R12 | 11 | 31 | 3.54 | | TRAIN |
| | R13 | 12 | 28 | 3.95 | | TRAIN |
| | R14 | 15 | 27 | 4.66 | | TRAIN |
| | R15 | 5 | 35 | 4.10 | | TRAIN |
| | R16 | 7 | 32 | 3.32 | | TRAIN |
| | R18 | 11 | 27 | 3.25 | | TRAIN |
| | R19 | 12 | 25 | 3.32 | | TRAIN |
| | R20 | 14 | 23 | 5.04 | | TRAIN |
| | R22 | 5 | 30 | 3.35 | | TRAIN |
| | R24 | 9 | 25 | 3.30 | | TRAIN |
| | R25 | 4 | 17 | 2.50 | | TRAIN |
| | R26 | 6 | 14 | 4.67 | | TRAIN |
| | R27 | 3 | 14 | 2.83 | | TRAIN |
| | R28 | 9 | 6 | 10.00 | | TRAIN |
| 1998 | R1 | 12 | 40 | 8.22 | | TRAIN |
| | R2 | 14 | 37 | 7.34 | | TRAIN |
| | R3 | 16 | 35 | 7.40 | | TRAIN |
| | R5 | 10 | 38 | 7.87 | | TRAIN |
| | R6 | 12 | 36 | 6.87 | | TRAIN |
| | R7 | 13 | 33 | 6.10 | | TRAIN |
| | R8 | 15 | 31 | 9.20 | | TRAIN |
| | R9 | 17 | 28 | 8.28 | | TRAIN |
| | R10 | 8 | 36 | 6.56 | | TRAIN |
| | R11 | 10 | 34 | 6.30 | | TRAIN |
| | R12 | 11 | 31 | 5.70 | | TRAIN |
| | R13 | 12 | 28 | 7.00 | | TRAIN |
| | R14 | 15 | 27 | 7.33 | | TRAIN |
| | R15 | 5 | 35 | 4.84 | | TRAIN |
| | R16 | 7 | 32 | 5.24 | | TRAIN |
| | R17 | 9 | 29 | 3.60 | | TRAIN |
| | R18 | 11 | 27 | 4.48 | | TRAIN |
| | R19 | 12 | 25 | 4.34 | | TRAIN |
| | R20 | 14 | 23 | 8.48 | | TRAIN |
| | R21 | 17 | 22 | 9.20 | | TRAIN |
| | R22 | 5 | 30 | 3.87 | | TRAIN |

**Table 4-4. (Continued)**

| Year | Well_ID | Input | | Target | Output | MF |
|---|---|---|---|---|---|---|
| | | X-Cord | Y-Cord | $NO_3$ (mg/L) | | |
| 1998 | R24 | 9 | 25 | 3.25 | | TRAIN |
| | R25 | 4 | 17 | 3.03 | | TRAIN |
| | R26 | 6 | 14 | 9.60 | | TRAIN |
| | R27 | 3 | 14 | 4.70 | | TRAIN |
| | R28 | 9 | 6 | 15.82 | | TRAIN |
| 2001 | R1 | 12 | 40 | 7.87 | | TRAIN |
| | R2 | 14 | 37 | 7.63 | | TRAIN |
| | R3 | 16 | 35 | 9.10 | | TRAIN |
| | R4 | 18 | 33 | 8.13 | | TRAIN |
| | R5 | 10 | 38 | 7.27 | | TRAIN |
| | R6 | 12 | 36 | 7.00 | | TRAIN |
| | R7 | 13 | 33 | 7.52 | | TRAIN |
| | R8 | 15 | 31 | 9.87 | | TRAIN |
| | R9 | 17 | 28 | 9.27 | | TRAIN |
| | R10 | 8 | 36 | 6.93 | | TRAIN |
| | R11 | 10 | 34 | 6.80 | | TRAIN |
| | R12 | 11 | 31 | 5.90 | | TRAIN |
| | R13 | 12 | 28 | 8.07 | | TRAIN |
| | R14 | 15 | 27 | 12.17 | | TRAIN |
| | R15 | 5 | 35 | 5.43 | | TRAIN |
| | R16 | 7 | 32 | 7.40 | | TRAIN |
| | R17 | 9 | 29 | 4.57 | | TRAIN |
| | R18 | 11 | 27 | 4.60 | | TRAIN |
| | R19 | 12 | 25 | 4.80 | | TRAIN |
| | R20 | 14 | 23 | 10.83 | | TRAIN |
| | R21 | 17 | 22 | 12.87 | | TRAIN |
| | R22 | 5 | 30 | 3.85 | | TRAIN |
| | R24 | 9 | 25 | 3.53 | | TRAIN |
| | R25 | 4 | 17 | 2.75 | | TRAIN |
| | R26 | 6 | 14 | 10.27 | | TRAIN |
| | R27 | 3 | 14 | 5.40 | | TRAIN |
| | R28 | 9 | 6 | 16.00 | | TRAIN |
| 2002 | R1 | 12 | 40 | 7.52 | | TRAIN |
| | R2 | 14 | 37 | 7.28 | | TRAIN |
| | R3 | 16 | 35 | 9.00 | | TRAIN |
| | R4 | 18 | 33 | 8.10 | | TRAIN |
| | R5 | 10 | 38 | 7.28 | | TRAIN |
| | R6 | 12 | 36 | 6.76 | | TRAIN |
| | R7 | 13 | 33 | 7.52 | | TRAIN |
| | R8 | 15 | 31 | 9.30 | | TRAIN |
| | R9 | 17 | 28 | 9.37 | | TRAIN |
| | R10 | 8 | 36 | 7.32 | | TRAIN |
| | R11 | 10 | 34 | 7.00 | | TRAIN |
| | R12 | 11 | 31 | 6.17 | | TRAIN |

**Table 4-4. (Continued)**

| Year | Well_ID | Input | | Target | Output | MF |
|---|---|---|---|---|---|---|
| | | X-Cord | Y-Cord | $NO_3$ (mg/L) | | |
| 2002 | R13 | 12 | 28 | 7.77 | | TRAIN |
| | R14 | 15 | 27 | 11.63 | | TRAIN |
| | R15 | 5 | 35 | 5.30 | | TRAIN |
| | R16 | 7 | 32 | 7.50 | | TRAIN |
| | R17 | 9 | 29 | 4.50 | | TRAIN |
| | R18 | 11 | 27 | 4.87 | | TRAIN |
| | R19 | 12 | 25 | 5.47 | | TRAIN |
| | R20 | 14 | 23 | 10.47 | | TRAIN |
| | R21 | 17 | 22 | 13.50 | | TRAIN |
| | R22 | 5 | 30 | 4.20 | | TRAIN |
| | R24 | 9 | 25 | 3.27 | | TRAIN |
| | R25 | 4 | 17 | 3.47 | | TRAIN |
| | R26 | 6 | 14 | 10.84 | | TRAIN |
| | R27 | 3 | 14 | 6.32 | | TRAIN |
| | R28 | 9 | 6 | 15.60 | | TRAIN |
| 2003 | R1 | 12 | 40 | 7.40 | | TRAIN |
| | R2 | 14 | 37 | 7.25 | | TRAIN |
| | R3 | 16 | 35 | 9.15 | | TRAIN |
| | R4 | 18 | 33 | 8.35 | | TRAIN |
| | R5 | 10 | 38 | 7.30 | | TRAIN |
| | R6 | 12 | 36 | 6.80 | | TRAIN |
| | R7 | 13 | 33 | 7.30 | | TRAIN |
| | R8 | 15 | 31 | 8.95 | | TRAIN |
| | R9 | 17 | 28 | 9.60 | | TRAIN |
| | R10 | 8 | 36 | 7.00 | | TRAIN |
| | R11 | 10 | 34 | 6.45 | | TRAIN |
| | R12 | 11 | 31 | 6.45 | | TRAIN |
| | R13 | 12 | 28 | 7.70 | | TRAIN |
| | R14 | 15 | 27 | 12.10 | | TRAIN |
| | R15 | 5 | 35 | 5.25 | | TRAIN |
| | R16 | 7 | 32 | 8.40 | | TRAIN |
| | R17 | 9 | 29 | 4.70 | | TRAIN |
| | R18 | 11 | 27 | 5.10 | | TRAIN |
| | R19 | 12 | 25 | 5.10 | | TRAIN |
| | R20 | 14 | 23 | 10.80 | | TRAIN |
| | R21 | 17 | 22 | 13.25 | | TRAIN |
| | R22 | 5 | 30 | 4.20 | | TRAIN |
| | R24 | 9 | 25 | 3.45 | | TRAIN |
| | R25 | 4 | 17 | 3.70 | | TRAIN |
| | R26 | 6 | 14 | 11.20 | | TRAIN |
| | R27 | 3 | 14 | 7.05 | | TRAIN |
| | R28 | 9 | 6 | 15.60 | | TRAIN |
| 2005 | R1 | 12 | 40 | 6.80 | | TRAIN |
| | R2 | 14 | 37 | 7.07 | | TRAIN |

**Table 4-4. (Continued)**

| Year | Well_ID | Input | | Target | Output | MF |
|---|---|---|---|---|---|---|
| | | X-Cord | Y-Cord | $NO_3$ (mg/L) | | |
| 2005 | R3 | 16 | 35 | 9.20 | | TRAIN |
| | R4 | 18 | 33 | 8.37 | | TRAIN |
| | R5 | 10 | 38 | 6.83 | | TRAIN |
| | R7 | 13 | 33 | 7.27 | | TRAIN |
| | R8 | 15 | 31 | 8.93 | | TRAIN |
| | R9 | 17 | 28 | 9.32 | | TRAIN |
| | R10 | 8 | 36 | 6.73 | | TRAIN |
| | R11 | 10 | 34 | 6.53 | | TRAIN |
| | R12 | 11 | 31 | 6.53 | | TRAIN |
| | R13 | 12 | 28 | 7.87 | | TRAIN |
| | R14 | 15 | 27 | 13.63 | | TRAIN |
| | R17 | 9 | 29 | 4.93 | | TRAIN |
| | R18 | 11 | 27 | 5.47 | | TRAIN |
| | R19 | 12 | 25 | 5.10 | | TRAIN |
| | R20 | 14 | 23 | 11.70 | | TRAIN |
| | R21 | 17 | 22 | 13.33 | | TRAIN |
| | R24 | 9 | 25 | 3.80 | | TRAIN |
| | R25 | 4 | 17 | 3.33 | | TRAIN |
| | R26 | 6 | 14 | 12.17 | | TRAIN |
| | R27 | 3 | 14 | 7.80 | | TRAIN |
| | R28 | 9 | 6 | 15.73 | | TRAIN |
| 1999 | R1 | 12 | 40 | 8.52 | | TEST |
| | R2 | 14 | 37 | 7.73 | | TEST |
| | R3 | 16 | 35 | 7.60 | | TEST |
| | R4 | 18 | 33 | 8.26 | | TEST |
| | R5 | 10 | 38 | 7.85 | | TEST |
| | R6 | 12 | 36 | 6.93 | | TEST |
| | R7 | 13 | 33 | 8.80 | | TEST |
| | R8 | 15 | 31 | 9.88 | | TEST |
| | R9 | 17 | 28 | 9.55 | | TEST |
| | R10 | 8 | 36 | 6.73 | | TEST |
| | R11 | 10 | 34 | 6.60 | | TEST |
| | R12 | 11 | 31 | 6.02 | | TEST |
| | R13 | 12 | 28 | 7.66 | | TEST |
| | R14 | 15 | 27 | 10.48 | | TEST |
| | R15 | 5 | 35 | 5.58 | | TEST |
| | R16 | 7 | 32 | 6.05 | | TEST |
| | R17 | 9 | 29 | 3.80 | | TEST |
| | R18 | 11 | 27 | 4.20 | | TEST |
| | R19 | 12 | 25 | 4.17 | | TEST |
| | R20 | 14 | 23 | 9.62 | | TEST |
| | R21 | 17 | 22 | 12.00 | | TEST |
| | R22 | 5 | 30 | 3.60 | | TEST |
| | R24 | 9 | 25 | 2.80 | | TEST |

**Table 4-4. (Continued)**

| Year | Well_ID | Input | | Target | Output | MF |
|---|---|---|---|---|---|---|
| | | X-Cord | Y-Cord | $NO_3$ (mg/L) | | |
| 1999 | R25 | 4 | 17 | 2.80 | | TEST |
| | R26 | 6 | 14 | 10.60 | | TEST |
| | R27 | 3 | 14 | 4.97 | | TEST |
| | R28 | 9 | 6 | 18.80 | | TEST |
| 2004 | R1 | 12 | 40 | 7.53 | | TEST |
| | R2 | 14 | 37 | 7.60 | | TEST |
| | R3 | 16 | 35 | 9.03 | | TEST |
| | R4 | 18 | 33 | 8.60 | | TEST |
| | R5 | 10 | 38 | 7.27 | | TEST |
| | R6 | 12 | 36 | 7.00 | | TEST |
| | R7 | 13 | 33 | 7.65 | | TEST |
| | R8 | 15 | 31 | 9.13 | | TEST |
| | R9 | 17 | 28 | 10.20 | | TEST |
| | R10 | 8 | 36 | 7.35 | | TEST |
| | R11 | 10 | 34 | 6.55 | | TEST |
| | R12 | 11 | 31 | 6.65 | | TEST |
| | R13 | 12 | 28 | 7.80 | | TEST |
| | R14 | 15 | 27 | 13.60 | | TEST |
| | R15 | 5 | 35 | 5.00 | | TEST |
| | R17 | 9 | 29 | 4.65 | | TEST |
| | R18 | 11 | 27 | 5.47 | | TEST |
| | R19 | 12 | 25 | 5.40 | | TEST |
| | R20 | 14 | 23 | 12.00 | | TEST |
| | R21 | 17 | 22 | 13.65 | | TEST |
| | R24 | 9 | 25 | 3.55 | | TEST |
| | R25 | 4 | 17 | 3.40 | | TEST |
| | R26 | 6 | 14 | 11.90 | | TEST |
| | R27 | 3 | 14 | 8.00 | | TEST |
| | R28 | 9 | 6 | 16.15 | | TEST |

With the model configuration presented in Table 4-4 different network architectures were evaluated until some consistency in results in terms of prediction accuracy and numbers of iterations was achieved. The model with high prediction accuracy and least epochs required was selected as best model and it was used to predict the nitrate concentrations in each grid of the wellfield. Determination of best model is discussed in detail in Results.

#### 4.1.3.3 Ames wellfield spatial model

Data from the Ames wellfield was modeled in a similar manner as the Cleospring and Ringwood spatial models. Figure 4-8 presents the area included in this model. A total of 154 nitrate and well location data from 1997 to 2005 (except 2000) were used in this model for training and testing. Among eight years data set, 1998 and 2004 data sets were used for testing and rest for training the model and they are presented in Table 4-5 presents these data arranged as training and testing respectively. The data are arranged in the same way as previously explained Tables 4-3 and 4-4.

This model was executed with different architectures to determine the best model. Model architectures and their performances evaluated in this effort are discussed in detail in Results section. A model which required least training time and consistent in results in terms of prediction accuracy was defined as a best. The best model was then used to predict the nitrate concentrations at the unmeasured locations.

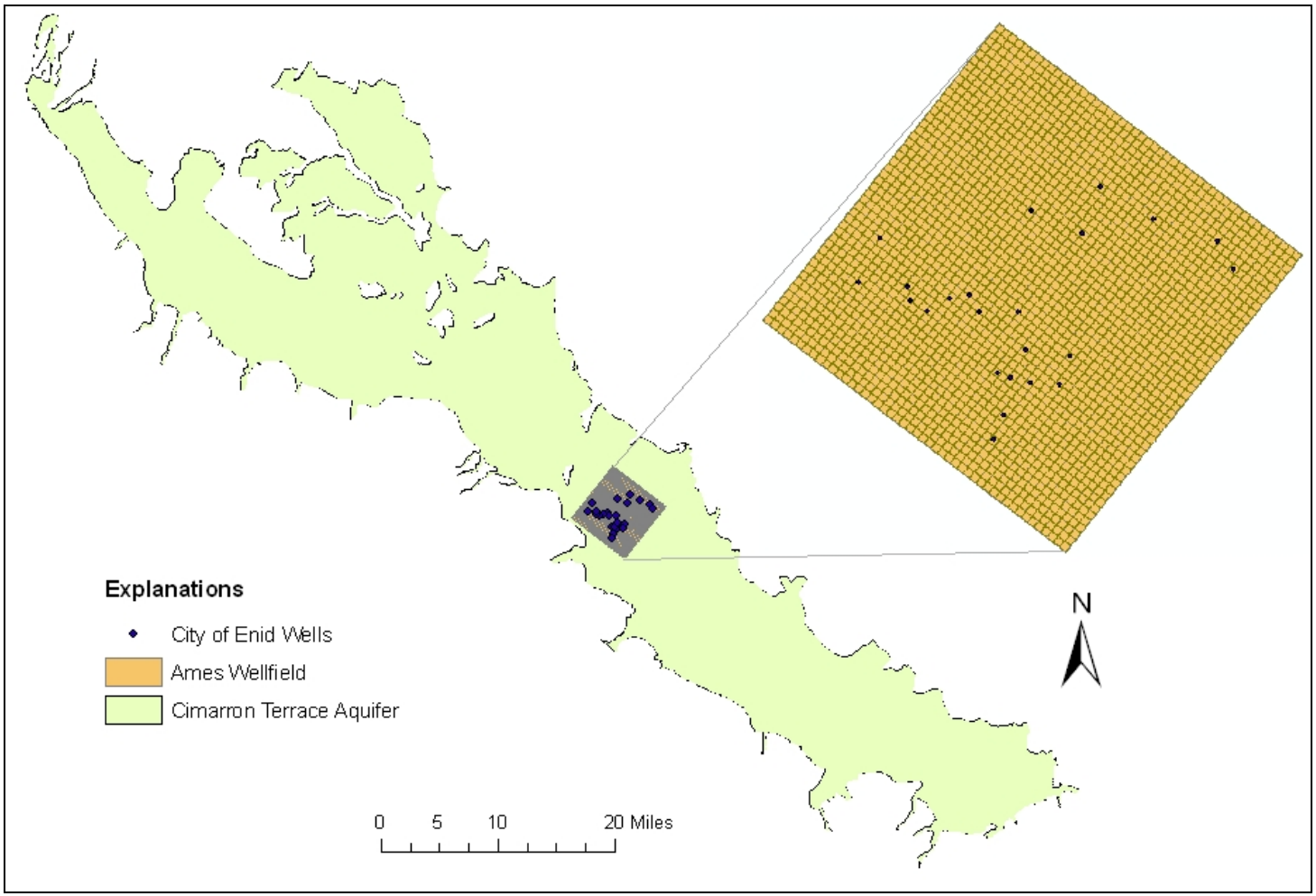


**Figure 4-8. Location of focused area in Ames wellfield model**

**Table 4-5. Training and testing data sets for Ames wellfield spatial model**

| Year | Well_ID | Input | | Target | Output | MF |
|---|---|---|---|---|---|---|
| | | X-Cord | Y-Cord | $NO_3$ (mg/L) | | |
| 1997 | A1 | 42 | 10 | 11.35 | | TRAIN |
| | A2 | 20 | 15 | 7.03 | | TRAIN |
| | A3 | 20 | 10 | 3.67 | | TRAIN |
| | A4 | 9 | 17 | 5.40 | | TRAIN |
| | A5 | 6 | 16 | 3.35 | | TRAIN |
| | A6 | 13 | 21 | 1.50 | | TRAIN |
| | A7 | 14 | 19 | 3.23 | | TRAIN |
| | A11 | 17 | 14 | 8.65 | | TRAIN |
| | A12 | 18 | 12 | 7.08 | | TRAIN |
| | A13 | 3 | 33 | 12.60 | | TRAIN |
| | A14 | 41 | 6 | 10.90 | | TRAIN |
| | A16 | 40 | 18 | 12.23 | | TRAIN |
| | A17 | 39 | 25 | 12.29 | | TRAIN |
| | A18 | 33 | 23 | 18.30 | | TRAIN |
| | A21 | 18 | 27 | 8.85 | | TRAIN |
| | A22 | 17 | 31 | 5.80 | | TRAIN |
| | A24 | 14 | 35 | 7.20 | | TRAIN |
| | A25 | 17 | 42 | 11.25 | | TRAIN |
| | A29 | 11 | 41 | 8.33 | | TRAIN |
| 1998 | A1 | 42 | 10 | 12.93 | | TRAIN |
| | A2 | 20 | 15 | 10.33 | | TRAIN |
| | A3 | 20 | 10 | 4.07 | | TRAIN |
| | A4 | 9 | 17 | 7.03 | | TRAIN |
| | A5 | 6 | 16 | 3.55 | | TRAIN |
| | A6 | 13 | 21 | 1.73 | | TRAIN |
| | A7 | 14 | 19 | 2.90 | | TRAIN |
| | A8 | 17 | 20 | 3.45 | | TRAIN |
| | A9 | 21 | 24 | 1.00 | | TRAIN |
| | A11 | 17 | 14 | 11.80 | | TRAIN |
| | A12 | 18 | 12 | 10.08 | | TRAIN |
| | A13 | 3 | 33 | 14.87 | | TRAIN |
| | A14 | 41 | 6 | 14.27 | | TRAIN |
| | A15 | 46 | 11 | 4.30 | | TRAIN |
| | A16 | 40 | 18 | 17.33 | | TRAIN |
| | A17 | 39 | 25 | 16.80 | | TRAIN |
| | A18 | 33 | 23 | 20.33 | | TRAIN |
| | A19 | 31 | 30 | 8.45 | | TRAIN |
| | A20 | 18 | 30 | 6.67 | | TRAIN |
| | A21 | 18 | 27 | 11.10 | | TRAIN |
| | A22 | 17 | 31 | 7.90 | | TRAIN |
| | A23 | 14 | 32 | 10.25 | | TRAIN |
| | A24 | 14 | 35 | 8.90 | | TRAIN |
| | A25 | 17 | 42 | 12.00 | | TRAIN |
| | A29 | 11 | 41 | 10.25 | | TRAIN |

**Table 4-5. (Continued)**

| Year | Well_ID | Input | | Target | Output | MF |
|---|---|---|---|---|---|---|
| | | X-Cord | Y-Cord | $NO_3$ (mg/L) | | |
| 2001 | A1 | 42 | 10 | 10.00 | | TRAIN |
| | A2 | 20 | 15 | 9.64 | | TRAIN |
| | A4 | 9 | 17 | 7.60 | | TRAIN |
| | A5 | 6 | 16 | 8.60 | | TRAIN |
| | A6 | 13 | 21 | 1.80 | | TRAIN |
| | A7 | 14 | 19 | 2.80 | | TRAIN |
| | A8 | 17 | 20 | 3.80 | | TRAIN |
| | A9 | 21 | 24 | 1.20 | | TRAIN |
| | A15 | 46 | 11 | 4.40 | | TRAIN |
| | A17 | 39 | 25 | 14.50 | | TRAIN |
| | A20 | 18 | 30 | 6.60 | | TRAIN |
| | A22 | 17 | 31 | 7.80 | | TRAIN |
| | A24 | 14 | 35 | 10.00 | | TRAIN |
| | A25 | 17 | 42 | 14.00 | | TRAIN |
| | A29 | 11 | 41 | 9.90 | | TRAIN |
| 2002 | A1 | 42 | 10 | 11.50 | | TRAIN |
| | A2 | 20 | 15 | 9.89 | | TRAIN |
| | A3 | 20 | 10 | 3.80 | | TRAIN |
| | A4 | 9 | 17 | 6.60 | | TRAIN |
| | A5 | 6 | 16 | 5.80 | | TRAIN |
| | A6 | 13 | 21 | 2.40 | | TRAIN |
| | A7 | 14 | 19 | 5.60 | | TRAIN |
| | A8 | 17 | 20 | 3.00 | | TRAIN |
| | A9 | 21 | 24 | 1.80 | | TRAIN |
| | A11 | 17 | 14 | 14.80 | | TRAIN |
| | A13 | 3 | 33 | 14.00 | | TRAIN |
| | A14 | 41 | 6 | 12.90 | | TRAIN |
| | A16 | 40 | 18 | 13.60 | | TRAIN |
| | A17 | 39 | 25 | 16.00 | | TRAIN |
| | A18 | 33 | 23 | 15.30 | | TRAIN |
| | A19 | 31 | 30 | 12.80 | | TRAIN |
| | A20 | 18 | 30 | 6.60 | | TRAIN |
| | A21 | 18 | 27 | 8.70 | | TRAIN |
| | A22 | 17 | 31 | 6.40 | | TRAIN |
| | A23 | 14 | 32 | 9.30 | | TRAIN |
| | A24 | 14 | 35 | 8.70 | | TRAIN |
| | A25 | 17 | 42 | 14.07 | | TRAIN |
| | A29 | 11 | 41 | 9.40 | | TRAIN |
| 2003 | A1 | 42 | 10 | 11.73 | | TRAIN |
| | A2 | 20 | 15 | 9.30 | | TRAIN |
| | A3 | 20 | 10 | 3.40 | | TRAIN |
| | A4 | 9 | 17 | 6.80 | | TRAIN |
| | A5 | 6 | 16 | 5.20 | | TRAIN |
| | A6 | 13 | 21 | 2.47 | | TRAIN |

**Table 4-5. (Continued)**

| Year | Well_ID | Input | | Target | Output | MF |
|---|---|---|---|---|---|---|
| | | X-Cord | Y-Cord | $NO_3$ (mg/L) | | |
| 2003 | A7 | 14 | 19 | 4.00 | | TRAIN |
| | A8 | 17 | 20 | 3.60 | | TRAIN |
| | A9 | 21 | 24 | 1.80 | | TRAIN |
| | A11 | 17 | 14 | 13.60 | | TRAIN |
| | A14 | 41 | 6 | 13.00 | | TRAIN |
| | A16 | 40 | 18 | 12.40 | | TRAIN |
| | A17 | 39 | 25 | 15.60 | | TRAIN |
| | A18 | 33 | 23 | 14.80 | | TRAIN |
| | A19 | 31 | 30 | 14.00 | | TRAIN |
| | A20 | 18 | 30 | 6.80 | | TRAIN |
| | A21 | 18 | 27 | 10.70 | | TRAIN |
| | A22 | 17 | 31 | 7.60 | | TRAIN |
| | A23 | 14 | 32 | 9.35 | | TRAIN |
| | A24 | 14 | 35 | 8.60 | | TRAIN |
| | A25 | 17 | 42 | 13.40 | | TRAIN |
| | A27 | 15 | 36 | 7.80 | | TRAIN |
| | A29 | 11 | 41 | 9.40 | | TRAIN |
| 2005 | A1 | 42 | 10 | 11.67 | | TRAIN |
| | A2 | 20 | 15 | 9.24 | | TRAIN |
| | A4 | 9 | 17 | 8.30 | | TRAIN |
| | A6 | 13 | 21 | 2.00 | | TRAIN |
| | A8 | 17 | 20 | 3.50 | | TRAIN |
| | A11 | 17 | 14 | 11.20 | | TRAIN |
| | A14 | 41 | 6 | 11.00 | | TRAIN |
| | A16 | 40 | 18 | 11.20 | | TRAIN |
| | A18 | 33 | 23 | 12.80 | | TRAIN |
| | A19 | 31 | 30 | 11.70 | | TRAIN |
| | A20 | 18 | 30 | 6.10 | | TRAIN |
| | A24 | 14 | 35 | 9.20 | | TRAIN |
| | A27 | 15 | 36 | 7.80 | | TRAIN |
| | A29 | 11 | 41 | 9.20 | | TRAIN |
| | A30 | 16 | 36 | 7.60 | | TRAIN |
| | A32 | 18 | 32 | 7.90 | | TRAIN |
| | A33 | 19 | 30 | 5.93 | | TRAIN |
| 1999 | A1 | 42 | 10 | 13.00 | | TEST |
| | A2 | 20 | 15 | 10.73 | | TEST |
| | A3 | 20 | 10 | 4.10 | | TEST |
| | A4 | 9 | 17 | 7.00 | | TEST |
| | A5 | 6 | 16 | 3.65 | | TEST |
| | A6 | 13 | 21 | 1.72 | | TEST |
| | A7 | 14 | 19 | 2.86 | | TEST |
| | A8 | 17 | 20 | 2.67 | | TEST |
| | A9 | 21 | 24 | 1.00 | | TEST |
| | A11 | 17 | 14 | 12.20 | | TEST |

**Table 4-5. (Continued)**

| Year | Well_ID | Input | | Target | Output | MF |
|---|---|---|---|---|---|---|
| | | X-Cord | Y-Cord | $NO_3$ (mg/L) | | |
| 1999 | A14 | 41 | 6 | 14.20 | | TEST |
| | A15 | 46 | 11 | 4.37 | | TEST |
| | A16 | 40 | 18 | 16.30 | | TEST |
| | A18 | 33 | 23 | 18.60 | | TEST |
| | A19 | 31 | 30 | 13.00 | | TEST |
| | A20 | 18 | 30 | 6.70 | | TEST |
| | A21 | 18 | 27 | 10.50 | | TEST |
| | A22 | 17 | 31 | 8.00 | | TEST |
| | A24 | 14 | 35 | 9.37 | | TEST |
| | A25 | 17 | 42 | 15.00 | | TEST |
| | A29 | 11 | 41 | 9.80 | | TEST |
| 2004 | A1 | 42 | 10 | 11.80 | | TEST |
| | A2 | 20 | 15 | 9.36 | | TEST |
| | A6 | 13 | 21 | 2.50 | | TEST |
| | A20 | 18 | 30 | 6.80 | | TEST |
| | A23 | 14 | 32 | 9.60 | | TEST |
| | A25 | 17 | 42 | 13.40 | | TEST |
| | A27 | 15 | 36 | 8.60 | | TEST |
| | A29 | 11 | 41 | 9.80 | | TEST |
| | A30 | 16 | 36 | 7.60 | | TEST |
| | A32 | 18 | 32 | 7.40 | | TEST |
| | A33 | 19 | 30 | 5.90 | | TEST |

#### 4.1.3.4 Drummond wellfield spatial model

Groundwater nitrate distribution in Drummond wellfield area was studied in this effort in the manner similar to other three individual wellfield spatial models. Figure 4-9 shows the area included in this model. A total of 121 data points from 1997 to 2005 (except 2000) were used in this model. The observed data shows that nitrate concentrations were relatively less in the wells of this wellfield compared with others since the aquifer is semi-confined and the percent of clay is also high in this area. Table 4-6 presents the training and testing data sets used in this model which are arranged in the same way as previously explained Tables 4-3, 4-4, and 4-5.

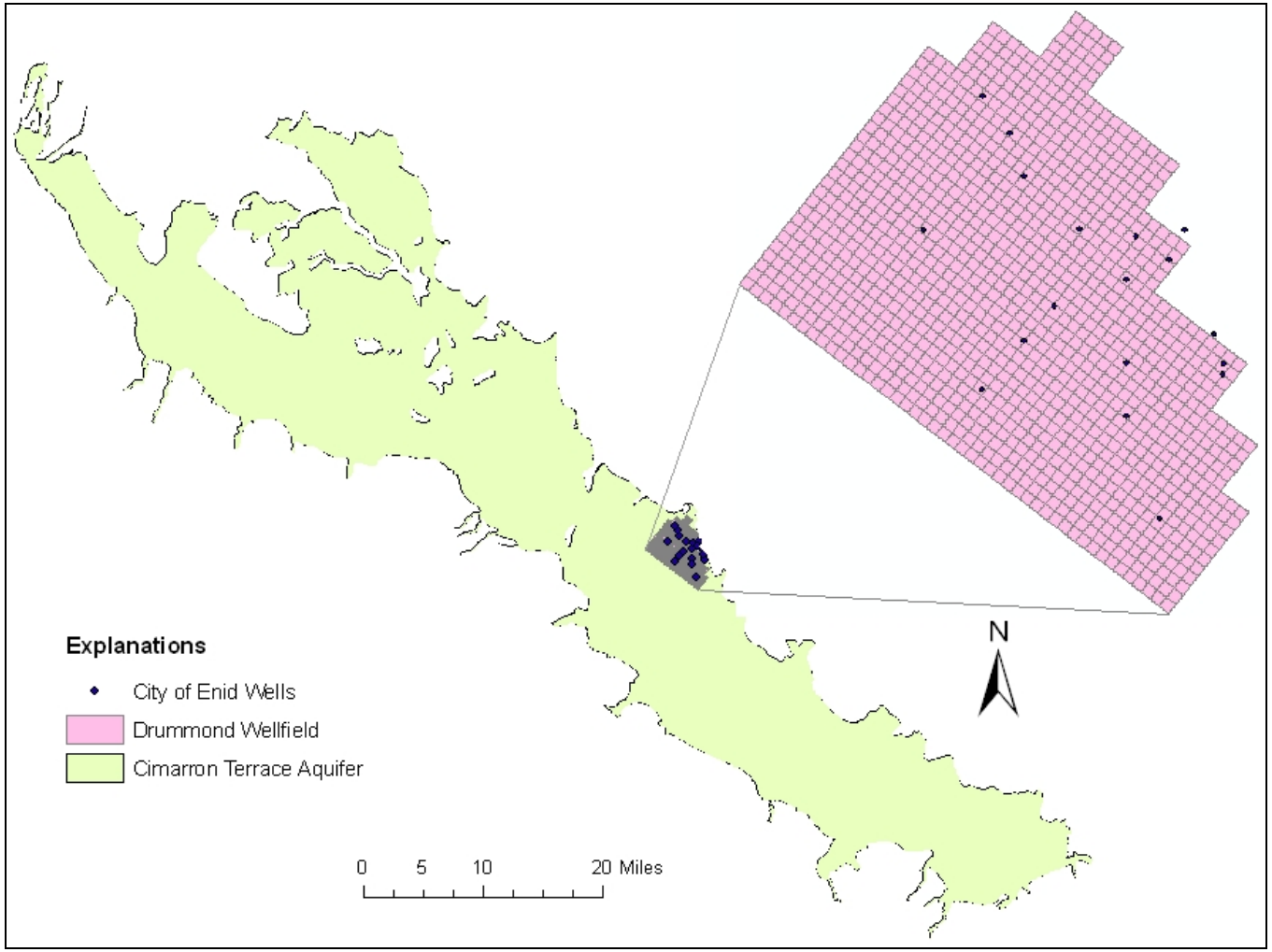


**Figure 4-9. Location of focused area in Drummond wellfield model**

**Table 4-6. Training and testing data sets for Drummond wellfield spatial model**

| Year | Well_ID | Input | | Target | Output | MF |
|---|---|---|---|---|---|---|
| | | X-Cord | Y-Cord | $NO_3$ (mg/L) | | |
| 1997 | D3 | 15 | 24 | 8.04 | | TRAIN |
| | D5 | 21 | 21 | 6.06 | | TRAIN |
| | D6 | 24 | 23 | 5.40 | | TRAIN |
| | D8 | 25 | 19 | 10.43 | | TRAIN |
| | D12 | 6 | 25 | 4.83 | | TRAIN |
| | D18 | 19 | 10 | 6.52 | | TRAIN |
| | D20 | 15 | 17 | 6.94 | | TRAIN |
| | D21 | 12 | 14 | 5.73 | | TRAIN |
| | D23 | 6 | 6 | 8.50 | | TRAIN |
| | D25 | 22 | 27 | 6.75 | | TRAIN |
| | D27 | 23 | 33 | 5.50 | | TRAIN |
| | D29 | 26 | 40 | 6.84 | | TRAIN |
| | D31 | 16 | 33 | 5.40 | | TRAIN |
| | D32 | 11 | 41 | 3.40 | | TRAIN |
| | D33 | 14 | 37 | 3.99 | | TRAIN |
| 1998 | D1 | 20 | 10 | 8.20 | | TRAIN |
| | D3 | 15 | 24 | 9.45 | | TRAIN |
| | D5 | 21 | 21 | 9.38 | | TRAIN |
| | D6 | 24 | 23 | 6.86 | | TRAIN |
| | D8 | 25 | 19 | 12.90 | | TRAIN |
| | D12 | 6 | 25 | 5.54 | | TRAIN |
| | D18 | 19 | 10 | 9.08 | | TRAIN |
| | D20 | 15 | 17 | 8.50 | | TRAIN |
| | D21 | 12 | 14 | 7.09 | | TRAIN |
| | D23 | 6 | 6 | 12.45 | | TRAIN |
| | D25 | 22 | 27 | 8.70 | | TRAIN |
| | D26 | 20 | 31 | 3.60 | | TRAIN |
| | D27 | 23 | 33 | 8.84 | | TRAIN |
| | D28 | 25 | 36 | 8.60 | | TRAIN |
| | D29 | 26 | 40 | 9.43 | | TRAIN |
| | D31 | 16 | 33 | 3.93 | | TRAIN |
| | D32 | 11 | 41 | 4.40 | | TRAIN |
| | D33 | 14 | 37 | 5.58 | | TRAIN |
| 2001 | D3 | 15 | 24 | 9.00 | | TRAIN |
| | D5 | 21 | 21 | 9.00 | | TRAIN |
| | D6 | 24 | 23 | 6.88 | | TRAIN |
| | D8 | 25 | 19 | 10.70 | | TRAIN |
| | D12 | 6 | 25 | 5.70 | | TRAIN |
| | D18 | 19 | 10 | 9.63 | | TRAIN |
| | D20 | 15 | 17 | 8.60 | | TRAIN |
| | D21 | 12 | 14 | 7.28 | | TRAIN |
| | D23 | 6 | 6 | 10.75 | | TRAIN |
| | D25 | 22 | 27 | 8.00 | | TRAIN |
| | D29 | 26 | 40 | 9.23 | | TRAIN |

**Table 4-6. (Continued)**

| Year | Well_ID | Input | | Target | Output | MF |
|---|---|---|---|---|---|---|
| | | X-Cord | Y-Cord | $NO_3$ (mg/L) | | |
| 2001 | D32 | 11 | 41 | 4.73 | | TRAIN |
| | D33 | 14 | 37 | 7.30 | | TRAIN |
| 2002 | D1 | 20 | 10 | 7.00 | | TRAIN |
| | D2 | 11 | 25 | 9.20 | | TRAIN |
| | D3 | 15 | 24 | 9.13 | | TRAIN |
| | D5 | 21 | 21 | 9.33 | | TRAIN |
| | D6 | 24 | 23 | 7.07 | | TRAIN |
| | D8 | 25 | 19 | 10.80 | | TRAIN |
| | D12 | 6 | 25 | 5.51 | | TRAIN |
| | D18 | 19 | 10 | 8.50 | | TRAIN |
| | D20 | 15 | 17 | 8.44 | | TRAIN |
| | D21 | 12 | 14 | 7.65 | | TRAIN |
| | D23 | 6 | 6 | 10.60 | | TRAIN |
| | D25 | 22 | 27 | 7.53 | | TRAIN |
| | D27 | 23 | 33 | 7.07 | | TRAIN |
| | D28 | 25 | 36 | 10.00 | | TRAIN |
| | D29 | 26 | 40 | 9.11 | | TRAIN |
| | D33 | 14 | 37 | 5.97 | | TRAIN |
| 2003 | D1 | 20 | 10 | 3.60 | | TRAIN |
| | D2 | 11 | 25 | 8.20 | | TRAIN |
| | D3 | 15 | 24 | 8.85 | | TRAIN |
| | D5 | 21 | 21 | 9.80 | | TRAIN |
| | D6 | 24 | 23 | 6.80 | | TRAIN |
| | D8 | 25 | 19 | 10.45 | | TRAIN |
| | D12 | 6 | 25 | 5.43 | | TRAIN |
| | D18 | 19 | 10 | 8.93 | | TRAIN |
| | D20 | 15 | 17 | 8.53 | | TRAIN |
| | D21 | 12 | 14 | 7.60 | | TRAIN |
| | D23 | 6 | 6 | 10.73 | | TRAIN |
| | D25 | 22 | 27 | 7.68 | | TRAIN |
| | D27 | 23 | 33 | 6.90 | | TRAIN |
| | D28 | 25 | 36 | 9.60 | | TRAIN |
| | D29 | 26 | 40 | 9.30 | | TRAIN |
| | D33 | 14 | 37 | 6.00 | | TRAIN |
| 2005 | D1 | 20 | 10 | 4.00 | | TRAIN |
| | D5 | 21 | 21 | 10.00 | | TRAIN |
| | D6 | 24 | 23 | 7.25 | | TRAIN |
| | D12 | 6 | 25 | 5.80 | | TRAIN |
| | D18 | 19 | 10 | 8.80 | | TRAIN |
| | D20 | 15 | 17 | 8.70 | | TRAIN |
| | D21 | 12 | 14 | 7.40 | | TRAIN |
| | D23 | 6 | 6 | 11.05 | | TRAIN |
| | D25 | 22 | 27 | 7.24 | | TRAIN |

**Table 4-6. (Continued)**

| Year | Well_ID | Input | | Target | Output | MF |
|---|---|---|---|---|---|---|
| | | X-Cord | Y-Cord | $NO_3$ (mg/L) | | |
| 2005 | D27 | 23 | 33 | 7.10 | | TRAIN |
| | D29 | 26 | 40 | 9.40 | | TRAIN |
| | D33 | 14 | 37 | 5.85 | | TRAIN |
| 1999 | D2 | 11 | 25 | 7.30 | | TEST |
| | D3 | 15 | 24 | 9.48 | | TEST |
| | D5 | 21 | 21 | 9.66 | | TEST |
| | D6 | 24 | 23 | 6.95 | | TEST |
| | D8 | 25 | 19 | 12.40 | | TEST |
| | D12 | 6 | 25 | 5.51 | | TEST |
| | D18 | 19 | 10 | 9.36 | | TEST |
| | D20 | 15 | 17 | 8.43 | | TEST |
| | D21 | 12 | 14 | 7.09 | | TEST |
| | D23 | 6 | 6 | 11.73 | | TEST |
| | D25 | 22 | 27 | 8.23 | | TEST |
| | D26 | 20 | 31 | 6.95 | | TEST |
| | D27 | 23 | 33 | 8.65 | | TEST |
| | D28 | 25 | 36 | 7.80 | | TEST |
| | D29 | 26 | 40 | 9.41 | | TEST |
| | D31 | 16 | 33 | 6.20 | | TEST |
| | D32 | 11 | 41 | 4.38 | | TEST |
| | D33 | 14 | 37 | 5.98 | | TEST |
| 2004 | D3 | 15 | 24 | 9.00 | | TEST |
| | D5 | 21 | 21 | 10.12 | | TEST |
| | D6 | 24 | 23 | 6.96 | | TEST |
| | D8 | 25 | 19 | 10.53 | | TEST |
| | D12 | 6 | 25 | 5.60 | | TEST |
| | D18 | 19 | 10 | 9.05 | | TEST |
| | D20 | 15 | 17 | 8.80 | | TEST |
| | D21 | 12 | 14 | 7.40 | | TEST |
| | D23 | 6 | 6 | 11.28 | | TEST |
| | D25 | 22 | 27 | 7.60 | | TEST |
| | D27 | 23 | 33 | 6.76 | | TEST |
| | D29 | 26 | 40 | 9.48 | | TEST |
| | D33 | 14 | 37 | 5.56 | | TEST |

With the configuration presented in Table 4-6 different network alternatives were evaluated by varying the network architecture until some consistency in results in terms of prediction accuracy and numbers of iterations were achieved. Performances of various networks evaluated in this effort are discussed in detail in results section. The architecture

with consistent prediction and least training time required was determined as best model. Finally, the best model was used to predict the nitrate concentrations at the locations where was not measured.

## 4.3 Constituent relationship models

With a spatial modeling approach, a relationship between the spatial locations of the aquifer and the nitrate concentrations was established. The constituent relationship models were developed for individual wellfield to establish the relationship between surface nitrogen application rate and nitrate concentrations in each well of the four wellfileds. The basic objective of developing constituent relationship models was to further expand these models as management models.

In a study KC (2007) performed logistic regression analysis to establish a relationship between groundwater nitrate and the type of land cover around the sampled wells in Cimarron Terrace Aquifer. The results reveled that land use at a 1,000 meter radial distance from the well had significant effect on nitrate concentration in the corresponding well. Figure 4-10 shows the land use types within this radial distance. Hence, nitrogen application rates in 1,000 meter radial distance of each well were determined. A county-wide fertilizer nitrogen of 110 kg/ha was apportioned equally to agricultural and developed land to account for residential fertilizer use.

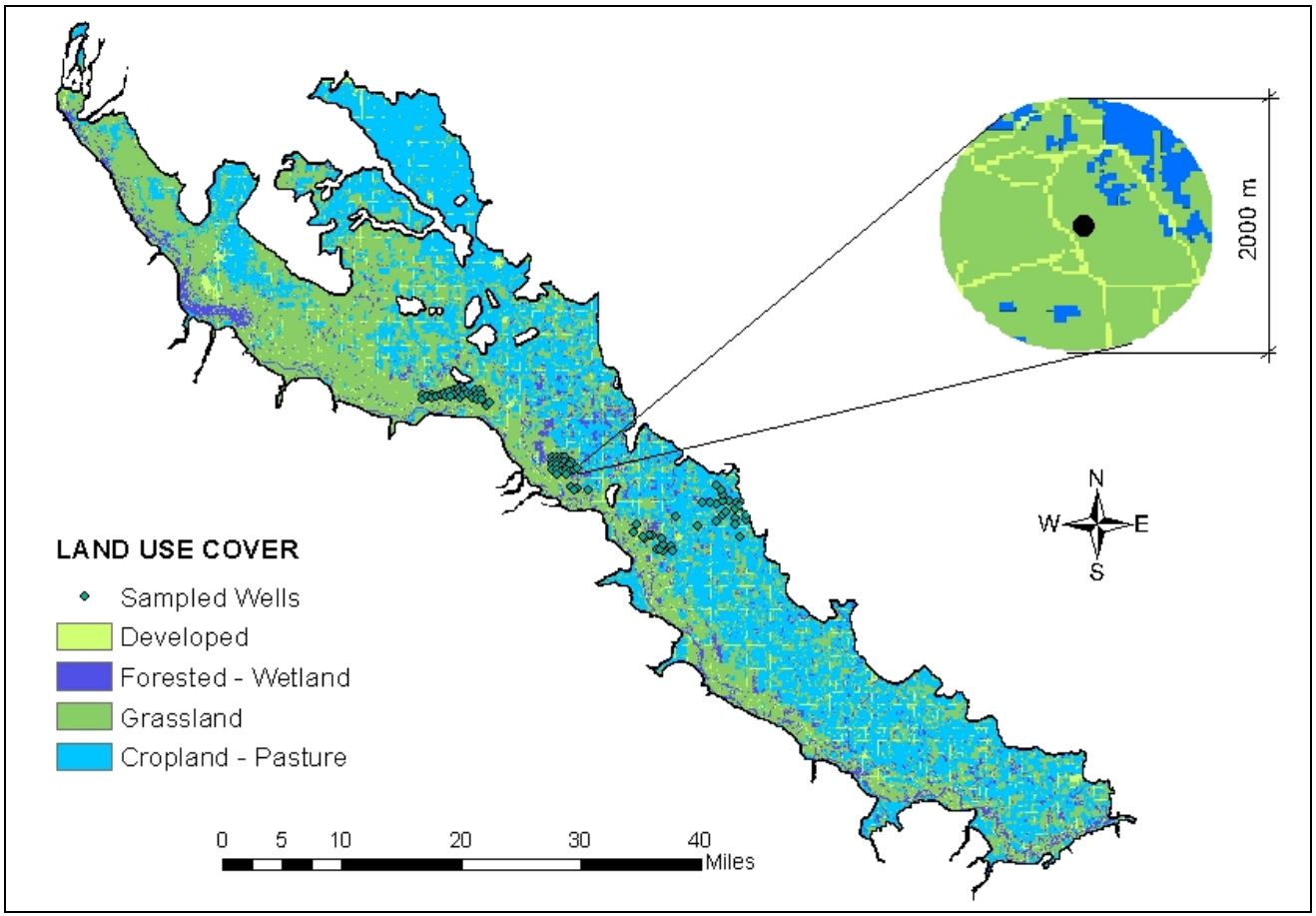


**Figure 4-10. Extractions of land cover variables within a statistical area of well influence around each groundwater well sampled in the Cimarron Terrace Aquifer (KC, 2007)**

Table 4-7 to 4-10 presents the model configuration for Cleospring, Ringwood, Ames, and Drummond constituent relationship model respectively. The first column of each model presents the well identification, and second column presents the nitrogen application rate in kg per square mile in 1000 meter radial distance of wells corresponding in column one. Third column presents the observed nitrate concentrations in the wells corresponding to column one. The output column presents the predicted nitrate concentrations in each well after training and testing the model, and the fifth "mode flag" column categorizes the target observed nitrate concentrations as training and testing. Twenty percent of randomly selected nitrate concentrations in each wellfields were used for testing and rest of them for training. To determine the best model, different alternatives were tried by varying the network architecture until some consistency in results in terms of prediction accuracy and numbers of iterations were achieved. The best model determination is described in detail in Results.

**Table 4-7. Cleospring wellfield constituent relationship model configuration**

| Well_ID | Input | Target | Output | MF |
|---|---|---|---|---|
| | Nitrogen Application (kg/sq. mile) | $NO_3$ (mg/L) | | |
| CS29 | 5.987 | 0.90 | | TEST |
| CS28 | 3.014 | 1.00 | | TRAIN |
| CS2 | 5.592 | 1.25 | | TRAIN |
| CS26 | 3.482 | 1.65 | | TRAIN |
| CS27 | 3.466 | 1.80 | | TRAIN |
| CS1 | 6.179 | 2.95 | | TRAIN |
| CS25 | 3.877 | 3.00 | | TEST |
| CS19 | 17.099 | 3.20 | | TEST |
| CS3 | 23.952 | 3.90 | | TRAIN |
| CS23 | 14.578 | 3.90 | | TEST |
| CS22 | 2.871 | 4.05 | | TRAIN |
| CS8 | 38.636 | 4.60 | | TRAIN |
| CS4 | 14.713 | 4.70 | | TEST |
| CS13 | 31.334 | 4.70 | | TRAIN |
| CS12 | 21.270 | 4.75 | | TRAIN |
| CS14 | 39.480 | 4.80 | | TRAIN |
| CS11 | 12.863 | 5.00 | | TRAIN |
| CS30 | 5.075 | 5.10 | | TRAIN |
| CS16 | 22.739 | 6.05 | | TRAIN |
| CS6 | 32.113 | 6.75 | | TEST |
| CS5 | 27.513 | 7.35 | | TRAIN |
| CS9 | 26.156 | 7.45 | | TRAIN |
| CS15 | 21.258 | 8.35 | | TRAIN |
| CS17 | 29.845 | 8.40 | | TRAIN |
| CS10 | 27.049 | 8.70 | | TRAIN |
| CS20 | 18.154 | 13.95 | | TRAIN |
| CS21 | 14.623 | 13.95 | | TRAIN |
| CS18 | 34.815 | 16.00 | | TRAIN |

**Table 4-8. Ringwood wellfield constituent relationship model configuration**

| Well_ID | Input | Target | Output | MF |
|---|---|---|---|---|
| | Nitrogen Application (kg/sq. mile) | $NO_3$ (mg/L) | | |
| R24 | 9.827 | 3.45 | | TEST |
| R25 | 4.171 | 3.70 | | TRAIN |
| R22 | 11.375 | 4.20 | | TRAIN |
| R17 | 11.353 | 4.70 | | TRAIN |
| R18 | 9.906 | 5.10 | | TRAIN |
| R19 | 8.975 | 5.10 | | TRAIN |
| R15 | 8.817 | 5.25 | | TRAIN |
| R11 | 8.749 | 6.45 | | TEST |
| R12 | 8.821 | 6.45 | | TEST |
| R6 | 6.202 | 6.80 | | TEST |
| R10 | 8.282 | 7.00 | | TRAIN |
| R27 | 7.487 | 7.05 | | TRAIN |
| R2 | 3.681 | 7.25 | | TRAIN |
| R5 | 3.327 | 7.30 | | TRAIN |
| R7 | 8.734 | 7.30 | | TRAIN |
| R1 | 3.568 | 7.40 | | TRAIN |
| R13 | 9.371 | 7.70 | | TRAIN |
| R4 | 16.089 | 8.35 | | TRAIN |
| R16 | 9.386 | 8.40 | | TRAIN |
| R8 | 8.007 | 8.95 | | TEST |
| R3 | 9.823 | 9.15 | | TRAIN |
| R9 | 24.777 | 9.60 | | TRAIN |
| R20 | 20.772 | 10.80 | | TRAIN |
| R26 | 15.584 | 11.20 | | TRAIN |
| R14 | 20.772 | 12.10 | | TRAIN |
| R21 | 48.624 | 13.25 | | TEST |
| R28 | 56.427 | 15.60 | | TRAIN |

**Table 4-9. Ames wellfield constituent relationship model configuration**

| Well ID | Input | Target | Output | MF |
|---|---|---|---|---|
| | Nitrogen Application (kg/sq. mile) | $NO_3$ (mg/L) | | |
| A9 | 27.25 | 1.80 | | TRAIN |
| A6 | 62.20 | 2.47 | | TEST |
| A3 | 47.99 | 3.40 | | TRAIN |
| A8 | 27.08 | 3.60 | | TRAIN |
| A7 | 52.75 | 4.00 | | TRAIN |
| A5 | 38.31 | 5.20 | | TRAIN |
| A4 | 45.10 | 6.80 | | TEST |
| A20 | 31.17 | 6.80 | | TRAIN |
| A22 | 32.69 | 7.60 | | TRAIN |
| A27 | 13.64 | 7.80 | | TRAIN |
| A24 | 20.36 | 8.60 | | TEST |
| A2 | 84.32 | 9.30 | | TRAIN |
| A23 | 30.72 | 9.35 | | TRAIN |
| A29 | 8.59 | 9.40 | | TRAIN |
| A21 | 40.56 | 10.70 | | TRAIN |
| A1 | 70.54 | 11.73 | | TRAIN |
| A16 | 104.10 | 12.40 | | TRAIN |
| A14 | 84.05 | 13.00 | | TRAIN |
| A25 | 32.48 | 13.40 | | TRAIN |
| A11 | 72.99 | 13.60 | | TRAIN |
| A19 | 78.41 | 14.00 | | TEST |
| A18 | 70.36 | 14.80 | | TEST |
| A17 | 90.64 | 15.60 | | TRAIN |

**Table 4-10. Drummond wellfield constituent relationship model configuration**

| Well_ID | Input | Target | Output | MF |
|---|---|---|---|---|
| | Nitrogen Application (kg/sq. mile) | $NO_3$ (mg/L) | | |
| D9 | 54.299 | 3.07 | | TRAIN |
| D1 | 70.101 | 3.60 | | TRAIN |
| D10 | 75.093 | 4.87 | | TEST |
| D12 | 118.352 | 5.43 | | TRAIN |
| D19 | 59.483 | 6.00 | | TRAIN |
| D33 | 105.436 | 6.00 | | TRAIN |
| D6 | 102.591 | 6.80 | | TRAIN |
| D27 | 117.188 | 6.90 | | TRAIN |
| D21 | 117.354 | 7.60 | | TRAIN |
| D25 | 103.895 | 7.68 | | TRAIN |
| D2 | 94.901 | 8.20 | | TRAIN |
| D20 | 83.662 | 8.53 | | TRAIN |
| D3 | 83.507 | 8.85 | | TRAIN |
| D18 | 79.283 | 8.93 | | TRAIN |
| D29 | 125.688 | 9.30 | | TEST |
| D28 | 123.273 | 9.60 | | TRAIN |
| D5 | 78.266 | 9.80 | | TEST |
| D8 | 88.997 | 10.45 | | TEST |
| D23 | 107.207 | 10.73 | | TRAIN |
| D7 | 101.759 | 12.00 | | TRAIN |

## 4.4 Management models

Control of potential contaminant sources and land use managements are the best options to protect the groundwater quality. The need to introduce management options to protect the groundwater quality of Cimarron Terrace Aquifer is of critical important. To identify the management options, management models were developed to represent current land use practices. The management modeling approach is based on the results of a study conducted by KC (2007) in Cimarron Terrace Aquifer.

In his study, KC (2007) also developed a multivariable logistic model which determined that developed land, fertilizer nitrogen, percent clay, and depth to water table were the most significant variables for the groundwater nitrate concentrations. Percent clay and depth of groundwater were the natural phenomenon and can not be altered to reduce groundwater nitrate contamination level. City of Enid and its surrounding areas are growing residential areas and reducing them may not be the practically feasible option. Therefore, reduction in application of fertilizer N was determined as a best option to protect the groundwater in Cimarron Terrace Aquifer.

Ames wellfield constituent relationship model with the best model architecture was used to developed management model since Ames wellfield was the most contaminated wellfield among the four. In this modeling effort, on ground nitrogen application rate was reduced and corresponding effect on the groundwater nitrate concentration in this wellfield was observed. The nitrate application rate was reduced 10% successively and the model was simulated to predict nitrate concentration. The nitrate application rate was reduced until the nitrate concentrations in each well of Ames wellfield were predicted below the MCL.

In order to accurately determine the amount of surface nitrogen application rates reduction, a separate Ames constituent relationship models was also developed for the wells with nitrate concentrations above 10 mg/L. Three data points with nitrate concentrations below 10 mg/L and less surface nitrogen application rate were also used to train the model; thus they could learn to predict low nitrate concentrations for less nitrogen application rate. Again, various networks with different architecture were executed to determine the best model. The developed best models were simulated with

subsequent 10 % reduction of surface nitrogen application rate until the nitrate concentrations in the wells were predicted below the MCL.

Table 4-11 presents the configuration of management model with nitrate concentration data above 10 mg/L and 10% reduction in nitrate application rate. Column one in the table presents the well of Ames wellfield with nitrate concentrations above 10 mg/L except wells A25, A27, and A29. Upper half of the column two presents the nitrogen application rate in current land use conditions and lower half of it presents the reduced value of nitrogen application by 10 %. Third column presents the observed nitrate concentrations in the wells corresponding to column one. The models were trained and tested to predict nitrate concentrations with reduced nitrogen application rate. The training and testing data were categorized as mentioned in the “mode flag” column.

**Table 4-11. Ames wellfield management model**

| Well_ID | Input | Target | Output | MF |
|---|---|---|---|---|
| | Nitrogen application (kg/sq. mile) | $NO_3$ (mg/L) | | |
| A1 | 32.48 | 13.40 | | TRAIN |
| A11 | 40.56 | 10.70 | | TRAIN |
| A14 | 70.36 | 14.80 | | TRAIN |
| A16 | 70.54 | 11.73 | | TRAIN |
| A17 | 72.99 | 13.60 | | TEST |
| A18 | 78.41 | 14.00 | | TRAIN |
| A19 | 84.05 | 13.00 | | TEST |
| A21 | 90.64 | 15.60 | | TRAIN |
| A24 | 104.10 | 12.40 | | TRAIN |
| A25 | 13.64 | 7.80 | | TRAIN |
| A27 | 20.36 | 8.60 | | TRAIN |
| A29 | 8.59 | 9.40 | | TRAIN |
| A1 | 29.23 | | | TEST |
| A11 | 36.50 | | | TEST |
| A14 | 63.32 | | | TEST |
| A16 | 63.49 | | | TEST |
| A17 | 65.69 | | | TEST |
| A18 | 70.57 | | | TEST |
| A19 | 75.65 | | | TEST |
| A21 | 81.58 | | | TEST |
| A24 | 93.69 | | | TEST |
| A25 | 12.28 | | | TEST |
| A27 | 18.32 | | | TEST |
| A29 | 7.73 | | | TEST |

## 4.5 Stochastic model

The Ames management model was used as a base for the stochastic or neural conditional simulation. The Ames management model employed nitrogen application rates as inputs, which were then targeted to predict nitrate concentrations in each well.

The Ames constituent relationship model was initiated as the base approach for additional simulations. The randomly selected neural estimation weights were altered sequentially and additional simulations were completed. The mean and standard deviation of predicted nitrate concentration in each well of Ames wellfield were determined with each successive simulation and plotted versus number of simulations. The conditional simulation was considered complete when these plot asymptoted to a constant value. The prediction of constant value indicated that the level of maximum precision had been reached.

Probability and cumulative density function were then developed for each well's nitrate concentration with @Risk (Palisades Crop, 2002) software. @ Risk is an excel based risk analysis software, which plots the various distribution functions for the given set of data and allows the user to preview and select the best fit curve. The distributions can be set up using percentiles as well as standard parameters. In this study distributions were set up using percentiles and the $50^{th}$ and $95^{th}$ percentile probability of predicted nitrate concentrations in each well of Ames wellfield were identified.

# CHAPTER 5

# RESULTS

This chapter presents the results of all the analysis methods explained in Chapter 4. This includes results of spatial models, constitutive relationship models, the management model, and the stochastic model.

## 5.1 Spatial models

In the following sections of spatial models, outputs of an overall aquifer spatial model, a central area spatial model, and individual wellfields spatial models are presented.

### 5.1.1 Overall aquifer model

In this modeling effort, the entire aquifer was considered. Table 5-1 lists the model architecture, and results obtained in terms of number of layers, neurons per layers, training tolerance, percentage of "Right" scores, and training epochs in this modeling approach**.**

**Table 5-1 Alternatives for building overall aquifer model**

| Network no. | No. of layers | Neurons per layer* | Training tolerance | % Right | Epochs |
|---|---|---|---|---|---|
| 1 | 3 | 2-20-1 | 0.1 | 85 | 18986 |
| 2 | 3 | 2-34-1 | 0.1 | 85 | 13256 |
| 3 | 3 | 2-46-1 | 0.1 | 85 | 8336 |
| 4 | 3 | 2-61-1 | 0.1 | 85 | 7774 |
| 5 | 3 | 2-46-1 | 0.2 | 85 | 7796 |
| 6 | 3 | 2-61-1 | 0.2 | 85 | 7632 |
| 7 | 3 | 2-70-1 | 0.2 | 85 | 9293 |
| 8 | 3 | 2-61-1 | 0.27 | 85 | 7395 |

* each value corresponds to number of neurons in input layer, hidden layer, and output layer respectively. Other parameters: Learning Rate = 1.0; Momentum = 0.9; Input Noise = 0; Testing Tolerance = 0.3, Error Limit = 0.01 (All the other parameters have default values except Error Limit)

The model was initially started with default parameter settings and a small number of neurons in the hidden layer. Subsequently, the numbers of neurons in hidden layers, and default value of training tolerance (0.1) were increased to see the effect on prediction precision and time required to train the model.

All of the three layers, back propagation network alternatives for this model had consistent prediction rate of 85% "Right". The percentage of "Right" scores was measured by the number of predictions within the specified tolerance limit of the testing data. Changes in number of hidden neurons and training tolerance had no effect on this percentage. However, the epochs required to train the model and root-mean-square (RMS) error were sensitive to these architectural modification.

Figure 5-1 presents the RMS error plots for the network alternatives presented in Table 5-1. RMS error plots, used to monitor the network training and testing process, present the differences between the actual output and the target output in training and testing data after every simulation. The RMS plots serve two purposes: (1) they tell us the maximum learning achieved and (2) they tell us the consistency in the learning approach (Kumar, 2000). Theoretically, when the training curve dips to zero on the y-axis, the

learning is said to be complete. If there are sharp peaks in the curve, rather than a gradual decent or a straight line, the network learning is considered inappropriate and the predictions are thought to be unreliable. In this case, learning was considered complete when the error graph achieved a constant value and plot achieved a straight line.

.

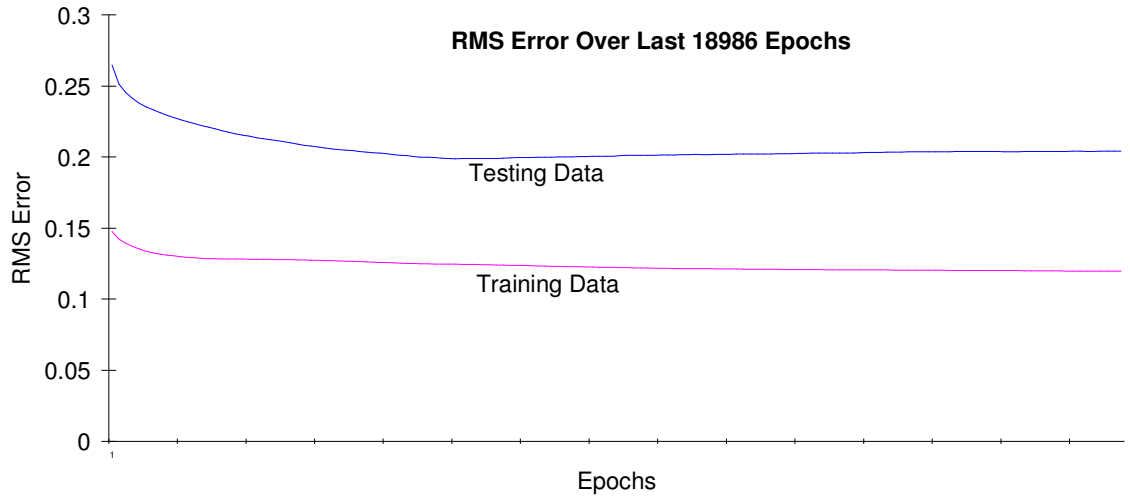


**Network no. 1**

**Figure 5-1. RMS error plots of various alternatives**

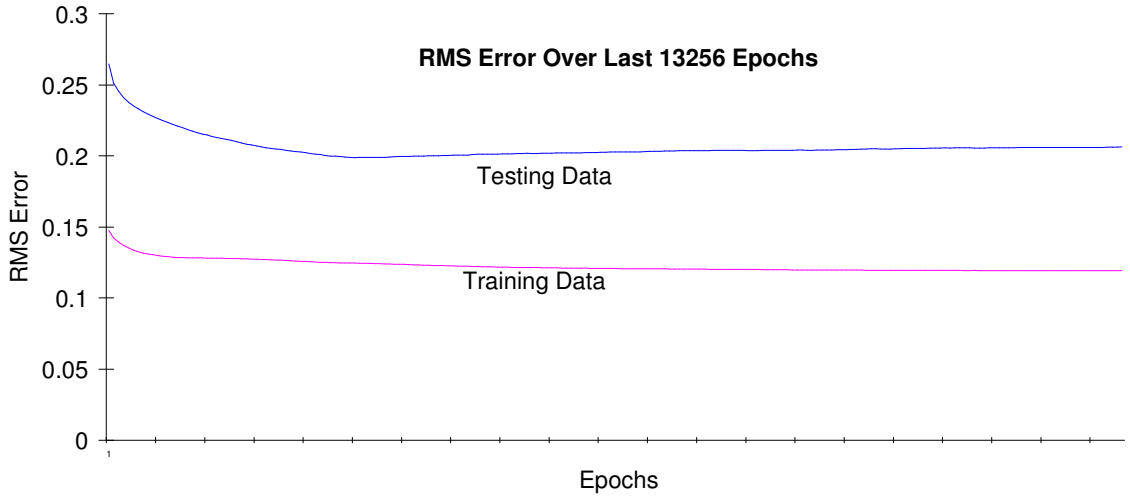

**Network no. 2**

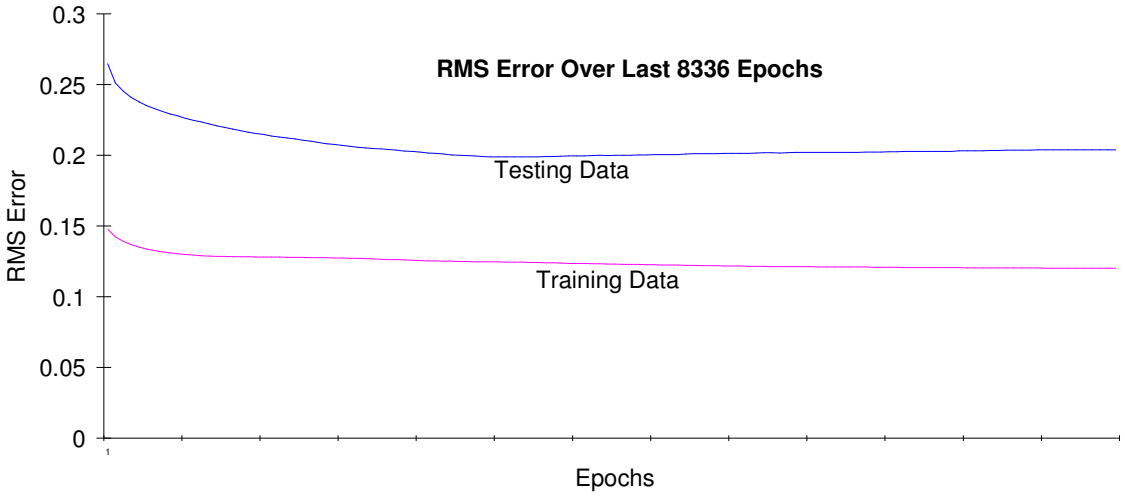


**Network no. 3**

**Figure 5-1. RMS error plots of various alternatives (Continued)**

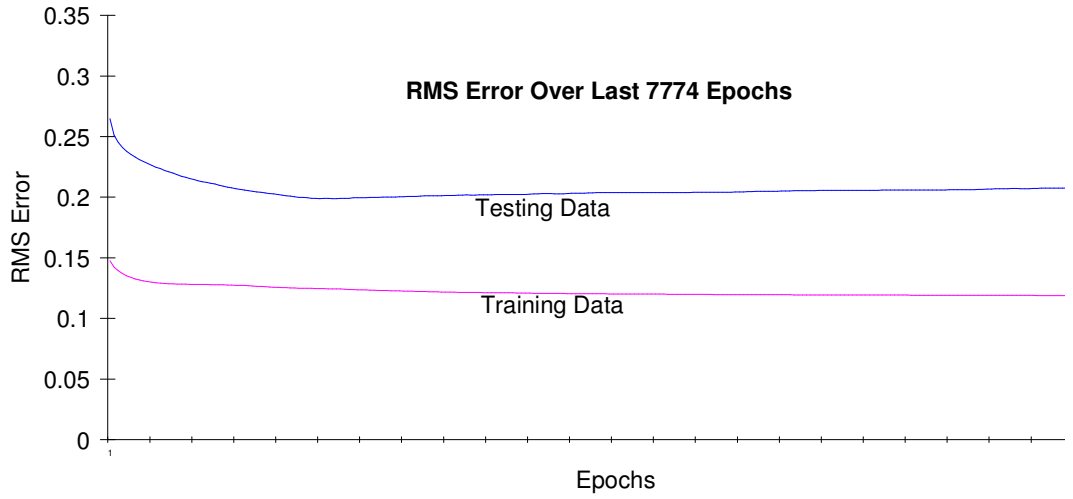


**Network no. 4**

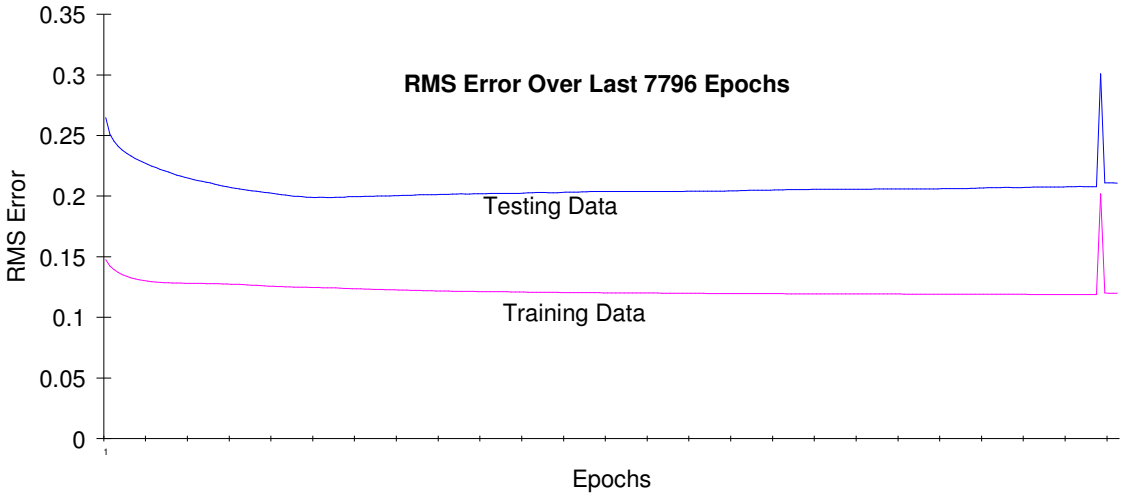


**Network no. 5**

**Figure 5-1. RMS error plots of various alternatives (Continued)**

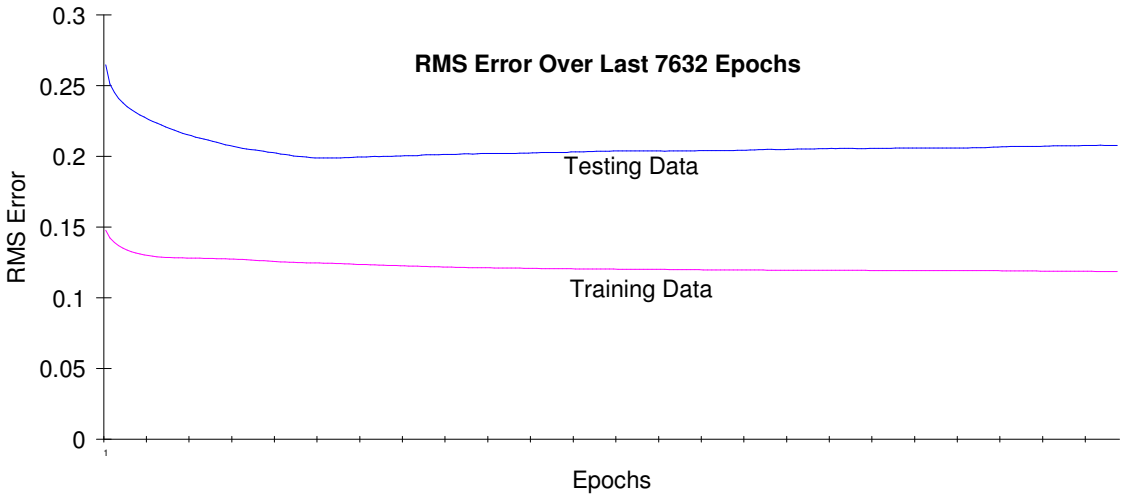


**Network no. 6**

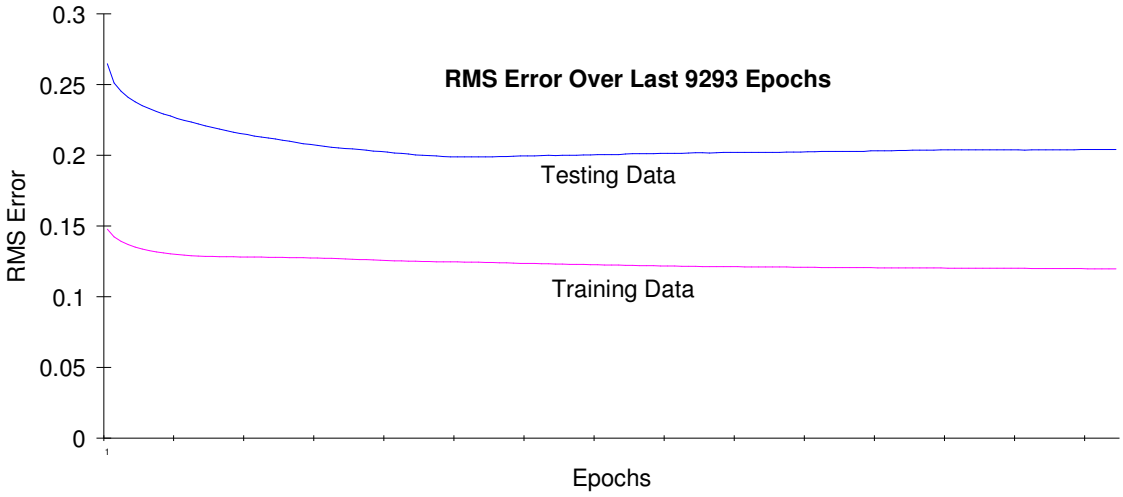


**Network no. 7**

**Figure 5-1. RMS error plots of various alternatives (Continued)**

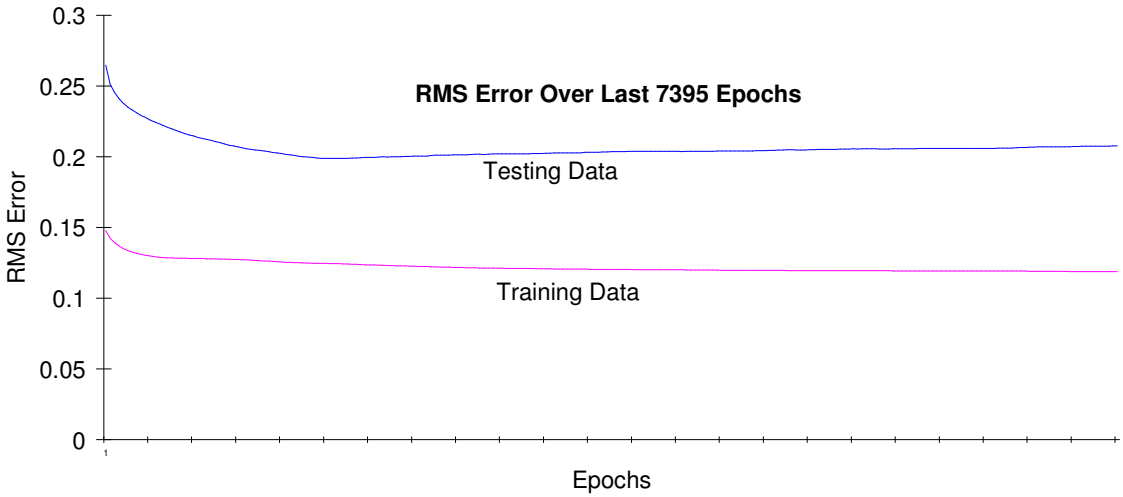


**Network no. 8**

**Figure 5-1. RMS error plots of various alternatives (Continued)**

With the exception of network number 5, all the RMS error plots for networks presented in Table 5-1 exhibited similar characteristics; a gradual stabilization over the epochs was achieved. After a while the plots achieve the constant straight lines indicating that the models had learned maximum and further training does not improve the learning of the models. This is considered to be ideal "learning" behavior (Kumar, 2000). Network with 61 neurons in the hidden layer (network no. 4, 6, and 8) exhibited the most consistent plot. Since, the percentage "Right" in all the cases was the same, the best model configuration was decided on the basis of the time required for training (i.e. epochs required for training). Network number 8 required the least training epochs and was selected as best model and was used to predict groundwater nitrate concentrations at other unmeasured locations. Table 5-2 presents the example of best model nitrate concentration predictions at the locations where nitrate concentrations were measured and they were used for training the model, at the locations where nitrate concentrations were measured and they were used for testing the model, and at the locations where nitrate concentrations were not measured.

**Table 5-2. Example of overall aquifer model outputs**

| Well_ID | Input | | Target | Output | MF |
|---|---|---|---|---|---|
| | X-Cord | Y-Cord | $NO_3$_2003 (mg/L) | $NO_3$_2003 (mg/L) | |
| W1 | 15 | 9 | 9.37 | 10.79 | TRAIN |
| W2 | 16 | 22 | 12.30 | 10.62 | TRAIN |
| W3 | 7 | 36 | 2.19 | 6.85 | TRAIN |
| A5,W14 | 13 | 72 | 4.71 | 8.03 | TRAIN |
| A4 | 14 | 72 | 6.80 | 8.38 | TRAIN |
| A23,A22,A20,W16 | 15 | 75 | 8.14 | 8.62 | TRAIN |
| D12 | 22 | 69 | 5.43 | 10.18 | TRAIN |
| D21,D20 | 24 | 67 | 8.07 | 10.10 | TRAIN |
| R22 | 14 | 90 | 4.20 | 7.79 | TRAIN |
| R24,R18 | 15 | 89 | 4.28 | 8.07 | TRAIN |
| R16,R17,R12,W21 | 15 | 90 | 5.31 | 8.02 | TRAIN |
| CS10 | 13 | 108 | 8.70 | 6.73 | TRAIN |
| CS17 | 14 | 107 | 8.40 | 6.91 | TRAIN |
| A21 | 15 | 74 | 10.7 | 8.65 | TEST |
| A18 | 18 | 73 | 14.8 | 9.51 | TEST |
| A16 | 20 | 72 | 12.4 | 9.88 | TEST |
| D2 | 23 | 69 | 8.2 | 10.06 | TEST |
| | 1 | 26 | | 4.73 | TEST |
| | 2 | 26 | | 5.07 | TEST |
| | 2 | 27 | | 5.05 | TEST |
| | 2 | 126 | | 3.51 | TEST |
| | 15 | 170 | | 0.56 | TEST |
| | 15 | 175 | | 0.26 | TEST |
| | 15 | 176 | | 0.20 | TEST |
| | 16 | 4 | | 11.28 | TEST |
| | 16 | 5 | | 11.25 | TEST |

The predicted nitrate concentrations are presented in the output column. Each value represents the nitrate concentrations in the grids represented by (X,Y) coordinates in column 2 and 3, respectively. The predicted concentrations were then linked to a GIS to develop the groundwater nitrate concentration map for the entire Cimarron Terrace Aquifer. The predicted nitrate concentrations were first categorized as low, moderate, and high according to the concentrations were below 4.0 mg/L, 4.1 to 10.0 mg/L, and above 10.1 mg/L, respectively, and presented in Figure 5-2.

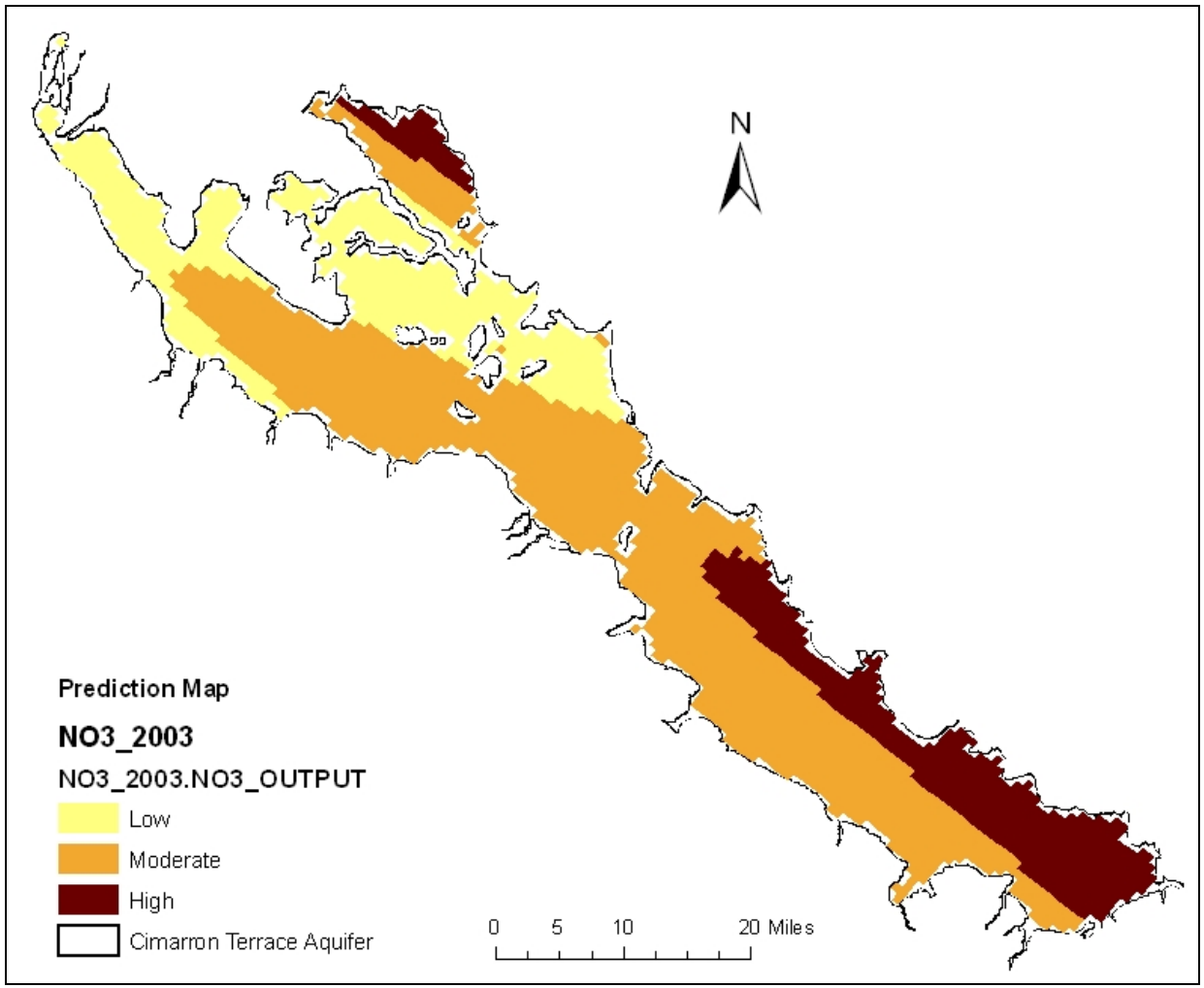


**Figure 5-2. Neural kriging estimation of groundwater nitrate distribution for the year 2003 in Cimarron Terrace Aquifer**

The model was able to expand the point data into block data identifying the general distribution pattern of nitrate concentrations in the entire aquifer. The map shows that the groundwater nitrate concentration gradually increases from northwest to southeast in the aquifer. The 2001 NLCD previously presented in Figure 2-3 shows that grasslands were predominant in the northwest and as aquifer progresses towards south east cultivated land were increased. The model predicted the low nitrate concentrations in grassland dominated areas and high concentrations in cultivated areas, which are evident. Table 5-3 presents the areas of aquifer in three ranges of predicted nitrate concentrations.

**Table 5-3. Areas of nitrate concentrations in three different ranges**

| **Concentration x (mg/L)** | **Area (square miles)** | **Percent of total area considered in overall aquifer model** |
|---|---|---|
| $x \leq 4$ | 230.65 | 22.73 |
| $4 < x \leq 10$ | 588.59 | 58.01 |
| $x>10$ | 195.34 | 19.25 |

The predicted nitrate concentrations shows that more then 50 percent of the Cimarron Terrace Aquifer has nitrate concentrations in the range of 4-10 mg/L. Nitrate concentrations of $\leq 4$ mg/L were predicted in 22.73 percent of the total area and 19.25 percent of the Cimarron Terrace Aquifer was contaminated above the MCL.

Table 5-4 presents the calculated mean absolute percentage error (MAPE) for the predicted nitrate concentrations. The error criteria suggest that nitrate concentrations were best predicted with this model configuration in moderate concentration range. High errors were associated with the low concentrations since the model tended to over predict the low values in comparison to the measured concentrations. Similarly, the mean

absolute percentage error of 41.18 percent for high concentrations, suggest that the model did not predicted the high concentrations adequately.

**Table 5-4. Calculated mean absolute percentage error (MAPE) for comparisons between observed and predicted nitrate concentrations by overall aquifer model**

| Concentrations (x mg/L) Evaluated | Mean Concentration (mg/L) | Calculated Error* (mg/L) | Percent of Mean |
|---|---|---|---|
| All | 8.30 | 3.42 | 41.36 |
| Low (x ≤ 4) | 2.30 | 4.14 | 176.74 |
| Moderate (4 < x ≤ 10) | 7.32 | 1.59 | 21.72 |
| High (10 < x) | 15.06 | 6.20 | 41.18 |

*$\text{Error}=1/N\sum_{i=1}^{N}|M-P|$

N = Number of samples
M = Measured concentration
P = Predicted concentration

The results showed that at the central part of the aquifer the predicted nitrate concentrations were in the range of 8.78 to10.20 mg/L. The observed nitrate concentrations in the Ames wellfield, which is located in the central part of the aquifer showed that nitrate concentration at this location were higher than this predicted range. A geostatistical study conducted by KC (2007) also showed that nitrate concentration in the central part of the aquifer was higher then that predicted by this model. This deficiency of the model may have been due to use of large amount of data in this model. Therefore, a model focusing only in the central part of the aquifer was developed.

### 5.1.2 Central area model

Table 5-5 lists the performance of nine neural network model architectures. The results obtained in terms of number of layers, neurons per layers, training tolerance, percentage of "Right" scores, and numbers of training epochs required in this modeling

approach are also listed. These models differed from the overall aquifer model in that they focused on that portion of the aquifer where the large model under-predicted nitrate concentrations. Initially a simple model with default parameters settings and small numbers of neurons in the hidden layer was developed. Subsequently the number of neurons in the hidden layers and training tolerance limit were increased in order to train the model in the least time and predict the results more accurately.

**Table 5-5. Alternatives for central area model**

| Network no. | No. of layers | Neurons per layer* | Training tolerance | % Right | Epochs |
|---|---|---|---|---|---|
| 1 | 3 | 2-10-1 | 0.1 | 73 | 10133 |
| 2 | 3 | 2-14-1 | 0.1 | 73 | 92134 |
| 3 | 3 | 2-19-1 | 0.1 | 73 | 19919 |
| 4 | 3 | 2-10-1 | 0.2 | 73 | 10235 |
| 5 | 3 | 2-14-1 | 0.2 | 73 | 8742 |
| 6 | 3 | 2-16-1 | 0.2 | 73 | 12076 |
| 7 | 3 | 2-10-1 | 0.25 | 73 | 10465 |
| 8 | 3 | 2-14-1 | 0.25 | 73 | 11635 |
| 9 | 3 | 2-61-1 | 0.27 | 73 | 9023 |

* each value corresponds to number of neurons in input layer, hidden layer, and output layer respectively. Other parameters: Learning Rate = 1.0; Momentum = 0.9; Input Noise = 0; Testing Tolerance = 0.3, Error Limit = 0.01 (All the other parameters have default values except Error Limit)

As before the percentage of "Right" scores was measured by the number of predictions within default tolerance limit (0.3) of the testing data. The testing data tolerance limit was same as that in overall aquifer model. All of the three layer back propagation network models had consistent predictions of 73% "Right". Changes in number of hidden neurons and training tolerance had no effect on this percentage. However, they had effect on epochs required to train the model and root-mean-square (RMS) error. Since, percentage "Right" in all the cases was same, the best model configuration was decided on the basis of time required for training i.e. epochs required

for training and RMS error plot. Network number 5 required the least training epochs, and the RMS error plot of network number 5 was a constant straight line after the maximum training was achieved. Figure 5-3 presents the RMS error plot of network no. 5. This network was selected as a best model among the alternatives evaluated and was used to predict groundwater nitrate concentrations at the locations of the central part of the aquifer where it was not measured. Figure 5-4 presents the predicted nitrate concentrations map at the central part of the Cimarron Terrace Aquifer.

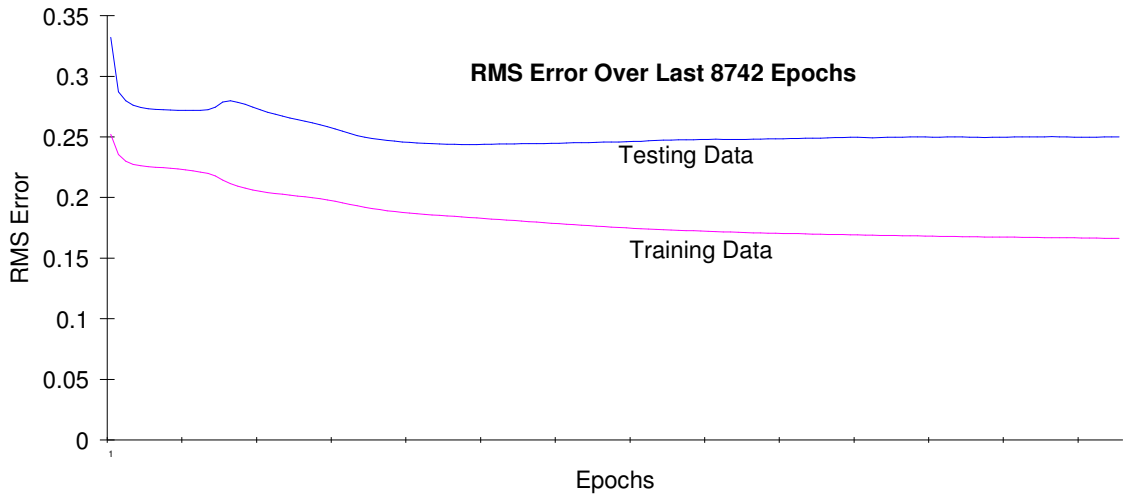


**Figure 5-3. RMS error plots of network no. 5**

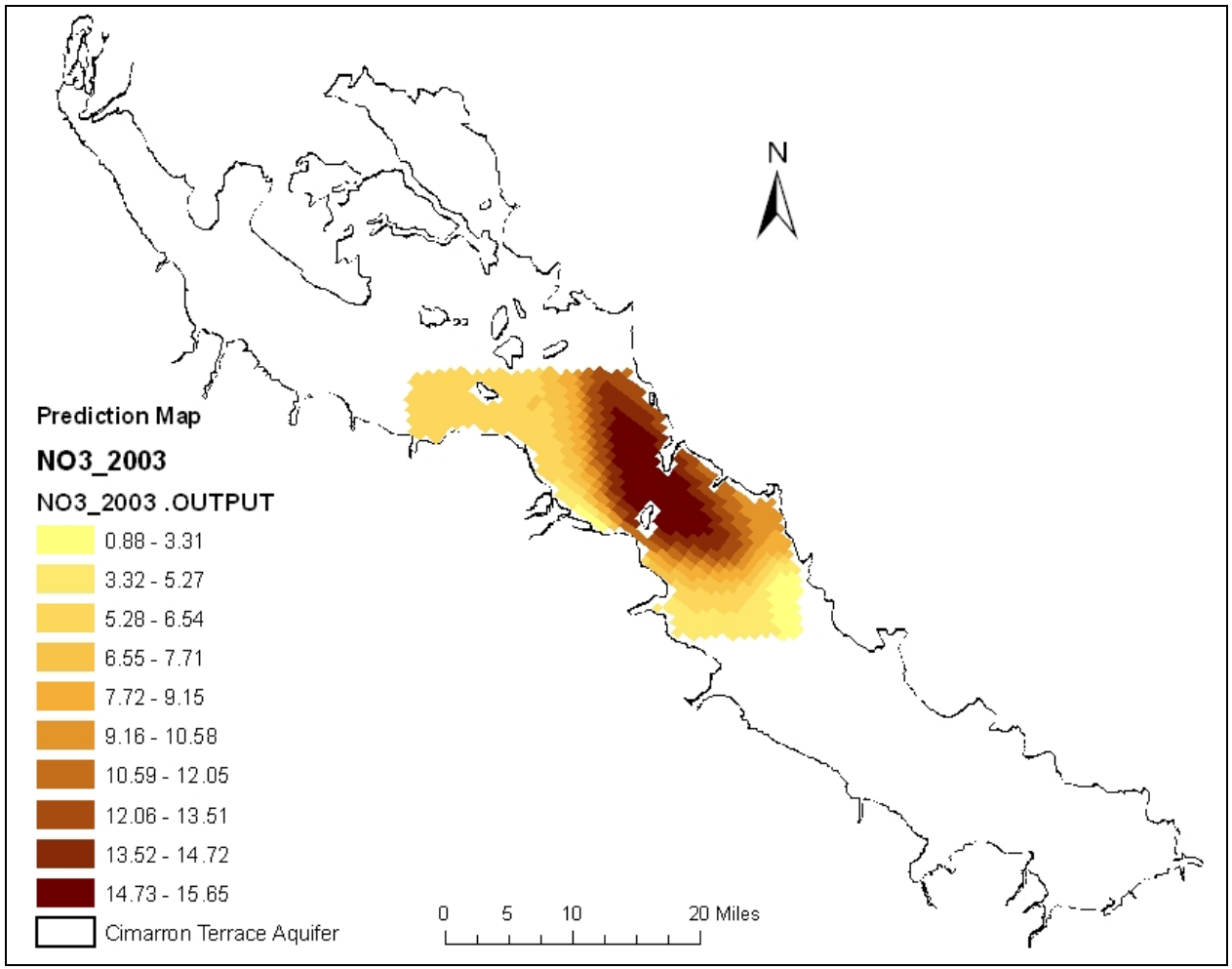


**Figure 5-4. Neural kriging estimation of groundwater nitrate distribution for the year 2003 in central area of Cimarron Terrace Aquifer**

The predicted concentrations showed that 115.87 sq. mile area at the core central part of the aquifer had nitrate concentration in the range of 10.59 mg/L to 15.65 mg/L. The predicted concentration was consistent with the results of kriging analysis conducted by KC (2007), which had estimated the nitrate concentration of 12.79 to 16.00 mg/L in the central area. Additionally, the highest measured nitrate concentrations of 15.3 mg/L in the Ames wellfield, which is at the central part of the aquifer, also verified the predicted concentrations.

Table 5-6 presents the mean absolute percentage error (MAPE) calculated to compare the observed and predicted concentrations.

**Table 5-6. Calculated mean absolute percentage error (MAPE) for comparisons between observed and predicted nitrate concentrations by central area model**

| Concentrations (x mg/L) Evaluated | Mean Concentration (mg/L) | Calculated Error* (mg/L) | Percent of Mean |
|---|---|---|---|
| All | 7.62 | 2.21 | 29.01 |
| Low ($x \leq 4$) | 2.41 | 4.63 | 192.04 |
| Moderate ($4 < x \leq 10$) | 7.18 | 1.45 | 20.17 |
| High ($10 < x$) | 13.37 | 2.46 | 18.36 |

*$\text{Error} = 1/N \sum_{i=1}^{N} |M-P|$

N = Number of samples
M = Measured concentration
P = Predicted concentration

The calculated error shows that the central area model predicted the high concentrations more accurately. The error for high values was 41.18 percent in the overall aquifer model which was reduced to 18.36 percent in this model. In this case the error for all data was also decreased to 29.01 percent from the previously calculated 41.36 percent for the overall aquifer model. The reductions in relative error indicated that the model could produce more accurate results when used for small areas. Therefore, separate models for the four individual wellfields were also developed.

### 5.1.3 Individual wellfield spatial model

Four City of Enid wellfields were modeled individually focusing on the small area of each wellfield in this effort. As the central aquifer model predicted better local results then the overall aquifer model, these models were expected to improve the plume predictions for each individual wellfield. Further, the grid size was also reduced to 200m×200m for these models, which would also increase the resolution.

#### 5.1.3.1 Cleospring wellfield spatial model

Table 5-7 lists the performance of an eight neural network model architecture. The table also presents the results obtained in terms of number of layers, neurons per layers, training tolerance, percentage of "Right" scores, and training epochs required in Cleosping wellfield model. These models differed from the previously explained overall aquifer model and central area model since they focused only on the Cleospring wellfield area. Also, in these models a smaller grid size and different architectures were used. The grid size was reduced to identify the spatial nitrate distributions more accurately and the different model architectures were evaluated to increase the accuracy as far as possible.

**Table 5-7. Alternatives for Cleospring wellfield spatial model**

| Network no. | No. of layers | Neurons per layer* | Training tolerance | % Right | Epochs |
|---|---|---|---|---|---|
| 1 | 3 | 2-13-1 | 0.1 | 100 | 2057 |
| 2 | 3 | 2-15-1 | 0.1 | 100 | 2067 |
| 3 | 3 | 2-18-1 | 0.1 | 100 | 4389 |
| 4 | 3 | 2-22-1 | 0.1 | 100 | 4358 |
| 5 | 3 | 2-25-1 | 0.1 | 100 | 5057 |
| 6 | 3 | 2-28-1 | 0.1 | 100 | 1859 |
| 7 | 3 | 2-32-1 | 0.1 | 100 | 1735 |
| 8 | 3 | 2-36-1 | 0.1 | 100 | 1891 |

* each value corresponds to number of neurons in input layer, hidden layer, and output layer respectively. Other parameters: Learning Rate = 1.0; Momentum = 0.9; Input Noise = 0; Testing Tolerance = 0.3, Error Limit = 0.01 (All the other parameters have default values except Error Limit)

In this effort the model development was initiated with a simple network using the default parameters settings; and a small number of neurons in the hidden layer. The first model executed predicted 100 % testing data "Right" with the default parameters settings therefore model alternatives were not required. Only the numbers of neurons in the hidden layer was changed to evaluate the effect on the training epochs required for the RMS error plot. A change in the number of neurons in the hidden layers had considerable effect on the epochs required to train the network. A best model configuration was determined based upon the least epochs required to train the model while achieving consistency in RMS error plot. Network no. 7 was determined to be the best model among the alternatives evaluated. Figure 5-5 shows the RMS error plot for this model. The plot show that both the testing and training data initially decreased rapidly and then slowed down and remained constant after maximum training was achieved.

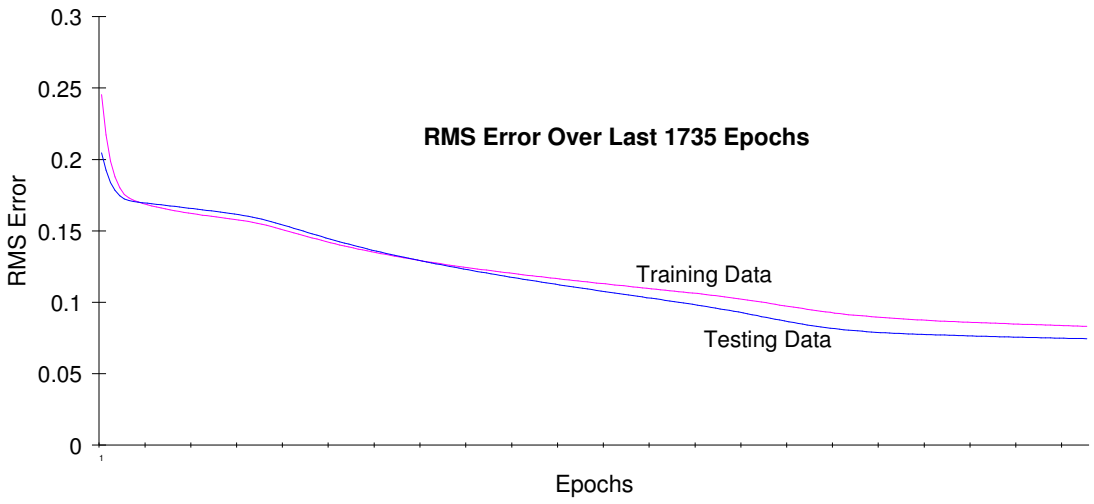


**Figure 5-5. RMS error plots of network no. 7**

This best network was used to predict the nitrate concentrations at the locations within the Cleospring wellfield where it was not measured. Figure 5-6 presents the map of these predicted nitrate concentrations. From the map two nitrate plumes were identified. The predicted values showed that 0.61 square mile of area in Cleospring wellfield was polluted by plume 1 with a contamination range of 10.01 to 19.91 mg/L. This plume occupied is 3.5 percent of total area considered in the model. Measured nitrate concentrations in wells C18, C13, and C21 had concentration level above 10 mg/L. These three wells are within the 0.61 square mile area of plume 1. This verifies that the plume was predicted in a reasonable location. The second plume identified was larger than plume 1. The predicted values showed that plume 2 had a highest concentration range of 6.97 to 9.69 mg/L over 1.07 square miles. None of the Enid sampling wells were located within this modeled area of area of plume 2. There were however, fourteen nearby wells of this wellfield with nitrate the contamination levels of less than 10 mg/L.

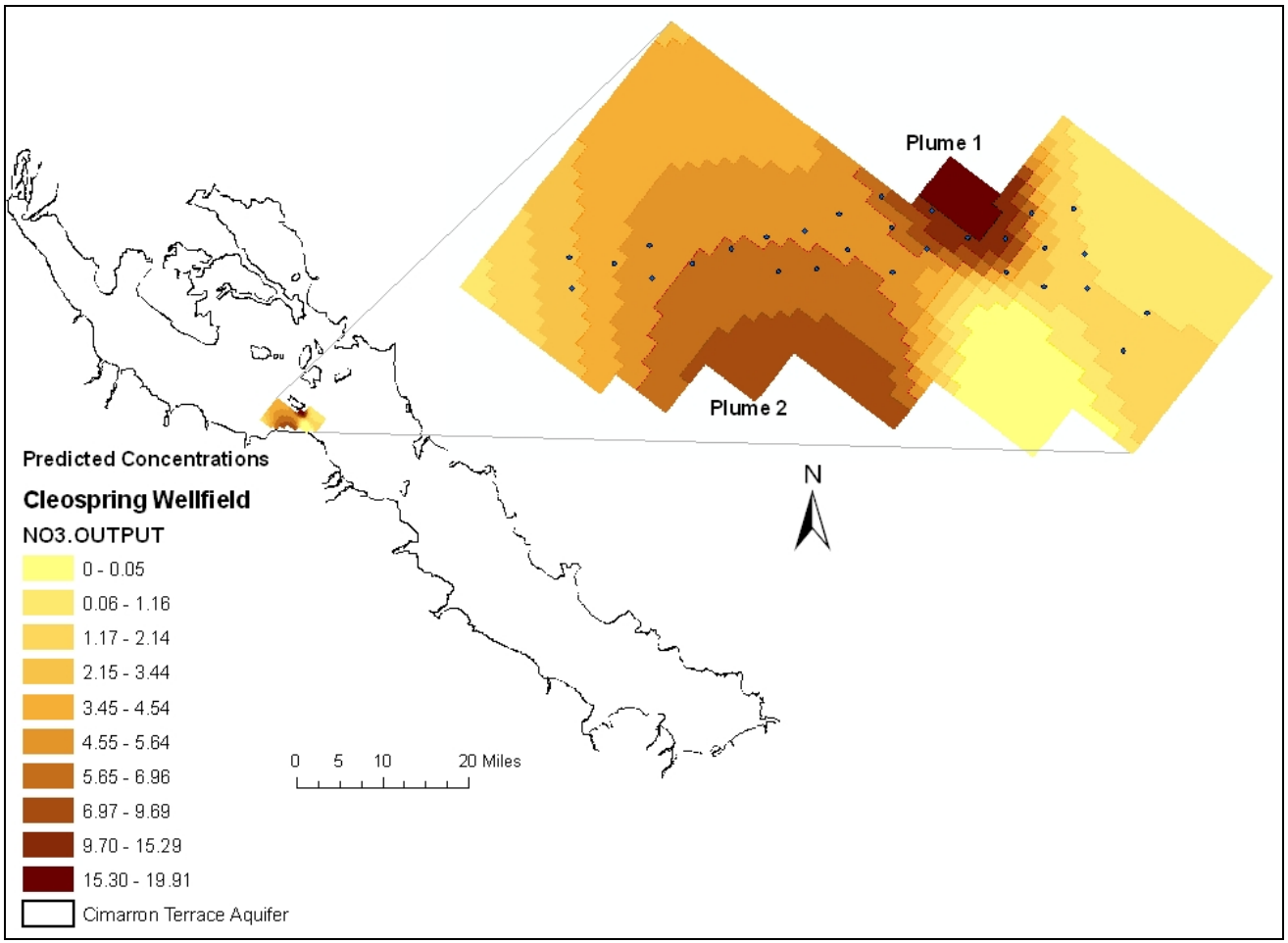


**Figure 5-6. Neural kriging estimation of groundwater nitrate distribution in Cleospring wellfield**

#### 5.1.3.2 Ringwood wellfield spatial model

Table 5-8 presents the structure and performance of six neural networks models attempted in this effort. The results obtained in terms of number of layers, neurons per layers, training tolerance, percentage of "Right" scores, and training epochs required in this modeling approach are also included in this table. The grid size used in these networks was same as that of the previously explained Cleospring wellfield model. As before, accurate results with a relatively simple model were achieved. These models were focused to predict nitrate concentrations in the Ringwood wellfield area.

**Table 5-8. Alternatives for Ringwood wellfield spatial model**

| Network no. | No. of layers | Neurons per layer* | Training tolerance | % Right | Epochs |
|---|---|---|---|---|---|
| 1 | 3 | 2-7-1 | 0.1 | 100 | 5562 |
| 2 | 3 | 2-11-1 | 0.1 | 100 | 19052 |
| 3 | 3 | 2-16-1 | 0.1 | 100 | 16053 |
| 4 | 3 | 2-20-1 | 0.1 | 100 | 5191 |
| 5 | 3 | 2-21-1 | 0.1 | 100 | 2899 |
| 6 | 3 | 2-23-1 | 0.1 | 100 | 16368 |

* each value corresponds to number of neurons in input layer, hidden layer, and output layer respectively. Other parameters: Learning Rate = 1.0; Momentum = 0.9; Input Noise = 0; Testing Tolerance = 0.3, Error Limit = 0.01 (All the other parameters have default values except Error Limit)

The modeling was started with a network using the default parameters setting and less number of neurons in the hidden layer. The first attempted network predicted 100% testing data "Right". Alternative architectures were not required to increase the prediction accuracy. However, the number of neurons in the hidden layers were changed to see the effect on the training time required for the model. Also, in this case, a change in number of neurons in the hidden layers had considerable effect on the epochs required to train the network. A best model configuration was again determined based upon the least epochs required to train the model and consistency of the RMS error plot. Figure 5-7 shows the

training and testing RMS error plot for network no. 5 which was determined to be the best model among the alternatives evaluated. The plot shows that initially the RMS errors of both training and testing data were gradually decreasing and after maximum training had achieved they remained constant and attaining straight lines in the plot.

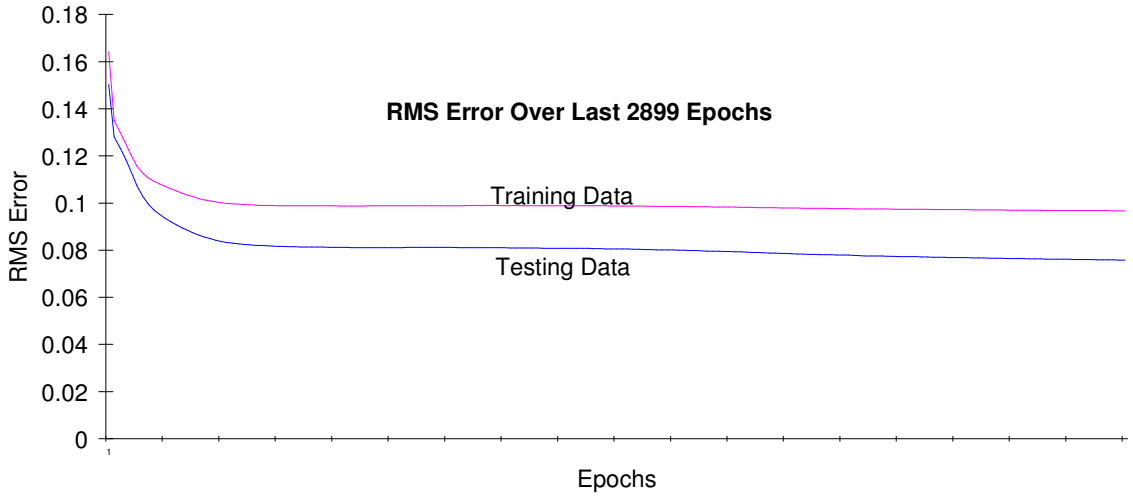


**Figure 5-7. RMS error plots of network no. 7**

Figure 5-8 shows the map of the predicted nitrate concentrations in the Ringwood wellfield. One plume was identified in this wellfield from the map. The plume is large, with 5.8 square miles of polluted area. This is 7.38 percent of total area considered in this model. Three wells: R28, R26, and R21 were identified in this high concentration range of the plume. Contamination levels in these three wells were measured above the MCL which verifies that the model was able to predict the correct position of plume and nitrate concentrations in it.

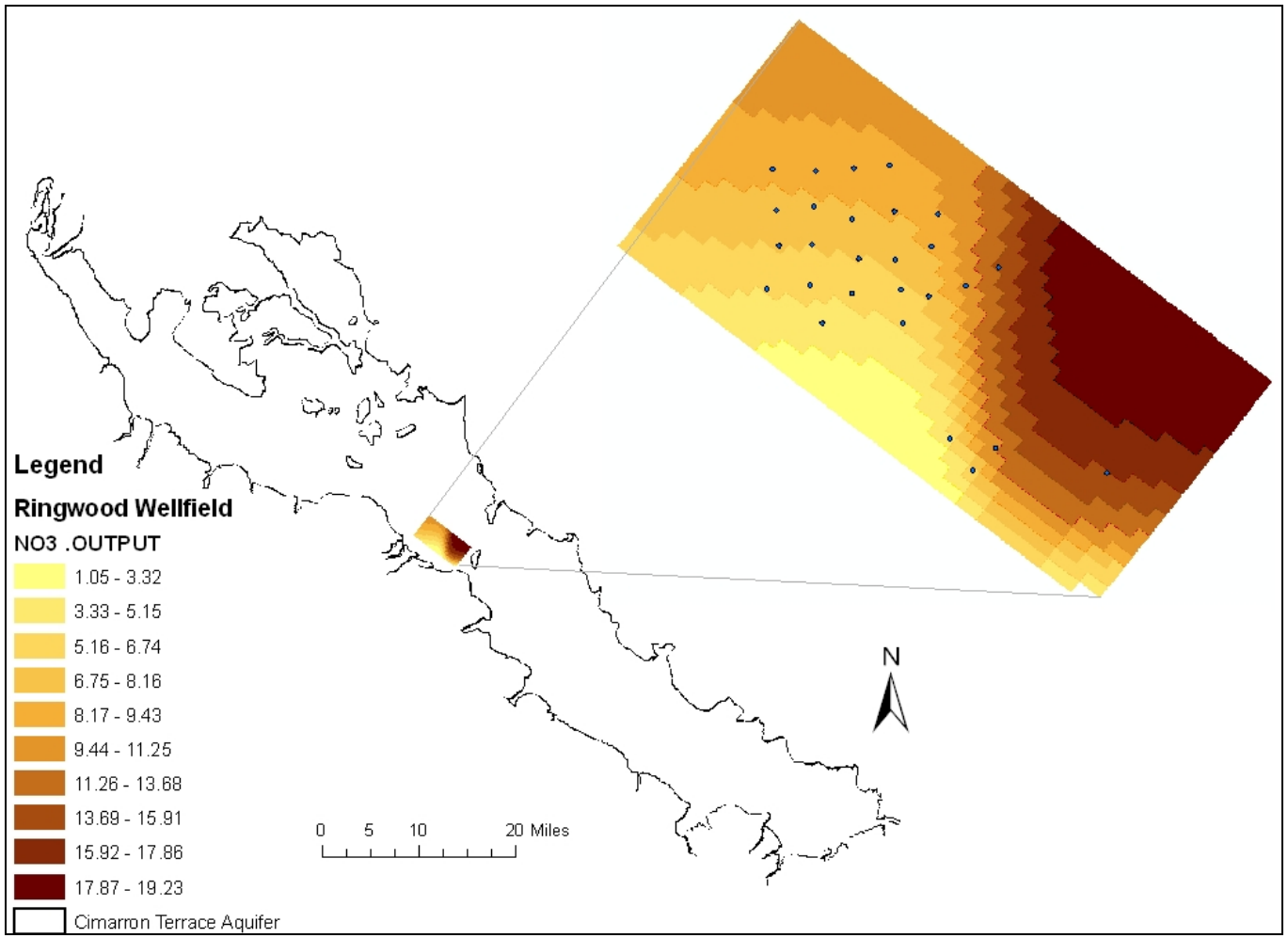


**Figure 5-8. Neural kriging estimation of groundwater nitrate distribution in Ringwood wellfield**

#### 5.1.3.3 Ames wellfield spatial model

Table 5-9 lists the structure of the five neural network models as well as the results obtained in terms of number of layers, neurons per layers, training tolerance, percentage of "Right" scores, and training epochs required in Ames wellfield model. The models were same as the previously explained Cleospring wellfield models and Ringwood wellfield models except in the area of focus. These models were developed to predict nitrate concentrations in the Ames wellfield which is located near the center of the aquifer.

**Table 5-9. Alternatives for Ames wellfield spatial model**

| Network no. | No. of layers | Neurons per layer* | Training tolerance | % Right | Epochs |
|---|---|---|---|---|---|
| 1 | 3 | 2-9-1 | 0.1 | 100 | 4142 |
| 2 | 3 | 2-12-1 | 0.1 | 100 | 6010 |
| 3 | 3 | 2-13-1 | 0.1 | 100 | 4230 |
| 4 | 3 | 2-15-1 | 0.1 | 100 | 4608 |
| 5 | 3 | 2-19-1 | 0.1 | 100 | 3288 |

* each value corresponds to number of neurons in input layer, hidden layer, and output layer respectively. Other parameters: Learning Rate = 1.0; Momentum = 0.9; Input Noise = 0; Testing Tolerance = 0.3, Error Limit = 0.01 (All the other parameters have default values except Error Limit)

As before, the modeling was started with a simple network structure using default parameters and few neurons in the hidden layer. In this wellfield all alternatives tried predicted testing data 100% "Right with the default parameters settings. As with the other individual wellfield models, a change in number of neurons in the hidden layers had considerable effect on the epochs required to train the network. A best model configuration was determined based upon the highest percentage "Right" and least epochs required training the model, and consistency in RMS error plot. Figure 5-9 shows the training and testing RMS error plot for network no. 5. With these criteria, network no.

5 was determined the best model and was used to predict the nitrate concentrations at the locations within the Ames wellfield where it was not measured.

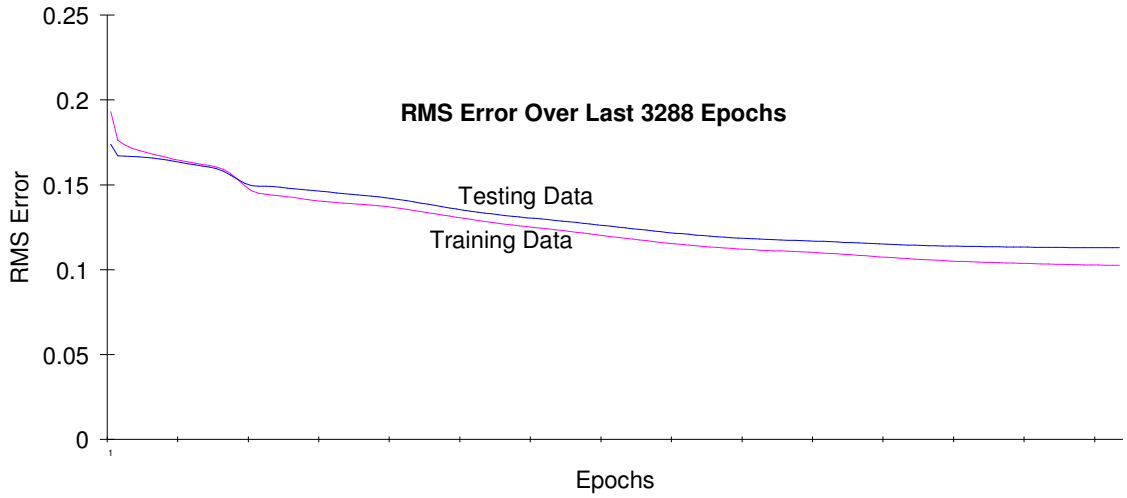


**Figure 5-9. RMS error plots of network no. 6**

The predicted nitrate concentrations in Ames wellfield, presented in Figure 5-10, showed that a 18.98 square mile area in the Ames wellfield was contaminated above the MCL. This is 58.57 percent of total area considered in this model. Out of twenty nine wells in this wellfield, eight wells: A13, A14, A16, A17, A18, A19, A25, and A29 were in the predicted area of concentration above the MCL. Nitrate concentrations in all of these wells except A29 were measured above 10 mg/L. This shows the Ames wellfield is highly contaminated by nitrate and the neural network model was able to identify its distribution pattern accurately.

In the Ames wellfield, two plumes connected with each other were identified. Both plumes have polluted 6.1 square mile area in the wellfield above 15 mg/L.

However, none of the wells were in this highest concentration location of the plumes. The lowest nitrate concentrations in the range of 2.28 to 4.14 mg/L were predicted towards the east side of the wellfield. Nitrate concentration gradually decreased on the left and right side of the plumes, while the central portion the wellfield had predicted nitrate concentration in the range of 4.15 to 6.09mg/L. Nine wells: A3, A4, A6, A7, A8, A9, A20, A21, and A33 are in the area of this concentration range.

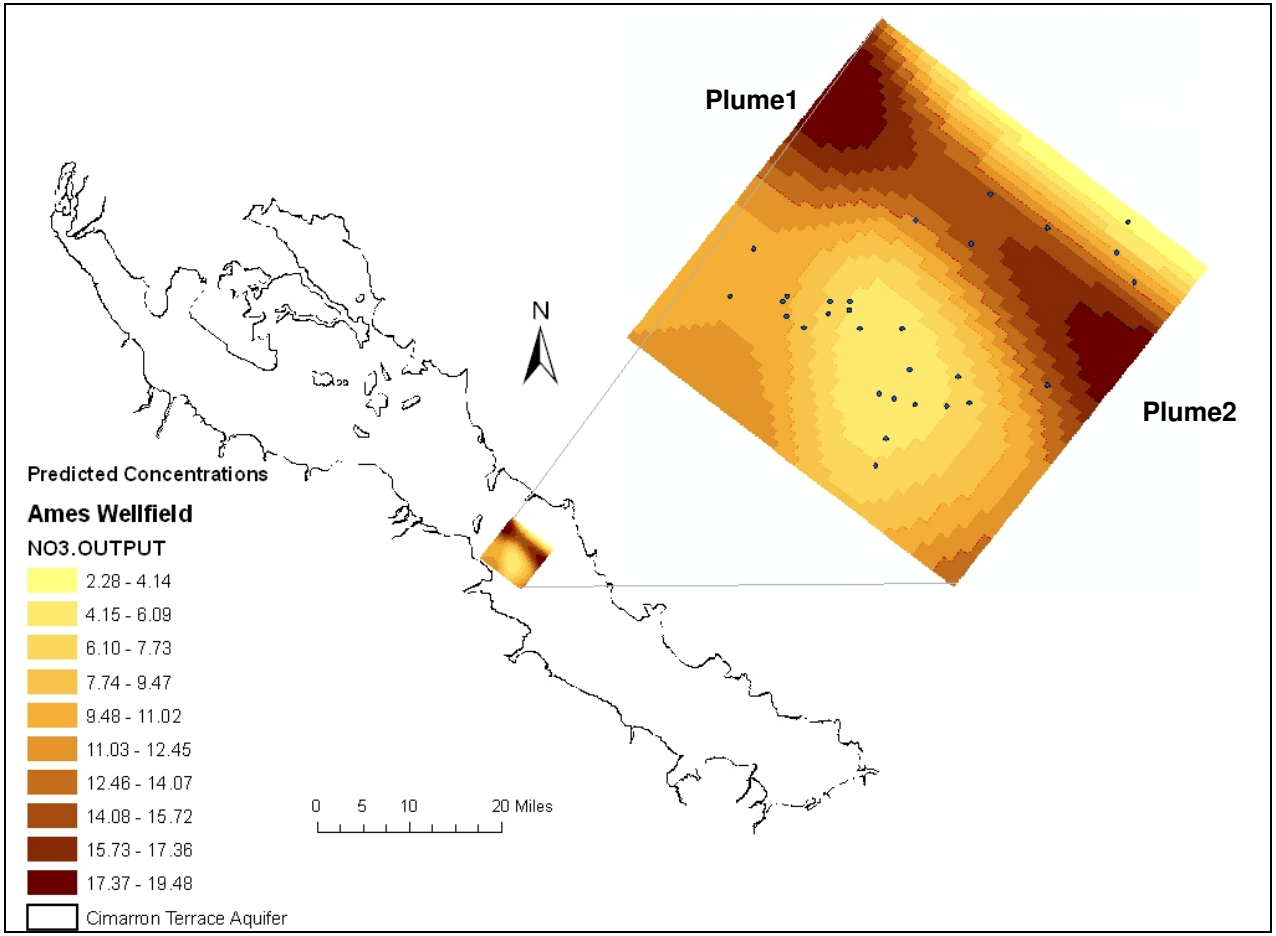


**Figure 5-10. Neural kriging estimation of groundwater nitrate distribution in Ames wellfield**

#### 5.1.3.4 Drummond wellfield spatial model

Table 5-10 lists the structure of six neural network model and their performance in terms of number of layers, neurons per layers, training tolerance, percentage of "Right" scores, and training epochs required. These networks were similar to previously explained three individual wellfield models but this model focused on the Drummond wellfield area.

**Table 5-10. Alternatives for Drummond wellfield spatial model**

| Network no. | No. of layers | Neurons per layer* | Training tolerance | % Right | Epochs |
|---|---|---|---|---|---|
| 1 | 3 | 2-6-1 | 0.1 | 100 | 4021 |
| 2 | 3 | 2-10-1 | 0.1 | 100 | 6281 |
| 3 | 3 | 2-14-1 | 0.1 | 100 | 4444 |
| 4 | 3 | 2-18-1 | 0.1 | 100 | 3720 |
| 5 | 3 | 2-19-1 | 0.1 | 100 | 3820 |
| 6 | 3 | 2-23-1 | 0.1 | 100 | 4911 |

* each value corresponds to number of neurons in input layer, hidden layer, and output layer respectively. Other parameters: Learning Rate = 1.0; Momentum = 0.9; Input Noise = 0; Testing Tolerance = 0.3, Error Limit = 0.01 (All the other parameters have default values except Error Limit)

The first network was executed using default parameters setting and less number of neurons in the hidden layer. Subsequently, the numbers of neurons in the hidden layers were increased. While all of the neural network alternatives predicted testing data 100% "Right" with default parameters settings, changes in number of neurons in the hidden layers had considerable effect on the epochs required to train the network. A best model configuration was determined based upon the least epochs required to train the model and consistency in RMS error plot. Network no. 4 was determined the best model among the alternatives tried with above mentioned two criteria. Figure 5-11 shows the training and testing RMS error plot for network no. 4, which shows that the error plot for both sets of data were consistent, decreased rapidly first and remained fairly constant

after that without any peaks and plateaus. The best network was then used to predict the nitrate concentrations at the locations where it not measured in Drummond wellfield.

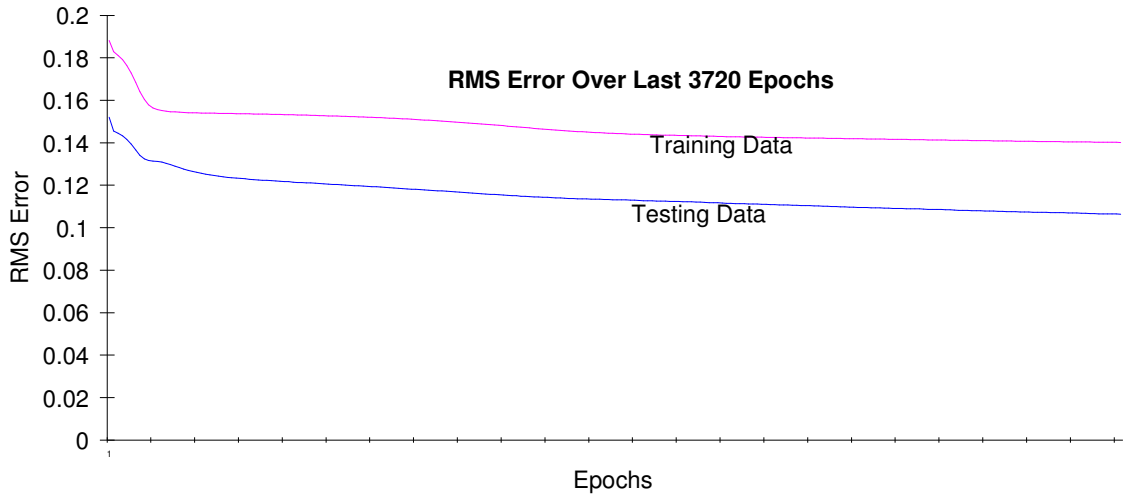


**Figure 5-11. RMS error plots of network no. 6**

Figure 5-12 shows the map of the predicted nitrate concentration in the Drummond wellfield. In this wellfield nitrate concentration was high at the south west end of the wellfield and increased towards the edge of the aquifer. In this wellfield one plume was identified towards the south west end of the wellfield. The plume had contaminated 1.14 square mile area of this wellfield above the MCL. One well, D23, is in the plume's highest concentration area and the highest measured concentration in this well was 11.1 mg/L. The highest predicted nitrate concentration in this wellfield was 13.29 mg/L which is less in comparison to the predicted nitrate concentrations in other three wellfields. The measured and predicted nitrate concentrations reveals that, this wellfield is less vulnerable in comparison to other three and that may have been due to the high percent of clay in this area of the aquifer and depth to water and partial confining layer.

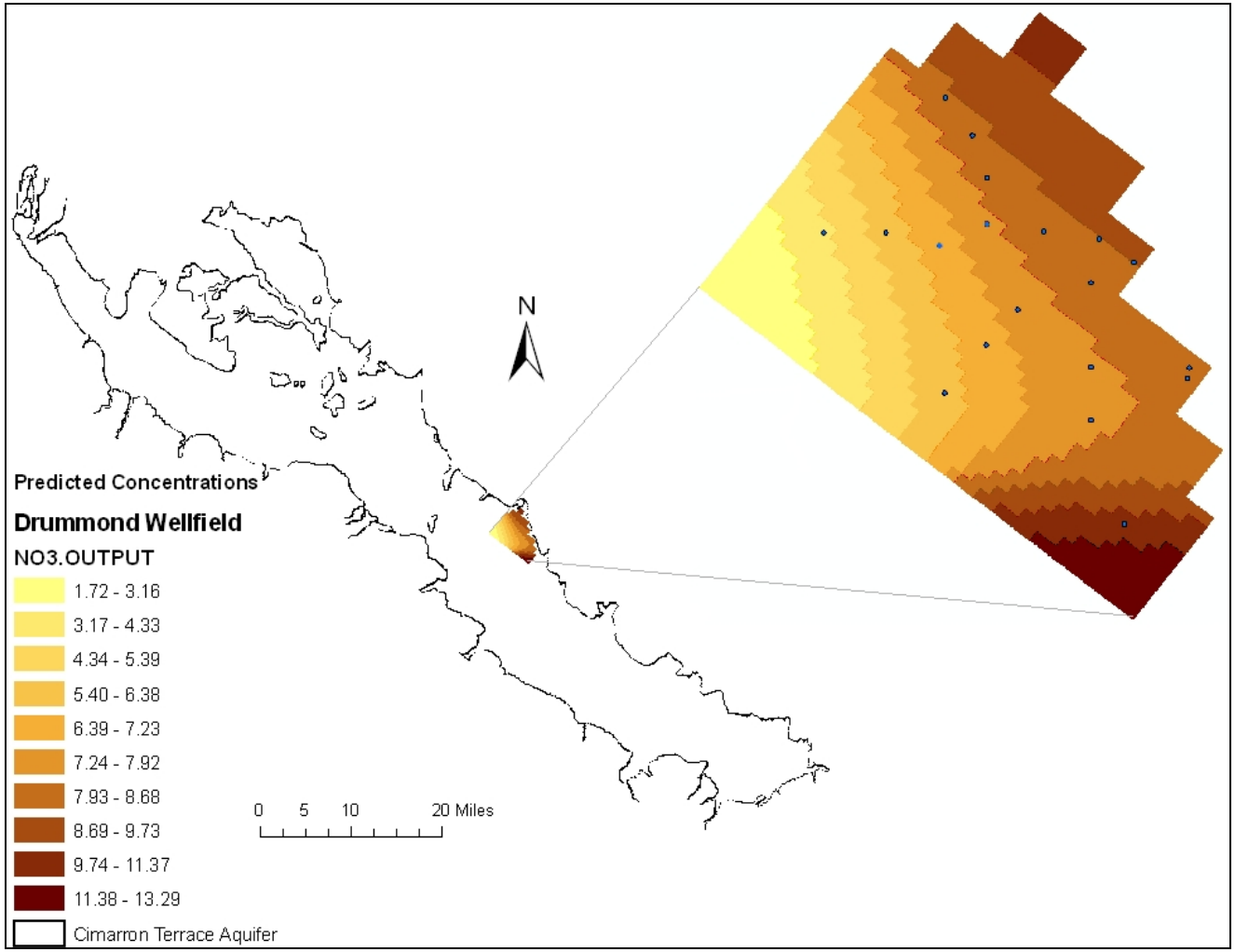


**Figure 5-12. Neural kriging estimation of groundwater nitrate distribution in Drummond wellfield**

## 5.2 Constituent Relationship Models

The spatial modeling approach projected nitrate concentrations throughout the overall aquifer, in the central region, and finally, in association with specific wellfields. In this constituent relationship modeling approach, nitrate concentrations in each well of the four wellfields were predicted as a function of surface nitrogen application rates.

### 5.2.1 Cleospring constituent relationship model

Table 5-11 presents the six alternative architectures attempted for the Cleospring wellfield constituent relationship model. The results obtained in terms of number of layers, neurons per layers, training tolerance, percentage of "Right" scores, and training epochs required are also presented.

**Table 5-11. Alternatives for Cleospirng wellfield constituent relationship model**

| Network no. | No. of layers | Neurons per layer* | Training tolerance | % Right | Epochs |
|---|---|---|---|---|---|
| 1 | 3 | 1-6-1 | 0.1 | 83 | 10342 |
| 2 | 3 | 1-11-1 | 0.1 | 83 | 15618 |
| 3 | 3 | 1-15-1 | 0.1 | 83 | 13250 |
| 4 | 3 | 1-19-1 | 0.1 | 83 | 14818 |
| 5 | 3 | 1-6-1 | 0.2 | 83 | 13520 |
| 6 | 3 | 1-15-1 | 0.2 | 83 | 16607 |

* each value corresponds to number of neurons in input layer, hidden layer, and output layer respectively. Other parameters: Learning Rate = 1.0; Momentum = 0.9; Input Noise = 0; Testing Tolerance = 0.3, Error Limit = 0.01 (All the other parameters have default values except Error Limit)

All of the attempted networks predicted nitrate concentration testing data at an 83% "Right" level with the default parameter settings. Changes in training tolerance did not affect the prediction precision and training time required in this model. The network no. 3 was decided as the best model among the alternatives since it required the fewest epochs to train the model. Figure 5-13 presents the training and testing data RMS error

plot of network no. 3 which shows the gradual stabilization of training and testing data RMS error. The curves became straight lines after the initial variation.

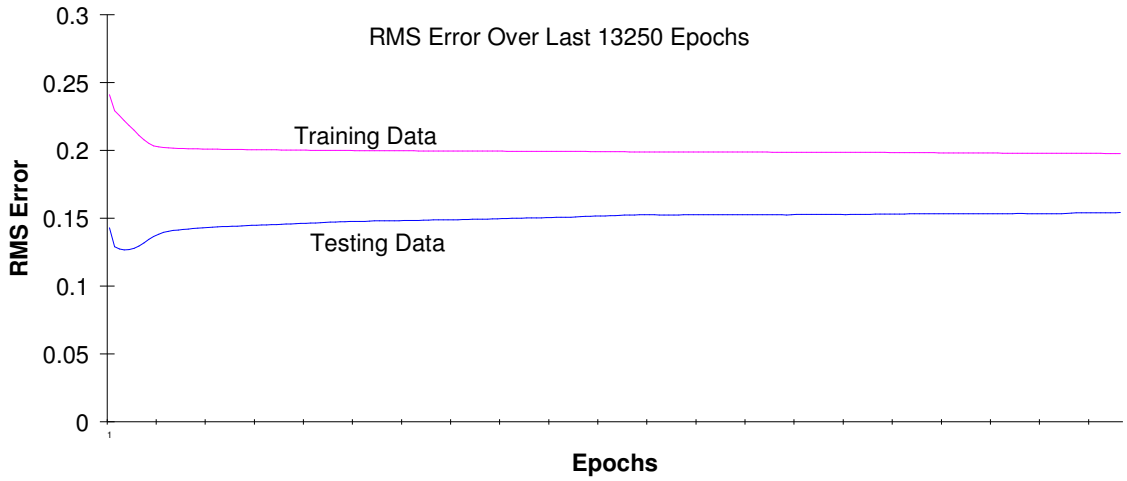


**Figure 5-13. RMS error plots of network no. 6**

Figure 5-14 presents the observed and predicted nitrate concentrations by this model in each well of the Cleospring wellfield. The plot shows that the model predicted all nitrate concentrations in wells below 8.0 mg/L. The predicted values were more accurate in wells C5, C6, and C9, while others showed some over-as well as under-prediction. The model could not match the highest concentrations. The surface nitrogen application rate within 1000m radius of wells C8 and C14 were calculated to be 38.63 kg/sq. mile and 39.47 kg/sq. mile, which were the highest rates in this wellfield, but the measured nitrate concentrations in these wells were 4.6 mg/L and 4.8 mg/L. On the other hand, surface nitrogen application rate at well C18 was 34.81 kg/sq. mile and the measured nitrate concentration in this well was 16.0 mg/L. A probable reason that the model was unable to establish the good relationship between the surface nitrogen application rates and measured high nitrate concentrations due to discrepancy in the input data. According to KC (2007) the percent clay and depth of groundwater are other two

significant variables besides surface nitrogen application rate for nitrate concentration level above 10 mg/L. The percent clay in 1000m radial distance of wells C8 and C14 were among the high values in this wellfield.

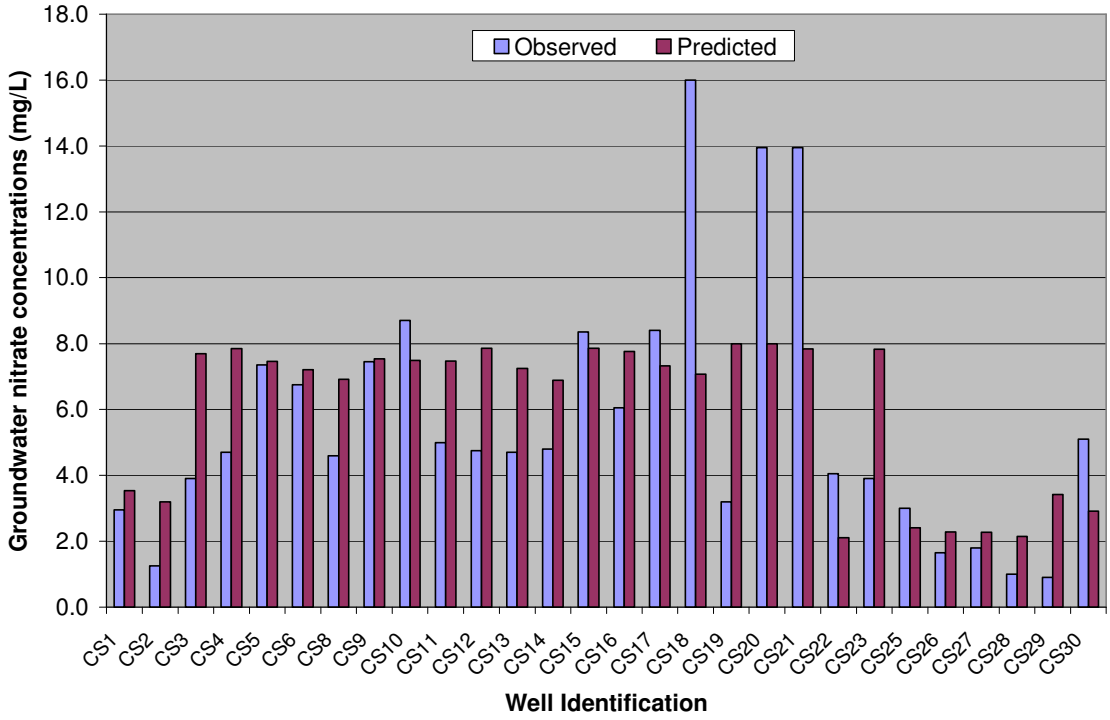


**Figure 5-14. Observed and predicted nitrate concentration by Cleospring constituent relationship model**

Table 5-12 presents the calculated mean absolute percentage error (MAPE) for the nitrate concentrations predicted by this model. The lowest mean absolute percentage error associated with moderate concentration range suggests that the model was best in predicting the moderate concentration range. The mean absolute percentage error for low range values was calculated highest, since most of the low range values were over-predicted. The mean absolute percentage error was calculated 47.82 for high range since all all the high range values were under-predicted. The under prediction of high values strongly suggests to development of a separate model for this range.

**Table 5-12. Calculated mean absolute percentage error (MAPE) for comparisons between observed and predicted nitrate concentrations by Cleospring wellfield constituent relationship model**

| Concentrations (x mg/L) Evaluated | Mean Concentration (mg/L) | Calculated Error* (mg/L) | Percent of Mean |
|---|---|---|---|
| All | 5.65 | 2.36 | 41.94 |
| Low (x ≤ 4) | 2.36 | 2.04 | 86.64 |
| Moderate (4 < x ≤ 10) | 6.05 | 1.66 | 27.50 |
| High (10 < x) | 14.63 | 6.99 | 47.82 |

$$*\text{Error}=1/N\sum_{i=1}^{N}|M-P|$$

N = Number of samples
M = Measured concentration
P = Predicted concentration

### 5.2.2 Ringwood constituent relationship model

The modeling approach of the Ringwood constituent relationship model was the same as that of Cleospring. The model related surface applied nitrogen loading, with measured nitrate concentrations in each well of the Ringwood wellfield.

Table 5-13 presents the four alternative architectures for this wellfield constituent relationship model. The results obtained in terms of number of layers, neurons per layers, training tolerance, percentage of "Right" scores, and training epochs required in Ringwood wellfield model are illustrated.

**Table 5-13. Alternatives for Ringwood wellfield constituent relationship model**

| Network no. | No. of layers | Neurons per layer* | Training tolerance | % Right | Epochs |
|---|---|---|---|---|---|
| 1 | 3 | 1-5-1 | 0.1 | 100 | 18410 |
| 2 | 3 | 1-9-1 | 0.1 | 100 | 24077 |
| 3 | 3 | 1-14-1 | 0.1 | 100 | 17216 |
| 4 | 3 | 1-18-1 | 0.1 | 100 | 19415 |

* each value corresponds to number of neurons in input layer, hidden layer, and output layer respectively. Other parameters: Learning Rate = 1.0; Momentum = 0.9; Input Noise = 0; Testing Tolerance = 0.3, Error Limit = 0.01 (All the other parameters have default values except Error Limit)

All of the alternatives attempted in this modeling effort predicted testing data 100% "Right" with default parameters settings. Since, the predictions were 100% "Right", the best model among the alternatives attempted was decided on epochs required to train the model and stable in RMS error plot. Network no. 3 was decided best with these criteria. Figure 5-15 shows the RMS error plot of network number 3.

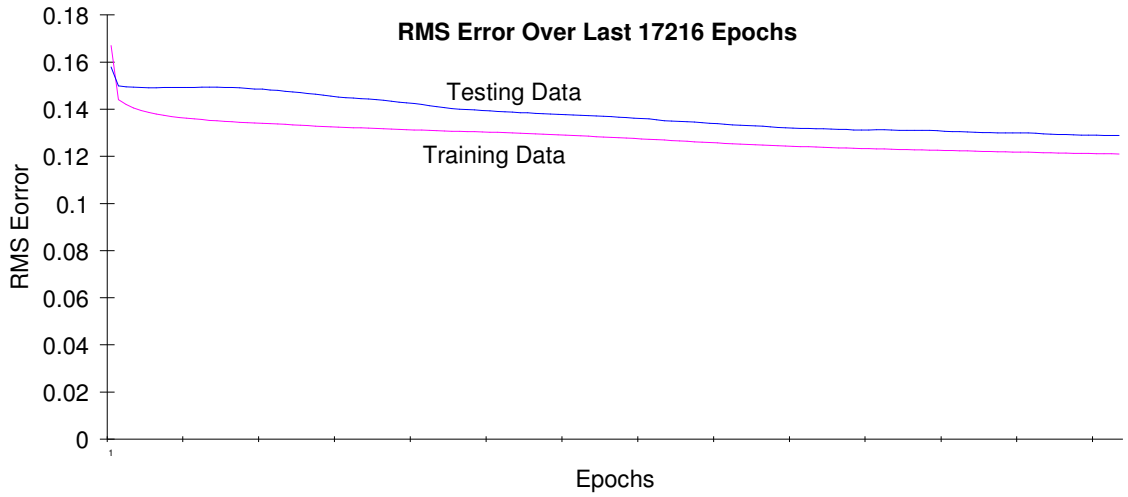


**Figure 5-15. RMS error plots of network no. 3**

In this wellfield the highest nitrate concentration of 15.33 mg/L in well R28 and lowest concentration of 6.57 mg/L in well R24 were predicted. The high nitrate concentrations were predicted at the wells where surface nitrogen application rates were also high. This indicates that high nitrate concentrations in this wellfield were due to the application of surface nitrogen. Figure 5-16 shows the plot of the observed and predicted nitrate concentrations in this wellfield. In most of the wells, predicted nitrate concentrations resembled the observed concentrations. The model was able to establish a good relationship between nitrate concentrations and surface nitrogen application rate

since most of the measured nitrate concentrations were consistent with the surface nitrogen application rate in this wellfield.

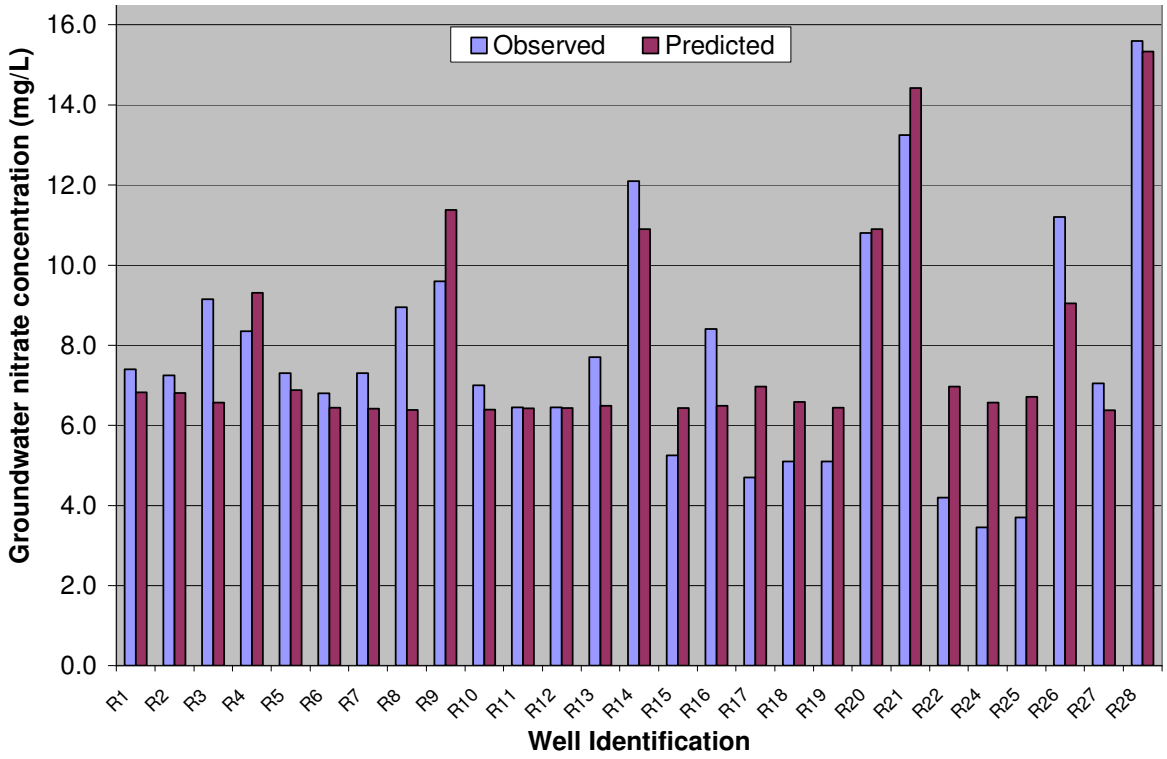


**Figure 5-16. Observed and predicted nitrate concentration by Ringwood constituent relationship model**

Table 5-14 presents the mean absolute percentage error associated with the various ranges of predictions. The high nitrate concentrations were accurately predicted by this model. Mean absolute percentage error of 7.76 for high values verifies the accuracy of the prediction of. Also, the model predicted moderate concentrations adequately with mean absolute percentage error of 17.24. The mean absolute percentage error for low concentration range was 85.71 since most of these concentrations were overestimated. The nitrogen application rate in wells R1, R2, and R5 were minimum in this wellfield but the measured nitrate concentration were 7.40 mg/L, 7.25 mg/L, and

7.30 mg/L respectively. The measured high concentrations in the low nitrogen application areas suggest the presence of some other sources too such as private septic tank system or high influence of geophysical setting.

**Table 5-14. Calculated mean absolute percentage error (MAPE) for comparisons between observed and predicted nitrate concentrations by Ringwood wellfield constituent relationship model**

| Concentrations (x mg/L) Evaluated | Mean Concentration (mg/L) | Calculated Error* (mg/L) | Percent of Mean |
|---|---|---|---|
| All | 7.76 | 1.3 | 16.73 |
| Low (x ≤ 4) | 3.58 | 3.06 | 85.71 |
| Moderate (4 < x ≤ 10) | 6.98 | 1.2 | 17.24 |
| High (10 < x) | 12.59 | 0.98 | 7.76 |

$$*\text{Error}=1/N\sum_{i=1}^{N}\left|M-P\right|$$

N = Number of samples
M = Measured concentration
P = Predicted concentration

### 5.2.3 Ames constituent relationship model

The Ames wellfield constituent relationship modeling approach was the same as that of previously described two constituent relationship models. Table 5-15 presents five alternatives attempted for the Ames wellfield constituent relationship model. The results obtained in terms of number of layers, neurons per layers, training tolerance, percentage of "Right" scores, and training epochs required are also presented.

**Table 5-15. Alternatives for Ames wellfield constituent relationship model**

| Network no. | No. of layers | Neurons per layer* | Training tolerance | % Right | Epochs |
|---|---|---|---|---|---|
| 1 | 3 | 1-10-1 | 0.1 | 100 | 31597 |
| 2 | 3 | 1-14-1 | 0.1 | 80 | 36278 |
| 3 | 3 | 1-20-1 | 0.1 | 80 | 38779 |
| 4 | 3 | 1-24-1 | 0.1 | 100 | 29760 |
| 5 | 3 | 1-27-1 | 0.1 | 100 | 30306 |

* each value corresponds to number of neurons in input layer, hidden layer, and output layer respectively. Other parameters: Learning Rate = 1.0; Momentum = 0.9; Input Noise = 0; Testing Tolerance = 0.3, Error Limit = 0.01 (All the other parameters have default values except Error Limit)

Among the networks used in this modeling effort, network number 1, 4, and 5 predicted the testing data 100% "Right" and network number 2, and 3 predicted 80% "Right". Default parameters were used for these model runs. In these models, precision of testing data prediction and epochs required to train the model were sensitive towards the number of neurons in the hidden layers. Among the alternatives evaluated, network number 4 required the fewest epochs and gave the 100% testing data "Right" with the default parameters settings. Figure 5-17 shows the RMS error plot of network number 4, which is consistent throughout the training and testing. Therefore, network number 4 was determined as a best among the alternatives evaluated.

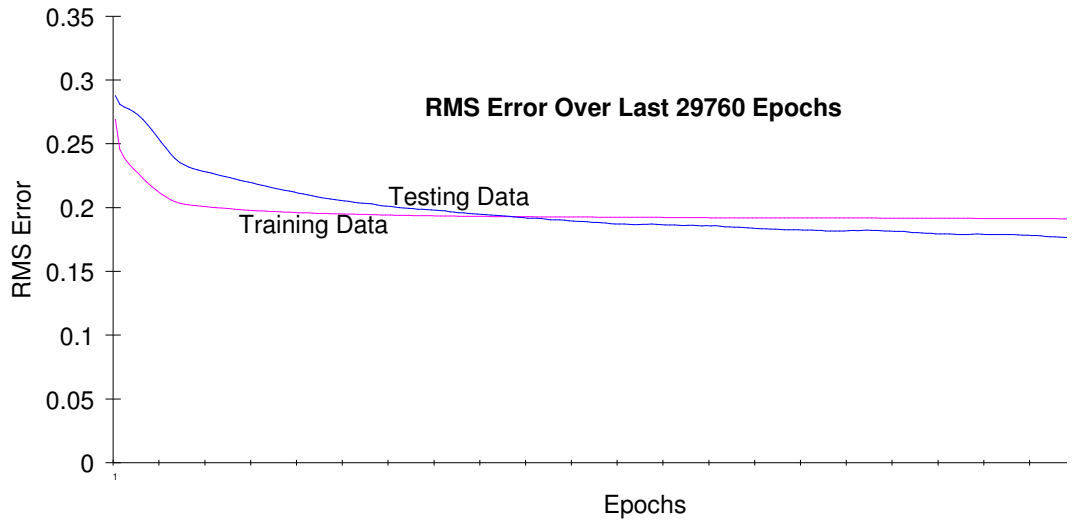


**Figure 5-17. RMS error plots of network no. 4**

Figure 5-18 shows the plot of observed and predicted nitrate concentrations in Ames wellfield constituent relationship model. The model predicted the highest nitrate concentration of 13.11 mg/L in well A19 where the measured concentration was 14.0 mg/L. Nitrate concentration of 12.66 mg/L was predicted in well A16 where nitrogen application was maximum and measured nitrate concentration was predicted 12.4 mg/L. Nitrogen application rates in this wellfield was highest among the four wellfields and the model predicted nitrate concentrations in 35 percent of wells in this wellfield above the MCL. This shows that the model had established the good association between the surface nitrogen application rate and groundwater nitrate concentrations. Table 5-16 presents the mean absolute percentage error associated with the various ranges of predicted nitrate concentrations. The mean absolute percentage error for the moderate range concentrations and high range concentrations were 9.35 and 15.61, which suggest that the model had predicted nitrate concentrations satisfactorily for these ranges. The

high error associated with the low range data suggests that the measured low range nitrate concentrations in this wellfield were not only the function of surface nitrogen application rate. Nitrate concentrations of 9.4 mg/L in well A29 where the surface nitrogen application rate was least, 8.59 kg/sq. mile, indicates the presence of other sources of nitrate around this well. In contradictory, nitrate concentrations were measured 2.47 mg/L, 3.4 mg/L, and 4.0 mg/L in the wells A6, A3, and A7 respectively where nitrogen application rate was in the range of 45 to 65 kg/ sq. mile. In these wells the model predicted nitrate concentrations above 5 mg/L. These discrepancies in the measured nitrate concentrations led the model to over predict the low range nitrate concentrations and signify the role of other geophysical variables.

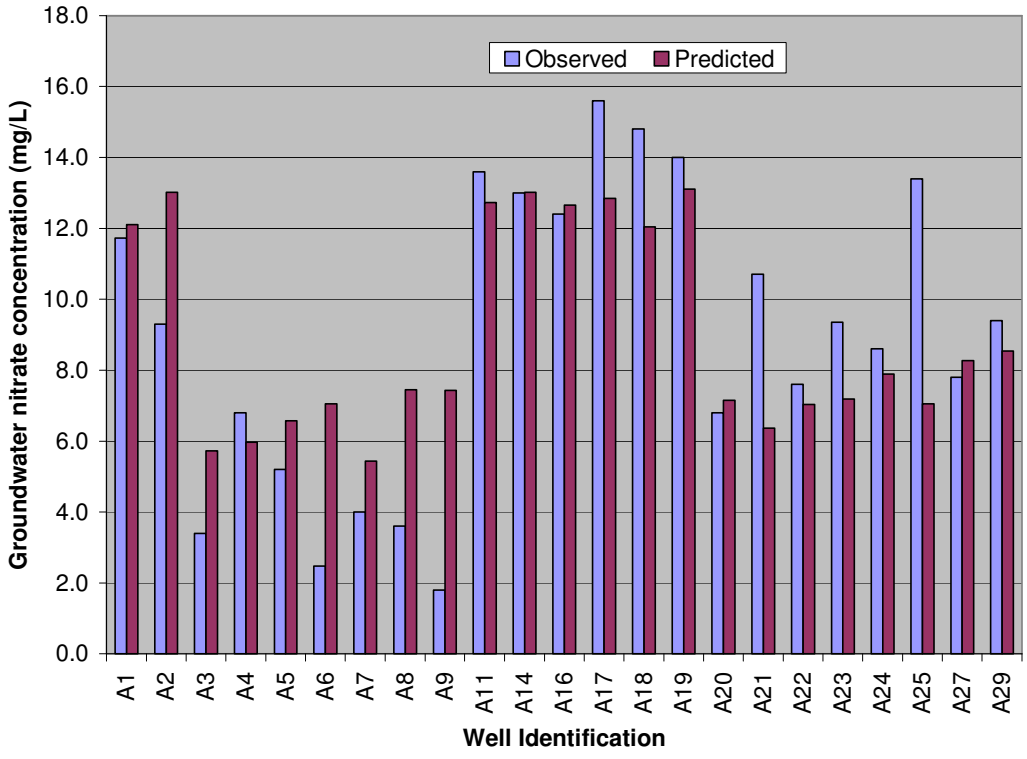


**Figure 5-18. Observed and predicted nitrate concentration by Ames constituent relationship model**

**Table 5-16. Calculated mean absolute percentage error (MAPE) for comparisons between observed and predicted nitrate concentrations by Ames wellfield constituent relationship model**

| Concentrations (x mg/L) Evaluated | Mean Concentration (mg/L) | Calculated Error* (mg/L) | Percent of Mean |
|---|---|---|---|
| All | 8.93 | 2.06 | 23.12 |
| Low (x ≤ 4) | 3.05 | 3.57 | 116.77 |
| Moderate (4 < x ≤ 10) | 7.87 | 0.74 | 9.35 |
| High (10 < x) | 13.25 | 2.07 | 15.61 |

$$*\text{Error}=1/N\sum_{i=1}^{N}|M-P|$$

N = Number of samples
M = Measured concentration
P = Predicted concentration

### 5.2.4 Drummond constituent relationship model

The Drummond wellfield constituent relationship modeling approach was the same as that of other constituent relationship models. Table 5-17 presents four alternatives attempted for the Drummond wellfield constituent relationship model with model architecture, and results obtained in terms of number of layers, neurons per layers, training tolerance, percentage of "Right" scores, and training epochs required.

**Table 5-17. Alternatives for Drummond wellfield constituent relationship model**

| Network no. | No. of layers | Neurons per layer* | Training tolerance | % Right | Epochs |
|---|---|---|---|---|---|
| 1 | 3 | 1-7-1 | 0.1 | 100 | 19509 |
| 2 | 3 | 1-10-1 | 0.1 | 100 | 22345 |
| 3 | 3 | 1-16-1 | 0.1 | 100 | 35567 |
| 4 | 3 | 1-21-1 | 0.1 | 100 | 25852 |

* each value corresponds to number of neurons in input layer, hidden layer, and output layer respectively. Other parameters: Learning Rate = 1.0; Momentum = 0.9; Input Noise = 0; Testing Tolerance = 0.3, Error Limit = 0.01 (All the other parameters have default values except Error Limit)

All the networks attempted in this modeling effort predicted the testing data 100% "Right" with the default parameters setting. Therefore, change in other parameters was not attempted. Among the alternatives evaluated, network number 1 required the fewest

epochs to train the model. Figure 5-19 shows the RMS error plot of network number 1, which shows that the error for training and testing data attained constant value when maximum training was achieved. The plot was stabilized after some initial undulations. Therefore, network number 1 was determined as the best model for this wellfield.

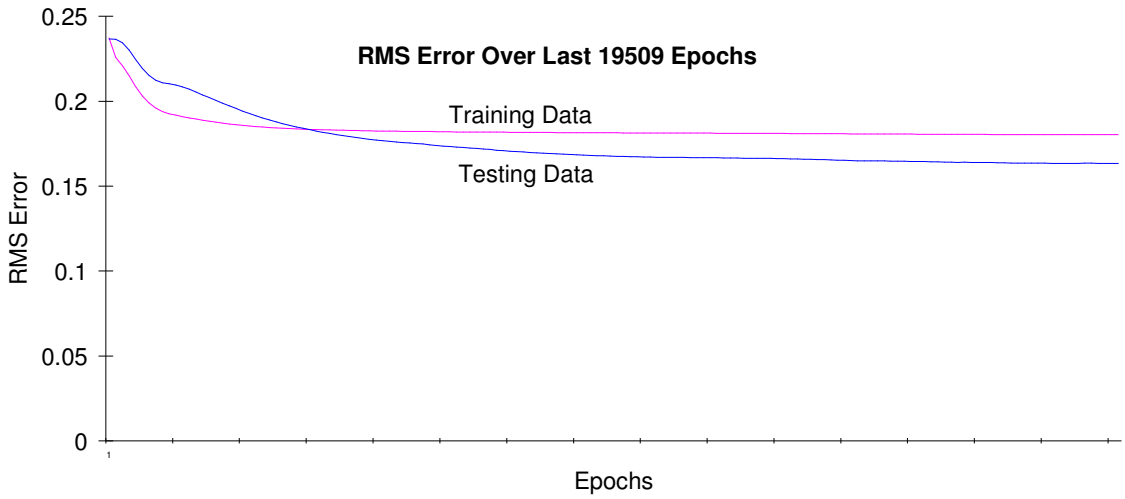


**Figure 5-19. RMS error plots of network no. 1**

Figure 5-20 shows the plot of observed nitrate concentrations and predicted nitrate concentrations by network number 1. In this wellfield the model predicted highest nitrate concentration of 9.16 mg/L in well D8 where measured concentration was 10.45 mg/L and nitrogen application rate was 125.69 kg/sq. mile, maximum in this wellfield. The model had predicted the concentrations in wells according to the surface nitrogen application rate. The model under-predicted the high nitrate concentrations measured in wells D7, D8, and D23, since these high nitrate concentrations were observed in wells where relatively less nitrogen were applied. The measured high concentration in wells with relatively less nitrogen application rates indicates the presence of other nitrate sources nearby and also the significant role of other geophysical variables. The mean

absolute percentage error of 16.13 for moderate concentration range presented in Table 5-18 verifies that the moderate nitrate concentrations were predicted more accurately. In comparison to the previously discussed three constituent relationship models, this model had best predicted the low range nitrate concentrations. However, this model also slightly over-predicted the low concentrations.

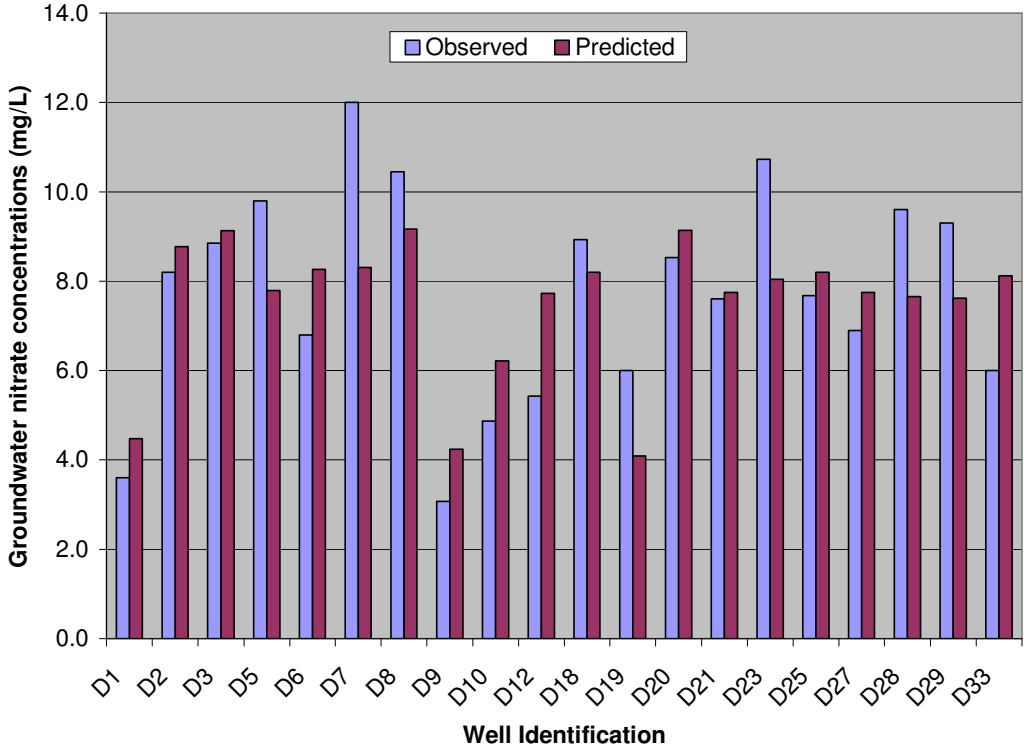


**Figure 5-20. Observed and predicted nitrate concentration by Drummond wellfield constituent relationship model**

**Table 5-18. Calculated mean absolute percentage error (MAPE) for comparisons between observed and predicted nitrate concentrations by Drummond wellfield constituent relationship model**

| Concentrations (x mg/L) Evaluated | Mean Concentration (mg/L) | Calculated Error* (mg/L) | Percent of Mean |
|---|---|---|---|
| All | 7.72 | 1.41 | 18.25 |
| Low (x ≤ 4) | 3.34 | 1.02 | 30.58 |
| Moderate (4 < x ≤ 10) | 7.63 | 1.23 | 16.13 |
| High (10 < x) | 11.06 | 2.55 | 23.08 |

$$*\text{Error}=1/N\sum_{i=1}^{N}|M-P|$$

N = Number of samples
M = Measured concentration
P = Predicted concentration

## 5.3 Management models

Management models were intended to identify the options to reduce the nitrate concentration below the MCL in the Cimarron Terrace Aquifer. Reduction of surface nitrogen application rate was identified as a feasible management option in reducing nitrate concentrations in the aquifer. The results of constituent relationship models showed that some wells in the Ames wellfield were contaminated beyond the limit of the drinking water standard due to excessive use of fertilizer nitrogen. The Ames wellfield constituent relationship model was used to developed management models. In this modeling effort, the land surface nitrogen application rate was reduced and the corresponding effect on the groundwater nitrate concentration in this wellfield was estimated. The nitrate concentration was reduced 10% each time and the model was employed to predict the corresponding nitrate concentration in the groundwater. Figure 5-21 shows the predicted nitrate concentrations with 10%, 20%, 30%, and 40% reduction of on ground application.

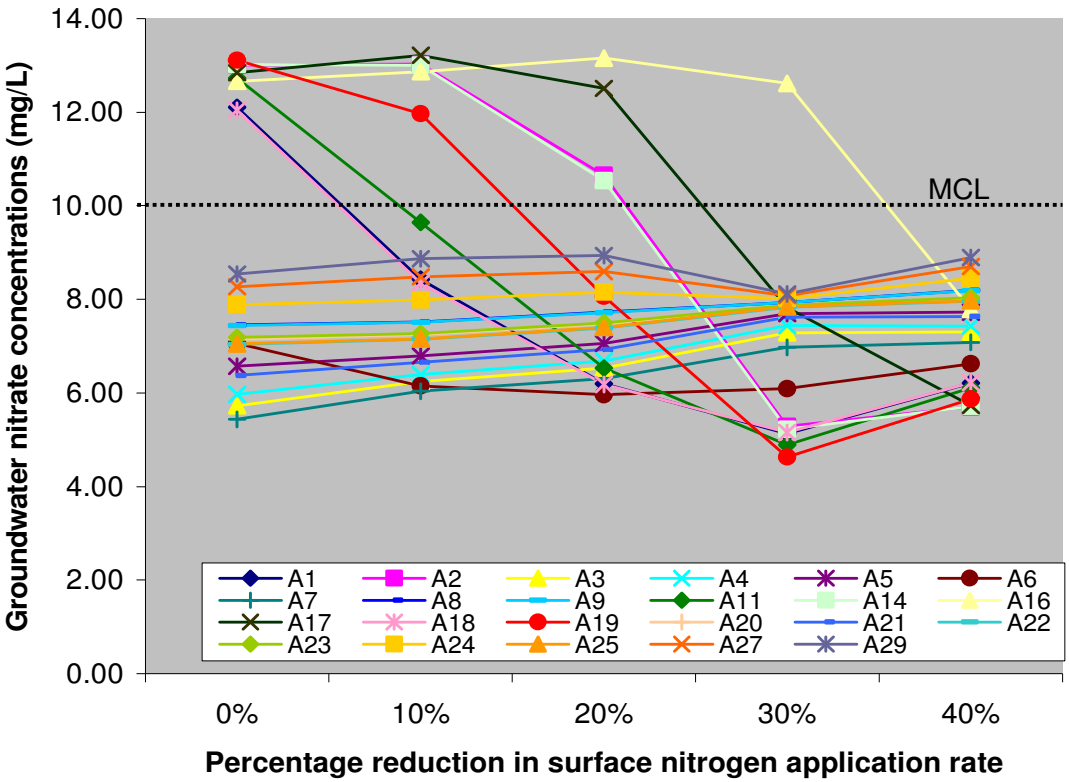


**Figure 5-21. Nitrate concentrations in all wells of Ames wellfield with varying on ground nitrogen application reduction**

The plot shows that the model with 40% reduction of surface nitrogen application predicted the nitrate concentration below the MCL in all wells in Ames wellfield. The model predicted the decreased nitrate concentrations corresponding to the decreased surface nitrogen application rate in the wells where contamination level was above 10 mg/L. As shown in the plot, in most of the wells where nitrate concentrations were below 10 mg/L, the model predicted increased concentrations with the decreased in the surface nitrogen application which was neither logically consistent nor acceptable. The results of this model suggested that separate models for the nitrate concentrations at different levels were needed.

Before simulating the management alternatives, a constituent relationship model for the high concentrations in the Ames wellfield was developed. Table 5-19 presents the

alternatives evaluated to determine the best network to predict the nitrate concentrations as a function of surface nitrogen application rate. Performances of the networks with different architectures are also presented in terms of percentage "Right" score and the epochs required to train the model.

**Table 5-19. Alternatives for Ames wellfield high concentrations constituent relationship model**

| Network no. | No. of layers | Neurons per layer* | Training tolerance | % Right | Epochs |
|---|---|---|---|---|---|
| 1 | 3 | 1-6-1 | 0.1 | 100 | 3082 |
| 2 | 3 | 1-10-1 | 0.1 | 100 | 2920 |
| 3 | 3 | 1-14-1 | 0.1 | 100 | 2517 |
| 4 | 3 | 1-19-1 | 0.1 | 100 | 6330 |

* each value corresponds to number of neurons in input layer, hidden layer, and output layer respectively. Other parameters: Learning Rate = 1.0; Momentum = 0.9; Input Noise = 0; Testing Tolerance = 0.3, Error Limit = 0.01 (All the other parameters have default values except Error Limit)

The modeling was started with the simple model with default parameters settings and a lower number of neurons in the hidden layer. The model predicted 100 % testing data "Right" at the first attempt. The number of neurons in the hidden layers were increased to see the effect on the training time required to train the model. The best model was again determined on the basis of highest percentage testing data "Right" score, fewest epochs required to train the model, and nature of RMS error plot. The percentage "Right" score of testing data were 100% in all the cases but the training epochs required was least for the network number 3. Figure 5-22 presents the RMS error plot for the network number 3. The plot of training and testing data attained straight lines after some initial undulations showing the model was trained adequately. Therefore, network number 3 was determined as a best model among the alternatives evaluated and was used to simulate with reduced nitrogen application rate.

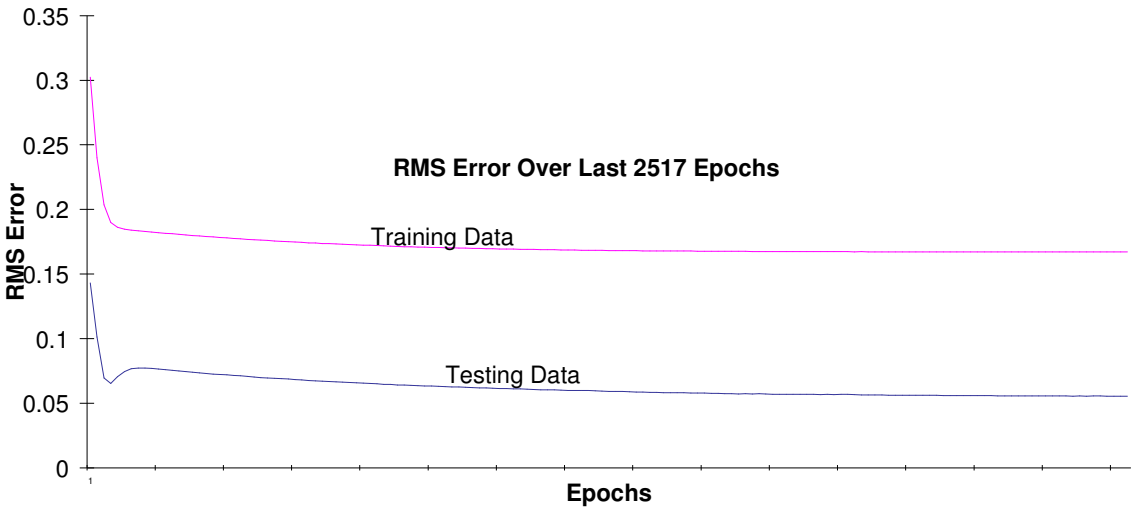


**Figure 5-22. RMS error plots of network no. 3**

Figure 5-23 presents the predicted nitrate concentrations in the wells of Ames wellfield where contamination leves were above 10 mg/L, corresponding to the subsequent 10% reduction of surface nitrogen application rate in the current land use conditions. The plot shows that with the decrease in nitrogen application rate, nitrate concentrations were decreased in all the considered wells. From the neural network model it was determined that, in order to reduce nitrate contamination level below 10mg/L, surface nitrogen application rate should be reduced by 80 percent of the current application rate.

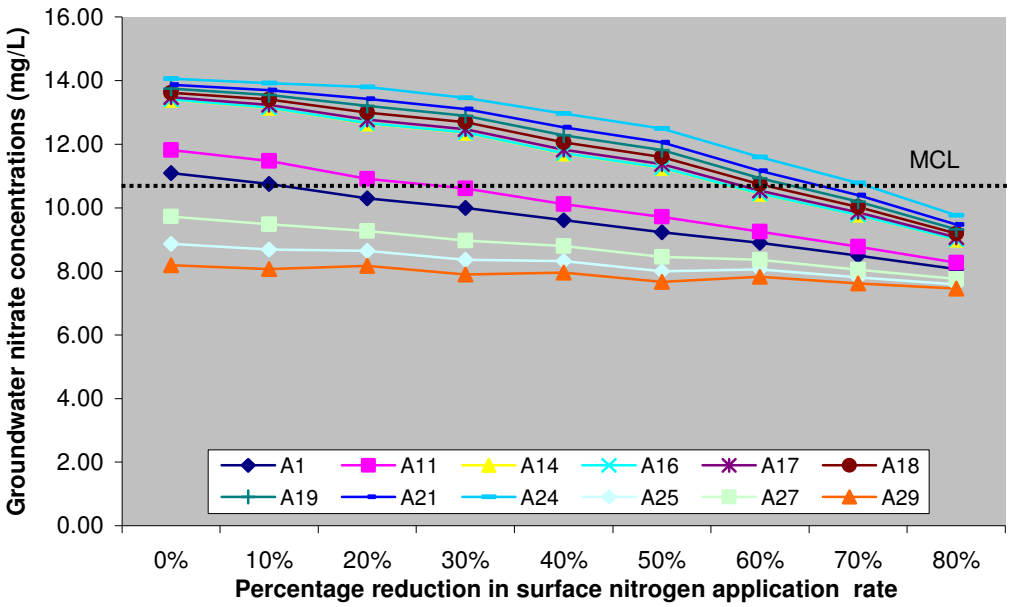


**Figure 5-23. Nitrate concentrations in wells of Ames wellfield having measured nitrate concentrations above 40 mg/L with varying on ground nitrogen application reduction**

## 5.4 Stochastic model

As described in the methodology chapter, the Ames constitutive relationship model was used for a neural conditional simulation. This analysis was conducted to determine the probabilities associated with the nitrate concentration predictions in the wells of Ames wellfield corresponding to the surface nitrogen application. Figure 5-24 and 5-25 presents the plots of running means and standard deviation of predicted nitrate concentrations in well A1 of Ames wellfield. When consecutive simulations predicted relatively constant values of nitrate concentrations, the stochastic modeling was considered finished, i.e. no additional information would be available for the subsequent

simulations. The running mean and standard deviation plots for other 22 wells of this wellfield are presented in appendix D.

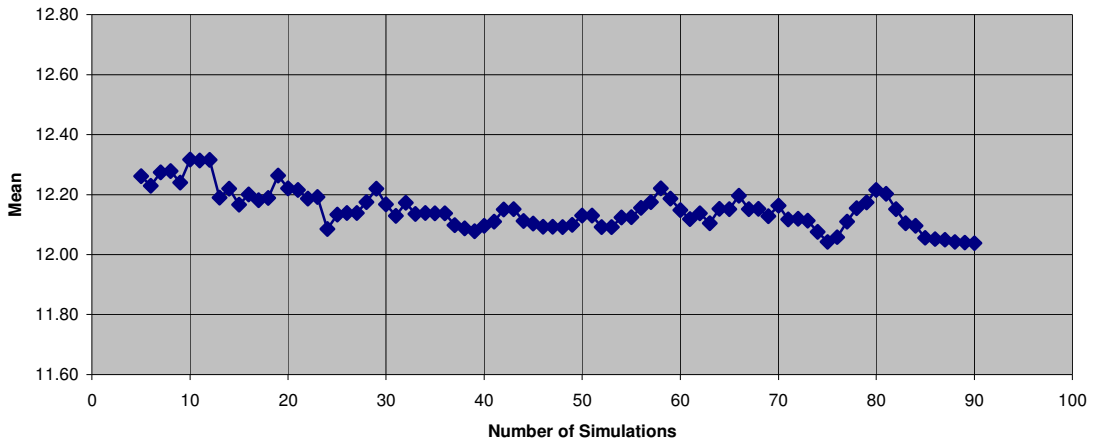


**Figure 5-24. Well A1: Mean versus number of simulations**

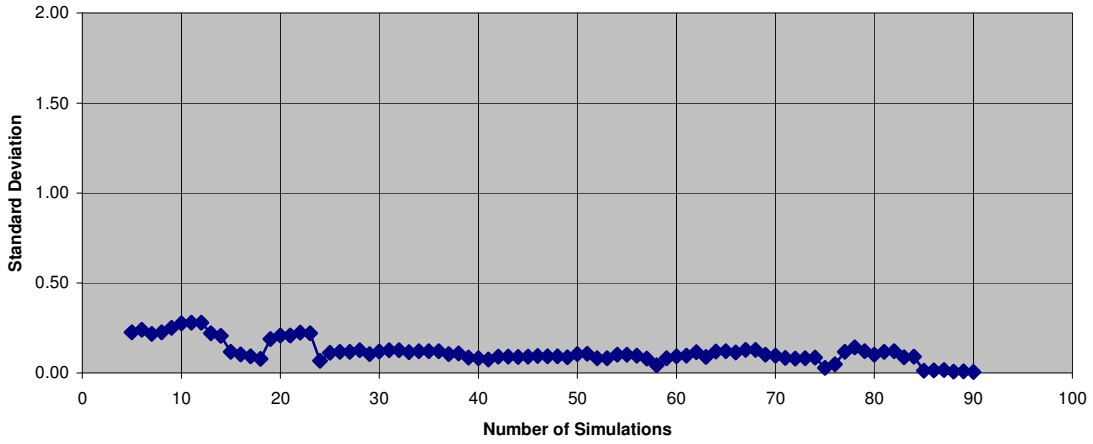


**Figure 5-25. Well A1: Standard deviation versus number of simulations**

These plots show that 90 individual simulations were adequate to achieve consistency in the mean and standard deviation of predicted nitrate concentrations. The predictions of these 90 simulations were then imported into probability and cumulative

density (pdf and cdf) plots using the program @Risk. Best fit curves were determined and ranked by the A-D (Anderson-Darling) method (Palisades Crop., 2002). Figure 5-26 and 5-27 shows the best fit curve for well A1.

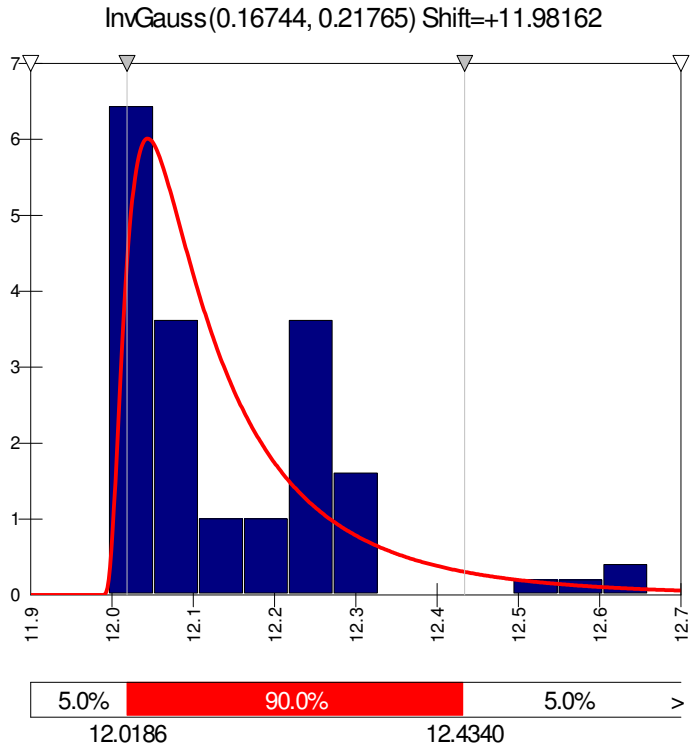


**Figure 5-26. Well A1: Best fit curve probability density**

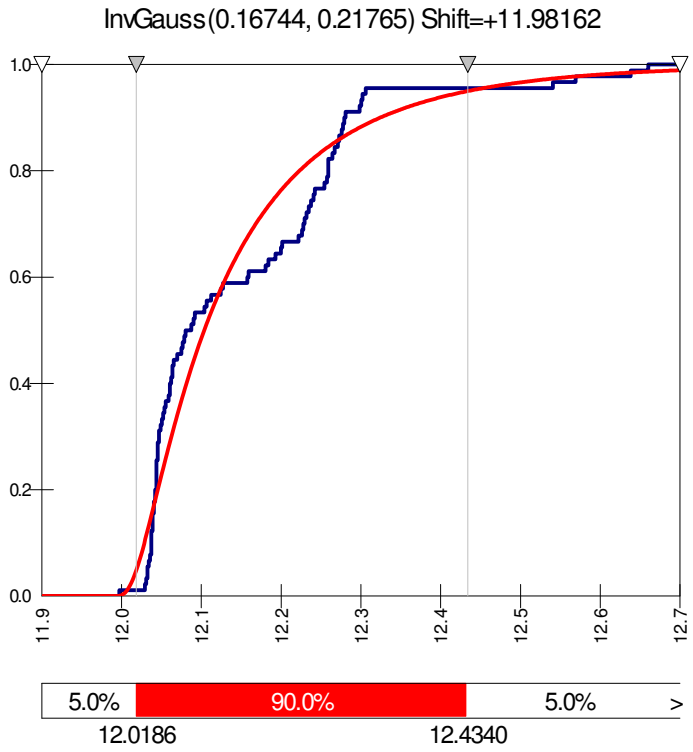


**Figure 5-27. Well A1: Best fit curve for cumulative density**

The plots show the nitrate concentrations expected for each well given the level of allowable uncertainty. For example, the 95$^{th}$ percentile concentration presents the nitrate concentration which is expected to be greater than or equal to 95% of all of the possible simulations which could occur for that well. Table 5-20 presents the 50$^{th}$ percentile and 95$^{th}$ percentile values of nitrate concentrations from best fit curves for all well of Ames wellfield.

**Table 5-20. Summary of results of best fit curves**

| Well_ID | $NO_3$_2003(mg/L) | 50th percentile | 95th percentile | Distribution |
|---|---|---|---|---|
| A1 | 11.73 | 0.17 | 12.43 | Inverse Gaussian |
| A2 | 9.30 | 0.68 | 13.14 | Beta General |
| A3 | 3.40 | 2.23 | 6.07 | Beta General |
| A4 | 6.80 | 54.67 | 6.31 | Beta General |
| A5 | 5.20 | 0.67 | 10.46 | Pearson |
| A6 | 2.47 | 41.46 | 7.68 | Beta General |
| A7 | 4.00 | 0.68 | 6.00 | Beta General |
| A8 | 3.60 | 7.42 | 7.88 | Logistic |
| A9 | 1.80 | 41.46 | 7.68 | Beta General |
| A11 | 13.60 | 12.37 | 12.73 | Triangular |
| A14 | 13.00 | 0.70 | 13.14 | Beta General |
| A16 | 12.40 | 34.71 | 13.48 | Pareto |
| A17 | 15.60 | 12.71 | 12.94 | Triangular |
| A18 | 14.80 | 11.93 | 12.53 | Log Logistic |
| A19 | 14.00 | 0.88 | 13.18 | Beta General |
| A20 | 6.80 | 0.44 | 7.77 | Beta General |
| A21 | 10.70 | 6.68 | 7.50 | Normal |
| A22 | 7.60 | 0.49 | 8.08 | Beta General |
| A23 | 9.35 | 0.44 | 7.71 | Beta General |
| A24 | 8.60 | 7.65 | 8.59 | Normal |
| A25 | 13.40 | 0.50 | 8.05 | Beta General |
| A27 | 7.80 | 4.99 | 8.50 | Beta General |
| A29 | 9.40 | 8.43 | 9.40 | Logistic |

# CHAPTER 6

# DISCUSSION

This chapter discusses the results of the study with respect to the statement of problems explained in Chapter 1. Results of spatial models, constitutive relationship models, management models, and stochastic model are discussed in this chapter. The spatial analysis included an overall or entire aquifer model, a central area model, and individual wellfield models. The constituent relationship models for each wellfield were developed to predict nitrate concentration in groundwater as a function of surface nitrogen application rate. The management models were developed to identify the management options needed to reduce the nitrate contamination below the MCL in Ames wellfield. The neural conditional simulation was performed in Ames constituent relationship model to define the probability of occurrence of the predicted nitrate concentrations.

## 6.1 Discussion on results of spatial models

Spatial models were developed to expand the sampled point data to the area of aquifer in order to identify the nitrate distribution pattern in the Cimarron Terrace Aquifer.

### 6.2.1 Discussion on results of overall aquifer spatial model

In the attempt to identify the pattern of nitrate distribution in the entire Cimarron Terrace Aquifer, an overall aquifer model was initially developed and analyzed. Nitrate concentration data from the city of Enid and from the USGS were used in this effort. Neural kriging method was used to expand the point data of nitrate concentrations taken at well locations over the entire space of the aquifer. The method adequately predicted the nitrate concentrations over the entire aquifer, identifying the pattern of its distribution. A map of predicted nitrate concentration in the entire aquifer (Figure 5-2) showed that nitrate concentration was at a minimum in the northwest section of the aquifer and was increasing towards the southeast. As shown in Figure 2-2 of the 2001 NLCD, grassland is a predominant land cover in the northwest of aquifer. In the south east portion of the study area the percentage of cultivated land increases. The predictions were consistent with earlier studies by Masoner and Mashburn (2004). Masoner and Mashburn studied the nitrogen isotopes in 45 well of Cimarron Terrace Aquifer. Among 45 samples, 28 were sampled in agricultural areas, 18 were in the mixed sources category (combination of synthetic fertilizer, septic or manure waste sources), one was in the septic source category, 17 were in grassland areas, and 4 were in the mixed category. According to them, the results of statistical analysis of the samples indicated that nitrate concentrations in agricultural areas were significantly greater than that in grassland areas. Hence, the model identified the evident trend of low concentrations in the grasslands and high concentrations in cultivated land. Additionally, the identified trend was consistent with the direction of the groundwater movement. In a study conducted by Adams and Bergman (1996), potentiometric surface of groundwater indicated that groundwater is

discharging to the intercepting tributaries and the Cimarron River. They also found that in several areas along the northwest boundary of the aquifer, groundwater is flowing away from the Cimarron River and its perennial tributaries.

The output of the neural kiging analysis identified the low, moderate, and high concentrations areas in the aquifer. The analysis showed that more then 50 percent area of the Cimarron Terrace Aquifer had nitrate concentrations in the range of 4-10 mg/L. The analysis also showed that 19.25 sq. mile areas in the north east and south corners of the aquifer are contaminated with nitrate above the MCL. This information and the predicted concentrations map can be very useful for the water managers to plan the groundwater protection programs in the Cimarron Terrace Aquifer.

Though the overall aquifer model acceptably produced the general picture of nitrate distribution in the Cimarron Terrace Aquifer, it under-predicted the nitrate concentrations in particular locations, especially at the central part of the aquifer. The measured nitrate concentrations in the Ames wellfield, which is near the center of the aquifer, and results of the kriging analysis conducted by KC (2007), showed that the central part of the aquifer was highly contaminated, which was not fully expressed in the overall aquifer model. Changes in the model architecture had no significant effect on the output of this model. Therefore, while the overall aquifer model provided the general picture of nitrate distribution throughout entire aquifer, additional resolution was needed in those areas of high nitrate concentrations.

### 6.2.2 Discussion on results of central area spatial model

In order to predict the nitrate concentrations more accurately in the central area of the Cimarron Terrace Aquifer where the concentrations were not fully expressed in the overall aquifer model, a central area model was subsequently developed. The model predicted that central 155.87 sq. mile area of the aquifer had nitrate concentrations above 10 mg/L. A map of predicted concentrations was shown in Figure. 5-4. Thirty nine percent of measured samples in the Ames wellfield which is towards the central area of the aquifer had nitrate concentrations above 10 mg/L. The predicted values closely resembled the observed nitrate concentrations and even the results of kriging analysis conducted by KC (2007). KC had determined the nitrate concentrations in the range of 12.79 to 16.0 mg/L in this area. Cultivated and developed lands were the principal land use types in the central area of the Cimarron Terrace Aquifer and the high nitrate concentrations in this area may have been due to the intensive application of fertilizer nitrogen in residential and agricultural lands.

### 6.2.3 Discussion on results of individual wellfield spatial model

The results of the overall aquifer model and the central area model concluded that the neural kriging method would be more accurate if it could be used in smaller area. This led to the development of individual wellfield models for the city of Enid's four wellfields.

The individual wellfield models addressed the areas in each wellfield. The grid size in this case was made smaller in order to identify nitrate distribution in detail. These models provided logical results by identifying the plumes which were reasonable in shape

and location. Besides, the predicted concentrations were higher than those used for training and testing the models. This indicates that the neural kriging method were able to adequately extrapolate the nitrate concentrations from training and testing data to areas where it was not measured. The maps of these outputs are illustrated in Figure 5-6, 5-8, 5-10, and 5-12. These maps can be useful in finding the less vulnerable well locations for new installation. They are also helpful for water managers to plan wellhead protection programs.

## 6.3 Discussion on results of constituent relationship models

After the identification of the spatial pattern of nitrate distribution, nitrate concentrations in each well of the four well fields were determined as a function of the surface nitrogen application rate. Nitrogen applied in the 1000m radius of each well was determined and used as input to predict nitrate concentration in the corresponding well.

Grassland is a principal land use type in the Cleospring wellfield. In this Cleospring wellfield, nitrate concentration was predicted in the range of 2.11 to 8.0 mg/L. The predicted concentration range was less then the measured concentration range which was in the range of 0.9 to 16.0 mg/L. In some of the wells of Cleospring wellfield, high concentrations were measured where surface nitrogen application rate were low. This indicates that surface nitrogen application is not only the source of groundwater nitrate in this wellfield. Wells in this wellfield can be contaminated from additional sources including septic systems, and the natural sources.

Nitrate concentration was predicted in the range of 6.57 to15.33 mg/L in the Ringwood wellfield. The high concentrations were predicted in the wells with high nitrogen application rate. Ringwood wellfield is one of the high residential areas with

relatively less cultivated land. Nitrogen fertilizers applied in the residential areas were the potential major sources of high nitrate concentrations in the wells of this wellfield.

Nitrate concentrations in the Ames wellfield were predicted in the range of 5.44 to 13.11 mg/L. The predicted concentration showed that about 35 percent of wells in the Ames wellfield were contaminated beyond the limit of drinking water standard. The Ames wellfield is in the area of high residential density and intensive agricultural activities. Thus the predicted high concentrations showed a strong association with the surface nitrogen application rate.

Cultivated lands are the major land use type in the Drummond wellfield area and hence surface nitrogen application rate was also high. However, nitrate concentrations were predicted in the range of 4.09 to 9.16 mg/L in this wellfield. The measured nitrate concentration was in the range of 3.07 to 12.0 which was relatively low with respect to the nitrogen application rate. Figure 6-1 percents the percentage clay map in the Cimarron Terrace Aquifer determined from the STATGO soil database. The map shows relatively high percentage of clay in the Drummond wellfield area compared to the other wellfields. Besides, depth of groundwater is also high in this wellfield. Though the nitrate application rates were high, high percentage of clay impeded the nitrate leaching into the deep groundwater.

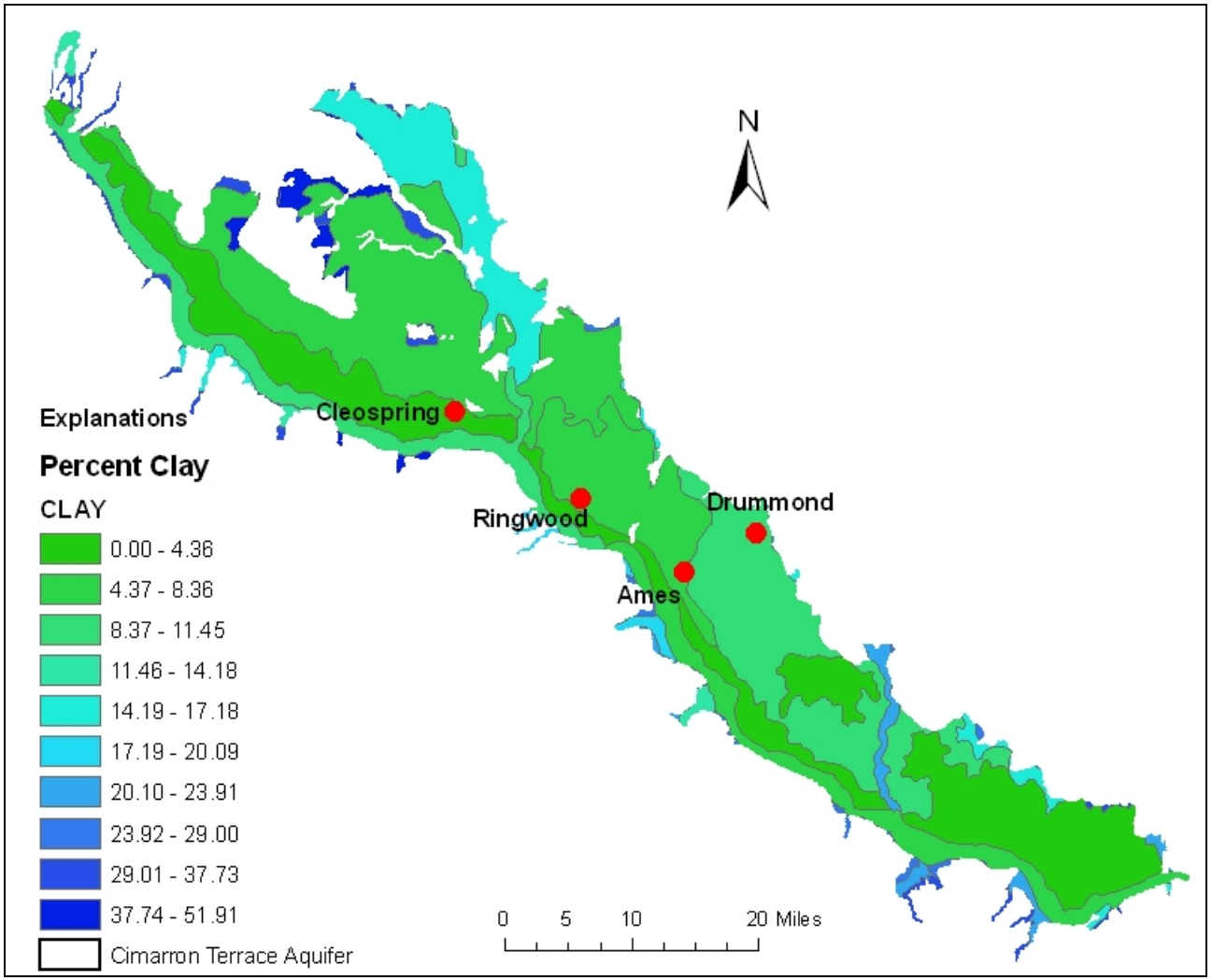


**Figure 6-1. Average soil profile clay content derived from STATSGO database**

Figure 6-2 presents the box plot of measured and predicted nitrate concentrations by Cleospring, Ringwood, Ames, and Drummond wellfield constitutive relationship models.

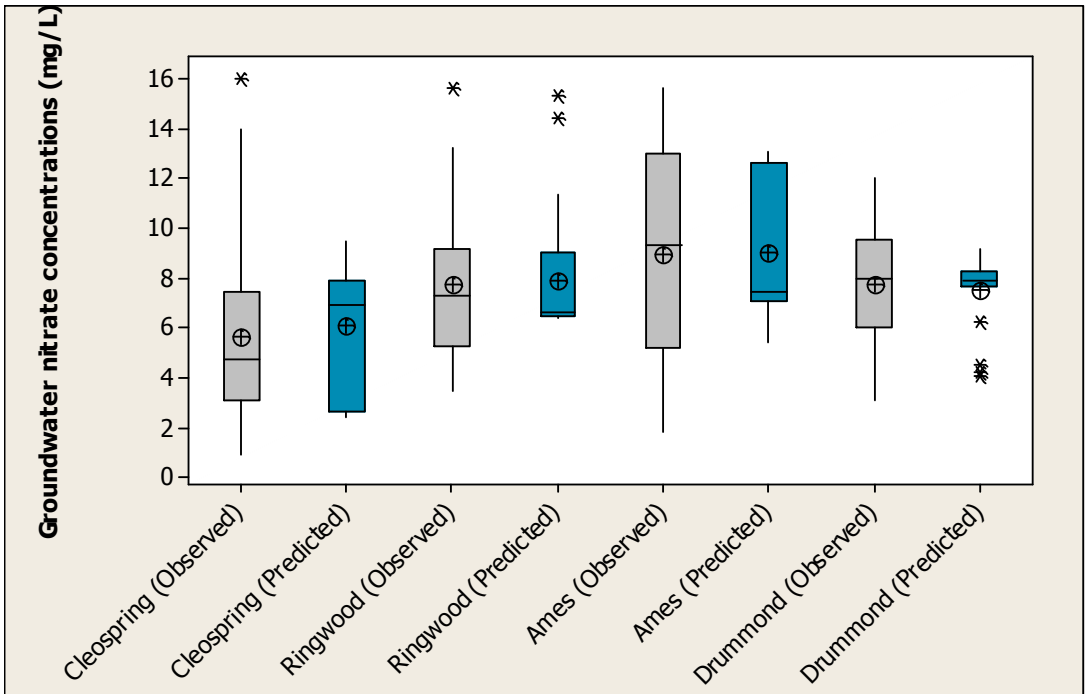


**Figure 6-2. Statistical summary (box plots) of observed and predicted nitrate concentrations in four wellfields**

The plot shows that the mean values of observed and predicted nitrate concentrations are almost equal in each wellfield. The ranges of predicted nitrate concentrations were decreased in all wellfields indicating that models over-predicted the low values and under-predicted the high values.

The Ringwood wellfield constituent relationship model best predicted the nitrate concentration corresponding to the measured values. The model predicted 100 percent of testing data “Right” with default testing tolerance 0.3 and the model had mean absolute percentage error (MAPE) of 16.73 for all data. High concentration values were accurately

predicted by this model. Mean absolute percentage error of 7.76 for values greater then 10 mg/L also verifies the prediction precision. Drummond, Ames, and Cleospring constituent relationship models also have predicted satisfactory results. Hundred percent testing data were “Right” in Drummond, 80 percent were “Right” in Ames, and 83 percent were “Right” in Drummond with default testing tolerance of 0.3. Mean absolute percentage error for all data was calculated 18.25, 23.12, and 43.56 in Drummond, Ames, Cleospring models, respectively. The inaccuracy that occurred in the Cleospring wellfield constituent relationship model may have been due to the fact that high nitrate concentrations were measured in areas of low nitrogen application rates. The Ames wellfield constituent relationship model had also predicted high values satisfactorily, with a mean absolute percentage error for high values of 15.61. The mean absolute percentage error of four wellfields suggested that the models were best in predicting moderate concentrations. All the models overestimated the low values. Lowest mean absolute percentage error for low values was 30.58 for Drummond wellfield constituent model relationship model. The error for low values for all other three models was more then 85 percent. The mean absolute percentage error calculated for three ranges of nitrate concentrations for all the constituent relationship models suggested the development of separate models for different ranges.

## 6.4 Discussion on results of management model

Among the four wellfields, percentage of measured and predicted nitrate concentrations were highest in the wells of Ames wellfield. Measured and predicted concentrations showed that about 39 percent of wells in this wellfield had nitrate

concentration above the MCL. Results of the constituent relationship model showed that high nitrate concentrations in this wellfield were due to the high surface nitrogen application rates. Thus the Ames wellfield constituent relationship model was used to determine the management options to reduce nitrate concentration below the MCL. The accessible management option for groundwater nitrate reduction was reduction of surface nitrogen application rate in this area. Therefore, the Ames wellfield constituent relationship model was simulated each time with subsequent 10% reduction in surface nitrogen application rate. The effect in groundwater nitrate concentration due to reduction in surface nitrogen application rate is shown in Figure 5-21. The model predicted that a 40% reduction in surface nitrogen application rate nitrate concentrations in wells which had concentration level above 10 mg/L would decrease the projected concentrations to below the MCL. The model also predicted that subsequent reductions in surface nitrogen application rate would result in increased nitrate concentrations in wells where they were below 10mg/L. Management models using the four most significant variables of surface nitrogen application rate, developed land, groundwater depth, and percentage clay were also developed but these models also predicted similar results as the bivariant model for concentrations below 10 mg/L. Thus, the results of these models were deemed not realistic. It was determined that significant differences in nitrate concentrations at threshold levels of 4.0 mg/L and 10.0 mg/L required condition-specific models. Similar observations were noticed by Nolan (2001), and KC (2007). This led to the development of separate models for concentrations above 10 mg/L.

The management model for the threshold level of 10mg/L suggested that surface nitrogen application rate should be reduced by 80 percent to decrease the nitrate

contamination below the MCL. Wheat, corn, and oats are the major agricultural products for the Cimarron Terrace Aquifer area (USDA, 1996). A study conducted by Edwards, Raun, Godsey, and Tyalor (2006) showed that around 70 to 80 kg/ha of nitrogen is generally enough to produce ample forage. Sustainable nutrient management approaches in nitrogen application method, fertilizer type, and timing of application can be adapted to reduce the surface nitrogen application.

## 6.5 Discussion on results of stochastic model

In order to determine the probability of occurrence of predicted nitrate concentrations by the Ames wellfield constituent relationship model, a set of stochastic tests were run. A total of 90 individual tests were needed to address the inherent variation in the model prediction. Each model was different from the others by the values of the initial random weights assigned by the code. After each model was completed, initial random weights of the neural network were reset. The cumulative density function (cdf) and probability density function (pdf) were also determined for the results of 90 simulations. The $50^{th}$ and $95^{th}$ percentile nitrate concentrations for each of wells in Ames wellfield were determined from the best fit curves and presented in Table 5-25. With the $50^{th}$ percentile probability, 26% of wells in Ames wellfield were predicted nitrate to have concentrations above the MCL, whereas with the $95^{th}$ percentile probability, 39% of wells were predicted to have nitrate concentrations above the MCL.

# CHAPTER 7

# CONCLUSIONS AND RECOMMENDATIONS

This chapter summarizes the techniques and results of spatial modeling, constituent relationship modeling, management modeling, and stochastic conditional modeling with respect to the problem statement. Some recommendations have also been suggested in the latter section of this chapter.

## 7.1 Conclusions

Identification of nitrate distribution pattern in groundwater is the most important feature for successful contaminant source control and groundwater remediation efforts. The deterministic neural network models provided an advanced technique for assessing the current state of groundwater quality, evaluating nitrate reduction goals below the MCL, and defining probability of occurrence of nitrate concentration in wells of the Cimarron Terrace Aquifer. The main features of the neural network models were:

- economical and simple due to less data and parameter requirements,
- easy to simulate multiple scenarios, and
- adaptive learning capability which captured subtle relationship in the data provided.

The critical issue in this study was model construction. Though the adaptive learning capability of the neural networks helps in modeling disaggregated data, the election of best model based on number of iterations required and optimal parameter specification was difficult. The best model was selected based on the percentage "Right" score of the testing data, number of epochs required to train the model, and the consistency exhibited in the learning process. The consistency in the learning process was evaluated by RMS error plot with the gradual dip. Sudden dips in the plot indicated inconsistent learning which lead to inaccurate predictions. The results of the best model led to the following conclusions:

1. Results of overall aquifer model was mapped and presented in Figure 5-2. The map showed that nitrate concentration in the Cimarron Terrace Aquifer was gradually increasing from northwest to south east. The predicted concentrations showed that groundwater in about 20 percent of the area of the Cimarron Terrace Aquifer were contaminated beyond the limit of EPA's drinking water criteria. Also, more then 50 percent of the area of the Cimarron Terrace Aquifer had nitrate concentrations in the range of 4 to 10 mg/L.
2. The central area model was developed in order to more precisely predict the nitrate concentration in the central area of the aquifer. Figure 5-4 presents the map of output concentrations. The predicted concentrations showed that 115.87 sq. mile area in the central part of the Cimarron Terrace Aquifer were contaminated above the MCL.
3. Four individual spatial models for Cleospring, Ringwood, Ames, and Drummond wellfields were developed and the outputs were mapped and shown in Figure 5-6, 5-8, 5-10, and 5-11. Figure 5-6 shows two nitrate plumes were identified in the

Cleospring wellfield. Plume 1 had contaminated 0.61 sq. mile area of this wellfield above the MCL. Three wells C13, C18, and C21 of this wellfield were within the high concentration area of the plume and they were contaminated above the maximum contamination level (MCL). One plume was identified in Ringwood wellfield from Figure 5-8. In this wellfield 5.8 sq. mile area was contaminated above 10 mg/L. Measured nitrate concentrations in wells: R21, R26, and R28 were above 10 mg/L and these wells were identified in the area of concentration range 9.44 to 19.23 mg/L of the plume. More then 50 percent area of the Ames wellfield had contamination levels beyond the drinking water standard. Two joined plumes were identified in this wellfield as shown in Figure 5-9. Seven wells A1, A13, A14, A16, A17, A18, and A19 were identified in the vicinity of the plumes and the measured nitrate concentrations showed they were contaminated beyond the MCL. One plume was identified in Drummond wellfield which had contaminated 1.14 sq. mile area of this wellfield above the MCL. One well D23, was identified in the plume's high concentration area. All the wellfield spatial models were able to extrapolate the patterns of locations and concentrations from training and testing data in excess of those measured.

4. Four constituent relationship models for each wellfield were determined to determine groundwater nitrate concentrations as a function of surface nitrogen application rates. Figure 5-13, 5-14, 5-15, and 5-16 presents the observed and predicted nitrate concentrations by Cleospring, Ringwood, Ames, and Drummond constituent relationship models, respectively. In all wellfields predicted nitrate concentrations showed strong association with the surface nitrogen application rate and groundwater

nitrate concentrations. The models predicted low concentrations in the Cleospring wellfield and high concentrations in Ames wellfield as grassland and residential land use is predominant in Cleospring wellfield and Ames wellfield respectively. The models were best in predicting moderate values of nitrate concentrations. They had satisfactorily predicted high concentrations but low concentrations were overestimated in all the cases.

5. Ames wellfield constituent relationship models were further developed as management models. The management option of reduced nitrogen application rates were simulated in this effort and the results of the management model for nitrate concentration threshold level 10 mg/L revealed that nitrogen application rate must be reduced by 80% to decrease nitrate concentration below 10 mg/L it in this wellfield.
6. In order to address the probability of occurrence of predicted nitrate concentrations by Ames wellfield constituent relationship model, a set of stochastic tests were run. A total of 90 individual tests were needed to address the inherent variation in this prediction. Cumulative density functions (cdf) and probability density functions (pdf) were determined for nitrate concentrations predicted in each well of Ames wellfield during 90 individual simulations. From the best fit curves of the data, $50^{th}$ and $95^{th}$ percentile concentrations for each well of the Ames wellfield were determined and presented in Table 5-15. With the $50^{th}$ percentile probability 26% of wells in Ames wellfield had nitrate concentrations above the MCL where as with the $95^{th}$ percentile probability 39% of wells had nitrate concentrations above the MCL.

## 7.2 Recommendations

The following recommendations are made from this research:

1. City of Enid sampling wells were closely cluster in central part of aquifer. In order to represent the entire aquifer, data from two agencies were used. Therefore, consistent sampling throughout the aquifer is recommended.
2. The neural kriging (NK) maps of nitrate concentrations of this research provide a general picture of nitrate concentrations in the entire aquifer and a more accurate one at the individual wellfield level. The maps can be utilized in delineating areas of high priority for further action and also in identifying potential vulnerable locations for new well installation.
3. The all data management model showed different results for nitrate concentrations above 4.0 mg/L and 10.0 mg/L. Therefore it is recommended to develope separate models for nitrate threshold level 4.0 mg/L, and 10.0 mg/L.
4. Ames wellfield is in the developed area with intensive agricultural activities. The management model suggested reducing 80 percent surface nitrogen application rate to decrease nitrate concentration below the MCL in this wellfield. Thus, research to optimize agricultural and residential nitrogen application in the Cimarron Terrace Aquifer area is recommended.
5. The results from this study showed that ANN is a promising tool for analyzing the complex physical systems with relatively simple approach. ANN system can be updated by including more subsurface-specific parameters. Therefore, detail investigations of subsurface-specific parameters are also recommended.

# REFERENCES

Adams, P. G., and Bergman, L. D., 1996. Geohydrology of alluvium and terrace deposits of the Cimarroan River from Freedom to Guthrie, Oklahoma: USGS Water Resources Investigations Reports 95-4066.

Aggarwal, R., and Song, Y., 1997. Artificial neural networks in power systems. Part 1 general introduction to neural computing: Power Engineering, v. 11, no. 3, p. 129-134.

Almasri, N. M., and Kaluarachchi, J. J., 2005. Modular neural networks to predict the nitrate distribution in ground water using the on-ground nitrogen loading and recharge data: Environmental Modeling and Software, v. 20, no. 7, p. 851-871.

Aral, M. M., Guan, J., and Maslia, L. M., 2001. Identification of contaminant source location and release history in aquifers: Journal of Hydrologic Engineering, v. 6, no. 3, p. 225-234.

Avery, A. A., 1999. Infantile methemoglobinemia: reexaming the role of drinking water nitrates: Environmental health perpectives, v. 107, no. 7, p. 583-586.

Basheer, I. A., Reddi, L. N., and Najjar, Y. M., 1996. Site characterization by neuronets: an application to the landfill sitting problem: Ground Water, v. 34, no. 4, p. 610-617.

Becker, C. J., 1994. Distribution and variability of nitrogen and phosphorus in the alluvial, high plains, rush springs, and Blaine aquifers in western Oklahoma: U.S. Geological Survey Open-File Report 97-41.

Bergsrud, F., Seelig, B., and Drickson, R., 1992. Treatment systems for household water supplies chlorination: AE-1046 <http://www.ag.ndsu.edu/pubs/h2oqual/watsys/ae1046w.htm>.

Bingham, R. H., and Bergman, D. L., 1980. Reconnaissance of the water resources of the Enid quadrangle, north central Oklahoma: Oklahoma Geological Survey Hydrologic Atlas 7, scale 1: 250,000, 4 sheets.

Bingham, R. H., and Moore, R. L., 1975. Reconnaissance of the water resources of the Oklahoma city quadrangle, central Oklahoma: Oklahoma Geological Survey Hydrologic Atlas 4, scale 1: 250, 000, 4 sheets.

Burkart, M. R. and J. D. Stoner, 2002. Nitrate in Aquifer beneath Agricultural Systems Water Science and Technology, v. 45, no.9, p.19-29.

Carr, J. E., and Bergman, D. L., 1976, Reconnaissance of the water resources of the Clinton quadrangle, west-central Oklahoma: Oklahoma Geological Survey Hydrologic Atlas 5, scale 1: 250, 000, 4 sheets.

Cheshire Engineering Corporation, 1994. Neuralyst User's Guide. Pasadena, California.

Chim, W. K., 1996. A neural-network-based local-field-effect correction scheme for quantitative voltage contrast measurements in the scanning electron microscope: Measurement Science and Technology, v. 7, no. 6., p. 882-887.

Edwards J., Raun, B., Godsey, C., and Taylor, G. C., 2006. Fall N requirement for wheat: OSU Wheat Production Newsletter, v. 3, no. 4, p. 2-3.

Faris, B., Nuttall, E., Spalding, R., Erhman, D., Roberts, K., Williams, A., and Hill, S., 2000: Emerging technologies for enhanced in situ biodenitrification (EISBD) of nitrate-contaminated ground water: Interstate Technology and Regulatory Cooperation Work Group Team Report, <http://www.itrcweb.org/Documents/EISBD-1.pdf>.

Hagen, M. T., Demuth, H. B., and Beale, M., 1996. Neural network design: PWS Publishing Company, Boston, MA.

KC, M., 2007. GIS-based statistical, geostatistical, and stochastic analyses of nitrate contamination in the Cimarron Terrace Aquifer in Oklahoma, M.S. Thesis, Oklahoma State University, Stillwater, Oklahoma.

Koike, K., Matsuda, S., Suzuki, T., and Ohmi, M., 2002. Neural Network-Based Estimation of Principal Metal Contents in the Hokuroku District, Northern Japan, for Exploring Kuroko-Type Deposits: Natural Resources Research, v. 11, no. 2, p. 135-156.

Kumar, A., 2000. Neural network solution for assessment of eutrophication in lake tenkiller: M. S. Thesis, Oklahoma State University, Stillwater, Oklahoma.

Kumar, A., DebRoy, T. 2006. Neural network model of heat and fluid flow in gas metal arc fillet welding based on genetic algorithm and conjugate gradient optimization: Science and Technology of Welding and Joining, v. 11, no. 1, p. 106-119.Li, Z.,

Li, Z., Rizzob, D., and Haydenc, N., 2006. Utilizing artificial neural networks to backtrack source location: University of Vermont <http://www.iemss.org/summit/papers/s2/175_Li_2.pdf>

Ling, G., and El-Kadi, A., 1998. A lumped parameter model for N transformation in the unsaturated zone: Water Resources Research, v. 34, no.2, p. 203-212.

Liu, L., Zechman, M. E., Brill, D. E., Maninthakumar, G., Ranjithan, S., Uber, J., 2006. Adaptive contamination source identification in water distribution systems using an evolutionary algorithm-based dynamic optimization procedure: 8th Annual Water Distribution Systems Analysis Symposium, Cincinnatti, OH.

Lui, C., and Ball, W. P., 1999. Application of inverse methods to contaminant source identification from aquitard diffusion profiles at dover AFB, DE: Water Resources Research, v. 35, no. 7, p. 1975.

Mahinthakumar, G., and Sayeed, M., 2005. Hybrid genetic algorithm-local search methods for solving groundwater source identification inverse problems: Water Resources Publications, v. 131, no. 1, pp. 45–57.

Makowski, A., 2006. Modeling nitrate transportation in Spanish Springs Valley, Washoe County, Neveda, M.S. Thesis, University of Nevada, Reno, Nevada.

Masoner, J. R., and Mashburn, S. L., 2004. Water quality and possible sources of nitrate in the Cimarron Terrace Aquifer, Oklahoma, 2003: U.S. Geological Survey Scientific Investigation Report 04-5221.

McGrail, B.P., 2001. Inverse reactive transport simulator (INVERTS): An inverse model for contaminant transport with nonlinear adsorption and source terms. Environmental Modelling & Software, v. 16, no. 8, p. 711-723.

McTernan, W. F. and B. V. Bonnett, 2002. Using Artificial Neural Network models to determine contaminant sources: Oklahoma State University, Report EA TIET 02-003.

Mendil, B., and Benmahammed, K., 1999. Simple activation functions for neural and fuzzy neural networks: Circuits and Systems, v. 5, p. 347-350.

Morshed, J., Kaluarachchi, J. J., 1998. Parameter estimation using artificial neural network and genetic algorithm for free-product migration and recovery: Water Resources Research v. 34 no. 5, p. 1101-1113.

Morton, R.B., 1992. Simulation of Ground-Water Flow in the Antlers Aquifer in Southeastern Oklahoma and Northeastern Texas: U.S. Geological Survey Water Resources Investigations Report 88-4208, 22 p.

Mueller, D. K., Ruddy, B. C., and Battaglin, W. A., 1993. Relation of nitrate concentrations in surface water to landuse in the upper midwestern United States, 1989-90: Water Resources Investigations Report 94-4015.

Murphy, P. A., 1991. Chemical process for denitrification of nitrates: PatentStrom LLC <http://www.patentstorm.us/patents/5616252-description.html>

Nolan, B. T., 2001. Relating nitrogen sources and aquifer susceptibility to nitrate in shallow ground waters of the United States: Ground Water, v. 39, no.2, p.290-299.

Nolan, B. T., B. C. Ruddy, K. J. Hitt, and D. R. Helsel, 1997. Risk of nitrate in ground waters of the United States- a national perspective: Environmental Science and Technology, v. 31, no. 8, p. 2229-2236.

Palisades Corporation, 2002. @Risk. http://www.palisade.com. Newfield, New York.

Postma, D., Boesen, C., Kristiansen, H. and Larsen, F., 1991. Nitrate reduction in an unconfined sandy aquifer: Water chemistry, reduction processes, and geochemical modeling: Water Resources Research v. 27, no.8, p. 2027–2045.

Reely, B. T., 1992. A linked optimization-simulation aquifer management model: Ph.D. Desertation, Oklahoma State University, Stillwater, Oklahoma.

Rizzo, M. D., and Dougherty, E. D., 1994. Characterization of aquifer properties using artificial neural networks: Neural kriging: Water Resources Research, v. 30, no. 2, p. 483-498.

Rogers, L. L., Dowla, F. U., and Johnson, V. M., 1995. Optimal field scale groundwater remediation using neural networks and the genetic algorithm: Environmental Science and Technology, v. 29, no. 5, p. 1145-1155.

Ryker, J. S. and Jones, L. J., 1995. Nitrate concentrations in ground water of the central Columbia Plateau: USGS Open-File Report 95-445.

Shrestha, R. K., and Ladha, J. K., 2002. Nitrate pollution in groundwater and strategies to reduce pollution: Water Science Technology v. 45, no. 9, p. 29-35.

Singh, M. R., and Datta, B., 2006. Artificial neural network modeling for identification of unknown pollution sources in groundwater with partially missing concentration observation data: Water Resources Management, v. 21., no. 3, p. 557-572.

Singh, R. M., Datta, B., and Jain, A., 2004. Identification of unknown groundwater pollution sources using artificial neural networks: Water Resources Planning and Management, v. 130, no. 6, p. 506-514.

Skaggs, T. H., and Kabala, Z. J., 1994. Recovering the release history of a groundwater contaminant: Water Resources Research, v. 30, no. 1, p. 71-80.

Solley, W.B., Pierce, R.R. and Perlman, H.A., 1998. Estimated use of water in the United States in 1995: United States Geological Survey Circular 1200, p. 1–71.

Spichak, V. V., 2006. Estimating temperature distributions in geothermal areas using a n euronet approach: Geothermics, v. 35, p. 181-197.

Tesoriero, A.J., and Voss, F.D., 1997. Predicting the probability of elevated nitrate concentrations in the Puget Sound Basin: Implications for aquifer susceptibility and vulnerability. Ground Water v. 35, no. 6, p.1029-1039.

U.S. Census Bureau, 1993. 1990 Census of Population. Characteristics of the Population, v. 1. Washington, DC:U.S. Government Printing Office.

U.S. Department of Agriculture, 1996. Extension toxicology network, pesticide information profiles: In Masoner, J. R. and S. L.Mashburn, 2004, Water quality and possible sources of nitrate in the Cimarron Terrace Aquifer, Oklahoma: USGS, Scientific Investigative Reports 2004-5221.

U.S. EPA, 1996. Drinking water regulations and health advisories, Washington, D.C., U.S. EPA, Office of water: US Government printing office.

United States: Environmental Science and technology, v. 34, no.7, p.1156-1165.

William, H., 2007. Remediation of drinking water for rural populations: USDA, <http://www.ars.usda.gov/research/publications/publications.htm?SEQ_NO_115=191344>.

Weyer, P., 2001. Nitrate in drinking water and human health. Center for Health Effects of Environmental Contamination (2001) University of Iowa Center for Health Effects of Environmental Contamination, <http://www.cheec.uiowa.edu/health.html>

Zurada, J.M., 1997. Introduction to Artificial Neural Systems. Jaico Publishing House, Delhi, p. 2226–2229.

APPENDIX A

NITRATE DATA

---

**Table A-1. Annual average nitrate concentrations in wells of (mg/L) in Cleospring wellfield**

| Well_ID | 1997 | 1998 | 1999 | 2000 | 2001 | 2002 | 2003 | 2004 | 2005 |
|---|---|---|---|---|---|---|---|---|---|
| CS1 | 4.52 | 4.47 | 3.80 | 2.74 | 3.92 | 3.24 | 2.95 | 2.00 | 1.80 |
| CS2 | 0.90 | 1.00 | | 0.63 | 1.36 | 1.40 | 1.25 | 1.00 | 1.10 |
| CS3 | 4.85 | 6.38 | 4.30 | 3.30 | 5.24 | 4.40 | 3.90 | 3.92 | 4.08 |
| CS4 | 3.08 | 3.63 | 4.40 | 5.16 | 5.40 | 4.64 | 4.70 | 4.23 | 3.56 |
| CS5 | | 8.30 | | 7.87 | 7.90 | 7.90 | 7.35 | 7.07 | 6.92 |
| CS6 | 7.70 | 9.53 | 8.12 | 7.34 | 7.88 | 7.65 | 6.75 | 6.43 | 6.00 |
| CS8 | 4.88 | 5.27 | 4.90 | 4.60 | 4.76 | 4.80 | 4.60 | 5.28 | 4.36 |
| CS9 | | 8.12 | 8.60 | 6.84 | 7.30 | 7.68 | 7.45 | 7.40 | |
| CS10 | 6.10 | 8.02 | 8.40 | 7.66 | 7.72 | 8.08 | 8.70 | 9.13 | 9.80 |
| CS11 | 4.06 | 4.82 | 4.45 | 4.28 | 4.68 | 4.92 | 5.00 | 4.93 | 4.80 |
| CS12 | | 4.74 | 5.60 | 4.34 | 4.56 | 4.88 | 4.75 | 4.53 | 4.36 |
| CS13 | 4.02 | 4.57 | 4.64 | 4.41 | 4.68 | 4.68 | 4.70 | 4.30 | 4.32 |
| CS14 | 3.80 | 4.47 | 4.83 | 4.70 | 4.88 | 5.00 | 4.80 | 4.73 | 4.76 |
| CS15 | 4.78 | 6.86 | 7.42 | 7.26 | 7.86 | 7.88 | 8.35 | 8.33 | 7.32 |
| CS16 | 4.03 | 5.40 | 5.90 | 5.43 | 5.70 | 5.75 | 6.05 | 5.57 | 5.28 |
| CS17 | 4.70 | 6.80 | 6.20 | 5.87 | 6.84 | 6.64 | 8.40 | 8.73 | 9.56 |
| CS18 | 11.26 | 19.23 | 18.50 | 16.94 | 16.44 | 15.96 | 16.00 | 15.37 | 14.88 |
| CS19 | 2.63 | 2.80 | 3.20 | 2.74 | 3.00 | 3.36 | 3.20 | 3.27 | 3.40 |
| CS20 | 11.37 | 15.63 | 16.90 | 11.93 | 13.50 | 14.48 | 13.95 | 13.40 | 13.04 |
| CS21 | 12.20 | 15.52 | 15.03 | 14.66 | 14.36 | 14.20 | 13.95 | 13.67 | 12.88 |
| CS22 | 2.70 | 3.06 | 3.02 | 3.96 | 3.27 | 4.05 | 4.05 | 4.07 | 3.96 |
| CS23 | 2.65 | 3.90 | 3.66 | 3.13 | 3.10 | 3.70 | 3.90 | 4.00 | 3.40 |
| CS24 | | 2.70 | | 0.87 | 0.88 | 0.40 | | | 4.00 |
| CS25 | 2.24 | 3.42 | 3.08 | 2.46 | 3.04 | 2.55 | 3.00 | 2.60 | 2.55 |
| CS26 | 1.00 | 0.65 | | 1.04 | 0.70 | 1.80 | 1.65 | 1.37 | 1.10 |
| CS27 | 1.45 | 1.38 | 1.42 | 1.10 | 1.52 | 1.96 | 1.80 | 1.47 | 1.45 |
| CS28 | | 0.07 | 0.37 | 0.44 | 0.40 | | 1.00 | 0.70 | |
| CS29 | 0.38 | 0.12 | 0.34 | 0.48 | 0.30 | 0.80 | 0.90 | 0.47 | 0.93 |
| CS30 | 3.28 | 3.60 | 4.08 | 3.99 | 4.24 | 4.76 | 5.10 | 4.37 | 4.30 |
| CS31 | 3.35 | 4.30 | 4.52 | 4.03 | 4.36 | 4.80 | 4.80 | 4.53 | 4.45 |

**Table A-2. Annual average nitrate concentrations (mg/L) in wells of Ringwood wellfield**

| Well_ID | 1997 | 1998 | 1999 | 2000 | 2001 | 2002 | 2003 | 2004 | 2005 |
|---|---|---|---|---|---|---|---|---|---|
| R1 | 5.64 | 8.22 | 8.52 | 7.80 | 7.87 | 7.52 | 7.40 | 7.53 | 6.80 |
| R2 | 4.28 | 7.34 | 7.73 | 7.40 | 7.63 | 7.28 | 7.25 | 7.60 | 7.07 |
| R3 | | 7.40 | 7.60 | 7.73 | 9.10 | 9.00 | 9.15 | 9.03 | 9.20 |
| R4 | 4.52 | | 8.26 | 7.77 | 8.13 | 8.10 | 8.35 | 8.60 | 8.37 |
| R5 | 5.70 | 7.87 | 7.85 | 7.23 | 7.27 | 7.28 | 7.30 | 7.27 | 6.83 |
| R6 | 4.46 | 6.87 | 6.93 | 6.80 | 7.00 | 6.76 | 6.80 | 7.00 | |
| R7 | | 6.10 | 8.80 | 7.10 | 7.52 | 7.52 | 7.30 | 7.65 | 7.27 |
| R8 | 5.56 | 9.20 | 9.88 | 8.71 | 9.87 | 9.30 | 8.95 | 9.13 | 8.93 |
| R9 | 5.22 | 8.28 | 9.55 | 8.69 | 9.27 | 9.37 | 9.60 | 10.20 | 9.32 |
| R10 | 3.38 | 6.56 | 6.73 | 6.56 | 6.93 | 7.32 | 7.00 | 7.35 | 6.73 |
| R11 | 3.70 | 6.30 | 6.60 | 6.76 | 6.80 | 7.00 | 6.45 | 6.55 | 6.53 |
| R12 | 3.54 | 5.70 | 6.02 | 5.74 | 5.90 | 6.17 | 6.45 | 6.65 | 6.53 |
| R13 | 3.95 | 7.00 | 7.66 | 7.30 | 8.07 | 7.77 | 7.70 | 7.80 | 7.87 |
| R14 | 4.66 | 7.33 | 10.48 | 9.37 | 12.17 | 11.63 | 12.10 | 13.60 | 13.63 |
| R15 | 4.10 | 4.84 | 5.58 | 4.99 | 5.43 | 5.30 | 5.25 | 5.00 | |
| R16 | 3.32 | 5.24 | 6.05 | 6.57 | 7.40 | 7.50 | 8.40 | | |
| R17 | | 3.60 | 3.80 | 3.33 | 4.57 | 4.50 | 4.70 | 4.65 | 4.93 |
| R18 | 3.25 | 4.48 | 4.20 | 4.18 | 4.60 | 4.87 | 5.10 | 5.47 | 5.47 |
| R19 | 3.32 | 4.34 | 4.17 | 4.10 | 4.80 | 5.47 | 5.10 | 5.40 | 5.10 |
| R20 | 5.04 | 8.48 | 9.62 | 8.85 | 10.83 | 10.47 | 10.80 | 12.00 | 11.70 |
| R21 | | 9.20 | 12.00 | 10.25 | 12.87 | 13.50 | 13.25 | 13.65 | 13.33 |
| R22 | 3.35 | 3.87 | 3.60 | 3.57 | 3.85 | 4.20 | 4.20 | | |
| R24 | 3.30 | 3.25 | 2.80 | 2.50 | 3.53 | 3.27 | 3.45 | 3.55 | 3.80 |
| R25 | 2.50 | 3.03 | 2.80 | 2.65 | 2.75 | 3.47 | 3.70 | 3.40 | 3.33 |
| R26 | 4.67 | 9.60 | 10.60 | 8.98 | 10.27 | 10.84 | 11.20 | 11.90 | 12.17 |
| R27 | 2.83 | 4.70 | 4.97 | 5.31 | 5.40 | 6.32 | 7.05 | 8.00 | 7.80 |
| R28 | 10.00 | 15.82 | 18.80 | 17.03 | 16.00 | 15.60 | 15.60 | 16.15 | 15.73 |

**Table A-3. Annual average nitrate concentrations (mg/L) in wells of Ames wellfield**

| Well_ID | 1997 | 1998 | 1999 | 2000 | 2001 | 2002 | 2003 | 2004 | 2005 |
|---|---|---|---|---|---|---|---|---|---|
| A1 | 11.35 | 12.93 | 13.00 | 10.40 | 10.00 | 11.50 | 11.73 | 11.80 | 11.67 |
| A2 | 7.03 | 10.33 | 10.73 | 10.76 | 9.64 | 9.89 | 9.30 | 9.36 | 9.24 |
| A3 | 3.67 | 4.07 | 4.10 | 3.80 | | 3.80 | 3.40 | | |
| A4 | 5.40 | 7.03 | 7.00 | | 7.60 | 6.60 | 6.80 | | 8.30 |
| A5 | 3.35 | 3.55 | 3.65 | | 8.60 | 5.80 | 5.20 | | |
| A6 | 1.50 | 1.73 | 1.72 | 1.64 | 1.80 | 2.40 | 2.47 | 2.50 | 2.00 |
| A7 | 3.23 | 2.90 | 2.86 | 5.10 | 2.80 | 5.60 | 4.00 | | |
| A8 | | 3.45 | 2.67 | 2.65 | 3.80 | 3.00 | 3.60 | | 3.50 |
| A9 | | 1.00 | 1.00 | 1.00 | 1.20 | 1.80 | 1.80 | | |
| A11 | 8.65 | 11.80 | 12.20 | | | 14.80 | 13.60 | | 11.20 |
| A12 | 7.08 | 10.08 | | 6.80 | | | | | |
| A13 | 12.60 | 14.87 | | | | 14.00 | | | |
| A14 | 10.90 | 14.27 | 14.20 | | | 12.90 | 13.00 | | 11.00 |
| A15 | | 4.30 | 4.37 | | 4.40 | | | | |
| A16 | 12.23 | 17.33 | 16.30 | | | 13.60 | 12.40 | | 11.20 |
| A17 | 12.29 | 16.80 | | 11.68 | 14.50 | 16.00 | 15.60 | | |
| A18 | 18.30 | 20.33 | 18.60 | | | 15.30 | 14.80 | | 12.80 |
| A19 | | 8.45 | 13.00 | | | 12.80 | 14.00 | | 11.70 |
| A20 | | 6.67 | 6.70 | 6.23 | 6.60 | 6.60 | 6.80 | 6.80 | 6.10 |
| A21 | 8.85 | 11.10 | 10.50 | | | 8.70 | 10.70 | | |
| A22 | 5.80 | 7.90 | 8.00 | 6.25 | 7.80 | 6.40 | 7.60 | | |
| A23 | | 10.25 | | 9.10 | | 9.30 | 9.35 | 9.60 | |
| A24 | 7.20 | 8.90 | 9.37 | 8.40 | 10.00 | 8.70 | 8.60 | | 9.20 |
| A25 | 11.25 | 12.00 | 15.00 | 12.05 | 14.00 | 14.07 | 13.40 | 13.40 | |
| A27 | | | | | | | 7.80 | 8.60 | 7.80 |
| A29 | 8.33 | 10.25 | 9.80 | 9.08 | 9.90 | 9.40 | 9.40 | 9.80 | 9.20 |
| A30 | | | | | | | | 7.60 | 7.60 |
| A32 | | | | | | | | 7.40 | 7.90 |
| A33 | | | | | | | | 5.90 | 5.93 |

**Table A-4. Annual average nitrate concentrations (mg/L) in wells of Drummond wellfield**

| Well_ID | 1997 | 1998 | 1999 | 2000 | 2001 | 2002 | 2003 | 2004 | 2005 |
|---|---|---|---|---|---|---|---|---|---|
| D1 | | 8.20 | | | | 7.00 | 3.60 | | 4.00 |
| D2 | | | 7.30 | 8.00 | | 9.20 | 8.20 | | |
| D3 | 8.04 | 9.45 | 9.48 | 8.10 | 9.00 | 9.13 | 8.85 | 9.00 | |
| D5 | 6.06 | 9.38 | 9.66 | 8.70 | 9.00 | 9.33 | 9.80 | 10.12 | 10.00 |
| D6 | 5.40 | 6.86 | 6.95 | 6.39 | 6.88 | 7.07 | 6.80 | 6.96 | 7.25 |
| D7 | 8.87 | 13.23 | 14.40 | 12.64 | 13.07 | 11.66 | 12.00 | 11.84 | 11.60 |
| D8 | 10.43 | 12.90 | 12.40 | 11.40 | 10.70 | 10.80 | 10.45 | 10.53 | |
| D9 | 1.55 | 1.60 | 1.53 | 1.51 | 2.87 | 3.30 | 3.07 | 2.73 | 2.85 |
| D10 | 3.72 | 5.26 | 5.34 | 4.70 | 5.50 | 5.80 | 4.87 | 4.92 | 4.73 |
| D12 | 4.83 | 5.54 | 5.51 | 5.33 | 5.70 | 5.51 | 5.43 | 5.60 | 5.80 |
| D18 | 6.52 | 9.08 | 9.36 | 8.46 | 9.63 | 8.50 | 8.93 | 9.05 | 8.80 |
| D19 | 3.67 | 4.52 | 4.84 | 4.94 | 5.40 | 6.40 | 6.00 | | |
| D20 | 6.94 | 8.50 | 8.43 | 7.69 | 8.60 | 8.44 | 8.53 | 8.80 | 8.70 |
| D21 | 5.73 | 7.09 | 7.09 | 6.81 | 7.28 | 7.65 | 7.60 | 7.40 | 7.40 |
| D23 | 8.50 | 12.45 | 11.73 | 10.67 | 10.75 | 10.60 | 10.73 | 11.28 | 11.05 |
| D25 | 6.75 | 8.70 | 8.23 | 6.66 | 8.00 | 7.53 | 7.68 | 7.60 | 7.24 |
| D26 | | 3.60 | 6.95 | 3.10 | | | | | |
| D27 | 5.50 | 8.84 | 8.65 | 8.07 | | 7.07 | 6.90 | 6.76 | 7.10 |
| D28 | | 8.60 | 7.80 | 7.80 | | 10.00 | 9.60 | | |
| D29 | 6.84 | 9.43 | 9.41 | 7.97 | 9.23 | 9.11 | 9.30 | 9.48 | 9.40 |
| D31 | 5.40 | 3.93 | 6.20 | 6.10 | | | | | |
| D32 | 3.40 | 4.40 | 4.38 | 4.16 | 4.73 | | | | |
| D33 | 3.99 | 5.58 | 5.98 | 5.90 | 7.30 | 5.97 | 6.00 | 5.56 | 5.85 |

**Table A-5. Nitrate concentrations (mg/L) in USGS study wells**

| Well ID | 2003 | Well ID | 2003 |
|---|---|---|---|
| W1 | 9.37 | W31 | 0.13 |
| W2 | 12.3 | W32 | 6.03 |
| W3 | 2.19 | W33 | 3.63 |
| W4 | 14.8 | W34 | 15.6 |
| W5 | 16.8 | W35 | 1.24 |
| W6 | 6.14 | W36 | 0.37 |
| W7 | 10.1 | W37 | 3.68 |
| W8 | 6.93 | W38 | 20.4 |
| W9 | 0.06 | W39 | 2.2 |
| W10 | 5.83 | W40 | 8.48 |
| W11 | 15.3 | W41 | 2.53 |
| W12 | 9.01 | W42 | 11.9 |
| W13 | 1.11 | W43 | 5.99 |
| W14 | 4.21 | W44 | 3.3 |
| W15 | 15.4 | W45 | 17.9 |
| W16 | 8.36 | | |
| W17 | 21.3 | | |
| W18 | 20.5 | | |
| W19 | 2.27 | | |
| W20 | 14.4 | | |
| W21 | 4.11 | | |
| W22 | 16.4 | | |
| W23 | 31.8 | | |
| W24 | 8.03 | | |
| W25 | 11.2 | | |
| W26 | 4.38 | | |
| W27 | 8.35 | | |
| W28 | 2.48 | | |
| W29 | 0.95 | | |
| W30 | 14.9 | | |

APPENDIX B

OUTPUTES OF FOUR INDIVIDUAL WELLFIELDS CONSTITUENT

RELATIONSHIP MODELS

---

**Table B-1. Outputs of Cleospring wellfield constituent relationship model**

| Well ID | N Applications (kg/ sq. mile) | $NO_3$ (mg/L) | Output | MF |
|---|---|---|---|---|
| CS29 | 5.987 | 0.90 | 2.84 | TEST |
| CS28 | 3.014 | 1.00 | 2.41 | TRAIN |
| CS2 | 5.592 | 1.25 | 2.67 | TRAIN |
| CS26 | 3.482 | 1.65 | 2.37 | TRAIN |
| CS27 | 3.466 | 1.80 | 2.37 | TRAIN |
| CS1 | 6.179 | 2.95 | 2.94 | TRAIN |
| CS25 | 3.877 | 3.00 | 2.36 | TRAIN |
| CS19 | 17.099 | 3.20 | 8.86 | TEST |
| CS3 | 23.952 | 3.90 | 7.51 | TRAIN |
| CS23 | 14.578 | 3.90 | 9.31 | TRAIN |
| CS22 | 2.871 | 4.05 | 2.43 | TRAIN |
| CS8 | 38.636 | 4.60 | 6.76 | TRAIN |
| CS13 | 31.334 | 4.70 | 6.94 | TRAIN |
| CS4 | 14.713 | 4.70 | 9.30 | TEST |
| CS12 | 21.270 | 4.75 | 7.93 | TRAIN |
| CS14 | 39.480 | 4.80 | 6.75 | TRAIN |
| CS11 | 12.863 | 5.00 | 9.20 | TEST |
| CS30 | 5.075 | 5.10 | 2.51 | TRAIN |
| CS16 | 22.739 | 6.05 | 7.68 | TRAIN |
| CS6 | 32.113 | 6.75 | 6.91 | TEST |
| CS5 | 27.513 | 7.35 | 7.15 | TRAIN |
| CS9 | 26.156 | 7.45 | 7.27 | TRAIN |
| CS15 | 21.258 | 8.35 | 7.93 | TRAIN |
| CS17 | 29.845 | 8.40 | 7.01 | TRAIN |
| CS10 | 27.049 | 8.70 | 7.19 | TEST |
| CS20 | 18.154 | 13.95 | 8.61 | TRAIN |
| CS21 | 14.623 | 13.95 | 9.30 | TRAIN |
| CS18 | 34.815 | 16.00 | 6.83 | TRAIN |

**Table B-2. Outputs of Ringwood wellfield constituent relationship model**

| Well_ID | N Applications (kg/ sq. mile) | $NO_3$ (mg/L) | Output | MF |
|---|---|---|---|---|
| R24 | 9.83 | 3.45 | 6.57 | TEST |
| R25 | 4.17 | 3.70 | 6.71 | TRAIN |
| R22 | 11.38 | 4.20 | 6.97 | TRAIN |
| R17 | 11.35 | 4.70 | 6.96 | TRAIN |
| R18 | 9.91 | 5.10 | 6.58 | TRAIN |
| R19 | 8.98 | 5.10 | 6.44 | TRAIN |
| R15 | 8.82 | 5.25 | 6.43 | TRAIN |
| R11 | 8.75 | 6.45 | 6.42 | TEST |
| R12 | 8.82 | 6.45 | 6.43 | TEST |
| R6 | 6.20 | 6.80 | 6.44 | TEST |
| R10 | 8.28 | 7.00 | 6.39 | TRAIN |
| R27 | 7.49 | 7.05 | 6.37 | TRAIN |
| R2 | 3.68 | 7.25 | 6.81 | TRAIN |
| R5 | 3.33 | 7.30 | 6.88 | TRAIN |
| R7 | 8.73 | 7.30 | 6.42 | TRAIN |
| R1 | 3.57 | 7.40 | 6.83 | TRAIN |
| R13 | 9.37 | 7.70 | 6.49 | TRAIN |
| R4 | 16.09 | 8.35 | 9.31 | TRAIN |
| R16 | 9.39 | 8.40 | 6.49 | TRAIN |
| R8 | 8.01 | 8.95 | 6.38 | TEST |
| R3 | 9.82 | 9.15 | 6.57 | TRAIN |
| R9 | 24.78 | 9.60 | 11.37 | TRAIN |
| R20 | 20.77 | 10.80 | 10.90 | TRAIN |
| R26 | 15.58 | 11.20 | 9.05 | TRAIN |
| R14 | 20.77 | 12.10 | 10.90 | TRAIN |
| R21 | 48.62 | 13.25 | 14.42 | TEST |
| R28 | 56.43 | 15.60 | 15.33 | TRAIN |

**Table B-3. Outputs of Ames wellfield constituent relationship model**

| Well_ID | N Applications (kg/ sq. mile) | $NO_3$ (mg/L) | Output | MF |
|---|---|---|---|---|
| A7 | 52.75 | 4.00 | 5.44 | TRAIN |
| A3 | 47.99 | 3.40 | 5.72 | TRAIN |
| A4 | 45.10 | 6.80 | 5.97 | TEST |
| A21 | 40.56 | 10.70 | 6.37 | TRAIN |
| A5 | 38.31 | 5.20 | 6.57 | TRAIN |
| A22 | 32.69 | 7.60 | 7.03 | TRAIN |
| A25 | 32.48 | 13.40 | 7.05 | TRAIN |
| A6 | 62.20 | 2.47 | 7.05 | TEST |
| A20 | 31.17 | 6.80 | 7.15 | TRAIN |
| A23 | 30.72 | 9.35 | 7.19 | TRAIN |
| A9 | 27.25 | 1.80 | 7.44 | TRAIN |
| A8 | 27.08 | 3.60 | 7.45 | TRAIN |
| A24 | 20.36 | 8.60 | 7.89 | TEST |
| A27 | 13.64 | 7.80 | 8.27 | TRAIN |
| A29 | 8.59 | 9.40 | 8.54 | TRAIN |
| A18 | 70.36 | 14.80 | 12.04 | TEST |
| A1 | 70.54 | 11.73 | 12.10 | TRAIN |
| A16 | 104.10 | 12.40 | 12.66 | TRAIN |
| A11 | 72.99 | 13.60 | 12.73 | TRAIN |
| A17 | 90.64 | 15.60 | 12.85 | TRAIN |
| A2 | 84.32 | 9.30 | 13.01 | TRAIN |
| A14 | 84.05 | 13.00 | 13.02 | TRAIN |
| A19 | 78.41 | 14.00 | 13.11 | TEST |

**Table B-4. Outputs of Drummond wellfield constituent relationship model**

| Well_ID | N Applications (kg/ sq. mile) | $NO_3$ (mg/L) | Output | MF |
|---|---|---|---|---|
| D19 | 59.48 | 6.00 | 4.09 | TRAIN |
| D9 | 54.30 | 3.07 | 4.24 | TRAIN |
| D1 | 70.10 | 3.60 | 4.47 | TRAIN |
| D10 | 75.09 | 4.87 | 6.21 | TEST |
| D29 | 125.69 | 9.30 | 7.62 | TEST |
| D28 | 123.27 | 9.60 | 7.65 | TRAIN |
| D12 | 118.35 | 5.43 | 7.73 | TRAIN |
| D21 | 117.35 | 7.60 | 7.74 | TRAIN |
| D27 | 117.19 | 6.90 | 7.75 | TRAIN |
| D5 | 78.27 | 9.80 | 7.79 | TEST |
| D23 | 107.21 | 10.73 | 8.04 | TRAIN |
| D33 | 105.44 | 6.00 | 8.12 | TRAIN |
| D25 | 103.90 | 7.68 | 8.20 | TRAIN |
| D18 | 79.28 | 8.93 | 8.20 | TRAIN |
| D6 | 102.59 | 6.80 | 8.26 | TRAIN |
| D7 | 101.76 | 12.00 | 8.31 | TRAIN |
| D2 | 94.90 | 8.20 | 8.77 | TRAIN |
| D3 | 83.51 | 8.85 | 9.13 | TRAIN |
| D20 | 83.66 | 8.53 | 9.14 | TRAIN |
| D8 | 89.00 | 10.45 | 9.16 | TEST |

# APPENDIX D

## RUNNING MEAN AND STANDARD DEVATION PLOT OF NITRATE CONCENTRATIONS PREDICTED BY NEUARL CONDITIONAL SIMULATIONS

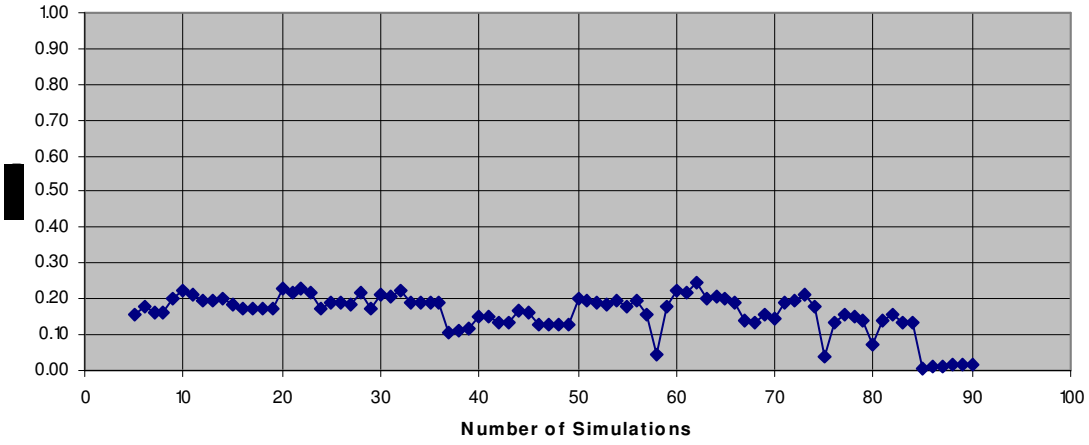


**(a)**

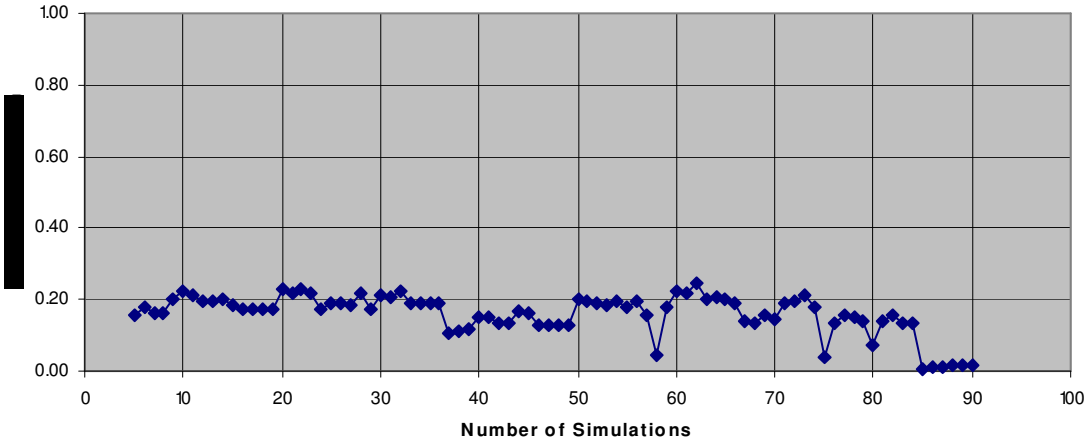


**(b)**

**Figure D-1. Well A2: (a) Mean versus number of simulations; (b) standard deviation versus number of simulations**

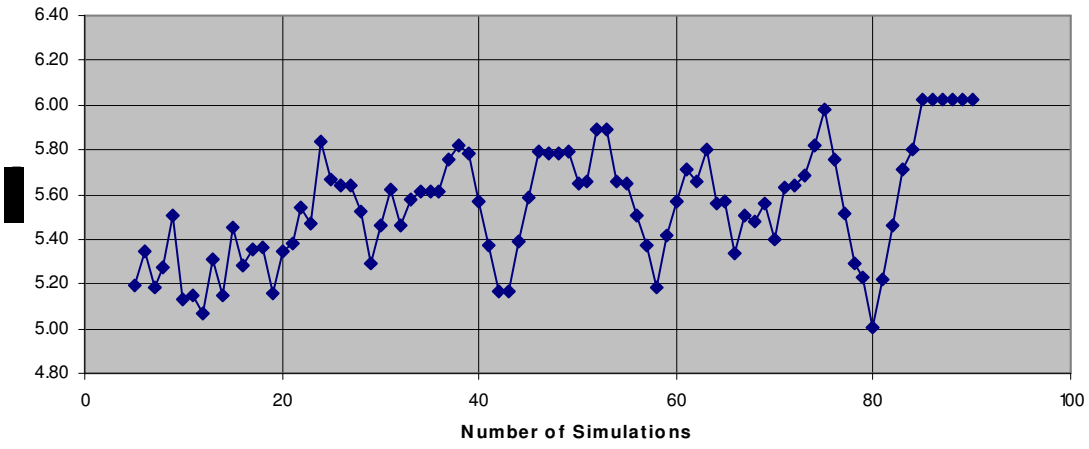


**(a)**

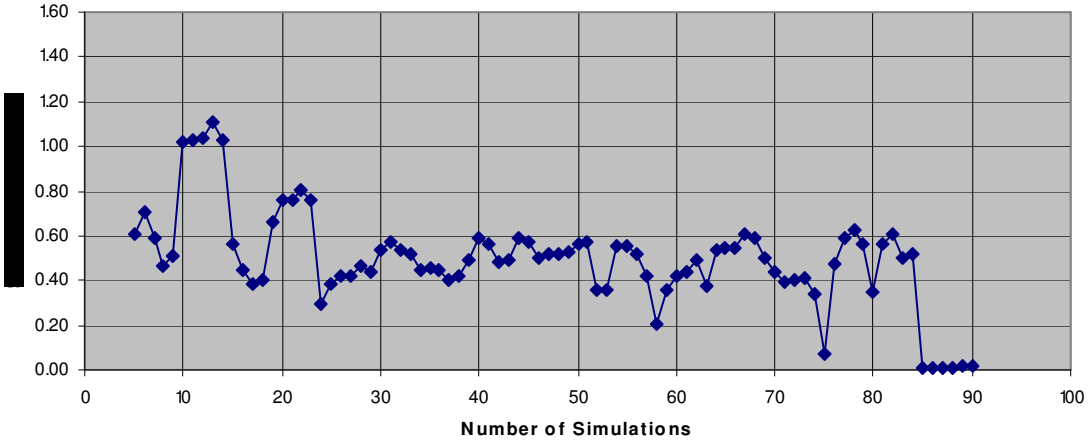


**(b)**

**Figure D-2. Well A3: (a) Mean versus number of simulations; (b) standard deviation versus number of simulations**

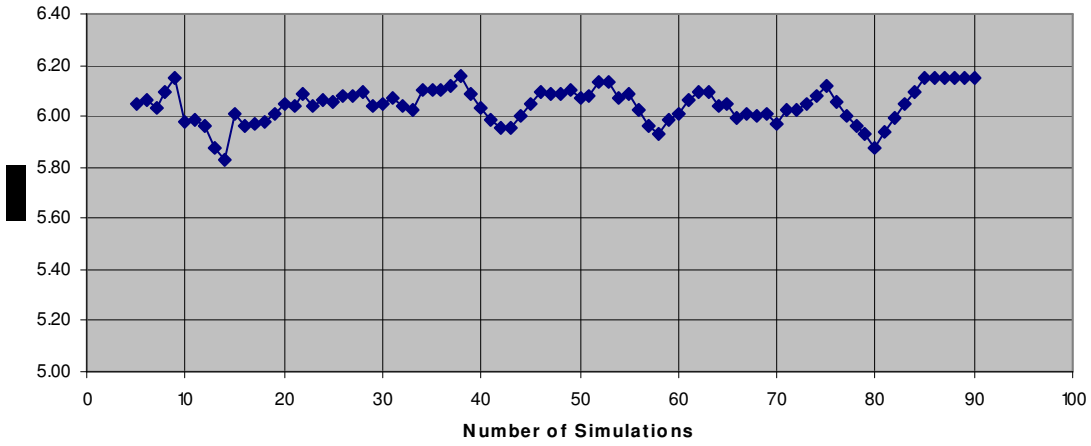


**(a)**

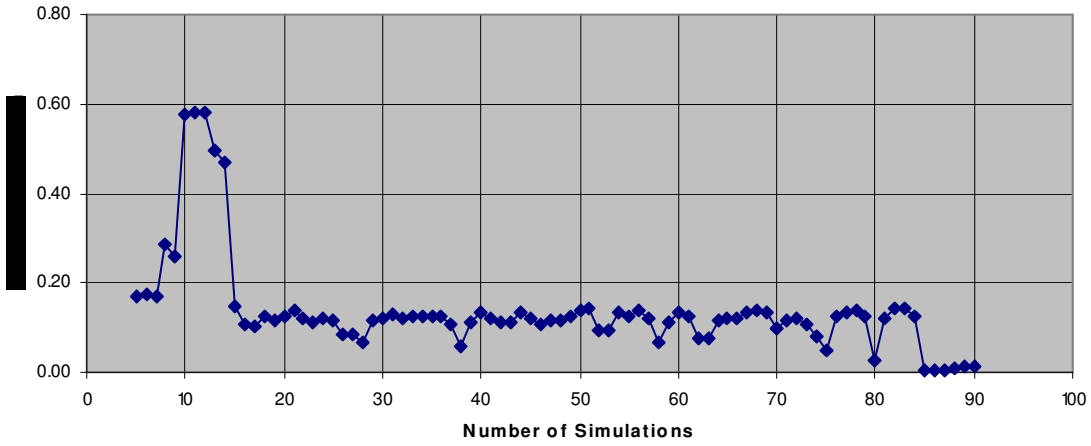


**(b)**

**Figure D-3. Well A4: (a) Mean versus number of simulations; (b) standard deviation versus number of simulations**

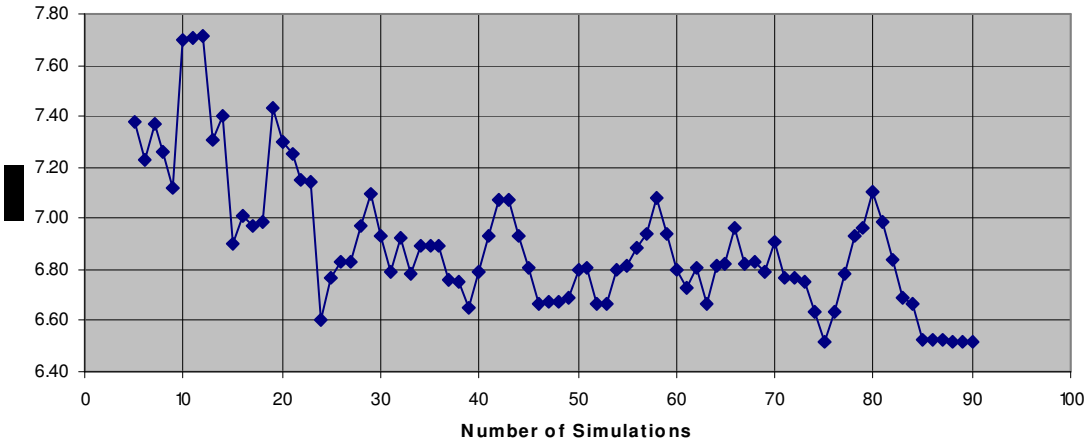


**(a)**

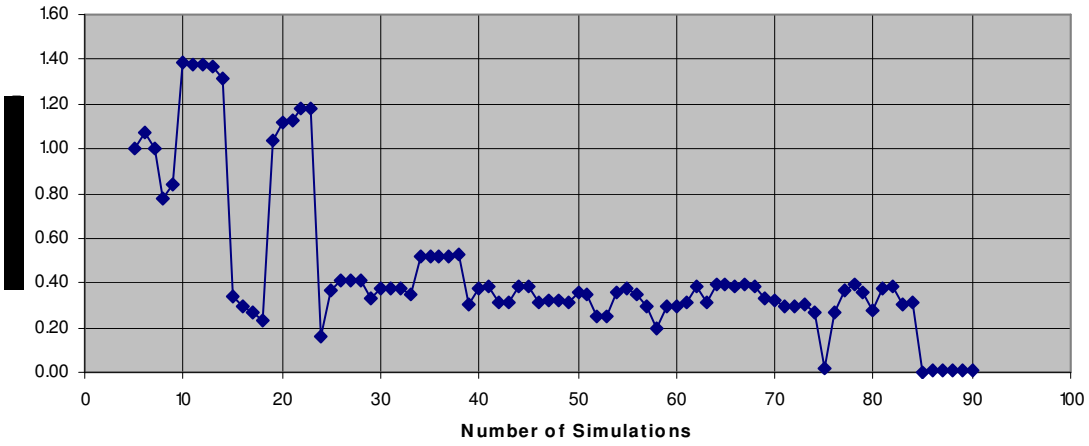


**(b)**

**Figure D-4. Well A5: (a) Mean versus number of simulations; (b) standard deviation versus number of simulations**

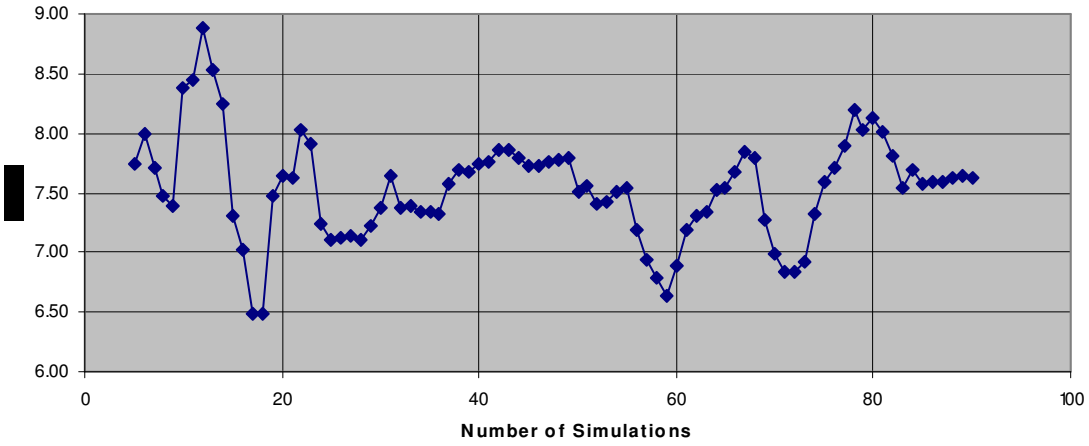


**(a)**

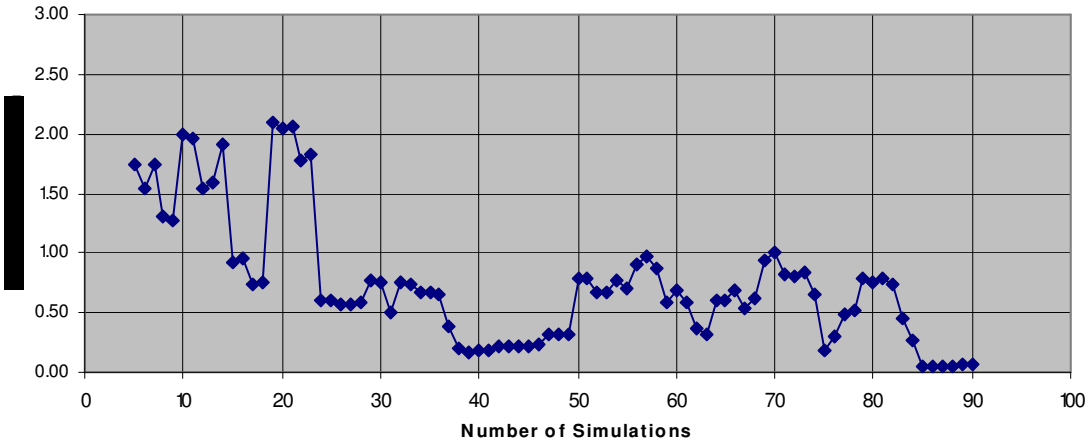


**(b)**

**Figure D-5. Well A6: (a) Mean versus number of simulations; (b) standard deviation versus number of simulations**

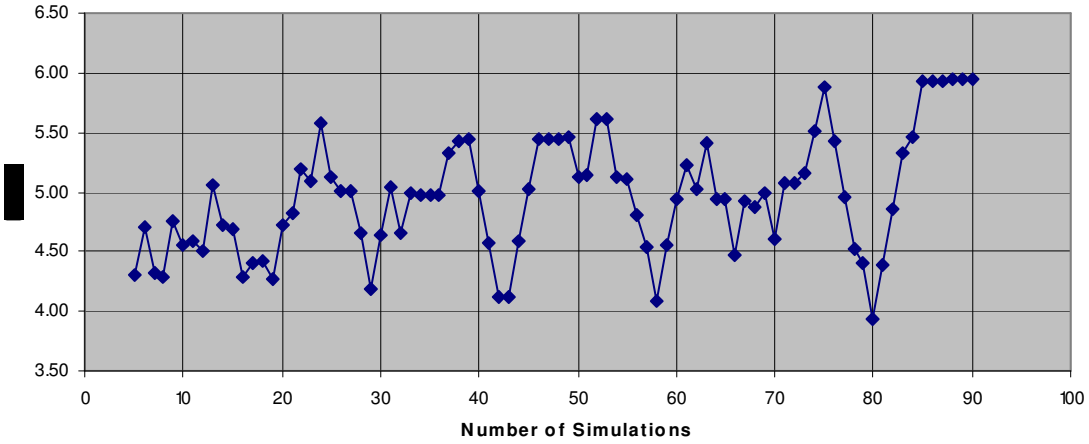


**(a)**

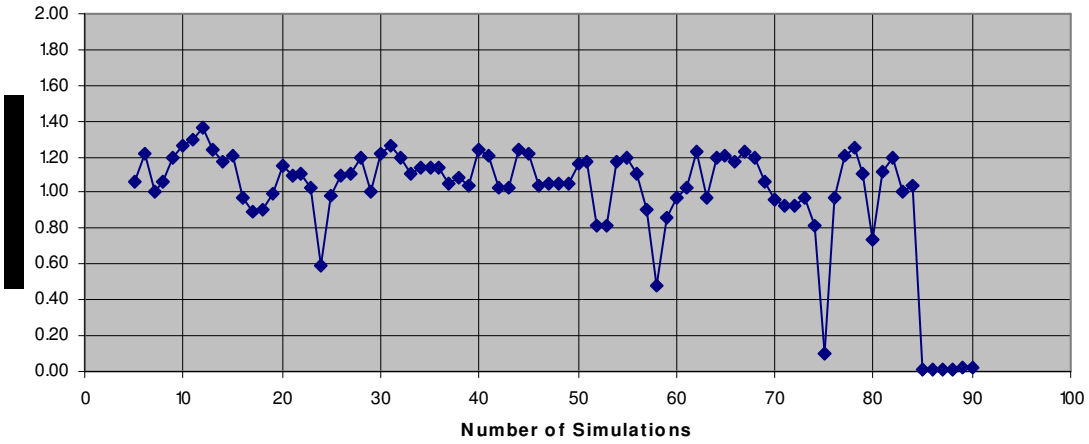


**(b)**

**Figure D-6. Well A7: (a) Mean versus number of simulations; (b) standard deviation versus number of simulations**

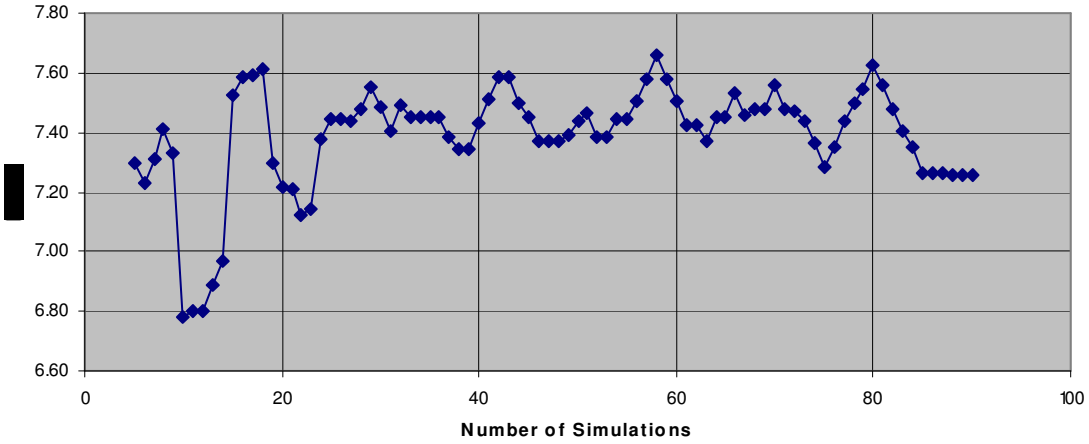


**(a)**

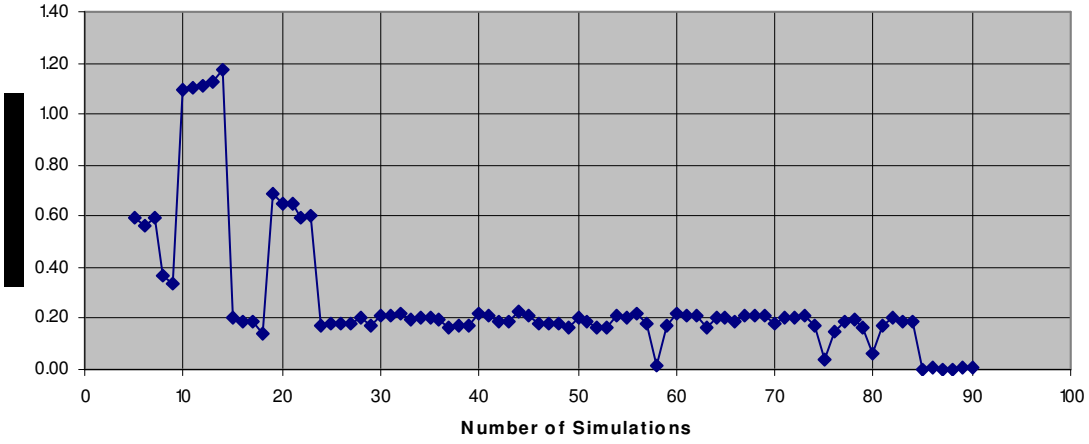


**(b)**

**Figure D-7. Well A8: (a) Mean versus number of simulations; (b) standard deviation versus number of simulations**

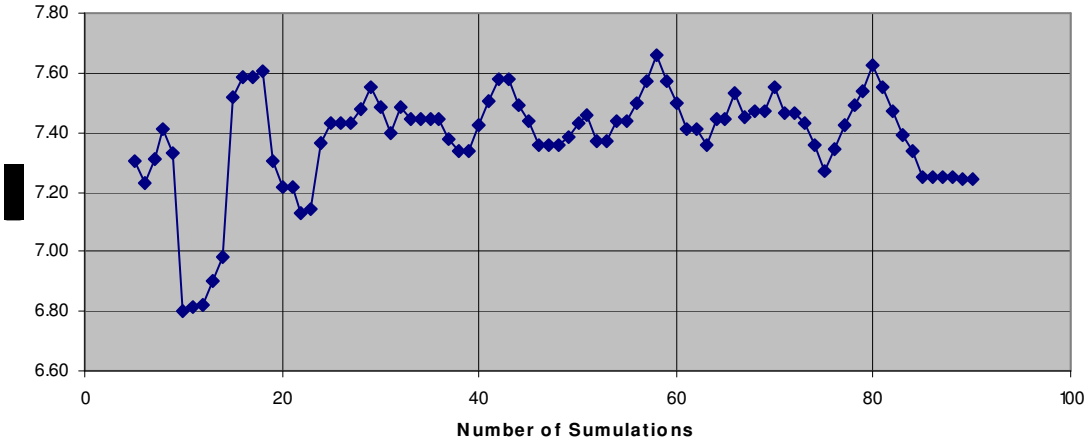


**(a)**

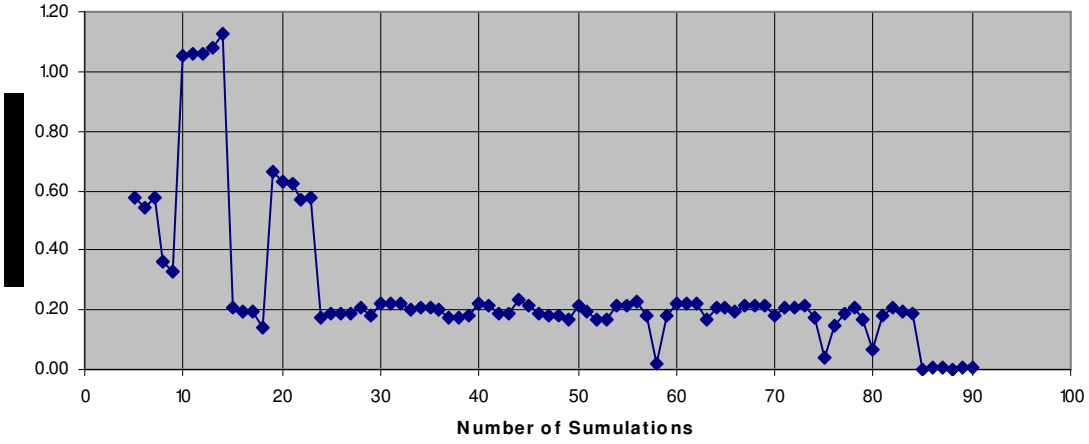


**(b)**

**Figure D-8. Well A9: (a) Mean versus number of simulations; (b) standard deviation versus number of simulations**

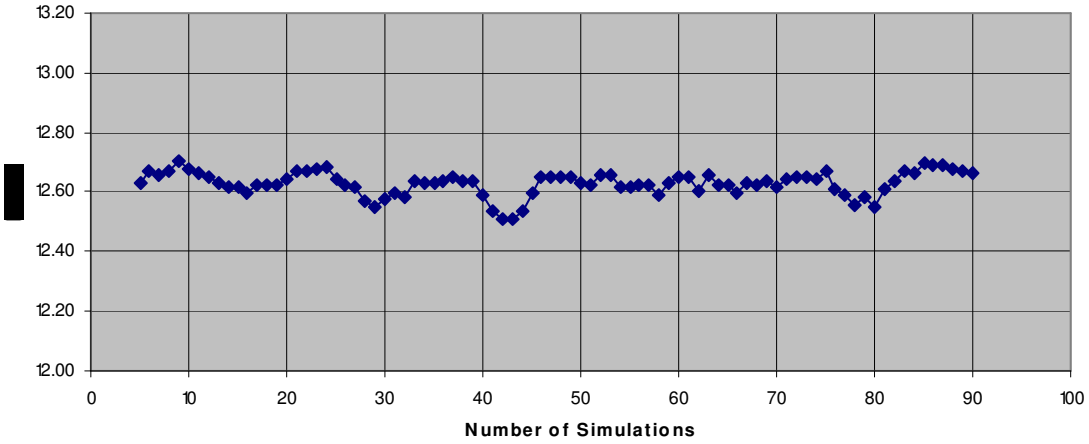


**(a)**

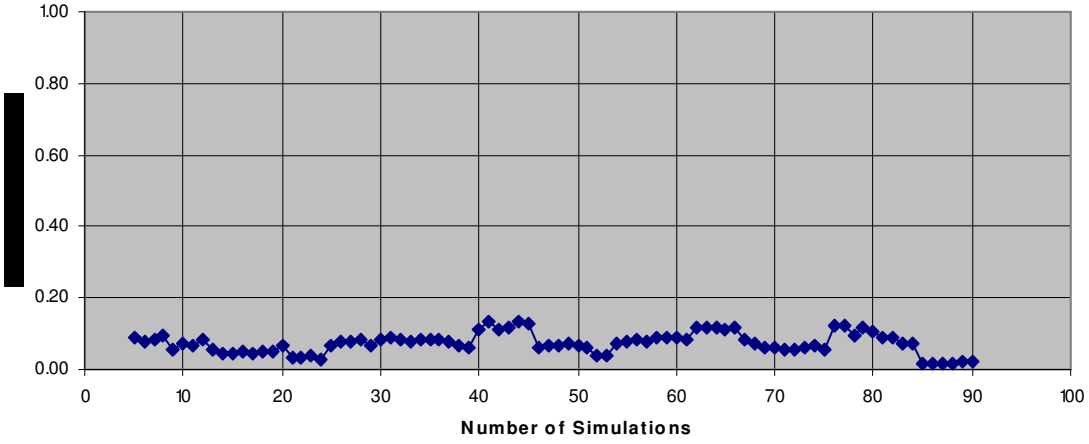


**(b)**

**Figure D-9. Well A11: (a) Mean versus number of simulations; (b) standard deviation versus number of simulations**

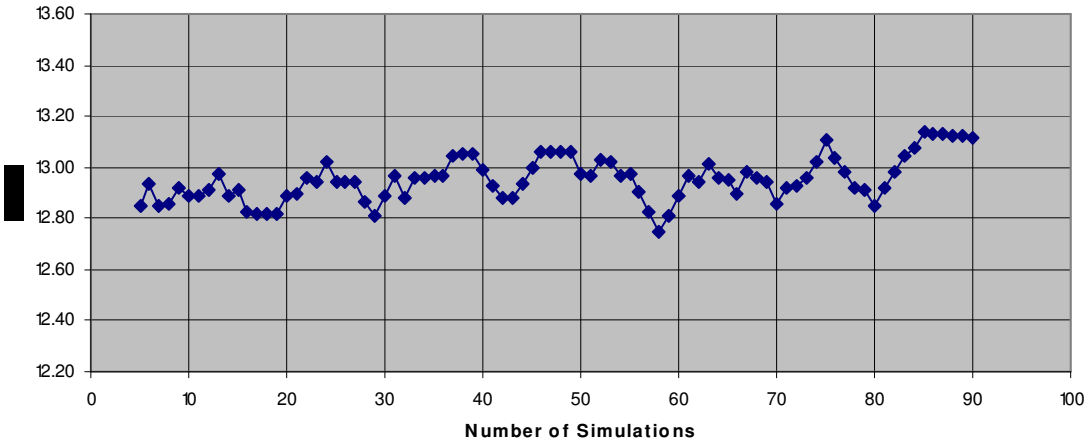


**(a)**

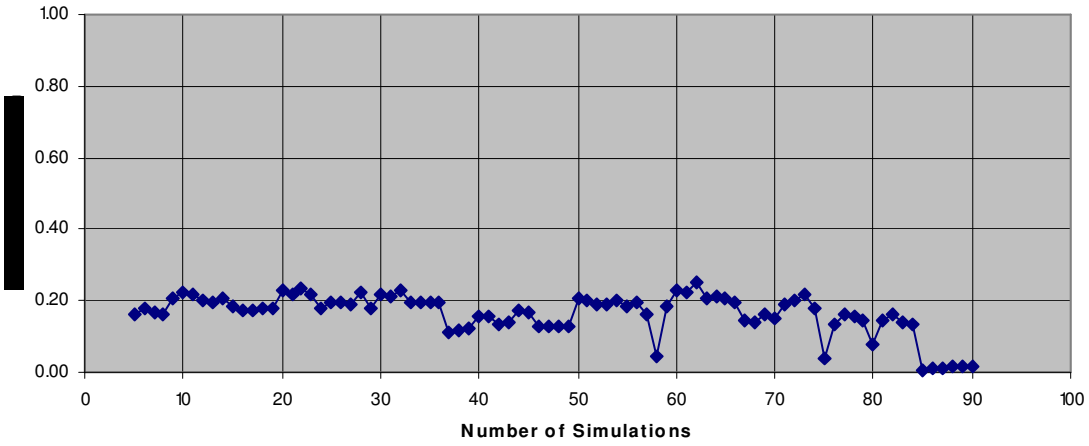


**(b)**

**Figure D-10. Well A14: (a) Mean versus number of simulations; (b) standard deviation versus number of simulations**

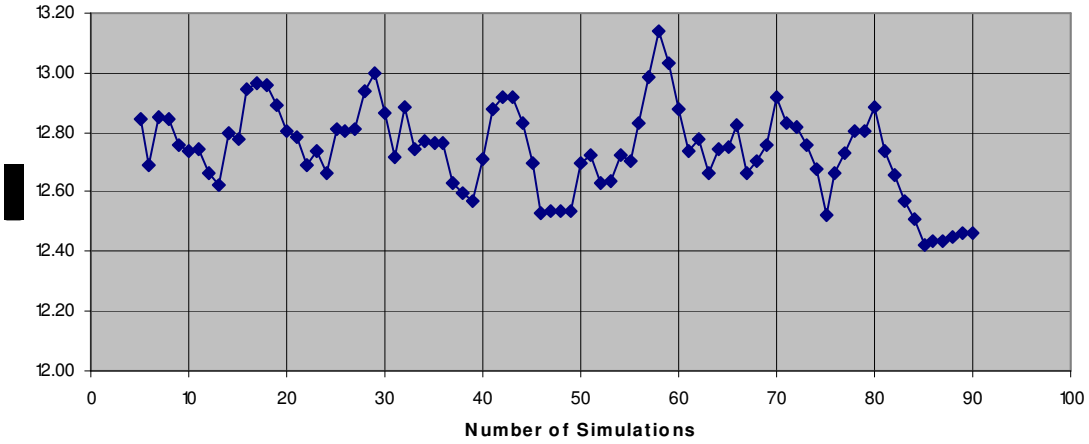


**(a)**

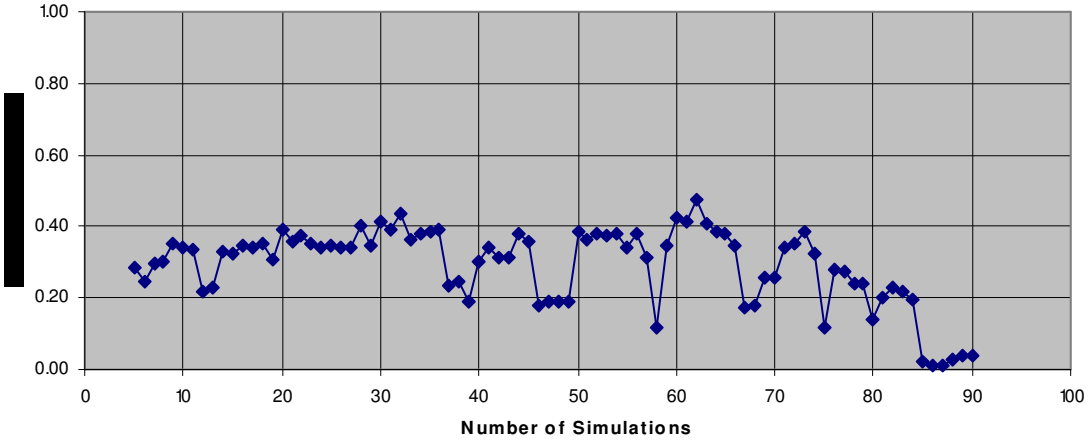


**(b)**

**Figure D-11. Well A16: (a) Mean versus number of simulations; (b) standard deviation versus number of simulations**

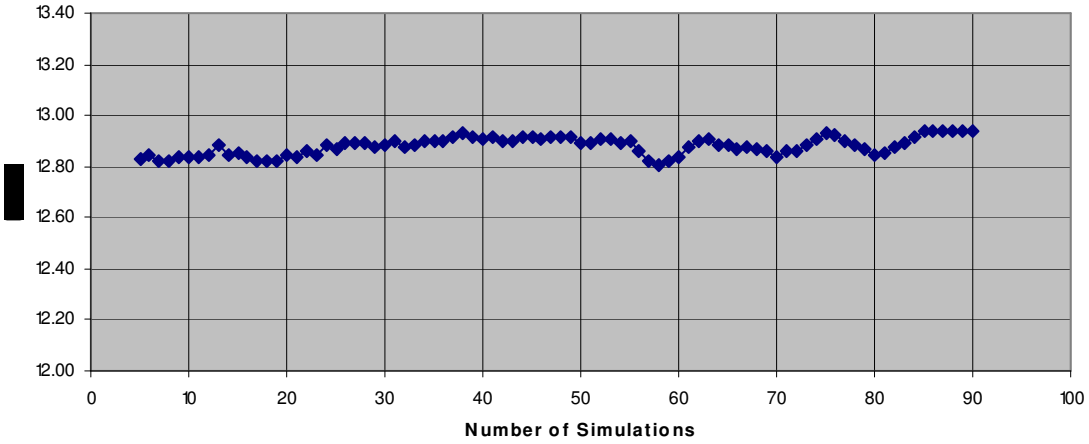


**(a)**

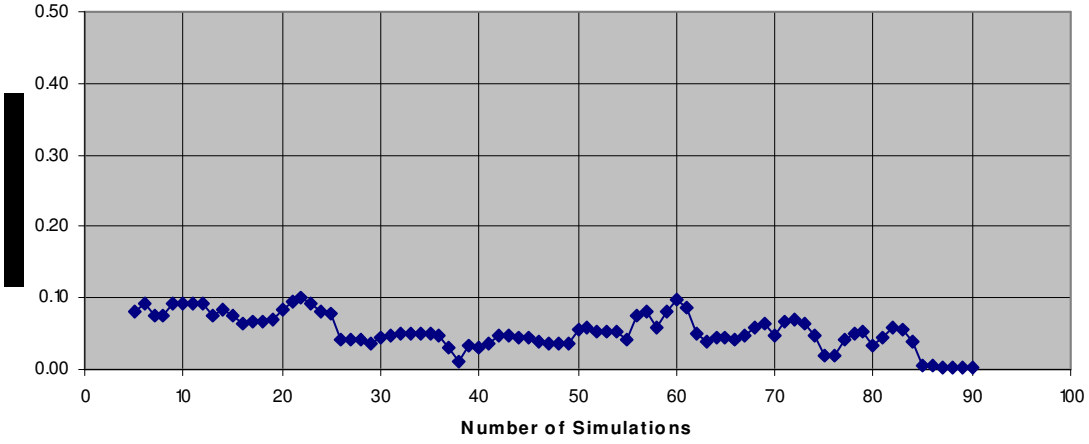


**(b)**

**Figure D-12. Well A17: (a) Mean versus number of simulations; (b) standard deviation versus number of simulations**

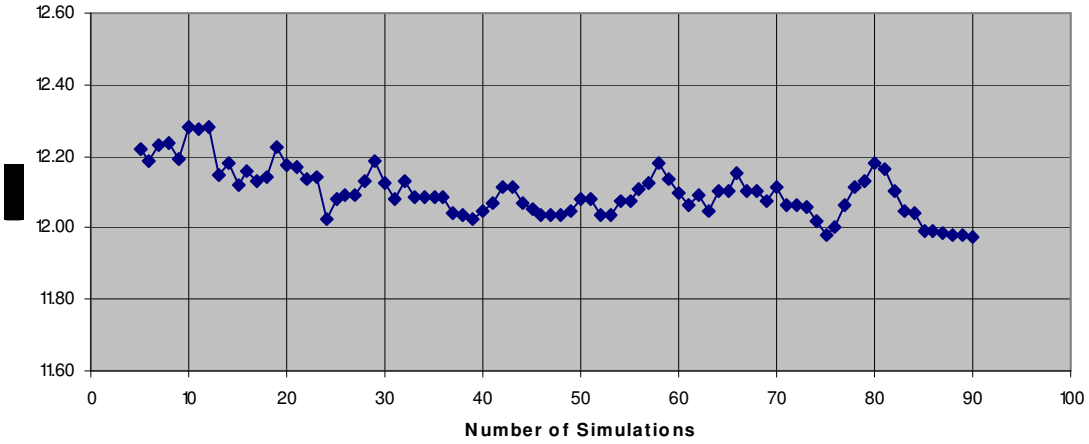


**(a)**

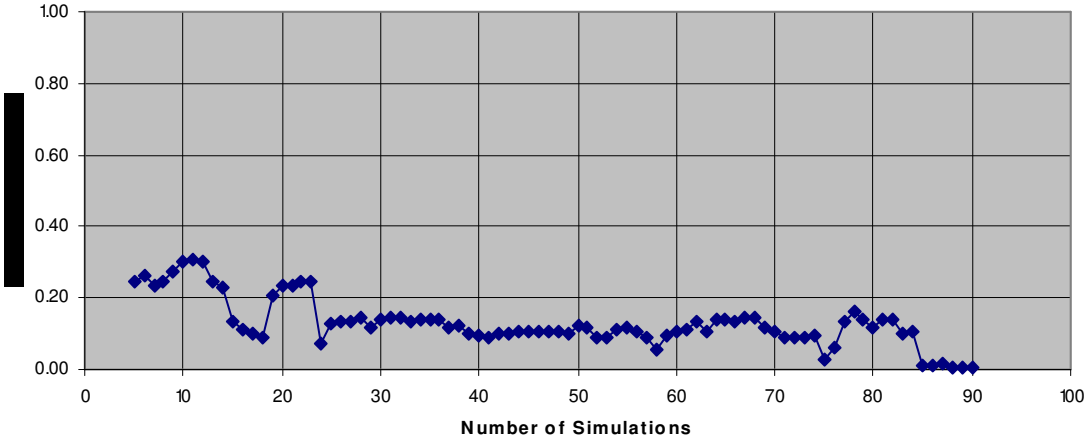


**(b)**

**Figure D-13. Well 18: (a) Mean versus number of simulations; (b) standard deviation versus number of simulations**

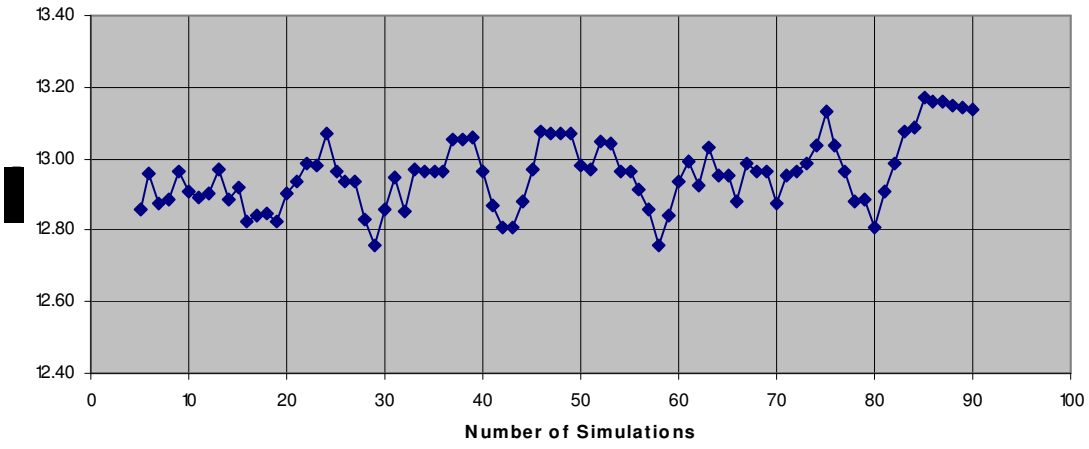


**(a)**

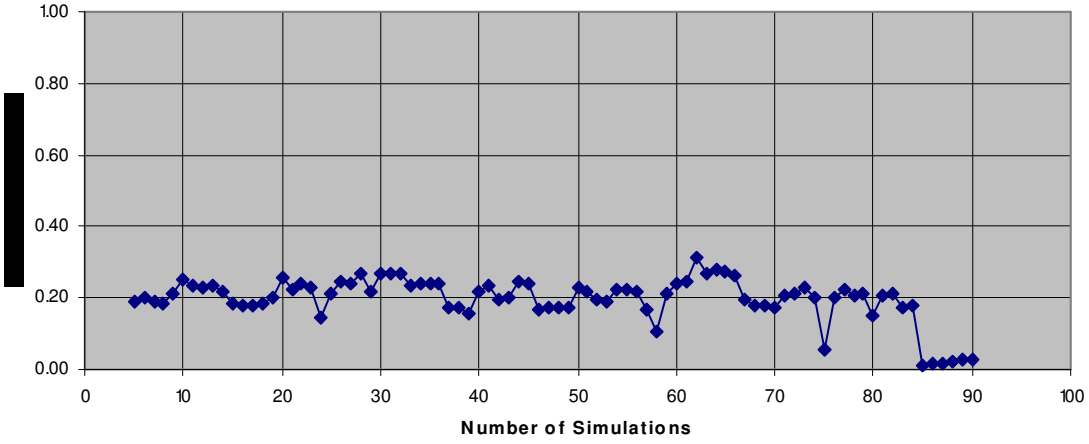


**(b)**

**Figure D-14. Well A19: (a) Mean versus number of simulations; (b) standard deviation versus number of simulations**

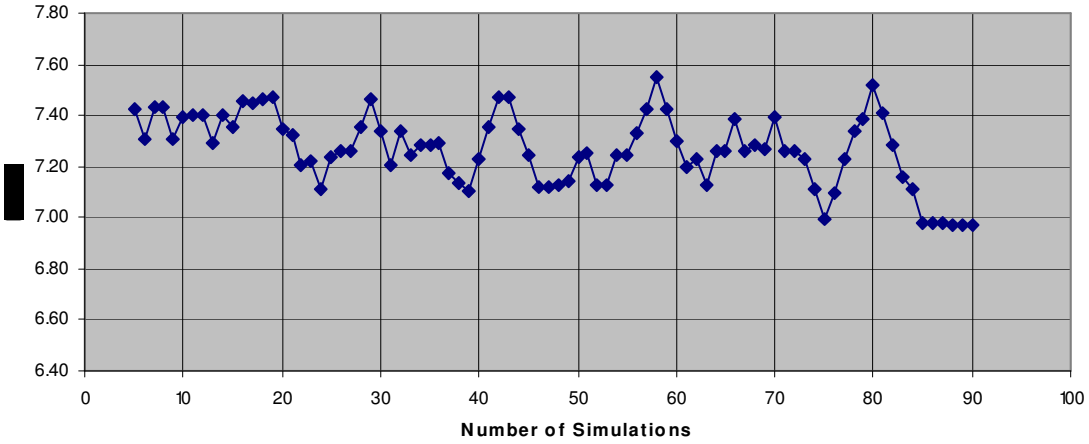


**(a)**

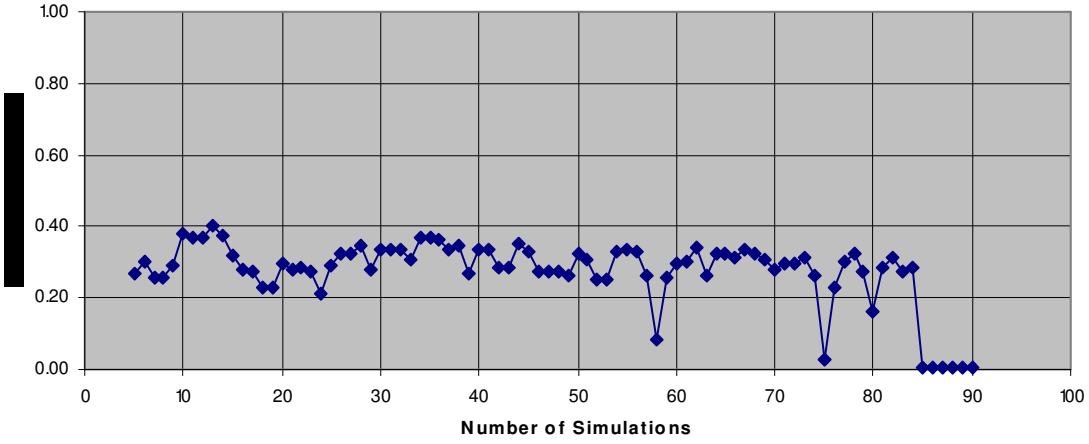


**(b)**

**Figure D-15. Well A20: (a) Mean versus number of simulations; (b) standard deviation versus number of simulations**

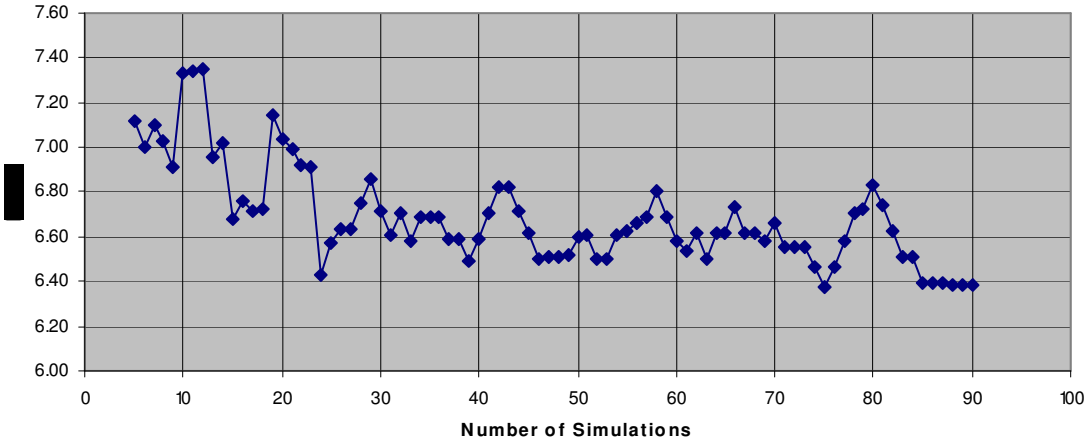


**(a)**

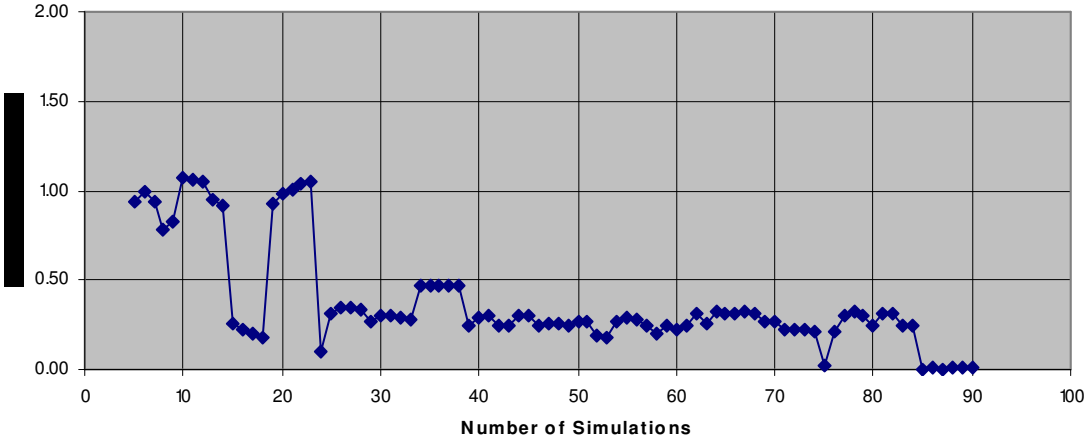


**(b)**

**Figure D-16. Well A21: (a) Mean versus number of simulations; (b) standard deviation versus number of simulations**

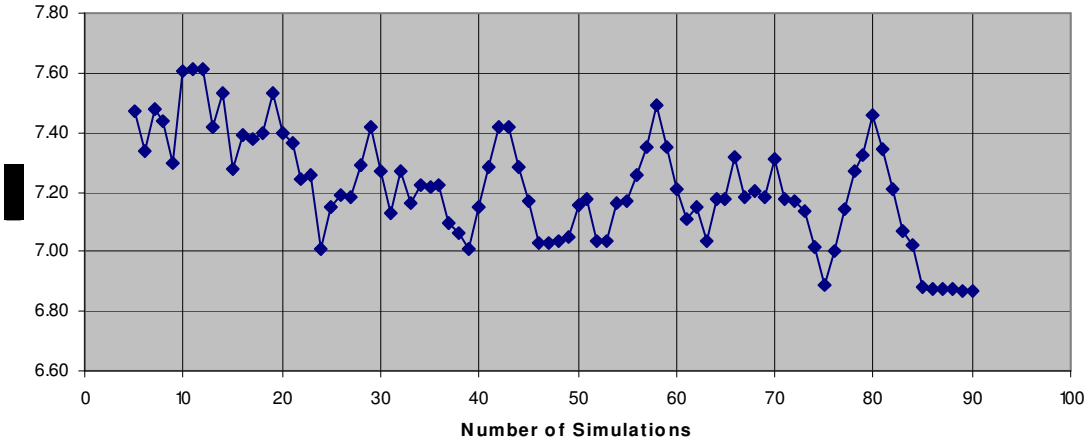


**(a)**

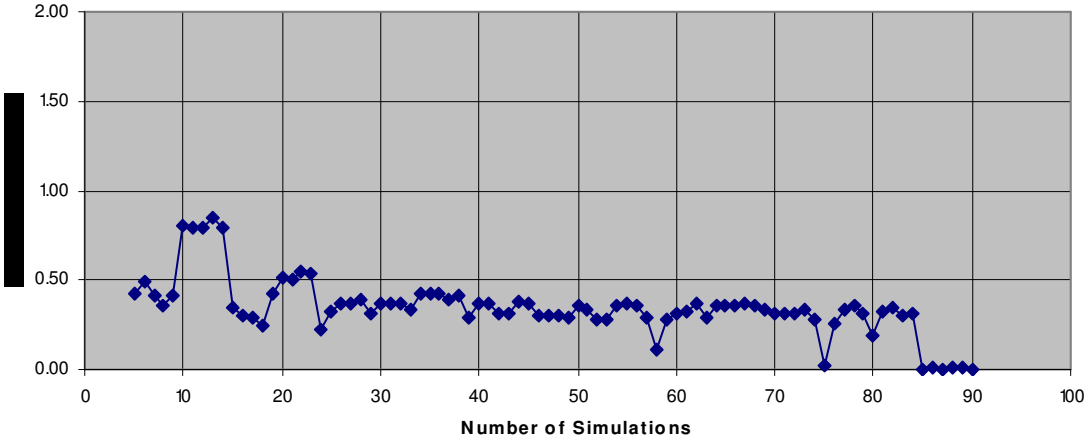


**(b)**

**Figure D-17. Well A22: (a) Mean versus number of simulations; (b) standard deviation versus number of simulations**

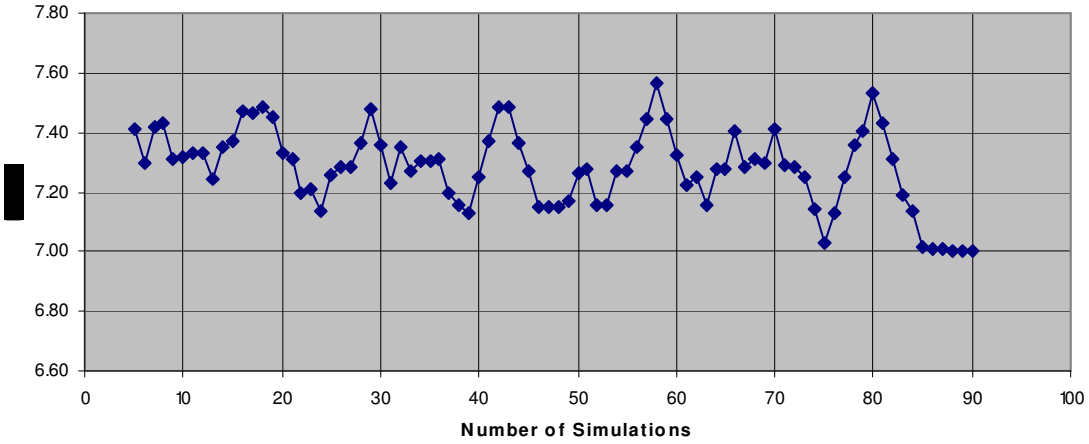


**(a)**

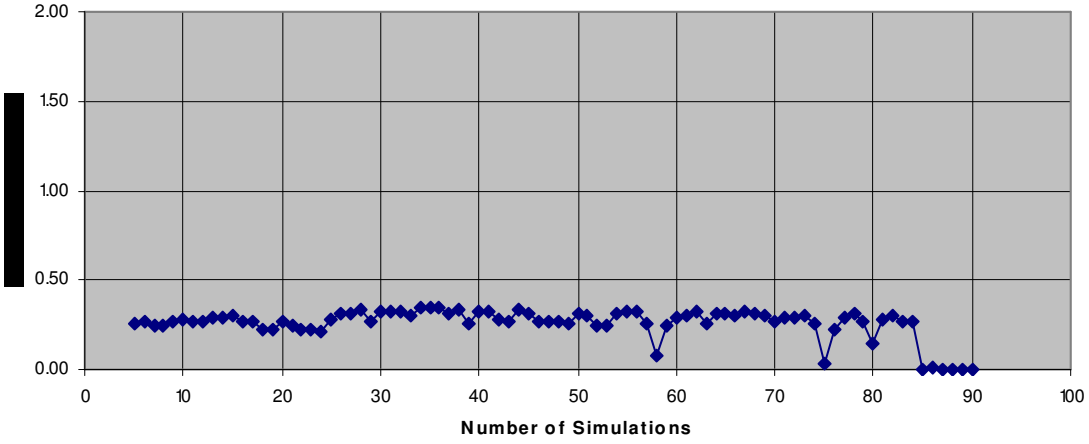


**(b)**

**Figure D-18. Well A23: (a) Mean versus number of simulations; (b) standard deviation versus number of simulations**

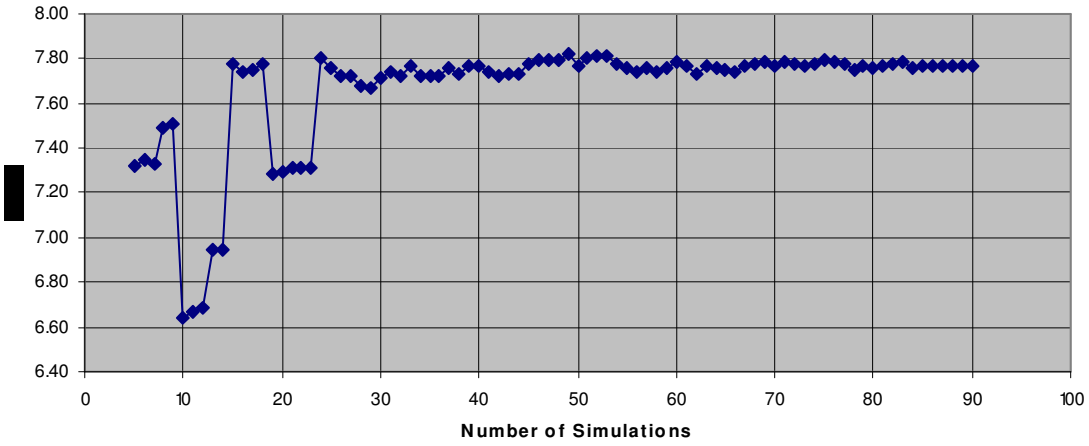


**(a)**

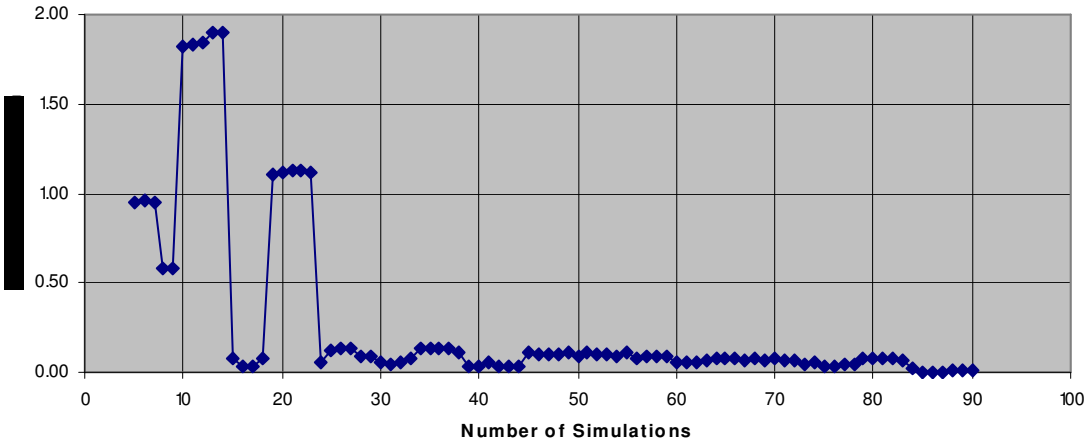


**(b)**

**Figure D-19. Well A24: (a) Mean versus number of simulations; (b) standard deviation versus number of simulations**

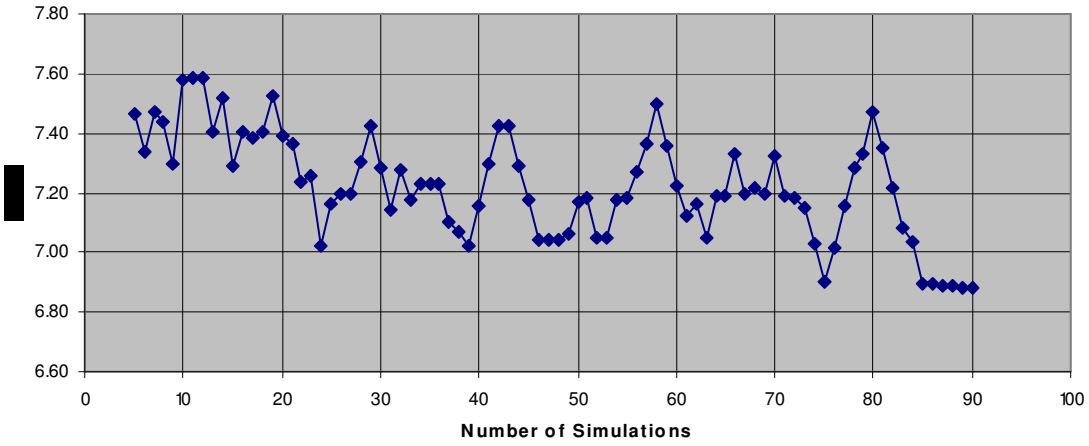


**(a)**

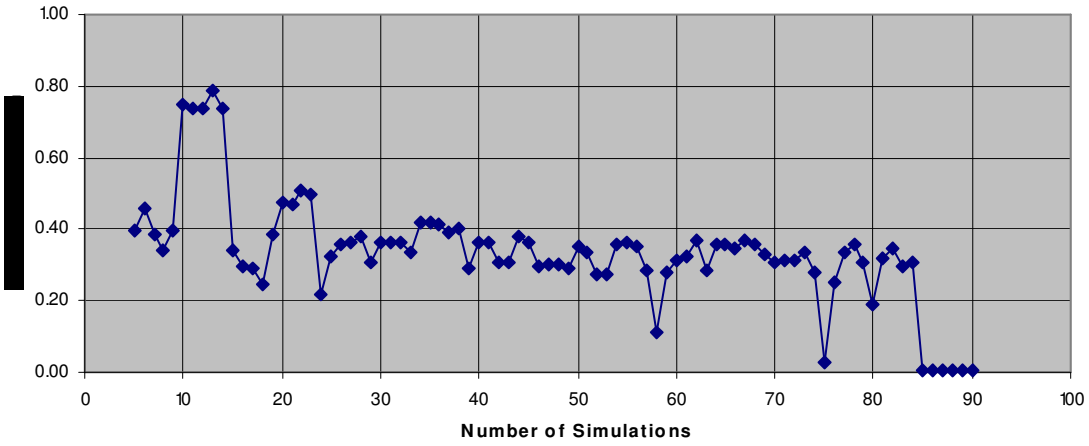


**(b)**

**Figure D-20. Well A25: (a) Mean versus number of simulations; (b) standard deviation versus number of simulations**

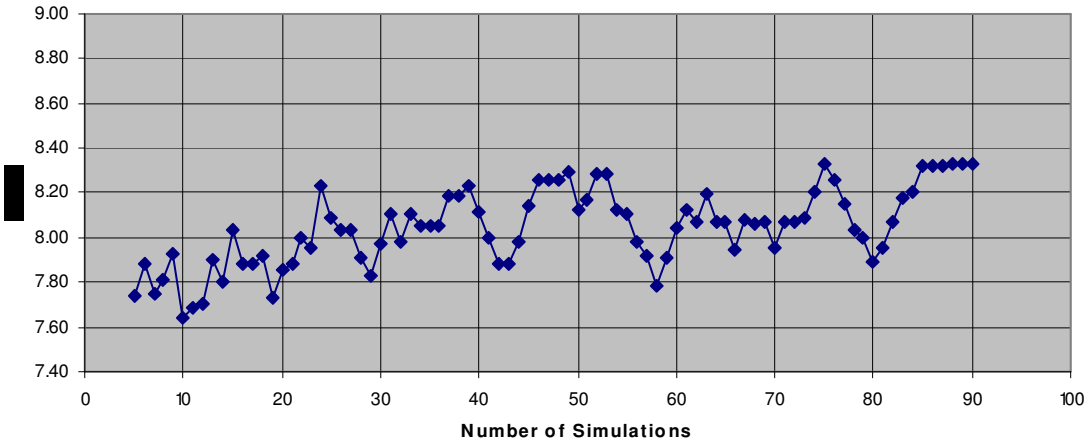


**(a)**

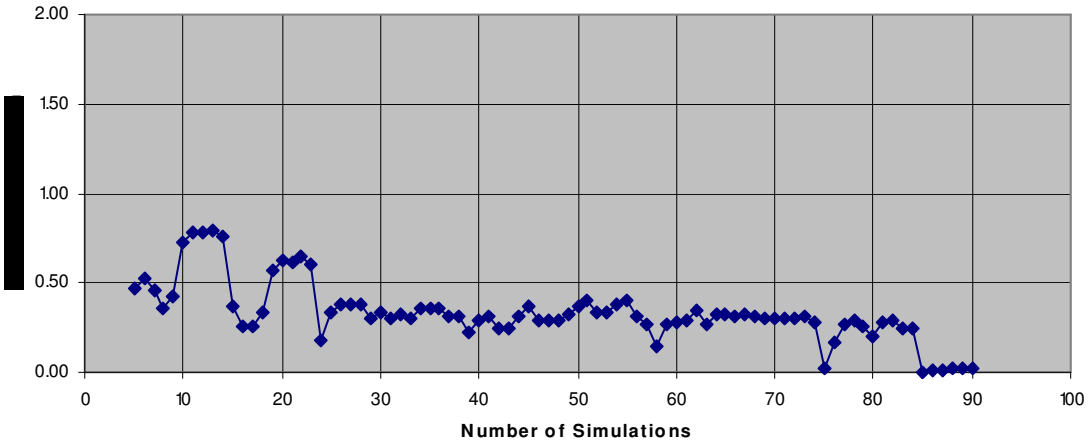


**(b)**

**Figure D-21. Well A27: (a) Mean versus number of simulations; (b) standard deviation versus number of simulations**

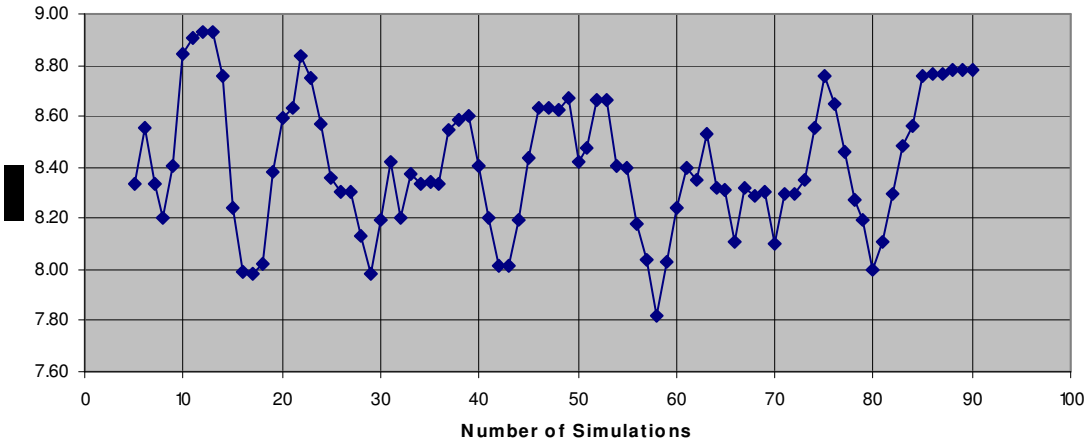


**(a)**

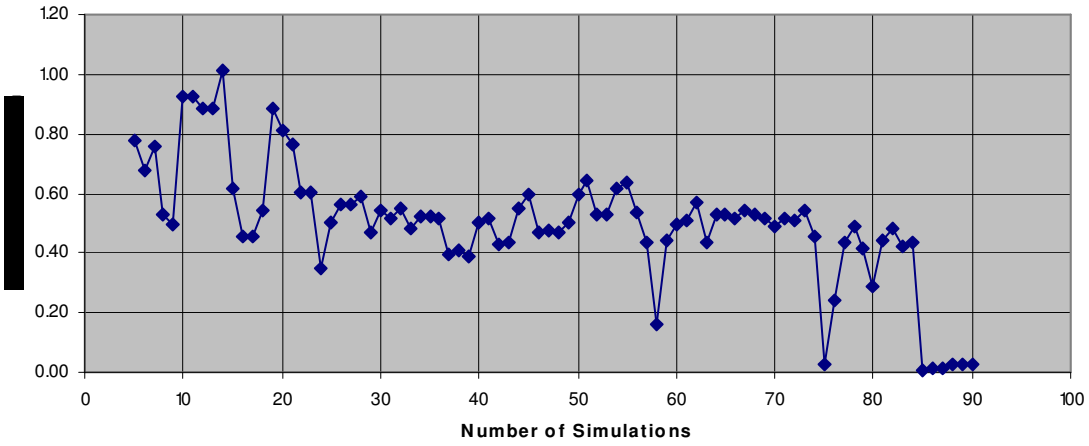


**(b)**

**Figure D-22. Well A29: (a) Mean versus number of simulations; (b) standard deviation versus number of simulations**

# APPENDIX E

# BEST FIT CURVES FOR THE RESULTS OF NEURAL CONDITIONAL SIMULATIONS

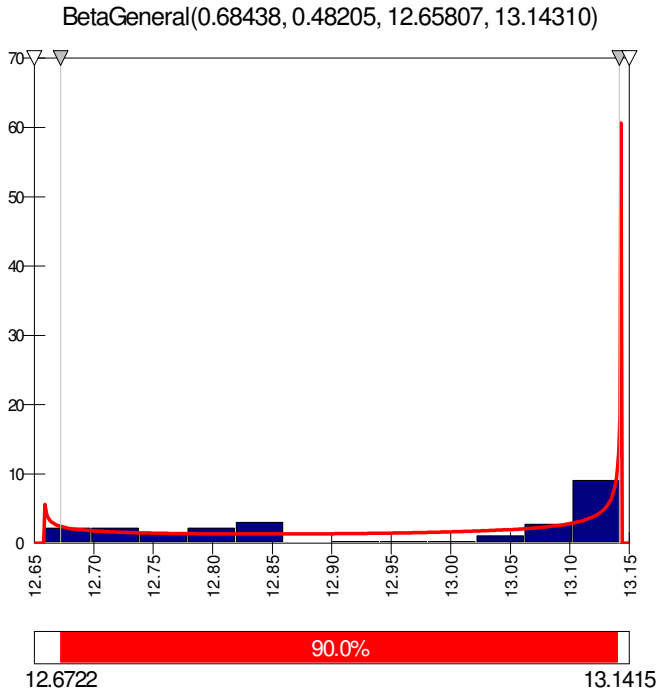


**(a)**

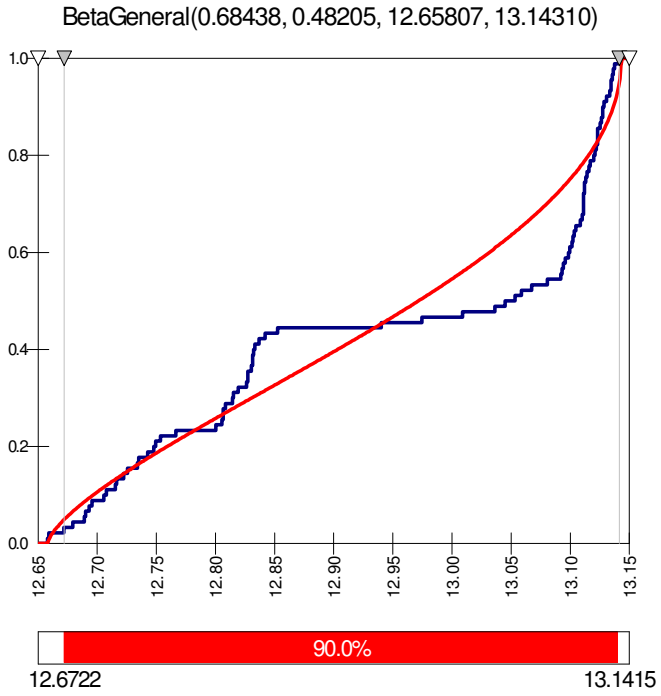


**(b)**

**Figure D-1. Well A2: Best fit curves (a) probability density; (b) cumulative density**

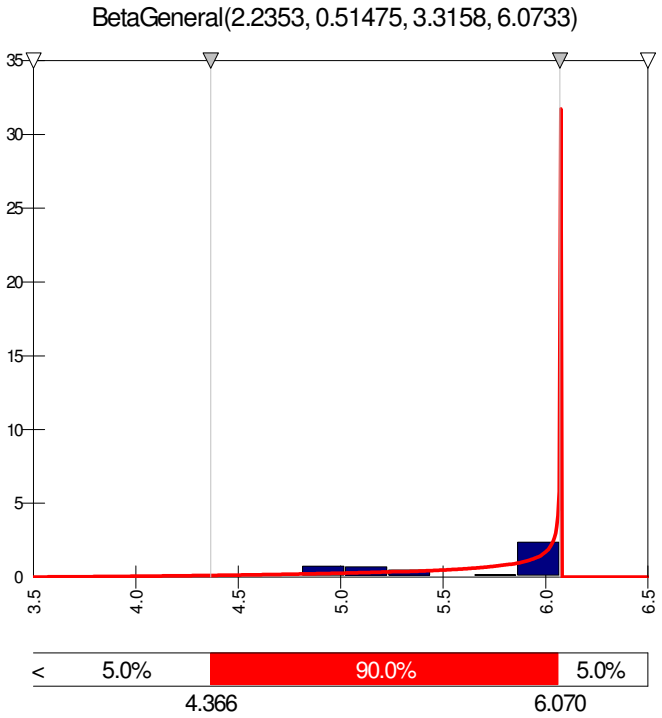


**(a)**

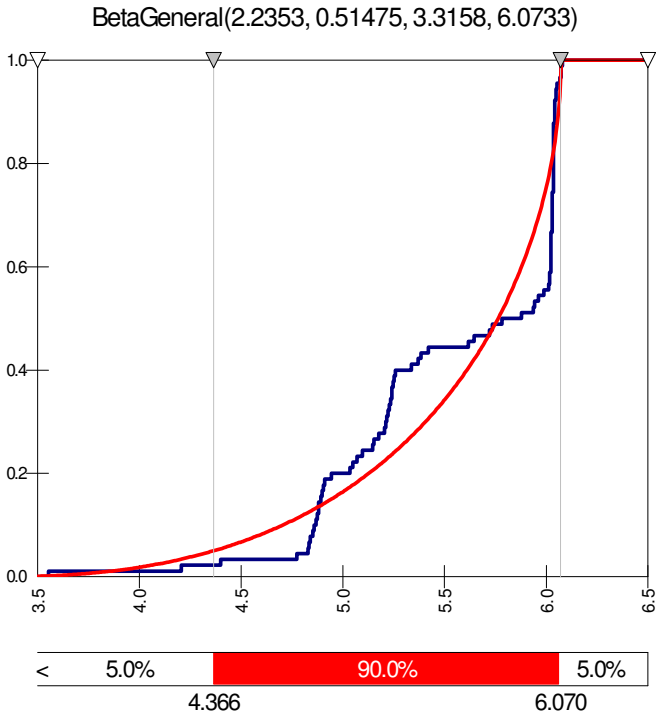


**(b)**

**Figure D-2. Well A3: Best fit curves (a) probability density; (b) cumulative density**

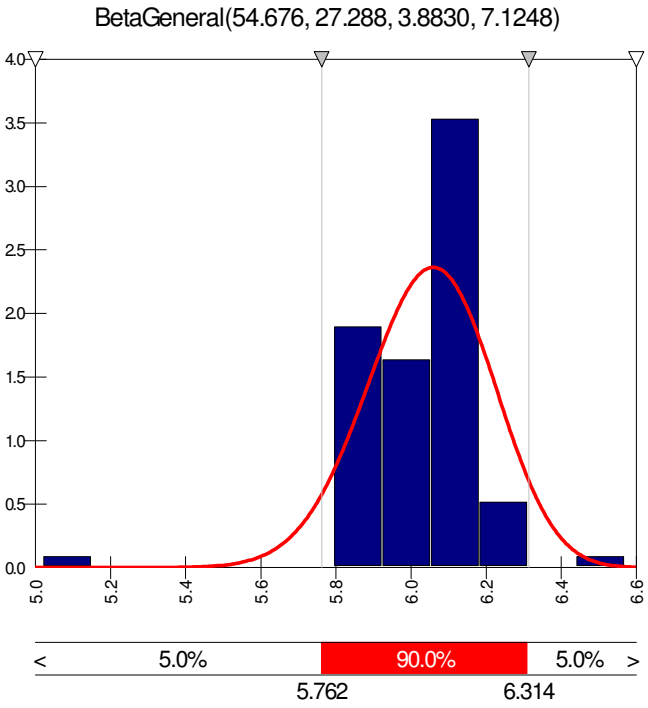


**(a)**

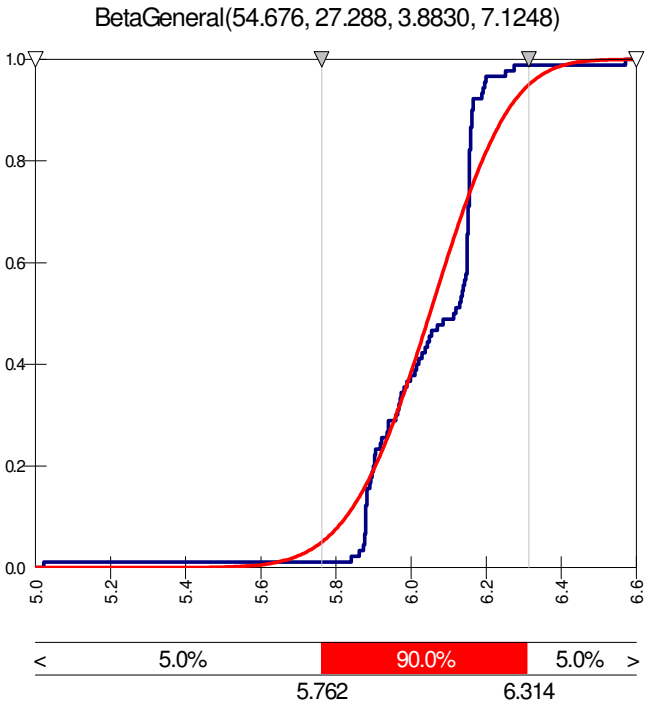


**(b)**

**Figure D-3. Well A4: Best fit curves (a) probability density; (b) cumulative density**

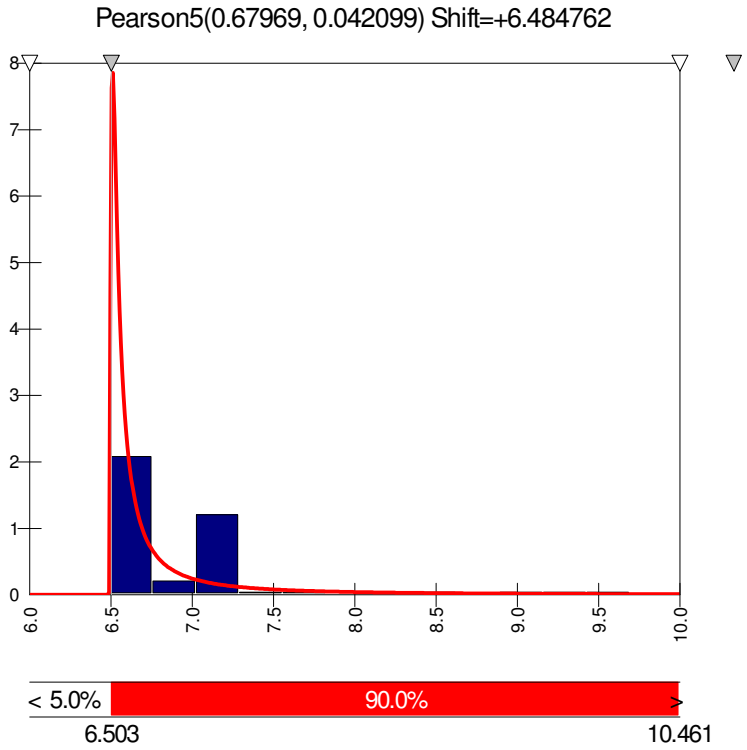


**(a)**

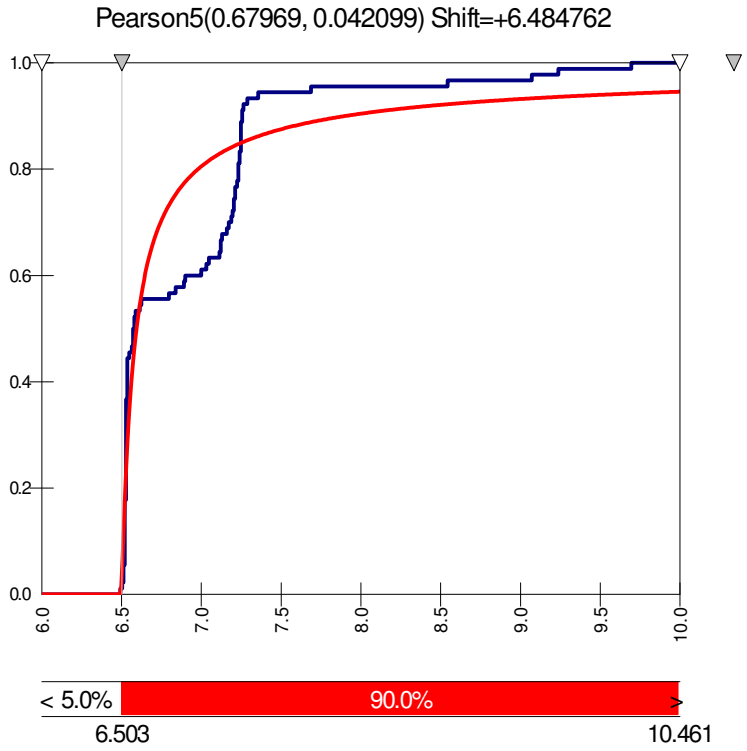


**(b)**

**Figure D-4. Well A5: Best fit curves (a) probability density; (b) cumulative density**

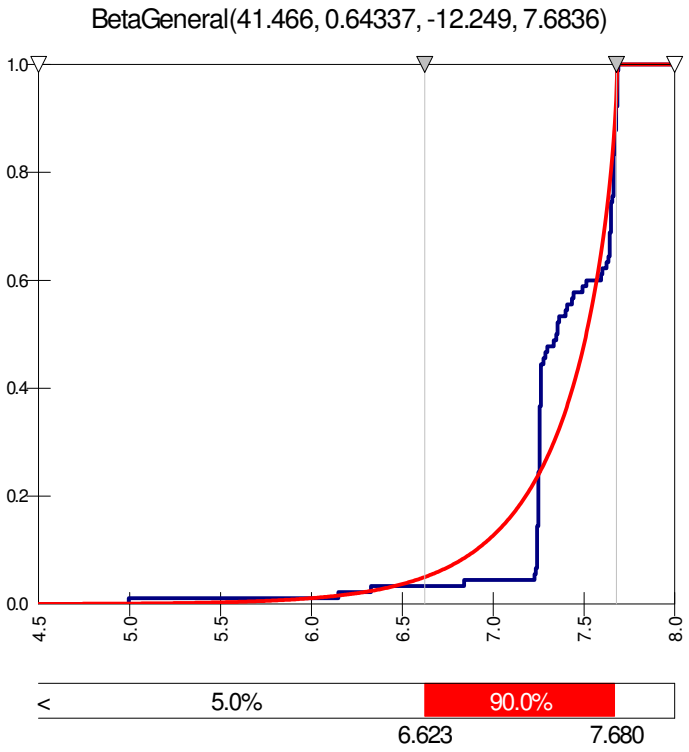


**(a)**

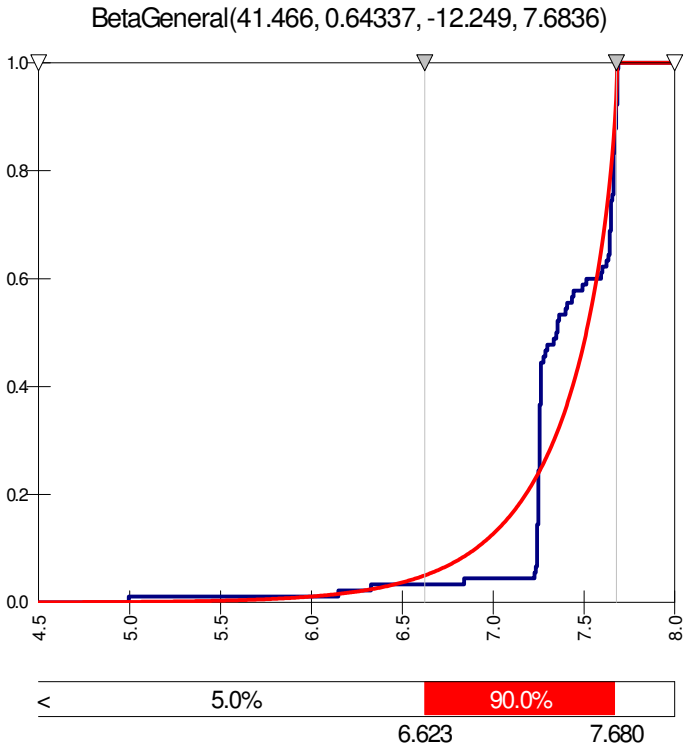


**(b)**

**Figure D-5. Well A6: Best fit curves (a) probability density; (b) cumulative density**

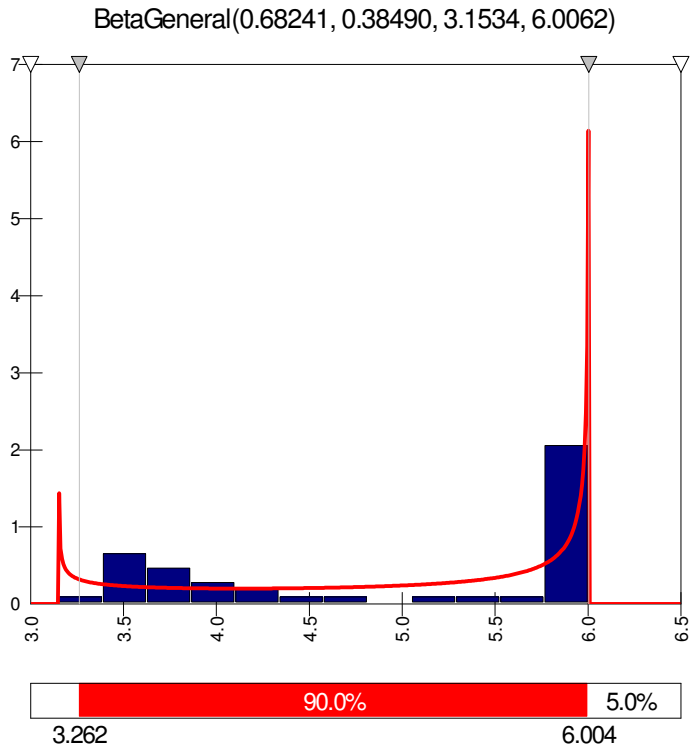


**(a)**

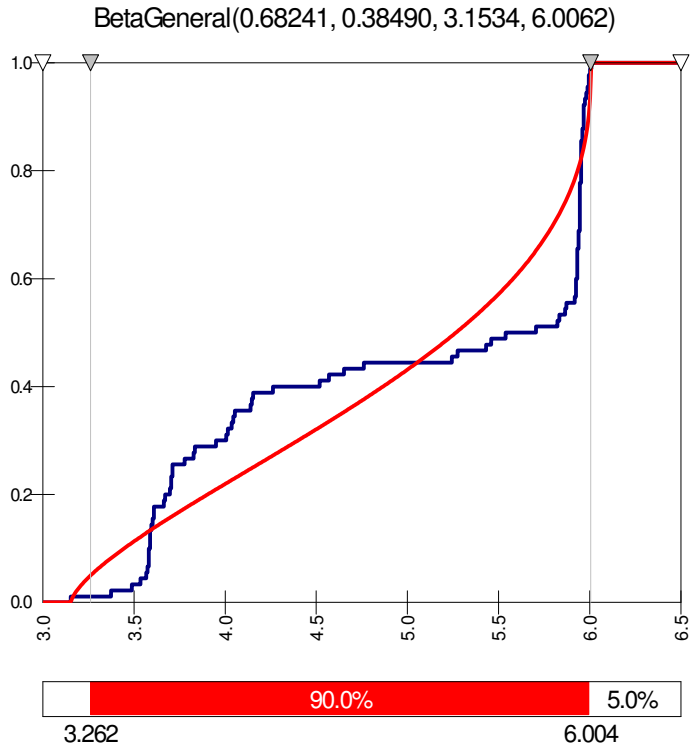


**(b)**

**Figure D-6. Well A7: Best fit curves (a) probability density; (b) cumulative density**

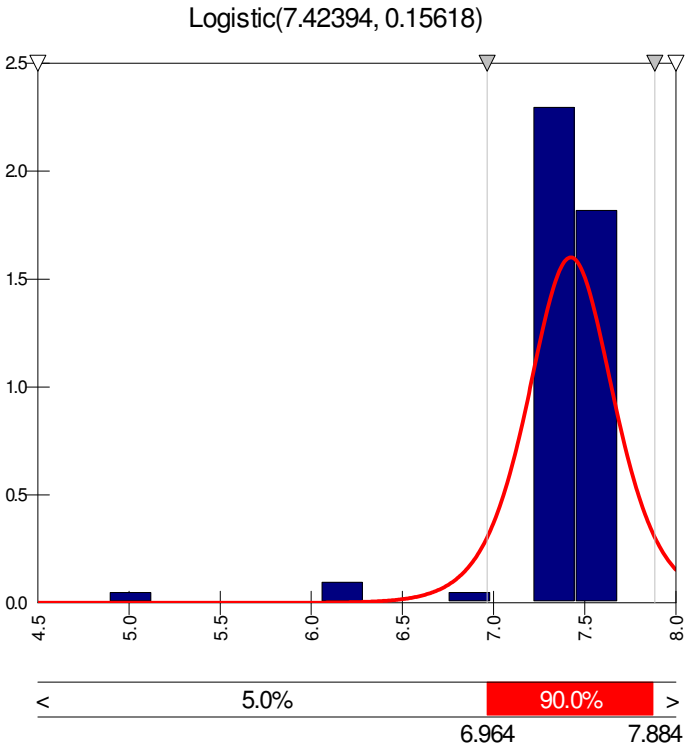


**(a)**

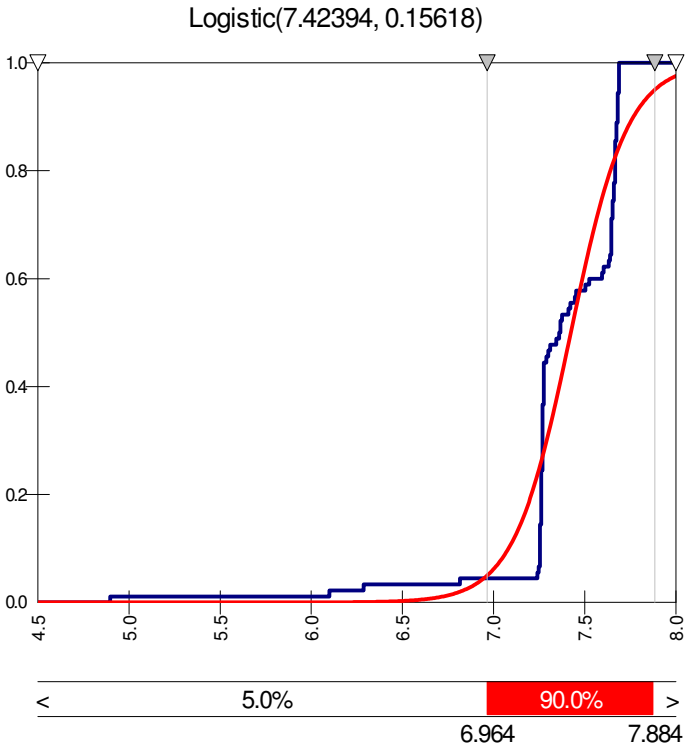


**(b)**

**Figure D-7. Well A8: Best fit curves (a) probability density; (b) cumulative density**

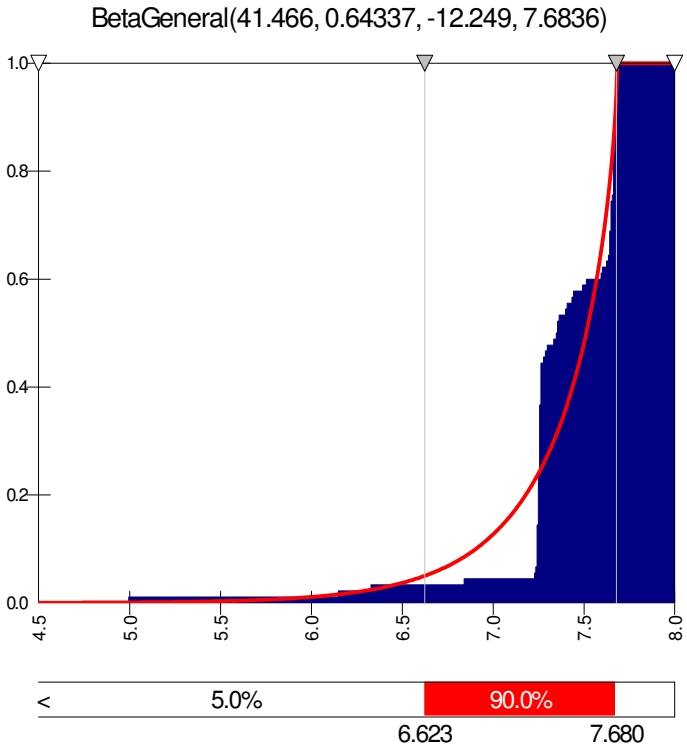


**(a)**

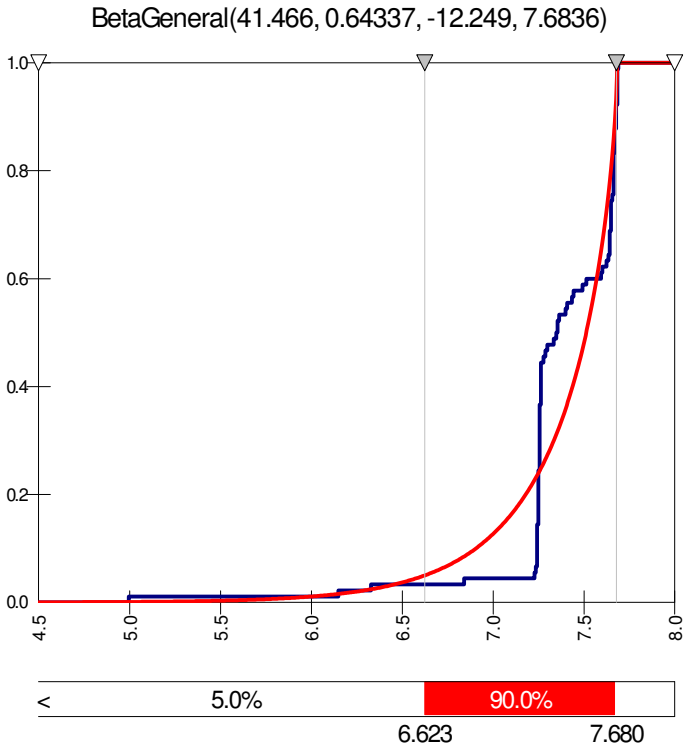


**(b)**

**Figure D-8. Well A9: Best fit curves (a) probability density; (b) cumulative density**

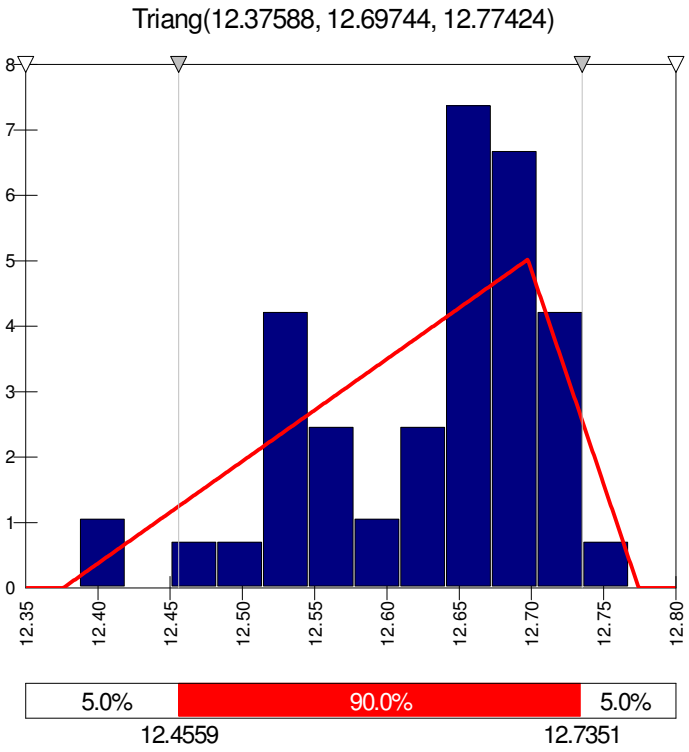


**(a)**

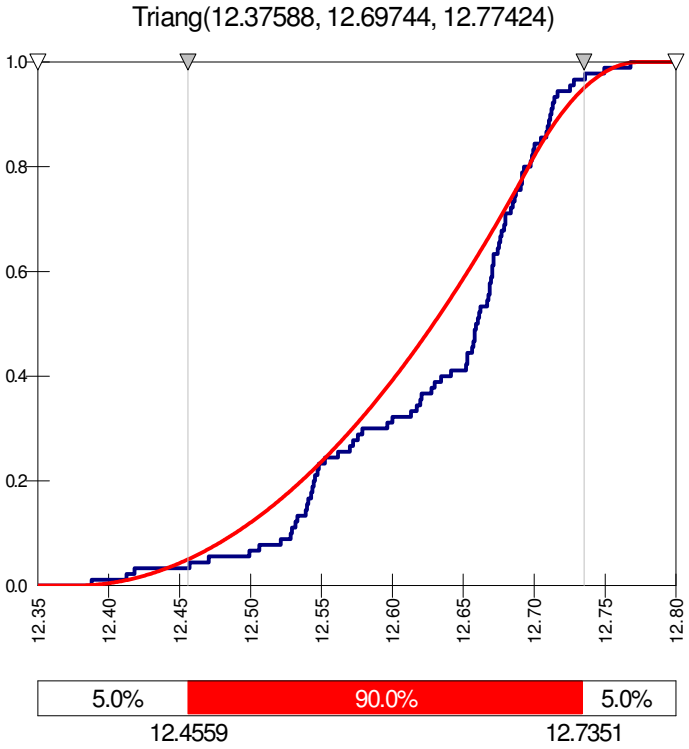


**(b)**

**Figure D-10. Well A11: Best fit curves (a) probability density; (b) cumulative density**

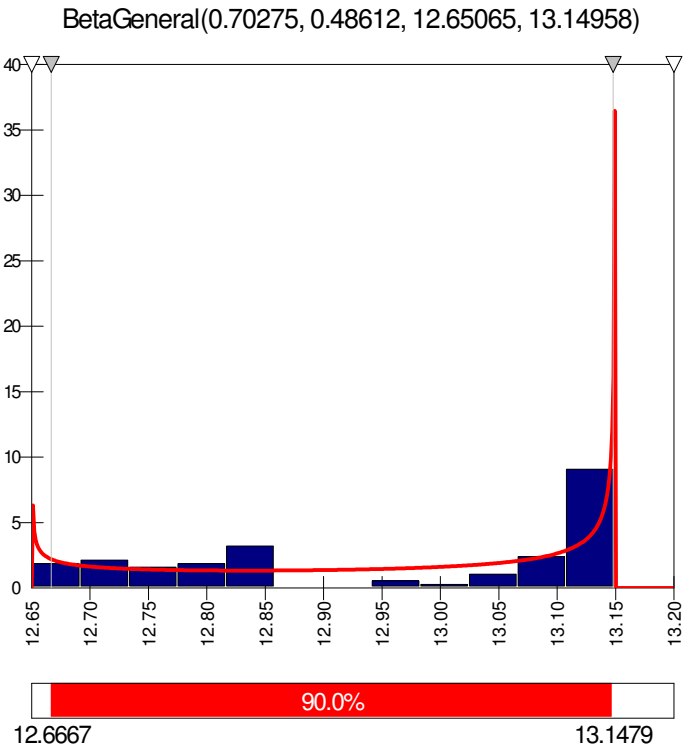


**(a)**

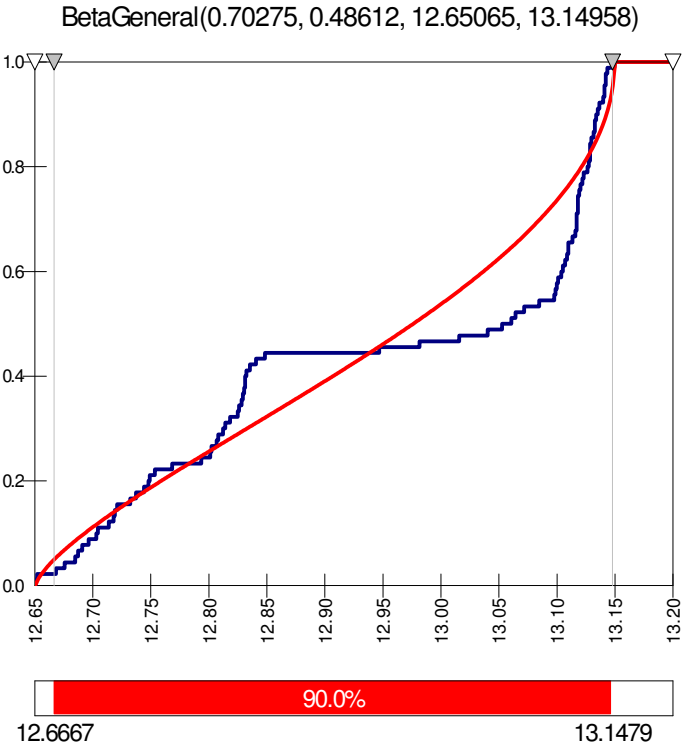


**(b)**

**Figure D-11. Well A14: Best fit curves (a) probability density; (b) cumulative density**

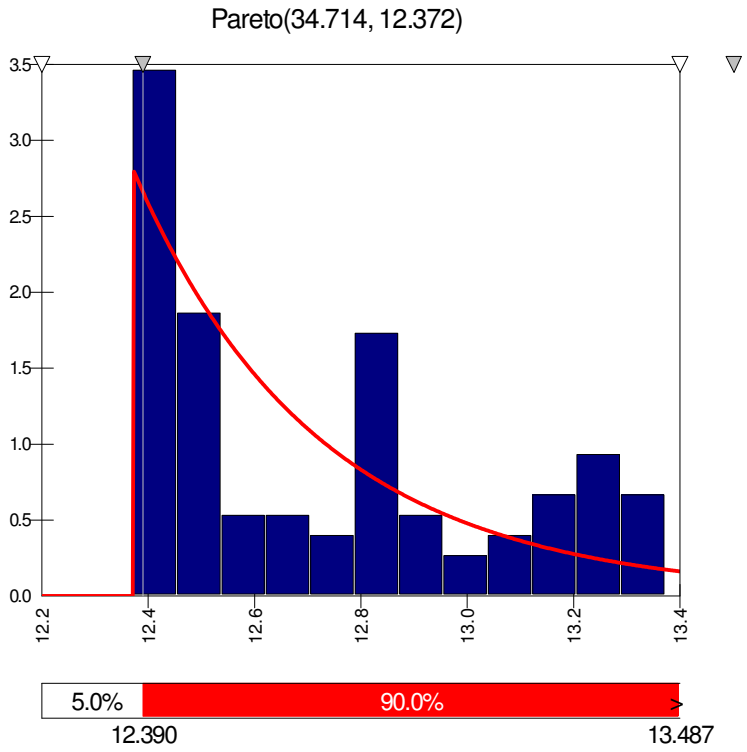


**(a)**

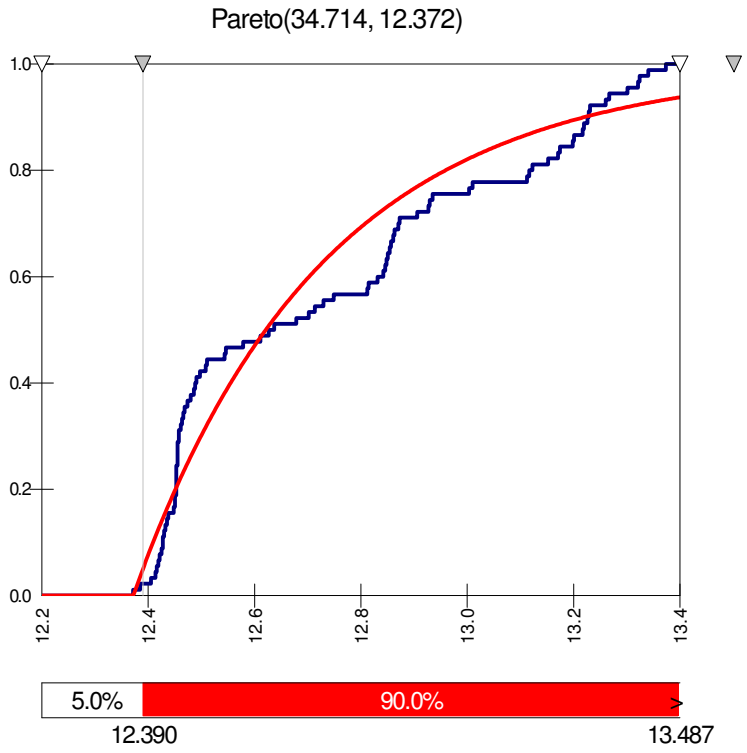


**(b)**

**Figure D-12. Well A16: Best fit curves (a) probability density; (b) cumulative density**

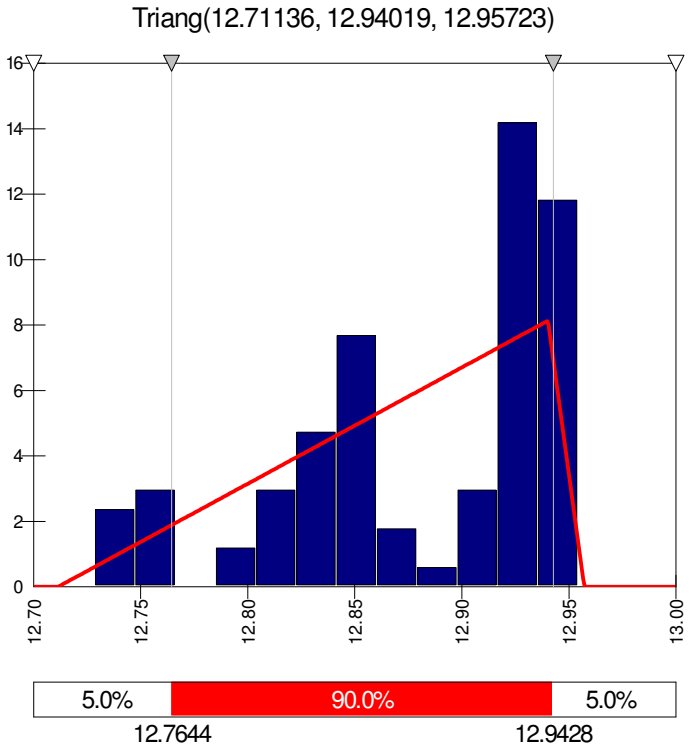


**(a)**

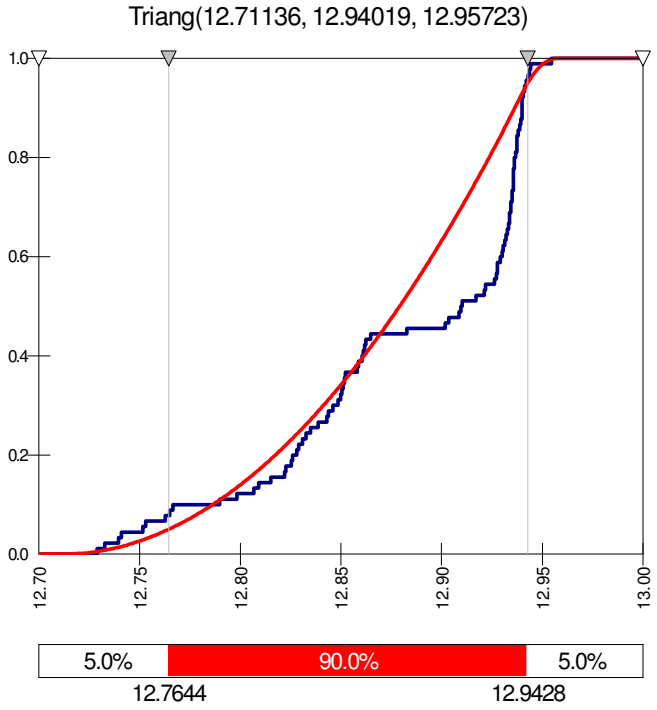


**(b)**

**Figure D-13. Well A17: Best fit curves (a) probability density; (b) cumulative density**

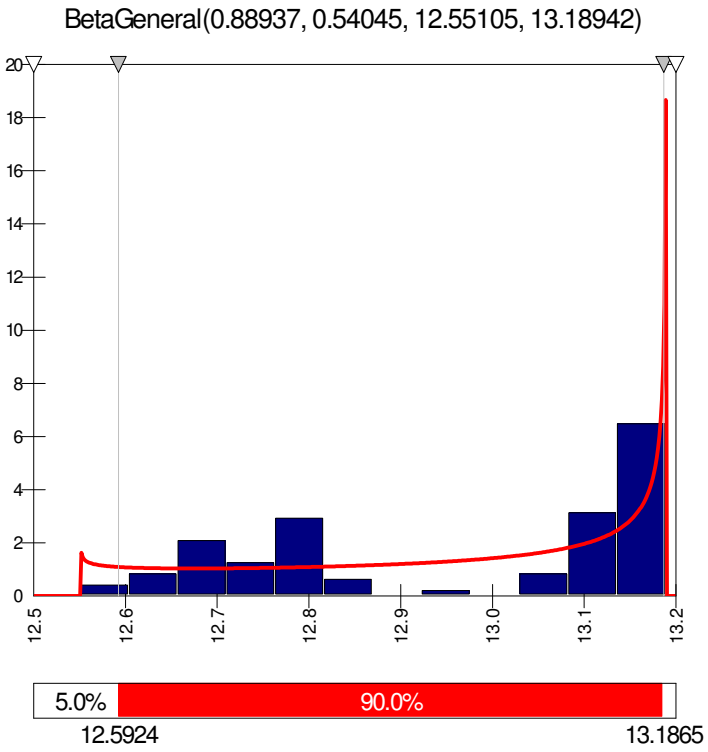


**(a)**

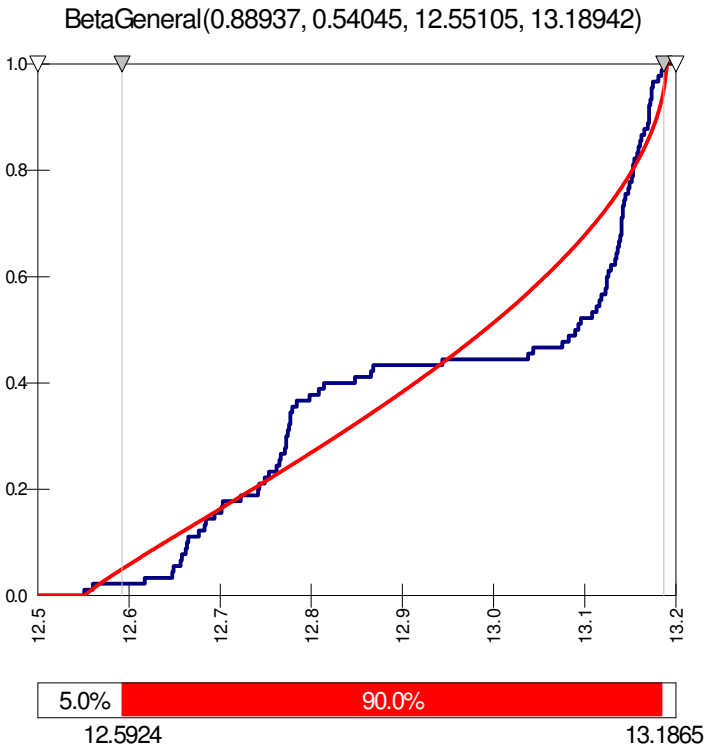


**(b)**

**Figure D-14. Well A19: Best fit curves (a) probability density; (b) cumulative density**

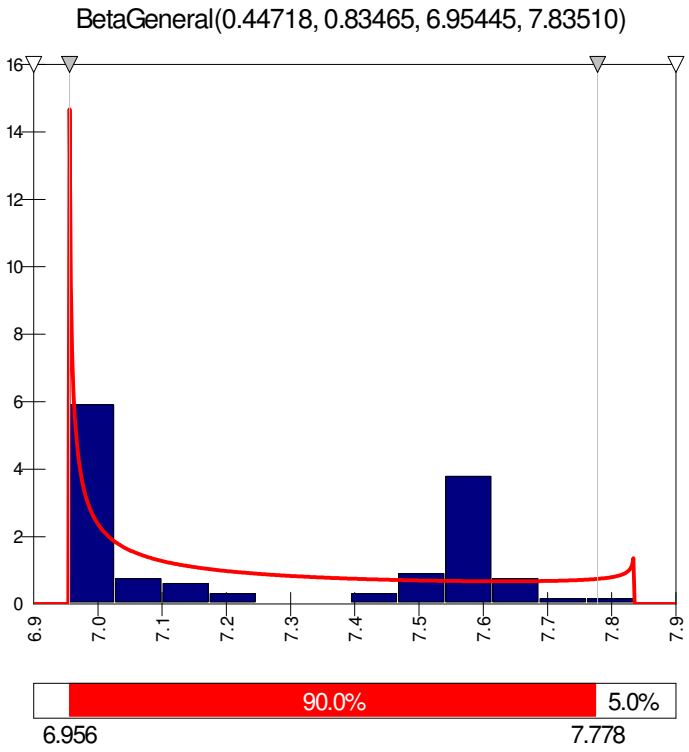


**(a)**

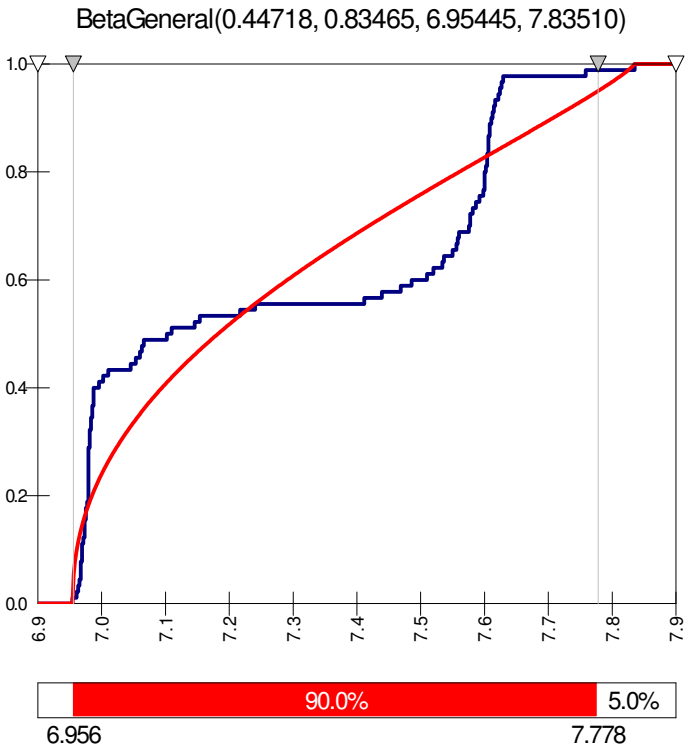


**(b)**

**Figure D-15. Well A20: Best fit curves (a) probability density; (b) cumulative density**

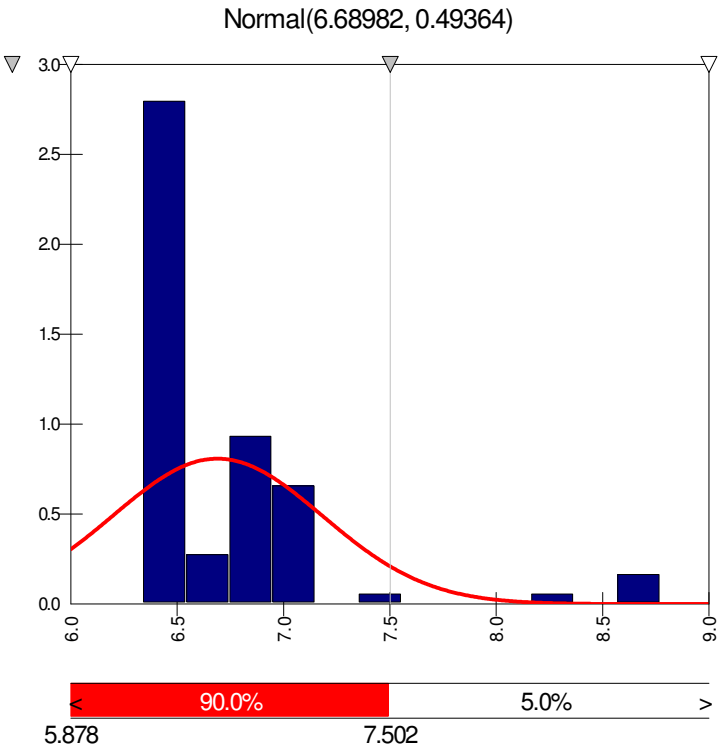


**(a)**

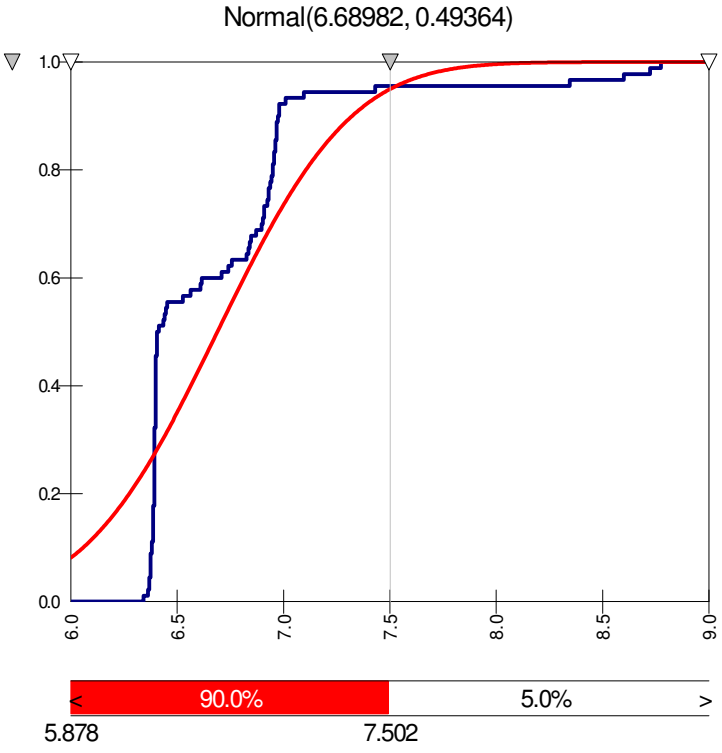


**(b)**

**Figure D-16. Well A21: Best fit curves (a) probability density; (b) cumulative density**

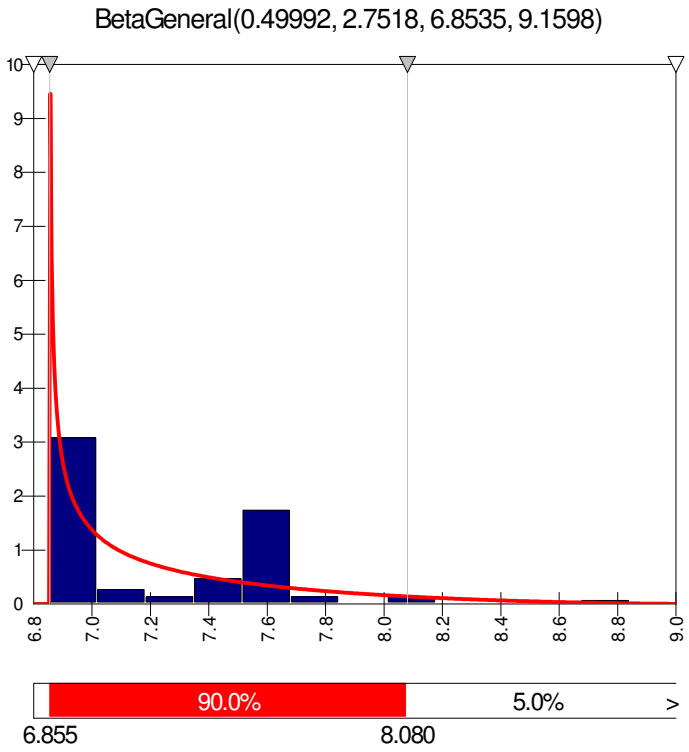


**(a)**

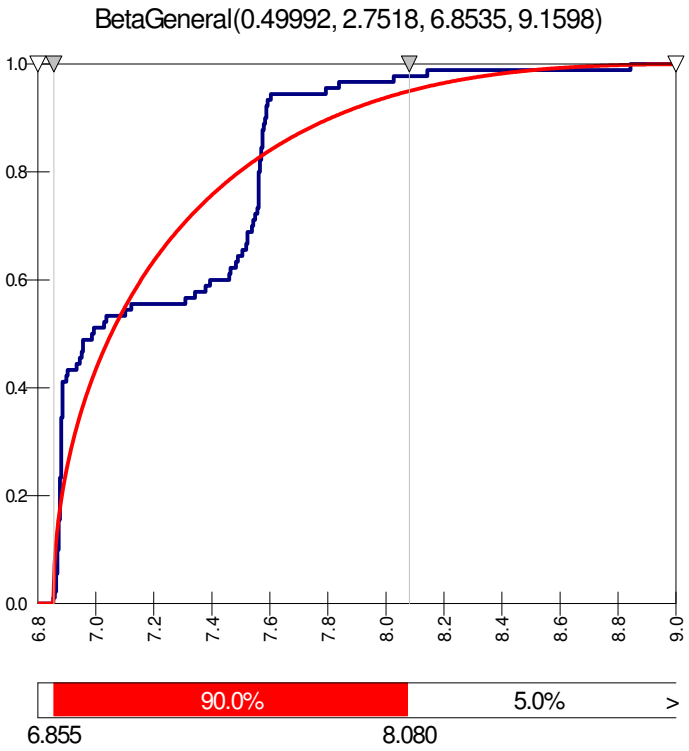


**(b)**

**Figure D-17. Well A22: Best fit curves (a) probability density; (b) cumulative density**

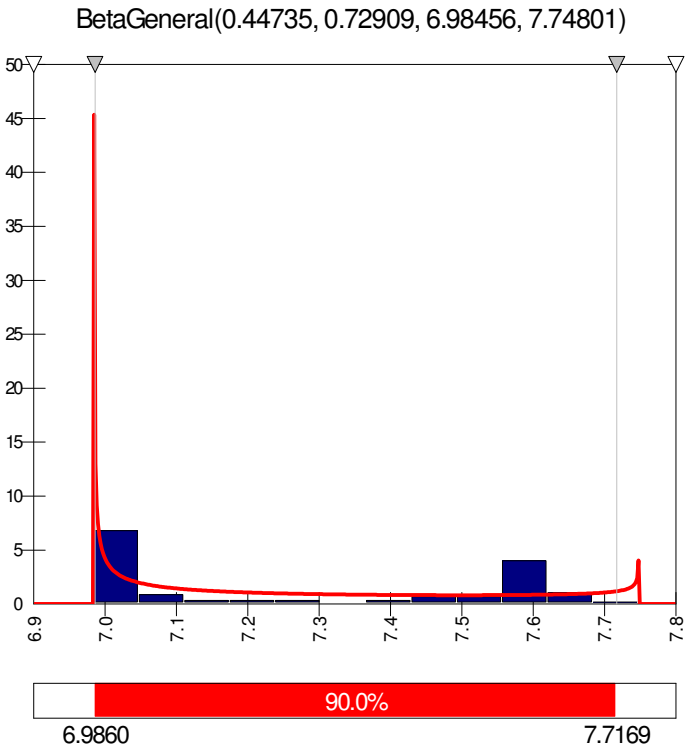


**(a)**

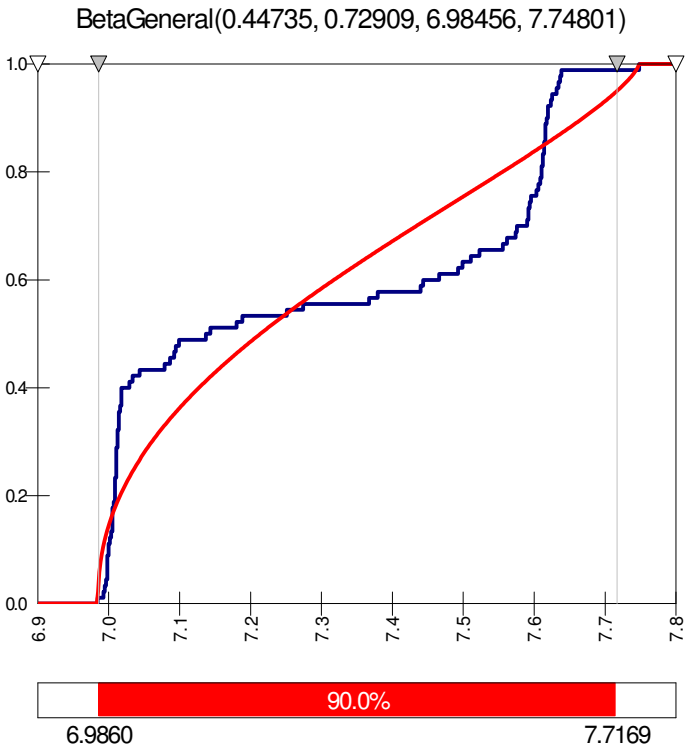


**(b)**

**Figure D-18. Well A23: Best fit curves (a) probability density; (b) cumulative density**

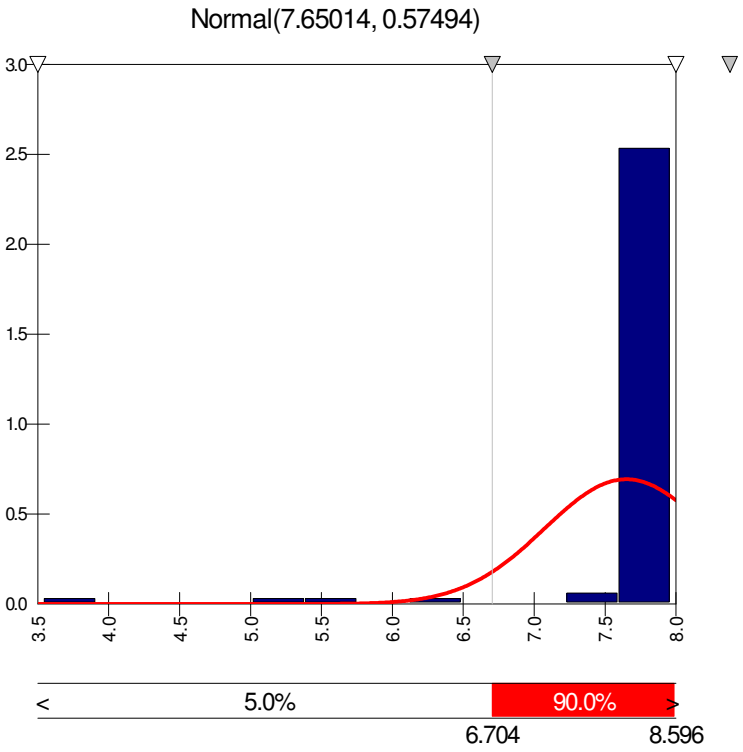


**(a)**

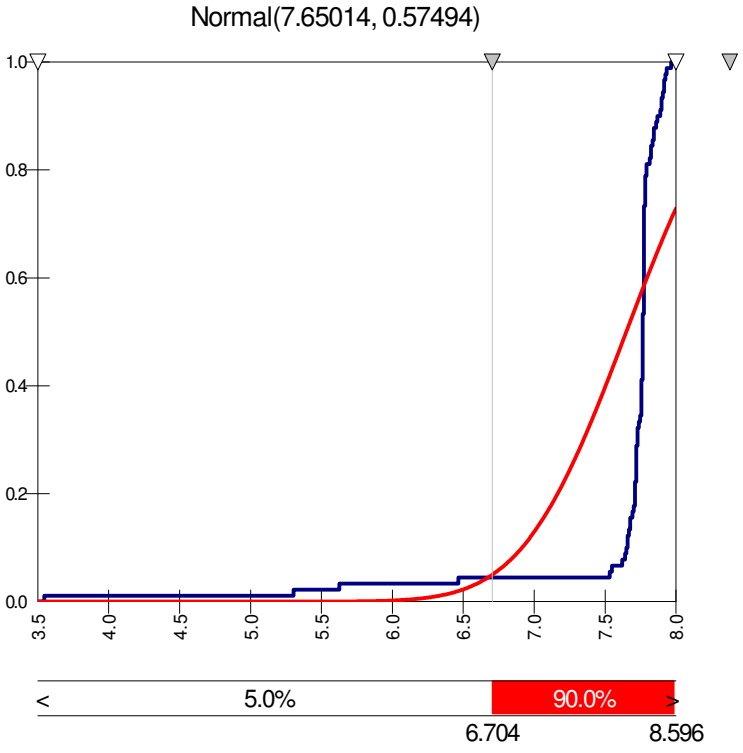


**(b)**

**Figure D-19. Well A24: Best fit curves (a) probability density; (b) cumulative density**

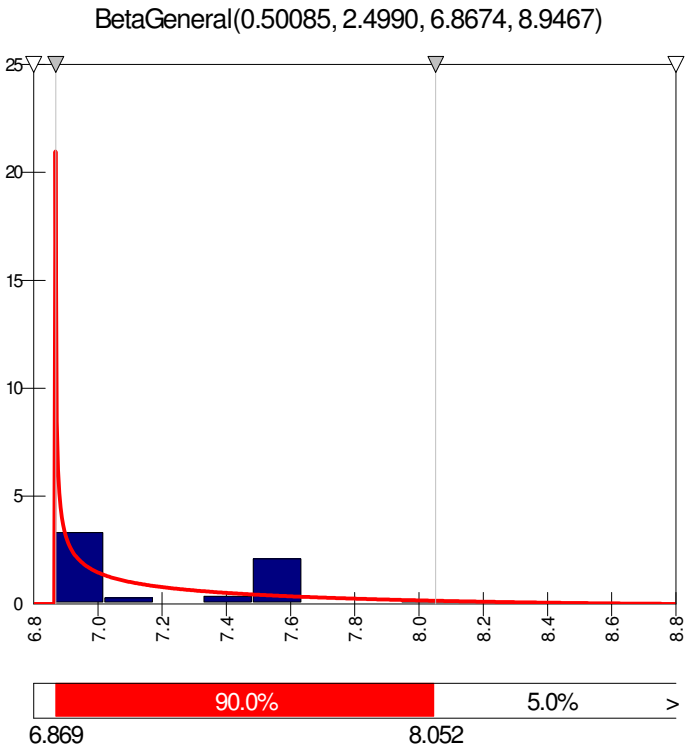


**(a)**

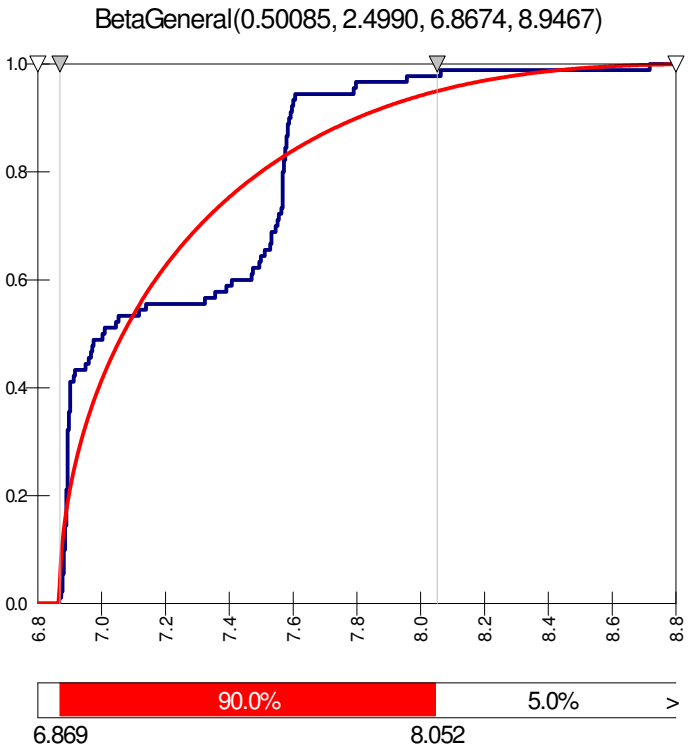


**(b)**

**Figure D-20. Well A25: Best fit curves (a) probability density; (b) cumulative density**

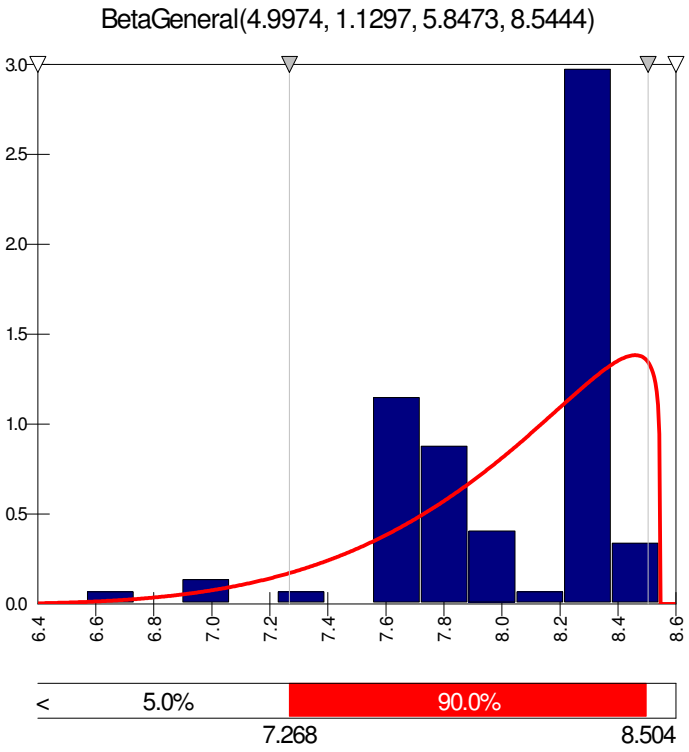


**(a)**

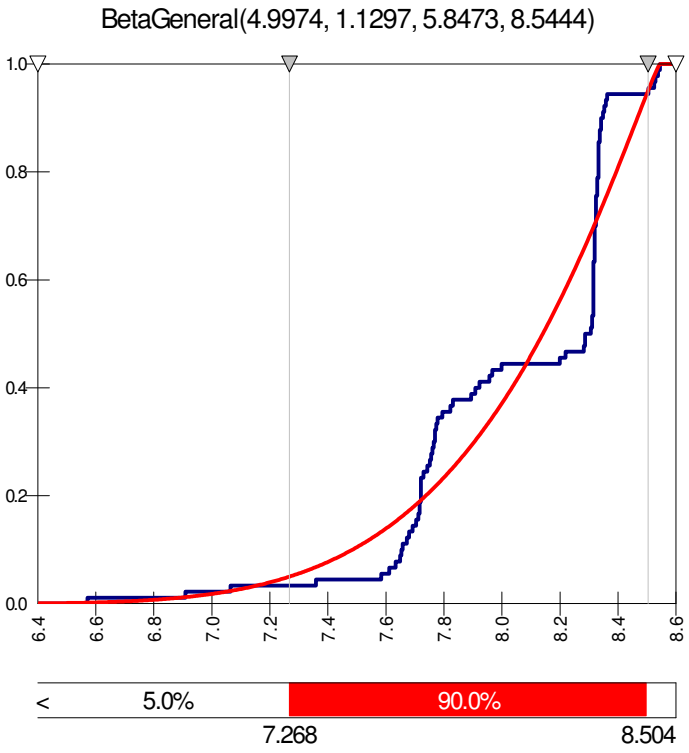


**(b)**

**Figure D-21. Well A27: Best fit curves (a) probability density; (b) cumulative density**

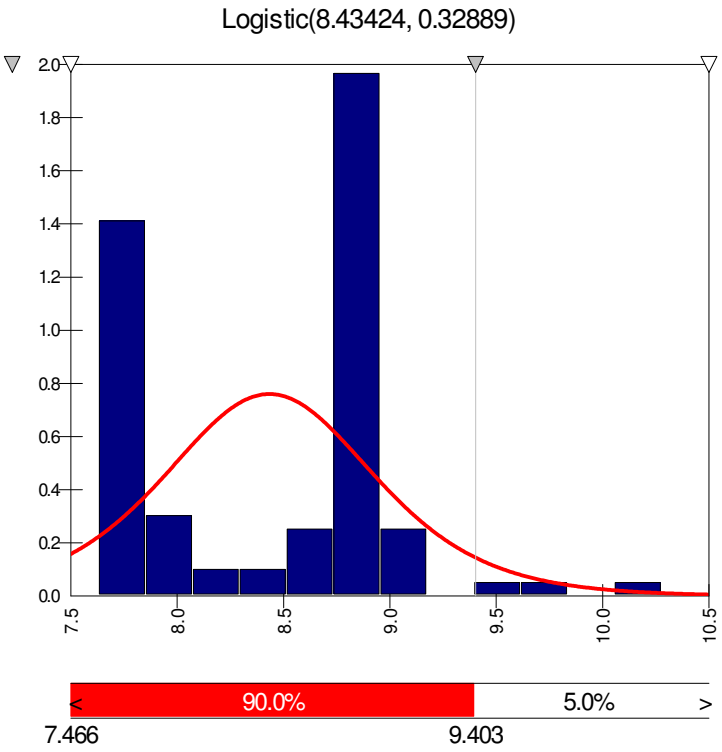


**(a)**

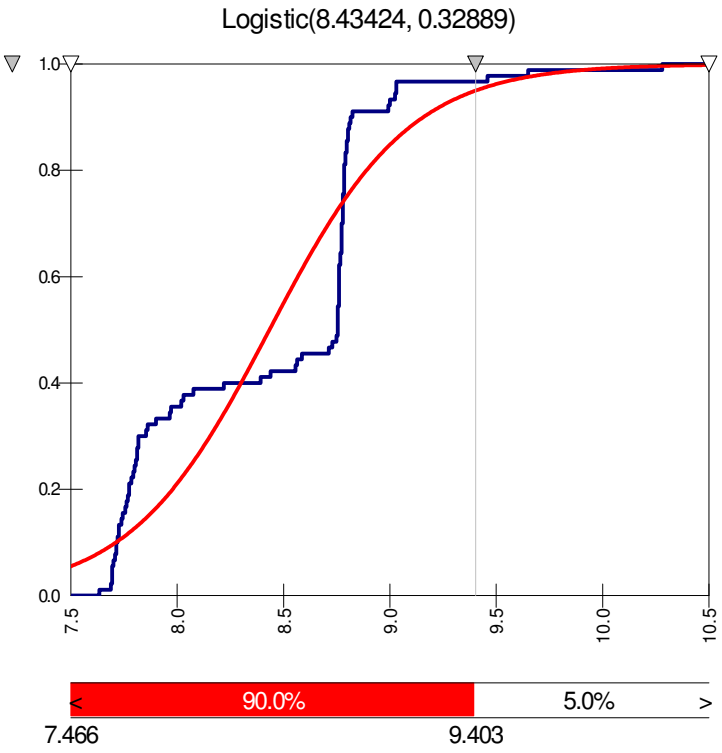


**(b)**

**Figure D-22. Well A29: Best fit curves (a) probability density; (b) cumulative density**

VITA

PRATIMA POUDYAL

Candidate for the Degree of

Master of Science

Thesis: ARTIFICIAL NEURAL NETWORKS TO PREDICT THE NITRATE DISTRIBUTION IN CIMARRON TERRACE AQUIFER, OKLAHOMA

Major Field: Civil Engineering

Biographical:

Personal Data: Born in Nepal, on Jun 27, 1980, the daughter of Giri Raj and Bindu Poudyal

Education: Graduated from Nepal Science Campus in July1998, Kathmandu Nepal; received Bachelor's Degree in Civil Engineering from Western Region Campus, Institute of Engineering, Tribhuvan University, Pokhara, Nepal in December 2003; completed the requirements for the Master of Science Degree in Civil Engineering (Emphasis in Environmental and Water Resources) at Oklahoma State University, Stillwater, Oklahoma in December 2007.

Experience: Employed with Khwopa Engineering College, Purbanchal University, Bhaktapur, Nepal from June 2004 to November 2006 as an assistant lecturer; employed by Oklahoma State University, Oklahoma Infrastructure Consortium, Department of Civil and Environmental Engineering as a graduate research assistant from August 2006 to December 2007.

Memberships: Member-Nepal Engineering Council; Oklahoma State University Chapter Member- Chi Epsilon, Oklahoma State University Chapter Member-American Society of Civil Engineerins

Name: Pratima Poudyal Date of Degree: December 2007

Institution: Oklahoma State University Location: Stillwater, Oklahoma

Title of Study: ARTIFICIAL NEURAL NETWORKS TO PREDICT THE NITRATE DISTRIBUTION IN CIMARRON TERRACE AQUIFER, OKLAHOMA

Pages in Study: 199 Candidate for the Degree of Master of Science

Major Field: Civil Engineering (Emphasis in Environmental and Water Resources)

Summary:

The artificial neural network (ANN) models were used to expand the groundwater nitrate data taken at well locations to the entire space of Cimarron Terrace Aquifer near the City of Enid, Oklahoma. These neural kriging methods were able to adequately extrapolate the nitrate concentrations from the measured point values over the area of concern.

Additional, a series management option models each with a 10 percent decrease nitrogen application rate were developed for the City of Enid's Ames wellfield. These models showed that significant differences existed between nitrate concentrations at threshold levels of 4.0 mg/L and 10.0 mg/L. A reduction of 80 percent of the surface nitrogen application rate was needed to cause a decrease to the nitrate MCL level.

Further, neural conditional simulation subsequently was applied to the Ames wellfield data to determine the probability and cumulative density functions and respective best fit curves for the predicted nitrate concentrations.

ADVISER'S APPROVAL: Dr. William F. McTernan and Dr. Avdhesh K. Tyagi